Fisheries and Oceans Canada | Pêches et Océans Canada
Science | Sciences

Canadian Science Advisory Secretariat (CSAS)

Research Document 2013/032

Pacific Region

State of physical, biological, and selected fishery resources of Pacific Canadian marine ecosystems in 2012

J.R. Irvine[1] and W.R. Crawford[2], editors

[1] Fisheries and Oceans Canada, Pacific Biological Station
3190 Hammond Bay Rd., Nanaimo, BC V9T 6N7

[2] Fisheries and Oceans Canada, Institute of Ocean Sciences,
9860 West Saanich Rd., Sidney, BC V8L 4B2

May 2013

Canada

Foreword

This series documents the scientific basis for the evaluation of aquatic resources and ecosystems in Canada. As such, it addresses the issues of the day in the time frames required and the documents it contains are not intended as definitive statements on the subjects addressed but rather as progress reports on ongoing investigations.

Research documents are produced in the official language in which they are provided to the Secretariat.

Published by:

Fisheries and Oceans Canada
Canadian Science Advisory Secretariat
200 Kent Street
Ottawa ON K1A 0E6

http://www.dfo-mpo.gc.ca/csas-sccs/
csas-sccs@dfo-mpo.gc.ca

ISSN 1919-5044

Correct citation for this publication:

Irvine, J.R. and Crawford, W.R. 2013. State of physical, biological, and selected fishery resources of Pacific Canadian marine ecosystems in 2012. DFO Can. Sci. Advis. Sec. Res. Doc. 2013/032. viii + 140 p.

TABLE OF CONTENTS

ABSTRACT

This report summarises results from the fourteenth annual workshop on the state of physical, biological, and selected fishery resources of primarily Pacific Canadian marine ecosystems.

The global temperature in 2012 was warmer than the 20th century average almost everywhere, but not in the northeast Pacific Ocean where cool waters have been present in almost every year since 2007, part of a Pacific-wide weather pattern associated with La Niña conditions of these years.

Sea surface measurements from shore stations along the coast of British Columbia and in the Salish Sea, confirm that ocean conditions were cooler in 2012 than in 2011 and 2010. Preliminary results of measurements by a Continuous Plankton Recorder through the eastern Gulf of Alaska were partially processed at press time, revealing somewhat lower biomass of large diatoms (a type of phytoplankton) than usual, and much larger biomass of copepods. Both these results are compatible with cool ocean surface waters. Satellite imagery results detected a very strong bloom of coccolithophores west of northern Vancouver Island in June 2012, the strongest bloom of the 11-year record.

An intense bloom of phytoplankton was observed by MODIS (Moderate Resolution Imaging Spectroradiometer) satellite in the Gulf of Alaska more than 200 nautical miles west of Haida Gwaii in August 2012. Its location, size and intensity suggest it may have been due to fertilization of the ocean with iron-rich material, as part of a project undertaken by the Haida Salmon Restoration Corporation.

Albacore Tuna catches in Canadian waters increased in 2012 relative to the previous year, but were probably related to increased effort. Off the west coast of Vancouver Island, the zooplankton community contained more cool-water zooplankton than average, which is associated with good local survival and growth of young salmon and other fish as well as plankton-eating seabirds including Cassin's Auklet. Walleye Pollock and Smooth Pink Shrimp densities increased in 2012, while Eulachon, Herring, and Sardine numbers remained relatively low. Nearshore fish populations in eelgrass and kelp beds of Pacific Rim National Park Reserve tend to vary more among areas than years.

Non-Fraser southern Sockeye Salmon stocks continued to exhibit re-building while those from the central and north coast continued a decadal-scale, sub-average return trend through 2012. The number of Pink Salmon returning in even-numbered years, including 2012, tend to be stable while populations returning in odd years, including the Fraser, are generally increasing. In 2012, juvenile Chum, Sockeye, Coho and Chinook Salmon catch rates were generally higher off the west coast of Vancouver Island (WCVI) and in the central coast than in 2011, and at or above the 1998-2012 long-term average for all species.

Waters of the Salish Sea, comprising Juan de Fuca Strait, Puget Sound and the Strait of Georgia and adjacent waters, host a separate ecosystem from offshore waters. A detailed study of Puget Sound waters since 1998 revealed systematic changes, many of which were due to intrusions of oceanic water. For instance, the average oxygen content of Puget Sound waters below 20 metres depth varies with the upwelling index off the west coast of Washington State. Oxygen concentration declined in the past 5 or so years, although it rebounded in 2012. A longer time series is available for the Strait of Georgia, where oxygen concentration in deep waters over the past 40 years declined, attributed to similar declines in deep waters on the continental shelf that advect into the Strait. This decline in oxygen is of concern because

oceanic sub-surface water in our region that is deficient in oxygen is often more acidic, and ocean acidity will increase everywhere as more carbon dioxide is added to the atmosphere.

Phytoplankton in the Strait of Georgia bloom in the late winter and early spring, reaching a peak when they have consumed all nutrients in the surface layer. The timing and duration of this peak of the spring bloom is believed to impact the survival of juvenile salmon and herring. The spring bloom of phytoplankton in the Strait of Georgia in 2012 was later than normal and similar in timing to the previous 6 years.

Juvenile salmon from the Fraser River generally enter the Strait of Georgia from April to June, many remaining there until the fall. A multi-year study of tagged sockeye salmon smolts exiting Chilko Lake in the Fraser River watershed found consistent early survival patterns among years. Tagged fish moved rapidly through the Strait of Georgia and Queen Charlotte Strait. Large catches of two-year-old juvenile Sockeye Salmon in research trawl surveys in the Strait of Georgia in 2012 resulted from record high returns to the Fraser River in 2010. Based on these research surveys in 2012, good returns are forecast for Fraser River Sockeye Salmon returning in 2014, and Coho and Pink Salmon returning in 2013, while poor returns of Chum and Chinook Salmon are expected in 2013 and 2014.

État des ressources physiques et biologiques et de certaines ressources halieutiques des écosystèmes des eaux canadiennes du Pacifique en 2011

RÉSUMÉ

Ce rapport résume le 14e atelier annuel sur l'état des ressources physiques et biologiques, ainsi que sur celui de ressources halieutiques sélectionnées, des écosystèmes marins de la région canadienne du Pacifique en particulier.

La température mondiale a été plus élevée que la moyenne du XXe siècle presque partout en 2012, sauf dans le nord-est de l'océan Pacifique, où des eaux fraîches sont présentes pour ainsi dire chaque année depuis 2007; ce phénomène fait partie des conditions météorologiques observées dans tout le Pacifique qui sont associées à La Niña de ces années-là.

Les mesures à la surface de l'océan prises par les stations le long de la côte de la Colombie-Britannique et dans la mer des Salish ont confirmé que les conditions océaniques ont été plus fraîches en 2012 qu'en 2011 et en 2010. Les résultats préliminaires des mesures d'un enregistreur continu du plancton dans l'est du golfe d'Alaska traitées en partie au moment de mettre sous presse révèlent que la biomasse des grosses diatomées (une sorte de phytoplancton) a été un peu moins importante qu'à l'habitude et que la biomasse des copépodes l'a été bien plus. Ces résultats sont tous deux compatibles avec des eaux fraîches à la surface de l'océan. L'imagerie satellitaire a permis de découvrir une très forte prolifération de coccolithophores à l'ouest du nord de l'île de Vancouver en juin 2012, la plus grosse enregistrée en 11 ans.

Un intense bloom phytoplanctonique a été observé par le satellite MODIS (Moderate Resolution Imaging Spectroradiometer : spectroradiomètre imageur à résolution moyenne) dans le golfe d'Alaska, à plus de 200 milles nautiques à l'ouest de Haida Gwaii, en août 2012. Son emplacement, sa taille et son ampleur donnent pourrait avoir été causé par la fertilisation de l'océan à l'aide d'un produit riche en fer réalisée dans le cadre d'un projet de la Haida Salmon Restoration Corporation.

Les prises de thon blanc ont augmenté en 2012 dans les eaux canadiennes par rapport à l'année précédente, mais cela vient probablement de ce que l'effort de pêche s'est accru. Au large de la côte ouest de l'île de Vancouver, la communauté zooplanctonique était composée de plus de zooplancton d'eau douce qu'elle ne l'est en moyenne, ce zooplancton étant associé à l'échelle locale à un bon taux de survie et à une croissance satisfaisante des jeunes saumons et autres poissons, et des oiseaux de mer planctonophages, comme le starique de Cassin. Les densités de goberges de l'Alaska et de crevettes océaniques ont augmenté en 2012, tandis que le nombre d'eulakanes, de harengs et de sardines est resté relativement faible. Les populations de poissons côtiers dans les herbiers de zostère et de varech de la réserve de parc national du Canada Pacific Rim varient plus selon les zones que selon les années.

Les stocks de saumons rouges de la partie sud de la côte, autres que ceux du Fraser, ont continué à se reconstituer, alors que la tendance décennale s'est poursuivie dans le centre et le nord de la côte, les stocks en montaison restant inférieurs à la moyenne tout au long de 2012. Le nombre de saumons roses qui reviennent frayer les années paires a tendance à être stable, comme ce fut le cas en 2012, tandis que les populations en montaison les années impaires, y compris celles du Fraser, sont en général à la hausse. En 2012, les taux des prises de saumons kéta, rouges, coho et quinnat ont été en règle générale plus élevés qu'en 2011 au large de la côte ouest de l'île de Vancouver et dans le centre de la côte, et ont atteint la moyenne à long terme de 1998-2012, ou ont été supérieurs à celle-ci, pour toutes les espèces.

Les eaux de la mer des Salish, formée du détroit de Juan de Fuca, de la baie Puget et du détroit de Georgie et des eaux avoisinantes, abritent un écosystème distinct de celui des eaux du large. Une étude détaillée des eaux de la baie Puget depuis 1998 a révélé des modifications systématiques, dont beaucoup sont dues à l'irruption d'eau océanique. Par exemple, la concentration moyenne en oxygène de l'eau de la baie à plus de 20 mètres de profondeur varie en fonction de l'indice des remontées d'eau au large de la côte ouest de l'État de Washington. La concentration en oxygène diminue depuis environ cinq ans, bien qu'elle ait rebondi en 2012. Il existe une série chronologique plus longue pour le détroit de Georgie, où la concentration en oxygène dans les eaux profondes a diminué au cours des 40 dernières années, ce qui est attribué à des diminutions semblables dans les eaux profondes du plateau continental qui pénètrent par advection dans le détroit. Cette réduction de l'oxygène est préoccupante parce que, dans notre région, les eaux de subsurface qui sont pauvres en oxygène sont souvent plus acides, et que l'acidité des océans augmentera partout en conséquence de l'ajout de dioxyde de carbone dans l'atmosphère.

Le phytoplancton prolifère dans le détroit de Georgie à la fin de l'hiver et au début du printemps, atteignant un sommet lorsqu'il a consommé tous les éléments nutritifs de la couche de surface. Au printemps, le moment et la durée de ce sommet influencent, semble-t-il, la survie des saumons et des harengs juvéniles. La prolifération printanière de végétaux planctoniques a eu lieu plus tard qu'à l'accoutumée en 2012 dans le détroit de Georgie, et à peu près au moment où elle s'est produite les six années précédentes.

Les saumons juvéniles du fleuve Fraser arrivent d'habitude dans le détroit de Georgie d'avril à juin, et beaucoup y restent jusqu'à l'automne. Une étude pluriannuelle sur des saumoneaux étiquetés qui quittaient le lac Chilkko, dans le bassin du fleuve Fraser, a révélé que la survie à ce stade est sensiblement la même d'une année à l'autre. Les poissons étiquetés sont rapidement passés dans le détroit de Georgie et le détroit de la Reine-Charlotte. Les larges prises de saumons rouges juvéniles vieux de deux ans effectuées en 2012 au cours des relevés au chalut dans le détroit de Georgie sont la conséquence des montaisons records dans le fleuve Fraser en 2010. En se fondant sur ces relevés, on prévoit que la montaison des saumons rouges du fleuve Fraser en 2014 et celle des saumons roses et coho en 2013 seront bonnes, mais que la montaison des saumons kéta et quinnat en 2013 et en 2014 sera médiocre.

1. INTRODUCTION

This report is the fourteenth in an annual series on the state of physical, biological, and selected fishery resources of Pacific Canadian marine ecosystems. The region supports important resident and migratory populations of invertebrates, groundfish and pelagic fishes, marine mammals and seabirds. Monitoring the physical and biological oceanographic conditions and fishery resources of the Pacific Region is done semi-regularly by scientific staff in several government departments, to understand the natural variability of these ecosystems and how they respond to both natural and anthropogenic stresses. Support for these programs is provided by Fisheries and Oceans Canada, Environment Canada, and Parks Canada. Additional information is provided by the province of British Columbia, US National Oceanographic and Atmospheric Aministration (NOAA), University of Victoria, and the University of British Columbia.

Information for this report was presented at the annual meeting of the Fisheries Oceanography Working Group (FOWG) at the Institute of Ocean Science, Sidney, BC, on February 20 to 21, 2013 chaired by Jim Irvine and Bill Crawford, both of Fisheries and Oceans Canada. They subsequently produced this summary report based on contributions by participants. Participants at the workshop are thanked for their contributions, especially those that contributed individual reports, and special thanks goes to Michael O'Brien for his hard work and attention to detail in helping to produce this report.

1.1. 2012 ASSESSMENT HIGHLIGHTS

Important highlights from the more detailed individual reports follow. The relevant individual reports are linked, with the author of each report indicated in blue.

1.1.1. Northeast Pacific - continuing cool along the west coast.

The global surface temperature in 2012 was warmer than average in most regions, but not in much of the eastern North Pacific near the west coast of North America (Crawford 1). Fig. 1 shows the extent to which surface temperature was relatively warm (shown in yellow and red) or cool (shown in blue and purple) in four individual months from September 2011 to February 2013.

All four panels of Fig. 1 show relatively cool ocean surface waters off the west coast of North America. These conditions have prevailed for most of the past six years. Only in February and March of 2010, an El Niño winter, were ocean temperatures significantly warmer than normal off the west coast. These cool conditions are linked to several Pacific-wide climate patterns, as described by Crawford 1.

The surface cooling extends down through the ocean, as revealed by measurements along Line P, a set of ocean climate stations sampled three times a year by Fisheries and Oceans Canada (DFO). Waters down to at least 1000 metres were cooler along this line in August 2012 than the previous August (Freeland and Robert). In addition, average temperatures in 2012 at shore stations in British Columbia were much lower than the average over the previous 30 years, and also lower than in 2011 (Chandler and Gower). The shift of coastal currents from winter to summer flow was late in 2012 (Hourston and Thomson 2). Much of the cooling through the Gulf of Alaska and along the coast since 2007 is linked to stronger westerly winds in the middle of the Gulf region (Crawford 1) during most of these years, and stronger northwesterly winds along the coast from 2008-2011 (Hourston and Thomson 1), although these winds were average strength in 2012 (Hourston and Thomson 1, Dewey et al.). These winds are associated with the positive phase of the North Pacific Gyre Oscillation (McKinnell), and are likely responsible for increased easterly flow in the North Pacific Current in 2012 (Freeland and Robert). The cooling

is expected to diminish within some years (McKinnell, Hourston and Thomson 1), but predictions of the timing are not reliable. Despite the continuing cool ocean into early 2013, water conditions are variable, leading to very different storm waves along the west coast from one year to the next, as measured by Ocean Networks Canada at the NEPTUNE array (Atkinson et al.) in Barkley Sound.

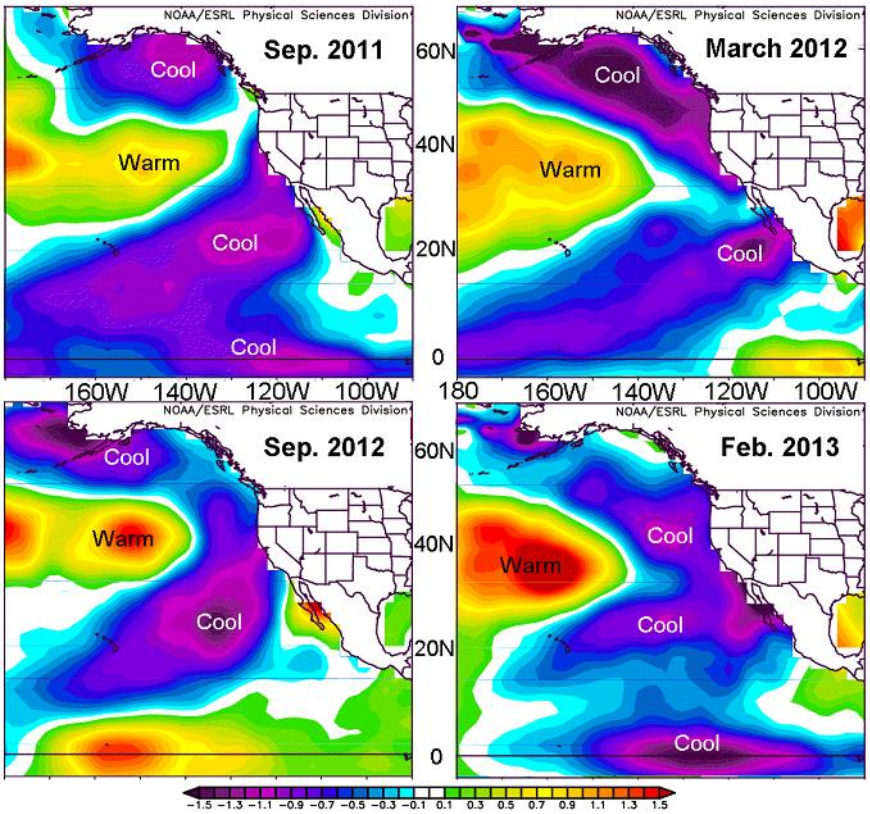

Figure 1. ***Sea surface temperature anomaly (SSTA)*** *in the eastern Pacific Ocean for Sept 2011 to Feb 2013. The maps extend from North America west to 180°, and from 5° South to 65° North. The equator is marked by the horizontal black line near bottom of each panel. The temperature anomaly scale in °C is at bottom. Positive and negative temperature anomalies are labelled warm and cool, respectively in each panel. Reference years for temperature anomaly are 1981 to 2010. Images provided by NOAA: http://www.esrl.noaa.gov/psd/cgi-bin/data/composites/printpage.pl*

Despite these relatively cool ocean waters since 2007, there is a trend toward warming of coastal waters since measurement began at shore stations in the early 20th century (Chandler and Gower) and in the upper 200 metres at Ocean Station Papa in the Gulf of Alaska at 50°N, 145°W since 1950 (Freeland and Robert).

1.1.2. Marine food chain of the Gulf of Alaska and continental shelf

Phytoplankton and zooplankton are microscopic plants and animals that are the base of the marine food chain, and interannual variability in their biomass can impact fish survival. Measurement of zooplankton and large phytoplankton by a continuous plankton recorder (CPR) have been undertaken since 2000 in the Northeast Pacific Ocean (Figure 2 a, b).

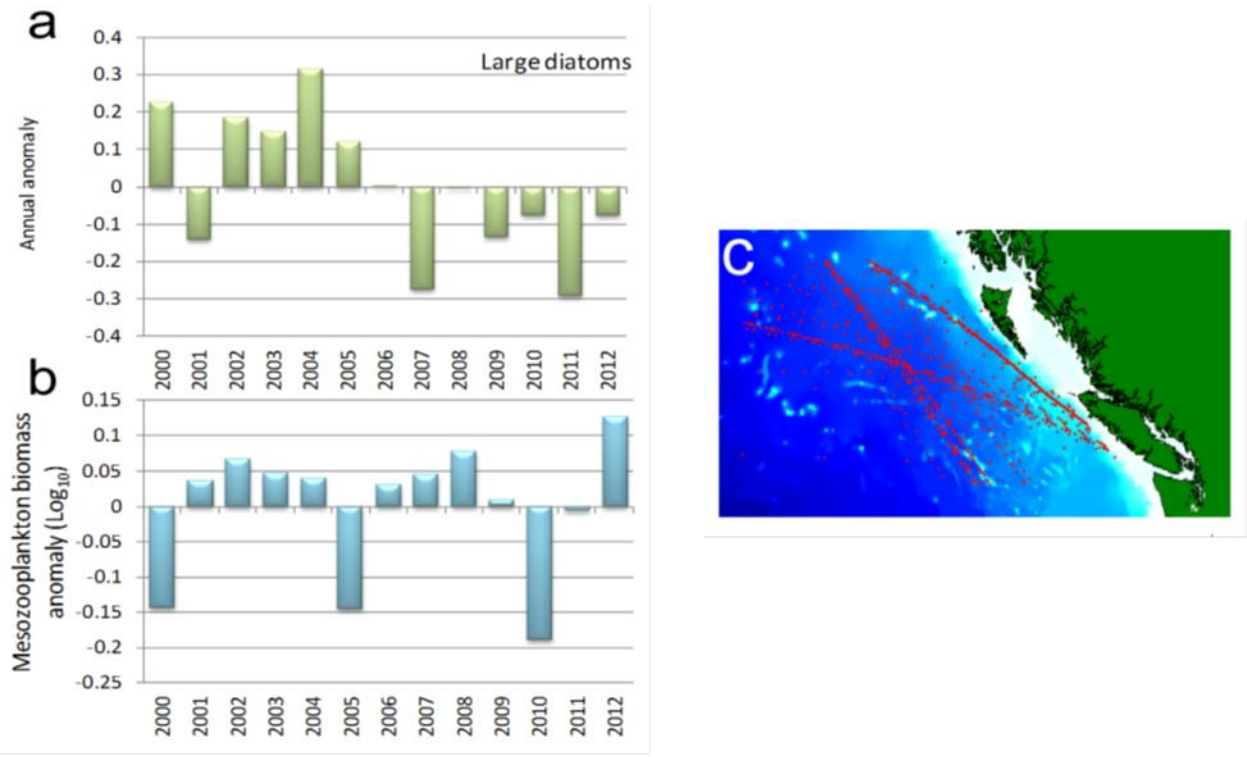

Figure 2. Large diatom (a) and meso-zooplankton annual biomass anomalies (b) based on data from the CPR survey for the sub-region of the Northeast Pacific shown in (c) (Batten).

Results for the eastern Gulf of Alaska (Fig. 2c) reveal that the concentration of large diatoms (a type of phytoplankton) has been rather low since 2007 (Fig. 2a) In contrast, the mesozooplankton biomass estimate of 2012 in the Gulf of Alaska was the largest of any year in the 13-year time series (Fig. 2b) (Batten). The timing of the mid-point of its seasonal cycle was also late in 2012. These features of large diatoms and zooplankton are consistent with cool conditions in the Gulf of Alaska.

We rely also on satellite images of ocean colour to reveal interannual changes in phytoplankton. A time series of visible light by Moderate Resolution Imaging Spectroradiometer (MODIS) satellite shows that the biomass of a bright *Coccolithophore* along the west coast of Vancouver Island (WCVI) in July 2012 was the second highest in the 11-year time series (Gower 1). This phytoplankton has shells rich in calcium carbonate that reflect white light, forming a distinctive white pattern on the ocean surface. Other phytoplankton are more easily detected by observing ocean colour, because they preferentially absorb blue light, turning the surface ocean green. An intense bloom of plankton was observed by MODIS satellite in the Gulf of Alaska more than 200 nautical miles west of Haida Gwaii in August 2012. Its location, size and intensity suggest it may be due to fertilization of the ocean with iron-rich material, as part of a project undertaken by the Haida Salmon Restoration Corportaion (Gower 2).

Along the Canadian west coast, annual anomalies of the cool-water copepod and chaetognath zooplankton species groups have been positive in most years since 2007, and were especially positive in 2012 for the “boreal shelf copepod” group (highest since the early-mid 1980s). Conversely, the warm-water southern-origin copepods and chaetognaths had negative anomalies, but less so than in 2007-2009. Euphausiid anomalies were positive and similar in magnitude to 2010. We now know that positive anomalies of the cool water zooplankton

community off Vancouver Island are also associated with good local survival and growth of juvenile salmon, sablefish, and planktivorous seabirds (Hipfner; Mackas et al. 1).

Studies of nearshore fish populations require special sampling techniques. Parks Canada scientists reported the results of a five-year survey by SCUBA divers of juvenile fish in eelgrass and kelp beds of Pacific Rim National Park Reserve. Fish assemblages in both kelp forest and eelgrass meadows assessed in these surveys did not appear to vary in 2012 anymore than was observed in previous years, and variation in fish assemblages was better explained by spatial variation then temporal (Yakimishyn and Zharikov).

Surveys in May 2012 found the biomass of *Pandalus jordani* shrimp off central Vancouver Island had increased from the low value in 2011 The biomass of "core" flatfish species remained lower in all surveyed areas in 2012 compared with the early 2000's, but higher than during the 1970's and 1980's. The biomass of Walleye Pollock (*Theragra chalcogramma*, a cold water species) was particularly high in 2012 in Areas 124-125, and slightly higher in Areas 121-123, compared with previous years (Perry et al.).

Eulachon have experienced long-term declines in many rivers throughout their distribution from California to Alaska. Indices of Eulachon abundance in central and southern British Columbia rivers remain at low levels. The estimated Eulachon spawning stock biomass in the Fraser River decreased during 1994-2010 with slight increases in 2011 and 2012 (Schweigert et al.).

The biomass of three major herring fishing stocks (Haida Gwaii, Central Coast, West Coast Vancouver Island) have been below fishery thresholds in recent years despite being closed to fishing; whereas two areas that are open to fishing have stable or high biomass estimates (Prince Rupert District, Strait of Georgia). Consideration of these biomass trends in combination with the declining trend in herring weight-at-age observed for all fishing stock areas, suggests that factors other than fishing may be influencing herring population trends. Changes in food supply and quality, predator abundance, and competition are factors that could affect trends in herring biomass and weight-at-age (Boldt et al.).

The most recent U.S. sardine assessment suggests that the California Current (Northeast Pacific) sardine population abundance off Canada and the U.S. increased rapidly through the 1980s and 1990s. WCVI survey catch densities of sardine decreased considerably from 2011 (Fig. 3), and density estimates were lower than other observations since 2006. The extremely low densities may be due to a combination of survey timing and unfavourable oceanographic conditions as well as decreased population abundance (Flostrand et al.).

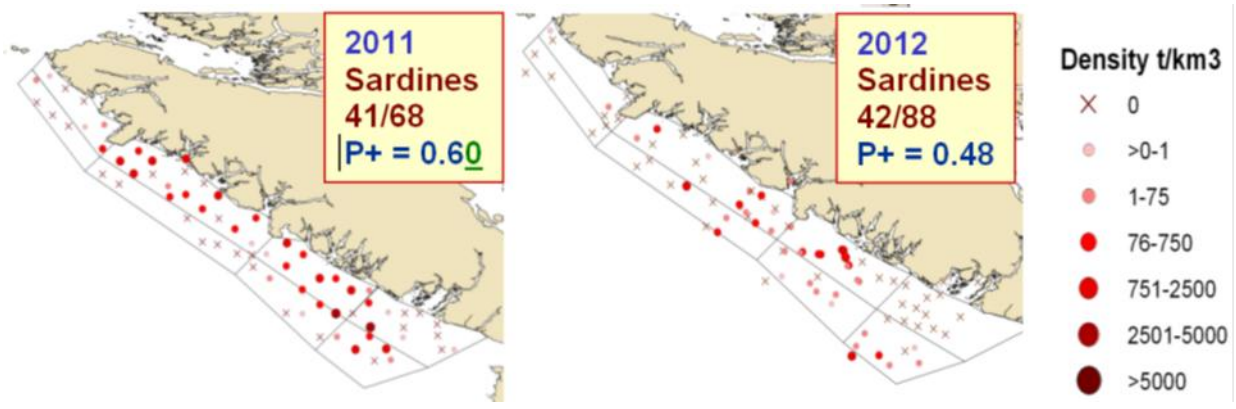

Figure 3. West coast of Vancouver Island summer trawl survey sampling locations and relative sardine catch densities for 2011 and 2012 (tonnes per km^3 trawled). P+ = the fraction of tows where sardine were caught.

All Pink Salmon spawn at 2 years of age such that fish that return to spawn in odd- and even-numbered years are genetically isolated from each other. Regional differences in even and odd year abundances have been known for more than a century. A DFO study used 5 statistical approaches to evaluate trends in the population time series of 23 Pink Salmon Conservation Units (CUs), which are largely genetically distinct biological units. Almost without exception, odd year CUs are doing better than even year CUs. Generally, even year CUs tended to have mostly neutral abundance trends while abundances of odd year CUs were increasing. In those areas with CUs of both even and odd year returning salmon, trends in odd years are always more positive than trends in even years (Irvine et al.).

Southern Sockeye Salmon stocks, with sea-entry into the northern California Current along the west coast continental shelf (Okanagan, and Barkley sockeye), exhibited rapid rebuilding to near record returns in 2009-2011. By contrast, the more northern Transboundary (Tahltan, Tatsamenie) and North Coast (Nass, Skeena) stocks continued a decadal-scale, sub-average return trend through 2012 (Hyatt et al.).

Mean June-July 2012 catch-per-unit-effort (CPUE) of juvenile Chum, Sockeye, Coho and Chinook Salmon were generally higher off the WCVI and in the central coast than in 2011 and at or above the 1998-2012 long-term average for all species. The utility of using these CPUEs as early indicators of future adult returns is not clear, as CPUEs may be correlated with smolt production from south of the region, smolt survivals, or both. Growth rates of juvenile Coho Salmon off WCVI increased above the 1998-2011 average in 2012 suggesting that marine survival will be average to above average for WCVI Coho Salmon returning in 2013 relative to 1999-2012 (Trudel et al.).

Historically, about 80% of the Canadian Albacore Tuna catch has occurred in American coastal waters off of Washington and Oregon (through access provisions in the Canada-US Albacore Tuna Treaty), approximately 14% has occurred in Canadian waters, and the remainder in adjacent high seas waters. Canadian vessels were not licensed to fish in coastal waters of the United States in 2012. As a result, harvesting activity by the Canadian fleet was focused in Canadian and adjacent international waters. Total catch of albacore in Canadian waters was 2,058 t (81% of the fishery), which is a 207% increase relative to the catch in 2011 (670 t) and reflects a 184% increase in effort in Canadian waters relative to 2011 (Holmes).

Marine birds can be effective indicators of the state of marine ecosystems because they gather in large and highly visible aggregations to breed and because, as a group, they feed at a variety of trophic levels (zooplankton to fish). Seabird breeding success is closely tied to the availability of key prey species, and as a result, can vary widely among years, depending on ocean conditions. Triangle Island (50°52' N, 129°05' W) in the Scott Island chain off northern Vancouver Island, supports the largest and most diverse seabird colony along the coast of British Columbia. The mean mass at 25 days of age of Cassin's Auklet nestlings in 2012 was above the 1996-2011 average. In general, the Auklets' offspring grow more quickly and fledge at heavier masses in cold-water years, because timing of their hatching is strongly temporally matched with the phenology of an important prey species, the copepod *Neocalanus cristatus*. Thus, the above-average 25-day mass was expected based on the relatively cold spring sea-surface temperatures in 2012 (Hipfner).

1.1.3. Salish Sea

Waters of the Salish Sea, comprising Juan de Fuca Strait, Puget Sound and the Strait of Georgia and adjacent waters, host a separate ecosystem from offshore waters; however, the nature of seawater in the Salish Sea varies in response to changes offshore. A detailed study of Puget Sound waters since 1998 reveals systematic changes inside Puget Sound, many of which are due to intrusions of oceanic water.

For example, the changes in thermal energy content (TEC, indicating temperature) of the top 50 metres of Puget Sound correlate well with the Pacific Decadal Oscillation (Fig. 4), itself a measure of surface temperature changes in the North Pacific Ocean. Puget Sound surface temperature at 0 to 50 m (related to heat content) has declined over the past 5 years or so (Krembs). Sampling in the Strait of Georgia reveals that temperature in this water body at most depths has been lower than average since 2008 (Masson).

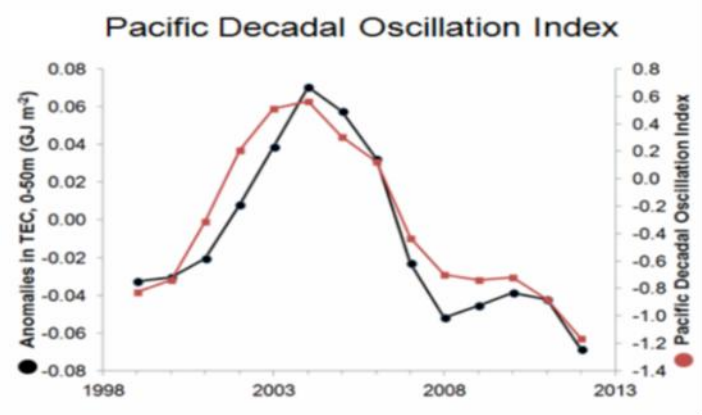

Figure 4. Average thermal energy content of the upper 50 metres of Puget Sound, based on an average over 27 sampling stations, (black) compared to the Pacific Decadal Oscillation Index (red). Both series have been passed through a 3-year running-mean, low-pass filter (Krembs).

The average oxygen content of Puget Sound waters, from 20 metres below ocean surface to bottom, varies with the upwelling index off the west coast of Washington State. Oxygen concentration declined in the past 5 or so years, although it rebounded in 2012 (Krembs). A longer time series is available for the Strait of Georgia, where oxygen concentration in deep waters over the past 40 years declined at an average rate of 0.02 millilitres per litre per year. Johannessen et al. attributed this to similar declines in deep waters on the continental shelf. This decline in oxygen is of special concern to the Salish Sea and entire west coast (Johannessen et al.), because oceanic sub-surface water in our region that is deficient in oxygen is often more acidic and ocean acidity will increase everywhere as more carbon dioxide is added to the atmosphere. Sub-surface seawater of the eastern Gulf of Alaska is already more acidic than most ocean regions, due to natural, prevailing oceanic flows.

Phytoplankton concentration in the Strait of Georgia increases rapidly in the late winter or early spring until they consume nutrients in the surface waters. This process is called the spring bloom, and the timing and duration of this event is believed to impact the survival of juvenile salmon and herring. Spring blooms are late if the weather has been cloudy and windy. A numerical model of this growth for conditions in 2012 reveals how abrupt these changes can be (Allen et al. Fig. 5). Observations by satellites sensing ocean colour generally agree with the model (Costa et al.)

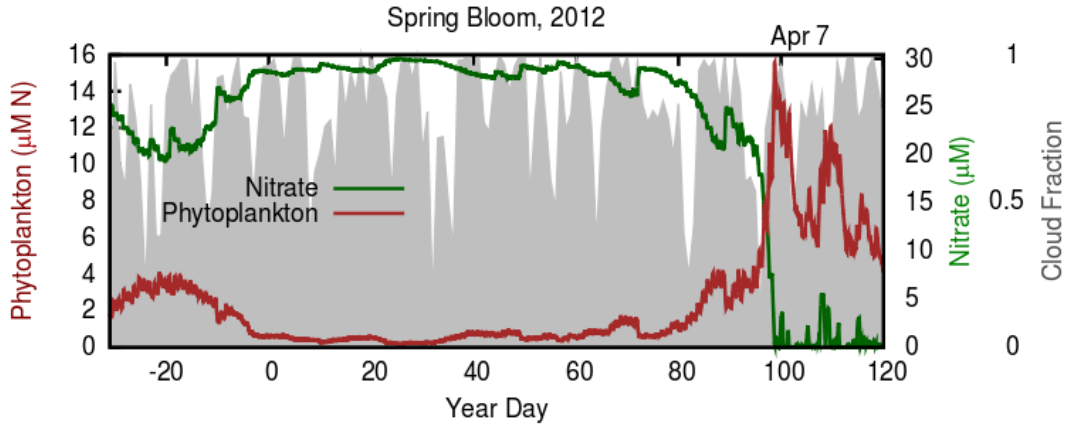

Figure 5. Hindcast of the 2012 spring bloom and related conditions in the Strait of Georgia, illustrating model outputs of temperature and nitrate and measured cloud fraction (Allen et al.).

According to the model, spring blooms from 2006-2011 were all later than March 29, meaning we have been in a period of stable, late spring blooms (Allen et al.). The prediction is for a late to very late spring bloom in 2013, similar to the previous 7 years.

The zooplankton biomass in the Strait of Georgia is dominated by copepods and euphausiids and these had low biomass in 1994-95 and very low biomass in 2005-07. Analysis of zooplankton samples that were collected opportunistically in 2011 and 2012 is not yet complete, but preliminary results indicate that the recovery from the 2005-2007 minimum of zooplankton biomass continued into 2012. Current levels appear to be similar to the high biomass in 1999-2002 (Mackas et al. 2).

1.1.4. Salmon of the Strait of Georgia

The official forecasts of returns of Fraser River Sockeye are based primarily on the numbers of spawners of the previous generation, which are derived from multiple studies estimating escapements in the Fraser River and its tributaries. The total forecasted 2013 Fraser Sockeye return largely falls (up to a three in four chance, based on past observations) below the cycle average (8,579,000), due to the below average 2009 and 2008 brood year escapements for most stocks. However, past experience has shown that actual returns can vary significantly from the predictions (Grant) and work is underway to determine more reliable confidence limits to the predictions.

A multi-year study of tagged Sockeye Salmon smolts exiting Chilko Lake in the Fraser River watershed found remarkably consistent early survival patterns among years. En-route freshwater mortality appears to be largely confined to clear water tributaries leading to Fraser, presumably due to predation, and survival down the Fraser River mainstem is very high. Once in the ocean, survival declines, and survival rates in the Strait of Georgia appear more stable relative to survival rates in the Discovery Passage/Queen Charlotte Strait region. Transit times indicate that large Fraser River Sockeye smolts are rapidly migrating out of the Strait of Georgia and Queen Charlotte Strait (Rechisky et al.).

Juvenile salmon generally enter the Strait of Georgia from April to June, with many individuals remaining there until the fall. In 2012, juvenile salmon were sampled during trawl surveys June

22 - July 2 and September 15 - 26. DFO scientists use a combination of the catch rates during these surveys along with oceanographic conditions in the Strait of Georgia to provide insight into the relative strength of returns in future years as adults (Neville and Sweeting).

Many of the juvenile Sockeye Salmon that entered the Strait of Georgia in 2012 were progeny of the record return of Sockeye Salmon to the Fraser River in 2010. It was, therefore, not surprising that the CPUE of juvenile Sockeye Salmon in the early summer survey of 2012 was the highest since regular sampling began in 1998 (Fig 6A), and almost double the long term average. While the average length of these juveniles in 2012 was the smallest observed in the time series (Figure 6B), the size of Sockeye juveniles in 2008, which resulted in the large 2010 return, was also small. Therefore, if there is no additional impact of the small size and if marine conditions are favourable along their subsequent migration route, Neville and Sweeting expect a good return of sockeye to the Strait of Georgia in 2014 .

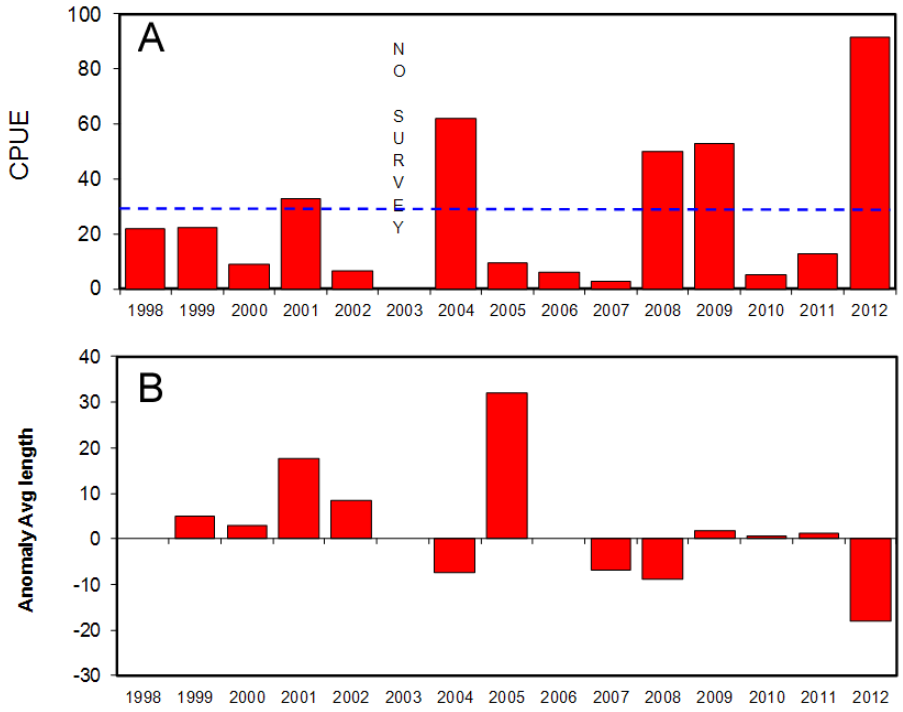

Figure 6. (A) (CPUE) and (B) anomaly of average length for juvenile Sockeye Salmon caught in the June/July trawl surveys in the Strait of Georgia 1998-2012. The juveniles in 2012 are from the record adult return to the Fraser River in 2010. Dashed line in (A) is average CPUE for 1998-2012. (Neville and Sweeting).

Based on surveys of juvenile salmon in the Strait of Georgia in 2011 and 2012, (Neville and Sweeting) anticipate the following marine survival and returns for future years, relative to other recent years:

Sockeye	2014	good
Coho	2013	good
Chum	2013, 2014	poor
Chinook	2013, 2014	poor
Pink	2013	good

2. APPENDIX 1 - INDIVIDUAL REPORTS

2.1. WCVI AND GULF OF ALASKA

2.1.1. Temperatures in 2012: globally warm, but cool in the Eastern Pacific

Bill Crawford, Fisheries and Oceans Canada

Global temperature anomaly in 2012 and its change since 1880

The global surface temperature in 2012 was warmer than average in most regions, but not in much of the eastern North Pacific, especially the Gulf of Alaska. Fig. 1 shows the extent to which surface temperature was relatively warm (shown in red) or cool (shown in blue) in 2012 compared to the reference period of 1981 to 2010. Relatively cool sea surface temperature (SST) in the Gulf of Alaska has been present every year since 2007 as part of a Pacific climate pattern associated with La Niña conditions at the equator and from Pacific-wide SST patterns such as the Pacific Decadal Oscillation (PDO) and the North Pacific Gyre Oscillation (NPGO). (The weather patterns that set up PDO and NPGO patterns are described below in association with Fig. 5.)

Ice melt and temperature increases were newsworthy elsewhere on the globe. The Arctic sea-ice as measured by satellites reached its smallest extent on 16 September 2012 at 3.41 million square kilometres. This was 18% less than the previous record low of 18 September, 2007 (Source WMO Press Release #966; http://www.wmo.int). Environment Canada reported that July through September 2012 was the warmest of any three-month period in Canada in 65 years.

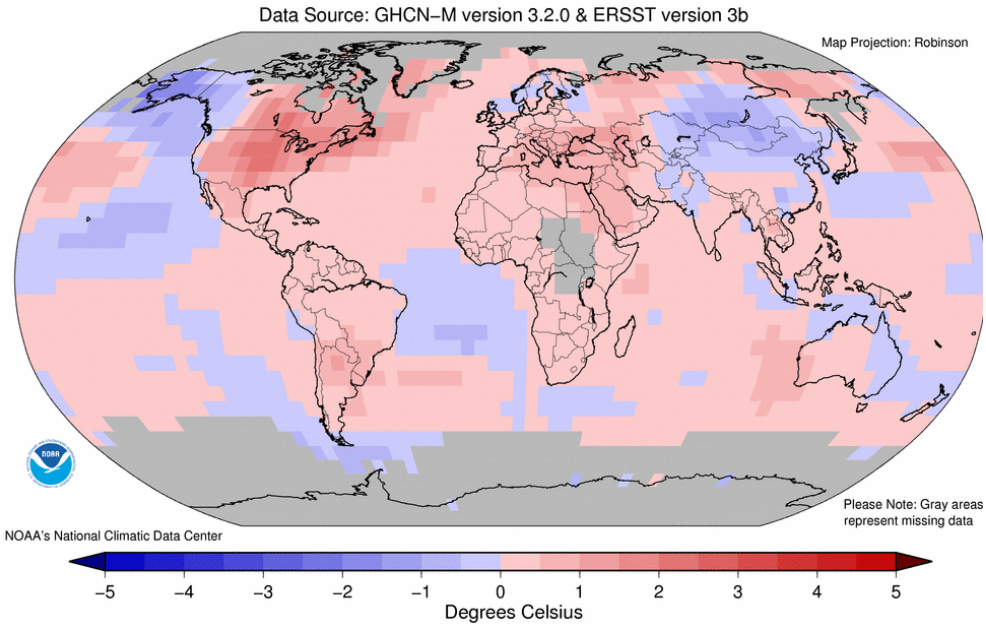

Figure 1.Global surface temperature anomaly for 2012 (°C), relative to the average of 1981 to 2010. Image provided by the National Climatic Data Center o of the US National Oceanic and Atmospheric Administration (NOAA). Figure available www.ncdc.noaa.gov/sotc/service/global/map-blended-mntp/201201-201212.gif

The long term global temperature anomaly is shown in Fig. 2. Red bars denote annual averages; black bars show 95% confidence intervals; blue line is a smoothed multi-year

average. Temperature in 2012 was cooler than typical temperatures since 1997, but warmer than temperatures prior to 1997. The year 2012 was the 10th warmest year since 1880.

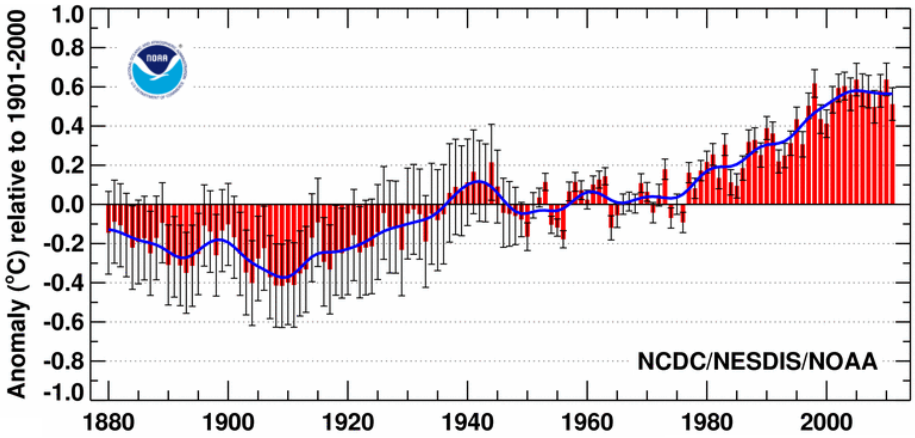

Figure 2. Global surface temperature anomalies from 1880 to 2012, relative to the 20th century average. Image provided by NOAA: http://www.ncdc.noaa.gov/cmb-faq/anomalies.html.

Climate of the Northeast Pacific Ocean

The prevailing air pressure pattern over the Gulf of Alaska in winter determines local ocean surface temperature through much of the year. Fig. 3a below shows the average sea surface pressure (SSP) from December 2012 to February 2013, compared, in Fig. 3b, to the SSP for December to February averaged over the years 1981 to 2010.

The relative positions and strengths of the major air pressure systems change from season to season. The Aleutian Low (**L** in Fig 3) expands in area and deepens in winter; The North Pacific High (**H** in Fig. 3) shrinks in area and its pressure decreases in winter. Fig. 3a reveals these two pressure systems of the most recent winter while Fig. 3b shows average winter conditions from 1981 to 2010. In the winter of Dec. 2012 to Feb 2013, SSP in the North Pacific High was higher and the centre of this system was shifted somewhat to the west compared to average winters.

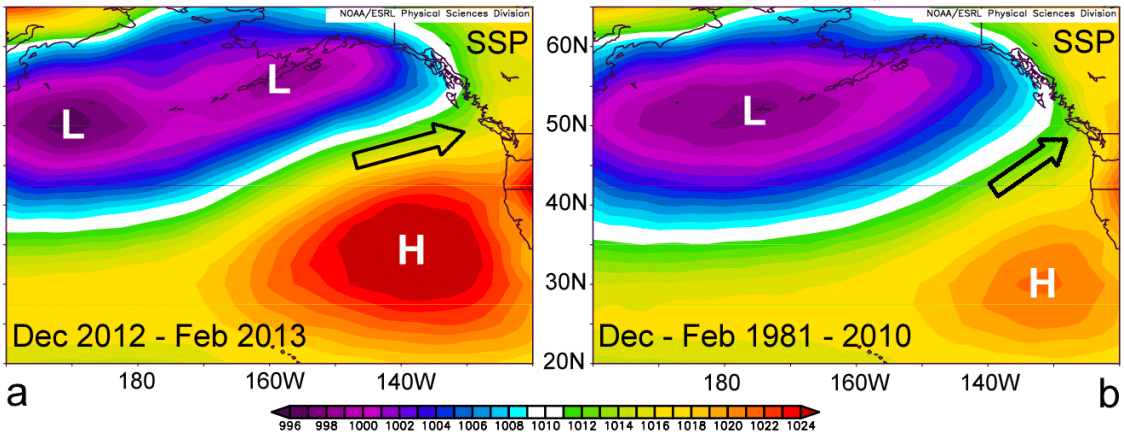

*Figure 3. **Sea surface pressure** in the Northeast Pacific Ocean and over western North America. (a) Average for Dec. 2012, Jan. 2013, Feb. 2013. (b) Average for the months of Dec., Jan., and Feb. for the 30-year period of 1981 to 2010. Contours represent isobars with units of millibars as shown in scale bar at bottom. Arrows show the general wind directions for these respective periods. **L** and **H** denote the Aleutian Low Pressure and North Pacific High Pressure, respectively. Images provided by NOAA:* http://www.esrl.noaa.gov/psd/cgi-bin/data/composites/printpage.pl

Winds in the lower atmosphere blow along isobars (line of constant pressure) with speeds that increase as isobars are spaced more closely together. The black arrows in Fig. 3 show the general wind direction in each panel. Note that winds of winter 2012-2013 blew more from the west than the 30-year average. In addition, isobars were closer than average in 2012-2013, indicating stronger winds. The combination of stronger winds blowing more from the west brings cooler SST to regions near North America, and these temperatures often persist for many months.

Anomalies of sea surface temperature (SSTA) in the eastern Pacific Ocean can be seen in Fig. 4 from September 2011 to February 2013.

All four panels of Fig. 4 show relatively cool ocean surface waters off the west coast of North America, and also on the Pacific Equator. These conditions have prevailed for most of the past six winters. Only in February and March of 2010, an El Niño winter, were ocean temperatures significantly warmer than normal off the west coast (Freeland and Robert).

Many of the winters with cool ocean temperature along our west coast are associated with La Niña episodes, or La Niña – type events on the Pacific equator. La Niña occurs when ocean temperature in mid-Pacific along the equator is more than 0.5 °C below normal for six to seven months; El Niño when temperature is more than 0.5 °C above normal. ENSO is the collective name for these two. Over the past fifteen years there have been six La Niña episodes and only four El Niño episodes, and the average La Niña episode has persisted longer. In the two decades prior to 1999 it was El Niño that dominated.

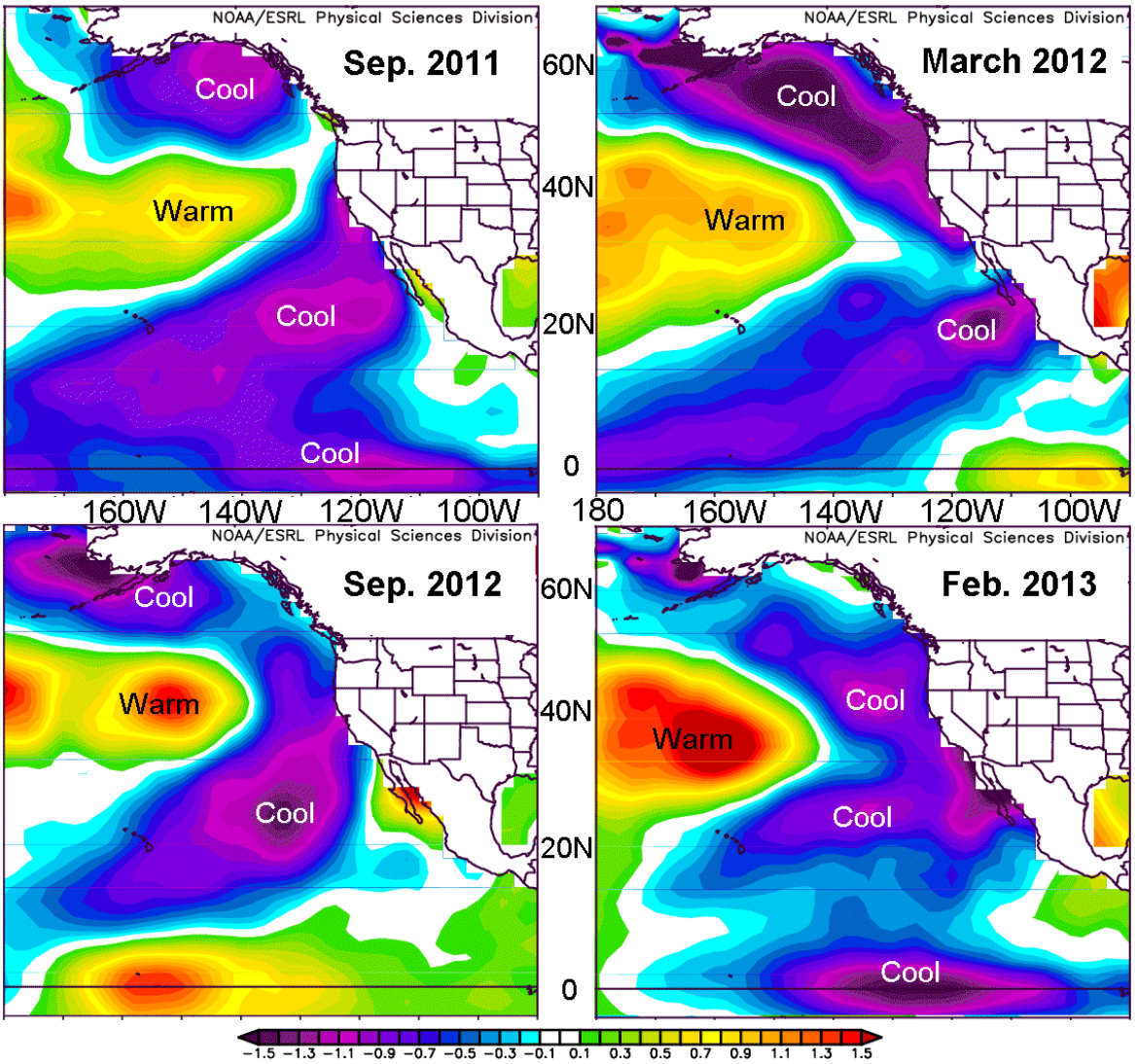

Figure 4. ***Sea surface temperature anomaly*** *in the eastern Pacific Ocean for Sept 2011 to Feb 2013. The maps extend from North America west to 180°, and from 5° South to 65° North. The equator is marked by the horizontal black line near bottom of each panel. The temperature anomaly scale in °C is at bottom. Positive and negative temperature anomalies are labelled warm and cool, respectively in each panel. Reference years for temperature anomaly are 1981 to 2010. Images provided by NOAA:* http://www.esrl.noaa.gov/psd/cgi-bin/data/composites/printpage.pl

The study of the atmosphere-ocean links extending across the Pacific can help interpret warm and cool conditions, such as the recent cool ocean temperatures west of coastal North America (Hourston and Thomson 1). Spatial patterns and time series of many of these patterns are presented next.

Linking Pacific-wide climate variations to local temperature: Patterns of the Pacific Decadal Oscillation and North Pacific Gyre Oscillation

How will ENSO affect our weather this year? What causes a cool winter or a warm summer in the Northeast Pacific? To try to answer these questions, scientists look at ocean temperature and/or air pressure in local and distant regions of the Pacific Ocean. From these, climate indices are developed whose changes in time are known to have far-reaching effects. The Southern

Oscillation Index and ENSO are the best known, but the PDO index and the NPGO index also reflect persistent SST patterns associated with weather systems (See Fig. 5).

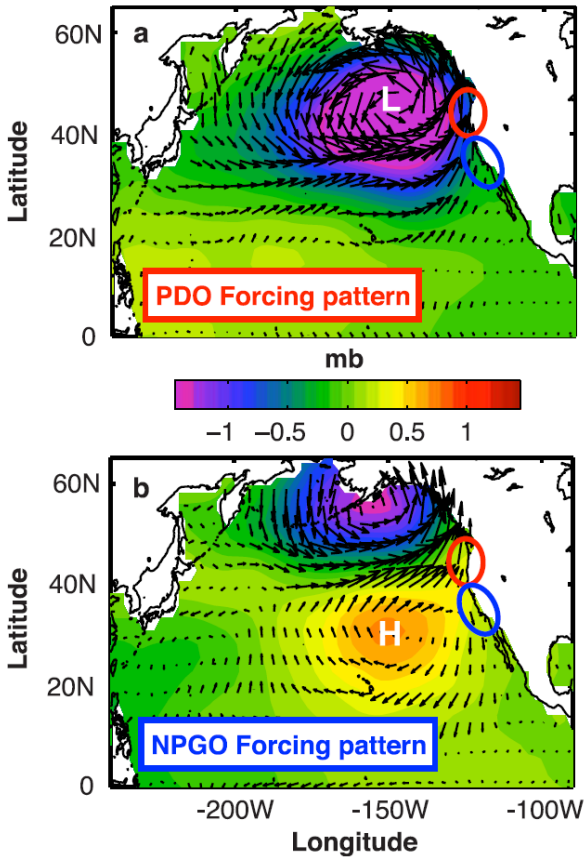

*Figure 5. Wind and air pressure patterns associated with (a) Pacific Decadal Oscillation, and (b) North Pacific Gyre Oscillation. **L** and **H** denote local low and high air pressure. Colours denote sea surface air pressure anomalies in millibars. Vectors denote prevailing winds. (Source: Fig. 3 in Di Lorenzo et al. 2008).*

The air pressure and wind patterns shown in Fig. 5 are associated with the positive phase of each index, as experienced in most years from 1977 to 1988 by the PDO and in most years from 1998 to 2012 by the NPGO (See Fig. 6). During the negative phase the wind vectors tend to reverse, and high and low air pressure regions change positions.

Generally, a positive PDO occurs during El Niño, and positive NPGO during La Niña. However, there are exceptions, and in general each phase of the PDO and NPGO persists for more years than does an El Niño or La Niña episode. During a positive phase of the PDO, severe winter storms tend to move to the northeast through the Gulf of Alaska and stall there. The cumulative effect of many storms over a winter is to create a low pressure system in mid-gulf of Alaska, with stronger winds from the south along the west coast, pushing warmer waters and air to the north. During a positive phase of the NPGO, the storms tend to arrive from farther north and reach the North American west coast, The cumulative effect of these storms is to bring stronger westerly winds and cooler air toward coastal waters.

Both a negative PDO and positive NPGO are associated with cool surface oceans of the eastern Gulf of Alaska, the conditions that have prevailed here starting in 2007. Time series of PDO and NPGO in Fig. 6 do indeed reveal these respective phases in recent years.

Time series of Pacific Ocean Variability

The weather pattern of the positive PDO in Fig. 5a dominated in most winters from 1977 to 1997; its negative phase has prevailed since 2007. The weather pattern of the negative NPGO in Fig. 5b dominated the winters of 1991 to 1997; its positive phase has dominated most winters since 1998. (Note that negative NPGO is red in Fig 6; positive is blue)

Fig. 6 presents five of these Pacific – wide indices, together with one graph of ocean temperature anomaly at Amphitrite Point, a light station on southwest coast of Vancouver Island.

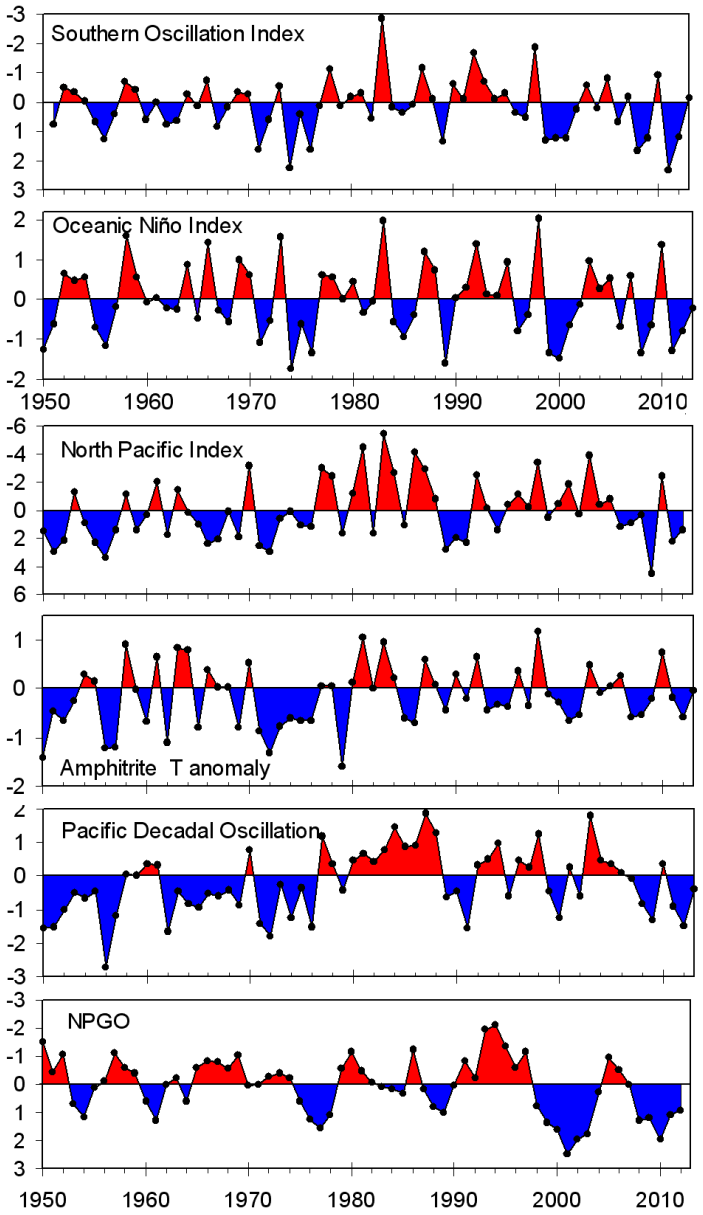

Figure 6. Five indices of Pacific Ocean climate, plus temperature anomaly (°C) at Amphitrite Point. Each point is an average over the months of November to March, and plotted for the calendar year of March. For example, an average of November 2011 to March 2012 is plotted as a data point for 2012. Three of the time series are inverted so their variability is in phase with other series. Indices for 2013 are for Nov. 2012 to Feb. 2013. Two indices are not yet available for 2013.

In general, blue for each index aligns with cool ocean temperature at Amphitrite Point and red with warm ocean temperature.

It is remarkable how all of the series of Fig. 6 are blue over the past three winters, and are mainly blue over the past seven winters. Only for the winter of 2010 stands out as red in most graphs.

The time series at top of Fig. 6 is the Southern Oscillation Index (SOI), which reflects the strength of the trade winds in the tropical Pacific Ocean, which in turn set up ENSO episodes. For example, a positive SOI in 2012 (blue in top panel of Fig. 6) coincided with stronger trade winds, which brought cooler waters to the mid-Pacific Equator and La Niña (positive Oceanic Niño Index in Fig 6). Stronger trade winds coincided with stronger westerly winds in the North Pacific Ocean, which created cooler waters in the eastern Gulf of Alaska and along the west coast of Canada and USA (negative anomaly at Amphitrite Point on the SW coast of Vancouver Island, Fig. 6). All these graphs are coloured blue in 2012.

The time series in Fig. 6 are explained in the next paragraphs. In general, blue regions prevailed prior to 1977, and red regions after then for about two decades until 1998. The Pacific Decadal Oscillation (PDO) shows this pattern best. Many time series shift from red to blue in the late 1990s and again the late 2000s. An exception is the North Pacific Index (NPI) which remained negative (red) through most years from late 1970s through to the mid 2000s. In general, cooling aligns with La Niña (negative ONI), negative PDO, NPGO and NPI, and positive SOI. Details of these time series are presented next.

Amphitrite temperature anomaly time series is based ocean surface temperature measured daily at the Amphitrite Lighthouse since 1934 on the southwest coast of Vancouver Island (Chandler and Gower). Reference years are 1981 to 2010. Monthly values are provided by Fisheries and Oceans Canada: http://www.pac.dfo-mpo.gc.ca/science/oceans/data-donnees/lighthouses-phares/data/amphitrt.txt

Oceanic Niño Index (ONI) is a measure of the anomaly of ocean surface temperature in the central tropical Pacific Ocean, and serves as the official index of the occurrence of El Niño and La Niña episodes as determined by the NOAA Climate Prediction Center. Although it is computed monthly, each value is based on a three-month period centred over the nominal month. The reference period for computing anomalies is 30 years and is updated every five years. A side effect of this particular reference-year system is to suppress climate change and some decadal variability in temperature. ONI is provided by the NOAA/ National Weather Service National Centers for Environmental Prediction Climate Prediction Center: http://www.cpc.ncep.noaa.gov/products/analysis_monitoring/ensostuff/ensoyears.shtml

Southern Oscillation Index (SOI) represents the anomaly of atmospheric sea surface pressure difference between the island of Tahiti and Darwin, Australia, which usually sets up the El Niño and La Niña ocean responses. A strong positive anomaly difference is associated with stronger trade winds and positive SOI (blue in Fig. 6), and generally sets up La Niña. Negative anomaly difference is associated with weaker trade winds, or even a reversal of wind direction in the tropical Pacific, and negative SOI (red in Fig. 6), and generally sets up El Niño. SOI is available at: http://www.cpc.ncep.noaa.gov/data/indices/soi.

North Pacific Index (NPI) is the area-weighted sea level pressure over the North Pacific from 30°N to 65°N and 160°E to140°W. It serves as an index of the impact of ENSO over the North Pacific Ocean. This index is a useful indicator of the intensity and areal extent of the Aleutian Low Pressure system. The NPI was generally negative from 1950 to 1976, and generally positive from 1977 to 2005. This change is attributed to strengthening of the Aleutian Low Pressure system in winter. Since 2005 is has been negative, due to weaker Aleutian Lows. Monthly time series of this index are provided by the Climate Analysis Section, NCAR, Boulder,

USA http://climatedataguide.ucar.edu/guidance/north-pacific-index-npi-trenberth-and-hurrell-monthly-and-winter based on Trenberth and Hurrell (1994) and Wallace and Gutzler (1981). Both monthly and winter-only values are available.

Pacific Decadal Oscillation (PDO) is based on analysis of Mantua et al. (1997) and Zhang et al. (1997). It is the first mode of ocean surface temperature variability in the North Pacific Ocean, and is often positive in El Niño years. However, its variability is slower than that of Oceanic Niño Index, and it is usually a good indicator of temperature patterns that persist for a decade or more. Prior to calculating the first mode of SST variability, the global average temperature for each month is subtracted from the SST at each data location in the North Pacific Ocean. As a result, the PDO time series does not include global warming (or cooling), and instead represents variability and change local to the North Pacific Ocean. The time series is provided at this Internet site of the Joint Institute for Studies of Atmosphere and Ocean of NOAA in Seattle: http://jisao.washington.edu/pdo/PDO.latest

North Pacific Gyre Oscillation (NPGO) is a climate pattern that emerges as the second dominant mode of sea surface height variability in the Northeast Pacific Ocean (Di Lorenzo et al.; 2008). The NPGO mode closely tracks the second mode of North Pacific SST, also referred to as the Victoria Mode. When positive (Fig. 5b and the blue intervals in Fig. 6), the westerly winds over the eastern North Pacific are often stronger than normal and the west coast and eastern Gulf of Alaska are cool. These conditions have dominated in most winters since 1999. The time series is available at this Internet site: http://www.o3d.org/npgo/

References

Di Lorenzo E., Schneider N., Cobb K.M., Chhak, K, Franks P.J.S., Miller A.J., McWilliams J.C., Bograd S.J., Arango H., Curchister E., Powell T.M. and Rivere, P. 2008. North Pacific Gyre Oscillation links ocean climate and ecosystem change. Geophys. Res. Lett. 35, L08607, doi:10.1029/2007GL032838.

Trenberth, K. and Hurrell, J. 1994. Decadal atmosphere-ocean variations in the Pacific. Climate Dynamics 9, DOI; 10.1007/BF00204745, 303-319.

Mantua, N.J., Hare, S.R., Zhang, Y., Wallace, J.M., and Francis, R.C. 1997. A Pacific interdecadal climate oscillation with impacts on salmon production. Bulletin of the American Meteorological Society 78, pp. 1069-1079.

Wallace, J. M., and Gutzler, D.S. 1981. Teleconnections in the geopotential height field during the Northern Hemisphere winter. Mon.Weather Rev. 109, 784-812

Zhang, Y., Wallace, J.M., and Battisti, D.S. 1997. ENSO-like interdecadal variability: 1900-93. J. Climate, 10, 1004-1020.

2.1.2. Ocean conditions in the Gulf of Alaska as seen by Argo and Line P

Howard Freeland and Marie Robert, Fisheries and Oceans Canada

The year 2012 was a big year for the Argo array. The global array acquired its millionth profile in November. Further, we are indebted to the Canadian Coast Guard for their agreement to divert a ship so that a large number of floats could be deployed in two areas that have always been under-sampled. The number of floats supplying profiles at 10-day intervals in the Gulf of Alaska is sufficient to provide continuous information at Ocean Station Papa at 50°N, 145°W. A contour plot of water density anomaly (specifically σ_t) versus time and depth is shown in Fig. 1 (note that depth is measured in decibars, which is a unit of pressure. Water pressure in the ocean increases by about a decibar for every metre of depth).

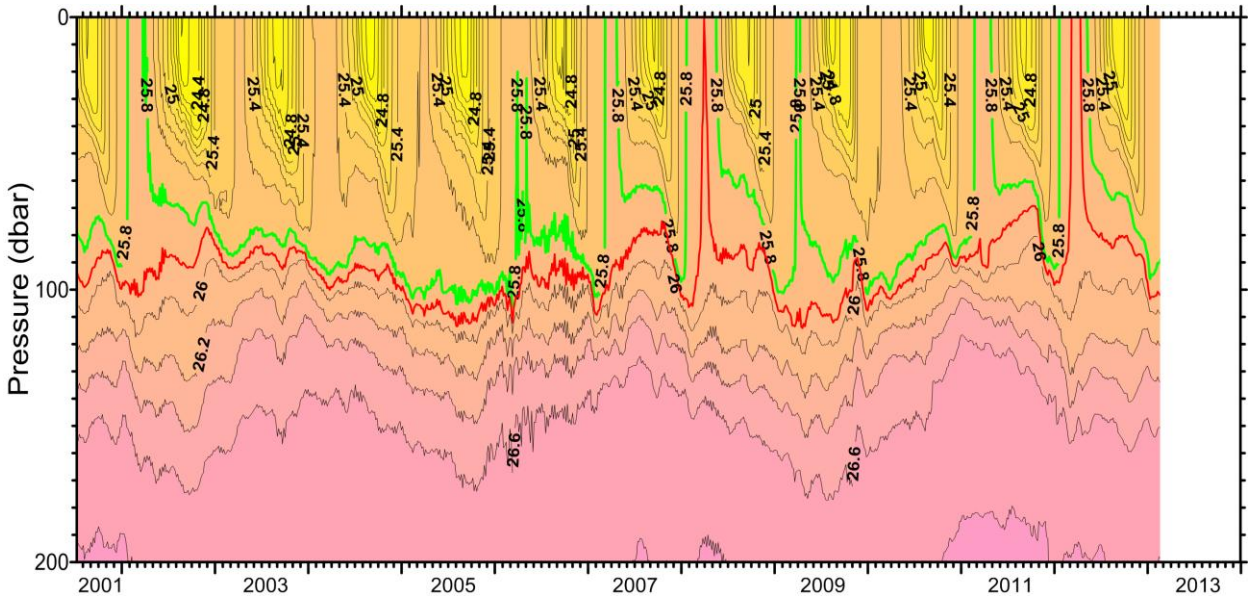

Figure 1. A plot versus time on the x-axis and water pressure on the y axis of density anomaly (σ_t) at Ocean Station Papa at 50°N, 145°W. The green contour marks a σ_t of 25.8 and the red line a σ_t of 25.9. (water densities of 1025.8 and 1025.9 kg/m^3, respectively). A decibar of water pressure is about one metre in depth.

Fig. 1 shows that in early 2013 mid-winter mixing had not yet reached the 25.8 σ_t contour and so was suggestive that the winter 2012/13 would end up accomplishing less mixing than has been seen in most recent years; this winter perhaps is looking more like the winters of 2002/3 through to 2005/6 and very different from the winter of 2011/12. Maps of mixed-layer depths support this view. At the end of January 2013 mixed layers at Ocean Station Papa reached only to about 90 metres depth, which is shallower than normal for this month.

Fig. 2 shows the contour plot of σ_t along along Line P in February 2013 (preliminary data) based on ship-board measurements. (Line P extends from the western end of Juan de Fuca Strait to Ocean Station Papa). This contour plot corroborates the shallow mixed layer at Station P shown by the Argo data.

Over the history of measurements at Ocean Station Papa we have seen reports of progressive freshening of the upper ocean along with the expected warming. Both of these changes tend to make the upper ocean less dense. It is possible to monitor this using the Argo array interpolating onto the stations occupied as part of the Line-P time series, and this procedure

shows the value of the two methods of sampling. The shipboard surveys happen relatively infrequently; nowadays we do surveys along Line-P only three times per year, but those surveys supply views of the ocean of very high precision and resolution, besides also allowing sampling of bio-geochemical variables, something that is very hard to do with Argo floats. The Argo simulated surveys can, however, be done at any time of the year. This allows us to combine the two sets of measurements and observe the progressive changes taking place at Ocean Station Papa and along Line-P.

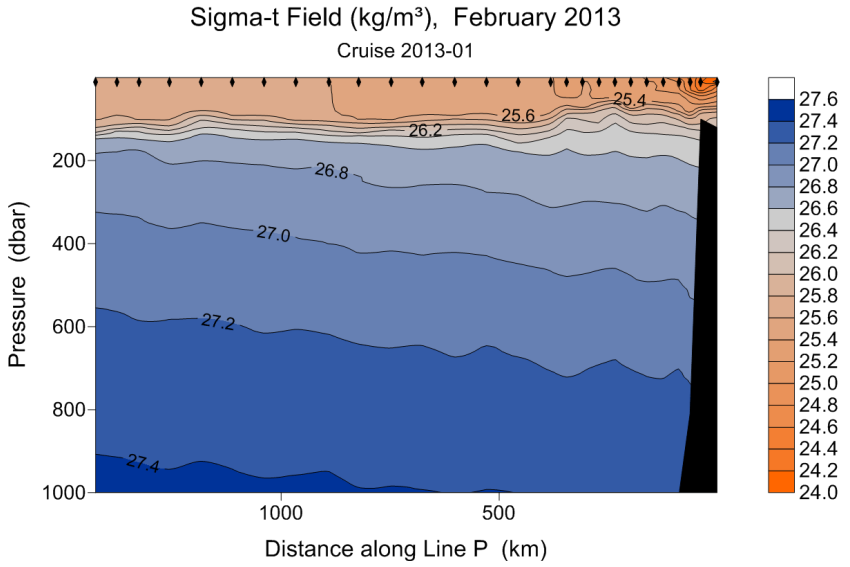

Figure 2. σ_t field along Line P in February 2013 (preliminary data). The mixed later is shallower than 100 metres. A decibar of water pressure is about one metre in depth.

Fig. 3 shows the rate at which temperature, salinity and density (computed from temperature and salinity) are varying with depth at Ocean Station Papa based on ship-board and Argo observations from 1950 to 2011. We see evidence of warming that is close to the 95% significance level (the shaded regions are 95% confidence bands) and extending down to 200 metres depth. The salinity changes are much more significant and the density trend in the upper 200 metres is dominated more by salinity than temperature changes.

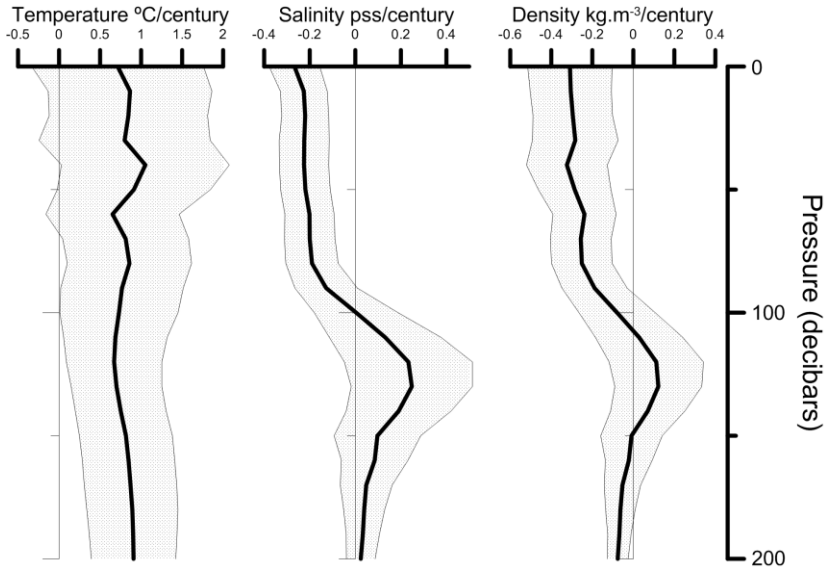

Figure 3. Trends in temperature, salinity and density plotted versus depth at Ocean Station Papa. A decibar of water pressure is about one metre in depth.

Fig. 4 shows the density trends as they are distributed along Line-P and showing that the results for Station Papa shown in Figure 3 are typical of the entire line until we get close to the continental shelf. This surface reduction in density coupled with the increased density in deeper water implies that the potential energy of the water column is being decreased. This inevitably must mean that to make a mixed layer of any given depth requires more work by mid-winter storms than was previously needed. Or as a corollary, if winter storminess remains the same, then mixed layers must be getting progressively shallower. The warming and freshening along Line P since 1950 agrees with trends reported for the lighthouse observations at the BC coast (Chandler and Gower).

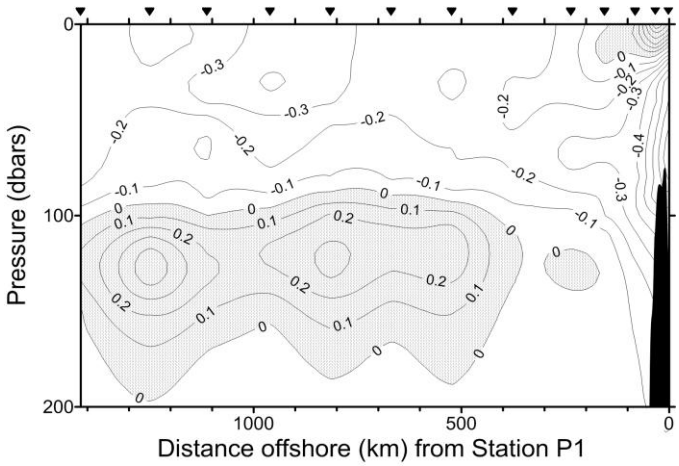

Figure 4. Trends in density plotted versus depth and distance along Line-P. The continental shelf is at right; Ocean Station Papa at left. Black symbols at top show stations along Line P that have been sampled regularly since the 1950s. A decibar of water pressure is about one metre in depth.

Although in general the Gulf of Alaska is warming, the year 2012 was colder than the previous year (Chandler and Gower) as can be seen on the next figure. Fig. 5 shows the difference between the temperature field along Line P in August 2012 and August 2011.

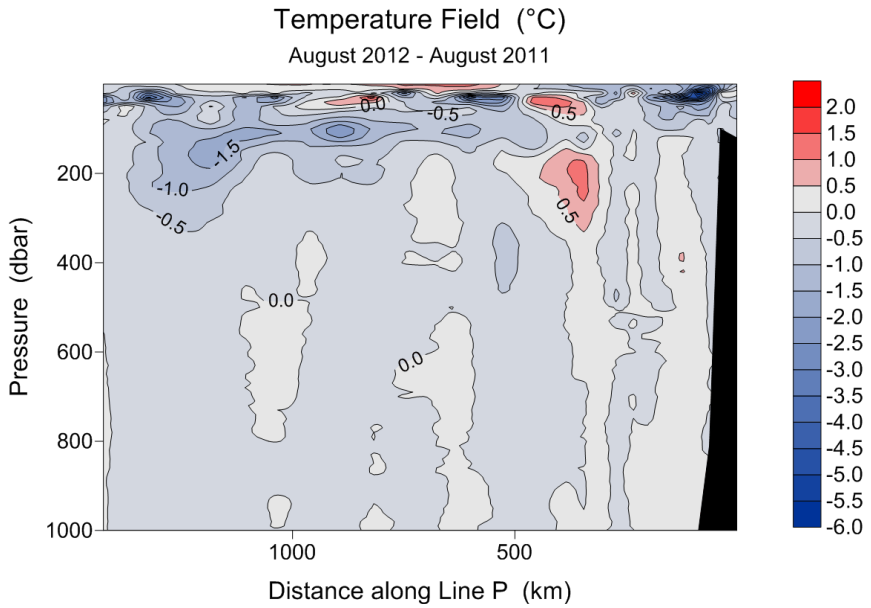

Figure 5. Temperature difference along Line P between August 2012 and August 2011. A decibar of water pressure is about one metre in depth.

Changes are also occurring on a shorter time scale as illustrated in Fig. 6, which shows plots of the deviations from normal salinity for four months selected between the start of 2012 and the time of writing this report (in Feb. 2013). As 2012 began there was an intense positive salinity anomaly centred near a depth of 120 metres. This anomaly had been present through most of the year in 2011 and persisted well into 2012, but had disappeared by August 2012. It is interesting that a detailed Line-P survey was carried out during the period August to September 2012, and the next survey did not occur until February 2013. In the meantime, however, the Argo array could supply low-resolution surveys along Line-P every month and these showed the development of a very intense negative salinity anomaly that shows most clearly in the panel at bottom left in Fig. 6, November 2012. This negative anomaly was intense but persisted only from about October 2012 through to January 2013. In February, when the next Line-P cruise took place it had almost completely disappeared. This, we believe, shows the power of seaboard measurements being supplemented by simulated surveys computed from the Argo observations.

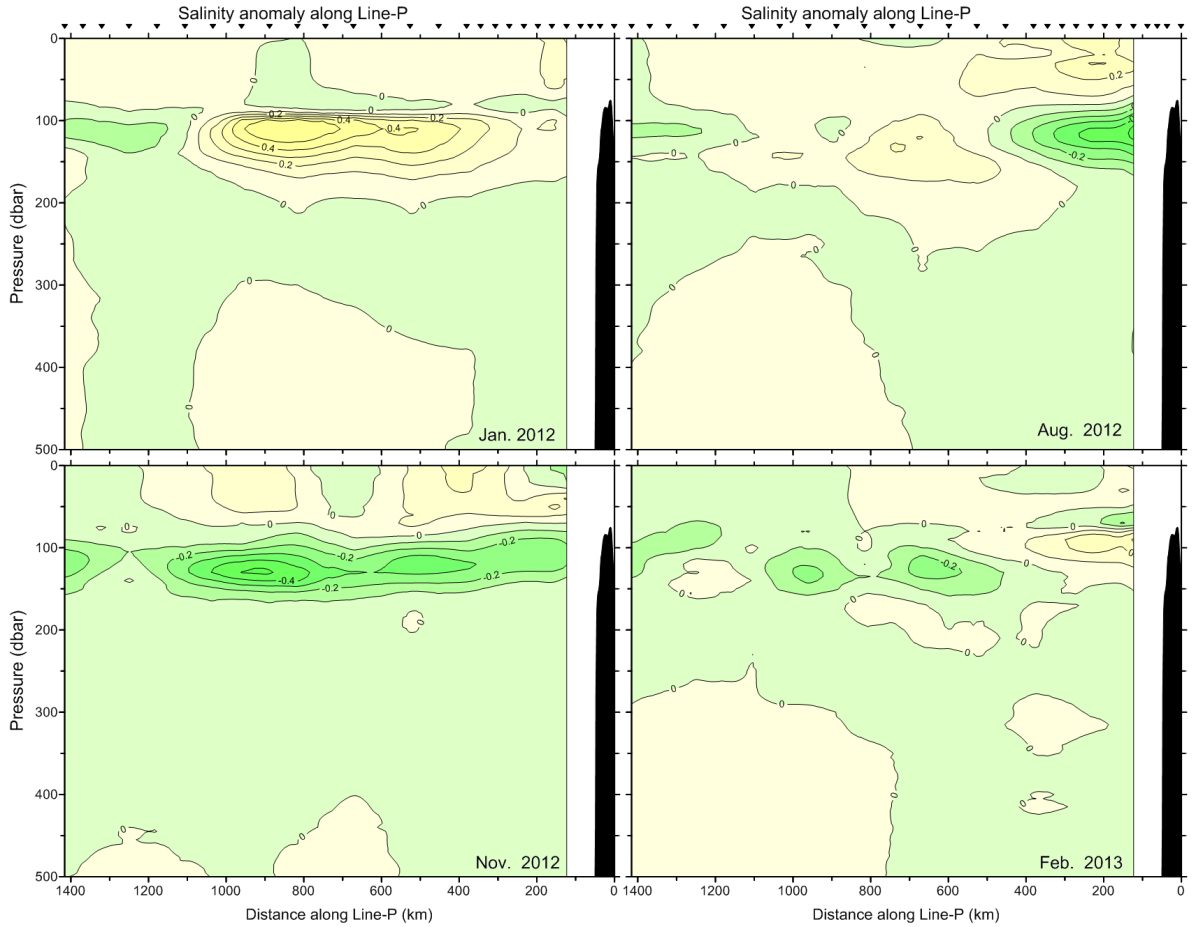

Figure 6. Deviation from normal salinity measured along Line-P for January 2012, August 2012, November 2012 and February 2013, interpolated from the Argo array. Black symbols at top show locations of sampling stations. A decibar of water pressure is about one metre in depth.

Fig. 7 shows some of the recent variations in the circulation patterns of the NE Pacific, compared with a circulation field (top left) that is an average over the last decade. We can see the dominant current systems. The North Pacific Current flows into NE Pacific from the Kuroshio extension far to the west; this is shown by the arrow labelled N. As it approaches the coast this current splits into a northbound branch that heads into the Gulf of Alaska (labelled G) and a southbound branch heading southwards into the California Current system (labelled C). The circulation patterns are computed monthly by projecting data from Argo floats (shown by the red dots in the monthly maps) onto a computer model of the NE Pacific. In January 2012 the general circulation of the NE Pacific was very close to the average over the last decade. As the year progressed the North Pacific Current, and the resulting bifurcation latitude, moved southwards. By the end of the year these were as far south as at any time since 2002. We are used to the presence of an intense circulation in the Gulf of Alaska centred near 54°N and 150°W, but towards the end of the year we saw a large strengthening of a cyclonic circulation near 50°N and 167°W. This was a surprise and something we have not seen before.

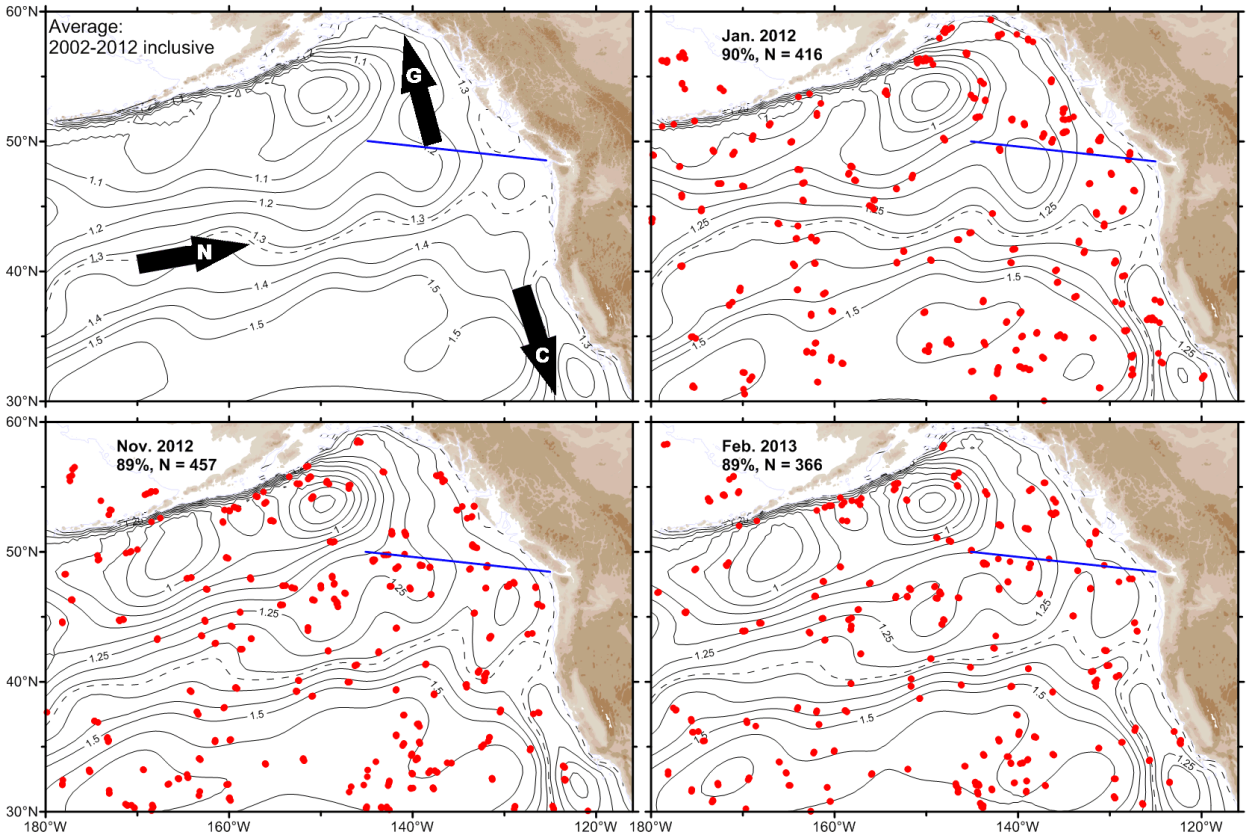

Figure 7: The circulation field of the northeast Pacific averaged over all months 2002-2012 (top-left) and the actual circulation patterns for Jan. 2012, Nov. 2012 and Feb. 2013. Stream lines are shown with black lines. The dashed line in each panel is a dividing streamline separating water that eventually flows south from that which eventually flows north. Closely spaced streamlines indicate stronger currents. The arrows labelled N, C and G identify the North Pacific, California and Alaska Currents, respectively. The blue line indicates the location of Line-P.

Fig. 8 illustrates the basic strength, observed monthly, of some of the major current systems. We see that the North Pacific Current (black line) passed through a deep minimum in the first few months of 2011 and indeed was quite weak as millions of tonnes of Japanese debris was washed into the ocean by a tsunami. Since that time there have been some large fluctuations but the background trend has been towards steadily stronger flow. In November 2012 and January 2013 we observed the strongest ever flow in the North Pacific Current since we have been able to monitor it. The fraction of water that eventually heads northwards is near average (the red line) and so it should be no surprise that both the flow into the Gulf of Alaska (blue line) and the southward flow into the California Current are very high. Interestingly, it is the flow into the Gulf of Alaska that is showing the greatest difference from previous observations.

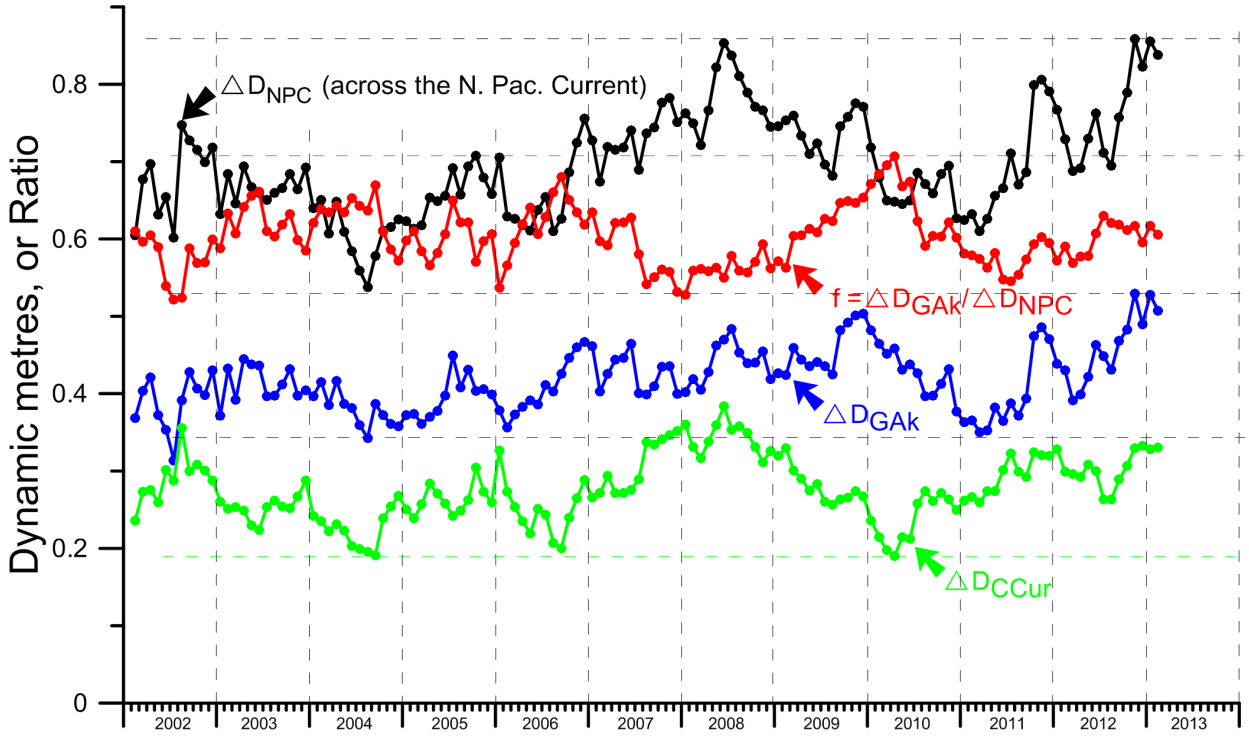

Figure 8. The difference in dynamic height between two points is a good surrogate for the strength of the current between those two points and flowing perpendicular to that line. The black, blue and green lines indicate the relative strength of flow in the three major currents in the Northeast Pacific Ocean. The red line is the ratio of the blue line divided by the black line and so represents the fraction of North Pacific Current water that flows northward into the Gulf of Alaska. The remaining water is carried to the south in the California Current.

Current information about the state of the N.E. Pacific as seen by Argo is available here:
http://www.pac.dfo-mpo.gc.ca/science/oceans/Argo/Alaska-Argo-eng.htm

Information about the Line P program is available here:
http://www.pac.dfo-mpo.gc.ca/science/oceans/data-donnees/line-p/index-eng.htm

2.1.3. Sea surface temperature and salinity trends observed at lighthouses and weather buoys in British Columbia, 2012

Peter Chandler and Jim Gower, Fisheries and Oceans Canada

Temperature and salinity are measured daily at the first daylight high tide at 13 shore stations (Fig. 1) as part of the DFO Shore Station Oceanographic Program. The first measurements began in 1914 and 13 stations continue to operate today, providing a database suitable to examine the long-term trends of conditions in coastal waters. Most stations are at lighthouses, with observations taken by lighthouse keepers. Several valuable time series ceased in previous years when lighthouses were destaffed.

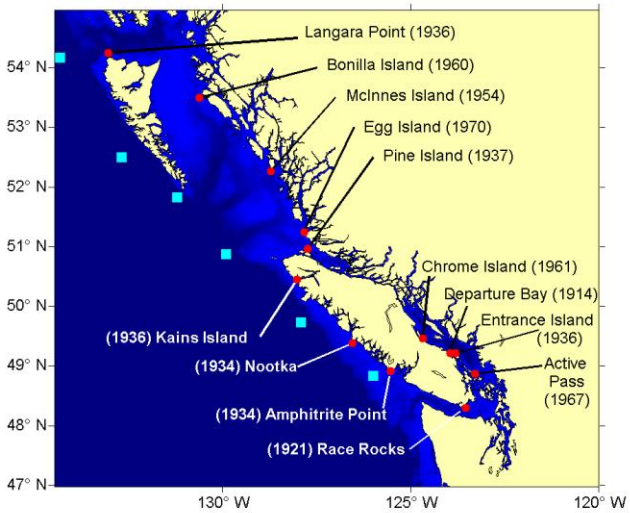

Figure 1. Red dots show the locations of 13 stations in the present shore station network with the first year of the data record in brackets. Blue squares show the locations of six of 17 weather buoys in the Canadian weather buoy network.

The observations at shore stations show the average daily sea surface temperature (Fig. 2) was cooler in 2012 than in 2011. On average the North and Central Coast (NCC) stations were 0.40 °C cooler; the West Coast Vancouver Island (WCVI) stations 0.26 °C cooler; and the Strait of Georgia (SG) stations 0.32 °C cooler than in the previous year. The average daily sea surface temperature at all stations in 2012 (except Nootka) was below the thirty-year average (1981 – 2010).

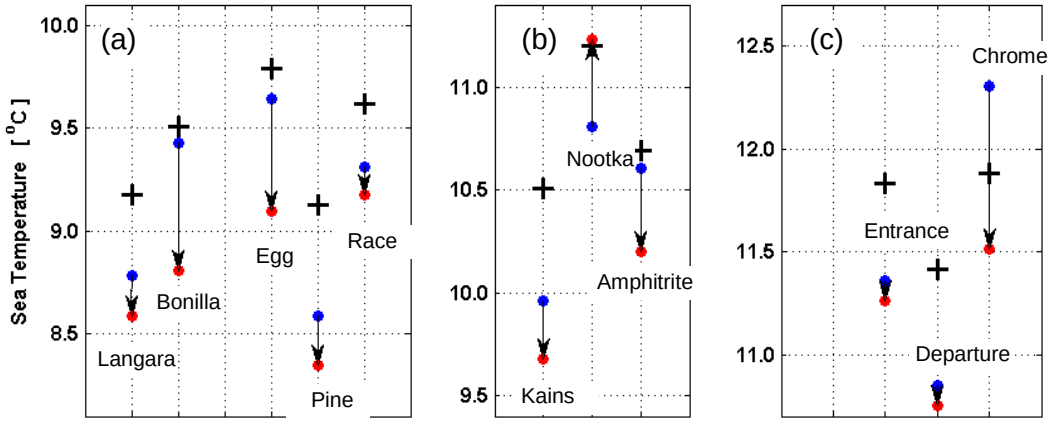

Figure 2. The average daily sea surface temperature in 2011 (blue dots) and 2012 (red dots) for shore stations in three regions (North and Central Coast (a), West Coast of Vancouver Island (b), and the Strait of Georgia (c); Race Rocks included here in the WCVI region for convenience). The crosses represent the mean annual temperature based on 30 years of data (1981-2010).

The average daily salinity observations (not shown) indicate WCVI conditions (Kains and Amphitrite) freshening, but little change for the NCC and SG, except Entrance Island in SG where the annual mean salinity increased by just under 1 psu.

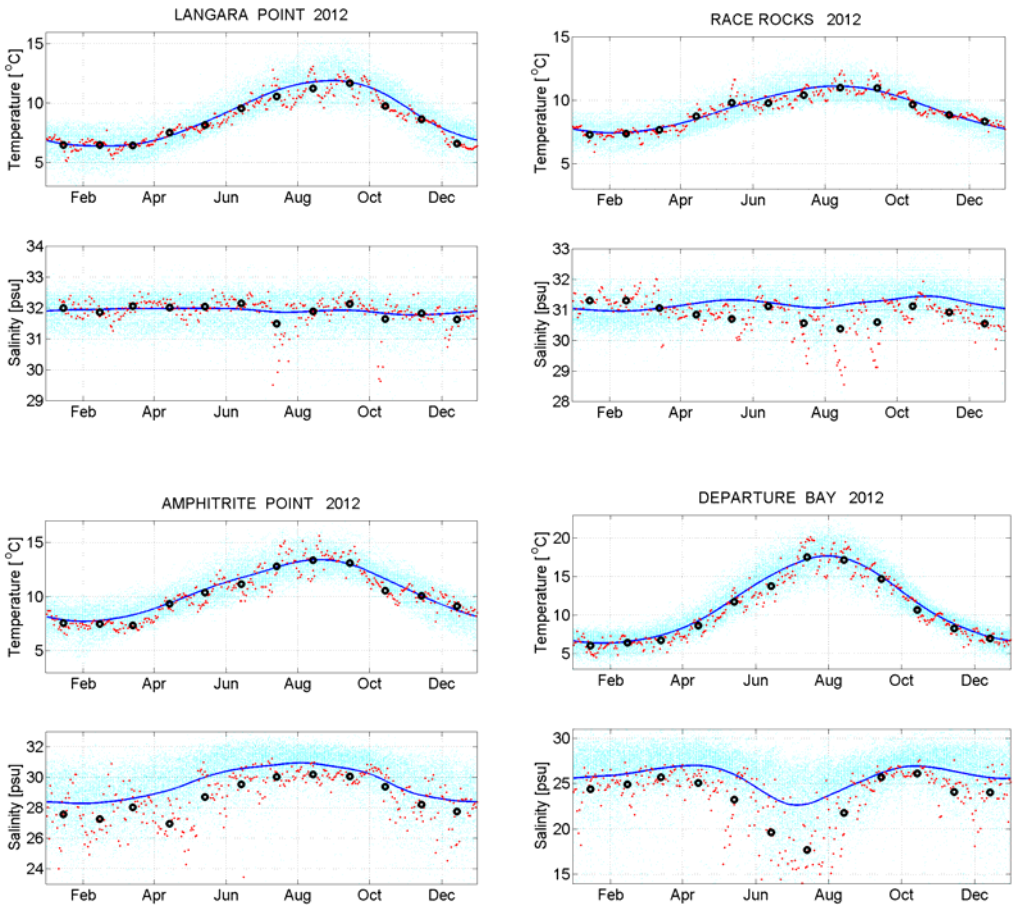

Figure 3. Daily temperatures and salinities observed in 2012 are shown in red. All observations from each station (record length given in Fig. 1) are shown in light blue with the dark blue line representing these data averaged using a 30-day running mean. The black circles represent the 2012 average monthly values.

The seasonal temperature cycles (Fig. 3, top) for four stations representative of the three regions show the expected summer warming and winter cooling. The salinity signal (Fig. 3, bottom) reflects the influences of the winter precipitation (Amphitrite) and the Fraser River freshet (Departure Bay). In 2012, generally below-normal temperatures were observed during the early summer, and fresher than normal conditions at many stations during the summer season and throughout the year at Amphitrite Point. The Fraser River freshet in 2012 was late to develop, but reached a near record maximum flow in July, influencing the summer salinity signal at Departure Bay in the Strait of Georgia.

Assuming a linear change over the entire data record, the time series of temperature at all of the BC shore stations show a warming trend. Fig. 4 shows this warming at representative stations for each of three regions. The right panel of Fig. 4 shows that sea surface temperature (SST) trend using all data up to the year shown on the x-axis. The slope of the trend varies with time, illustrating the impact of the recent cool phase of the PDO (Crawford 1). Temperature anomalies in 2012 continue the cooling phase evident since 2005. A similar trend analysis applied to the salinity data (Fig. 5) shows a trend toward fresher water along the BC Coast. Local influences are more prominent in the salinity signal and thus the data are not as representative of the salinity characteristics of the broader region beyond the lighthouse location.

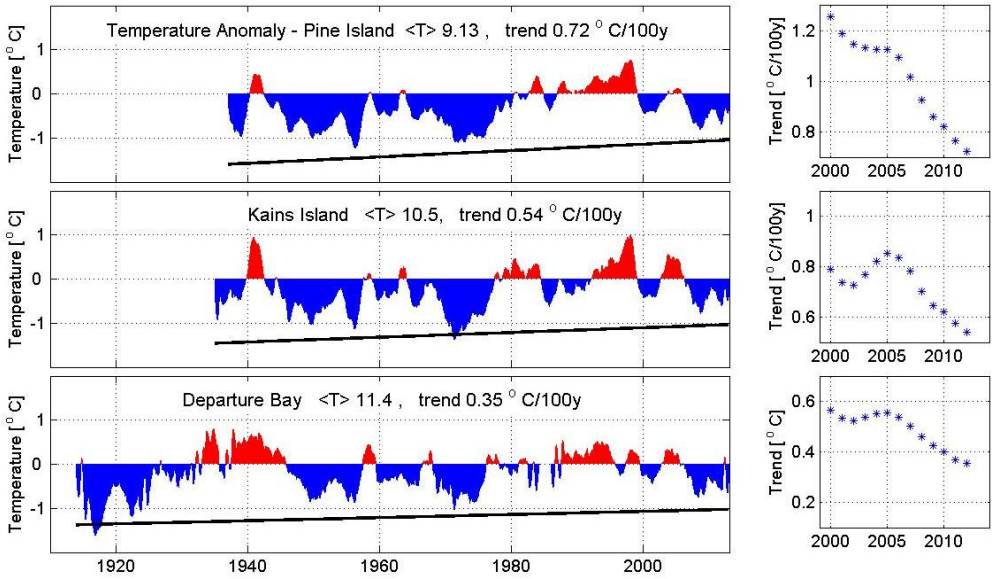

Figure 4. Time series of daily temperature observations, averaged over 12 months, at stations representing the North and Central Coast, West Coast Vancouver Island and Strait of Georgia. Positive anomalies from the average temperature <T> are shown in red, negative in blue. The panel to the right shows the slope of the trend lines calculated using only data up to the year shown on the x-axis.

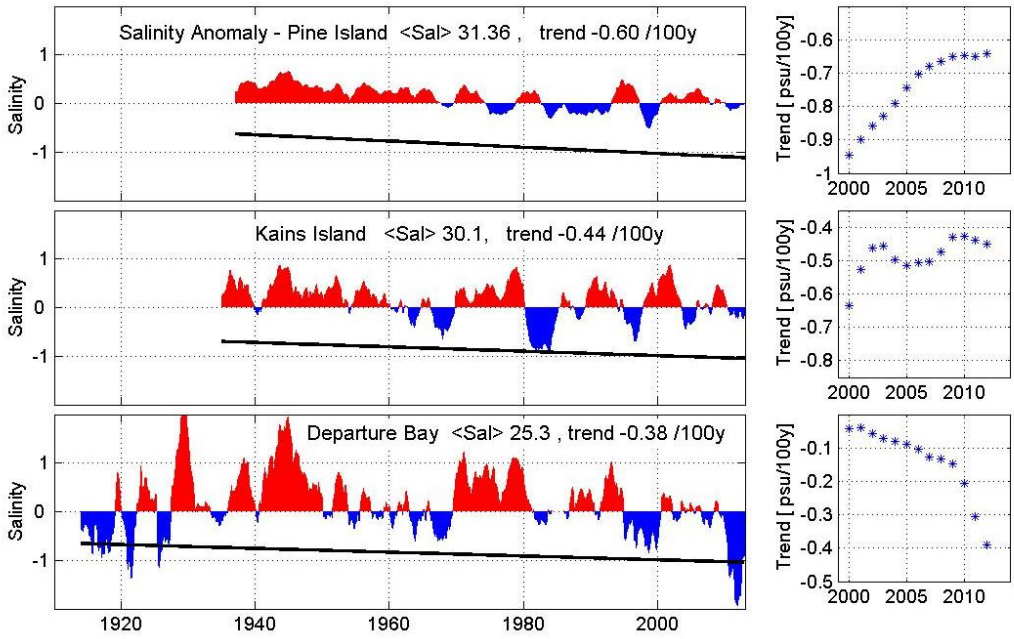

Figure 5. Time series of daily salinity observations, averaged over 12 months, at stations representing the North and Central Coast, West Coast Vancouver Island and Strait of Georgia. Positive anomalies from the average salinity <Sal> are shown in red, negative in blue. The panel to the right shows the slope of the trend lines calculated using only data up to the year shown on the x-axis.

The data from six of the 17 buoys in the Canadian weather buoy network (station locations shown in Fig. 1) show 2012 sea surface temperature continuing cooler than in the 1990's (Fig. 6). These buoys record hourly winds, waves, and air and sea temperatures, and sea

temperature is measured at about 1 m depth. The pattern of warm 1990's, cool 1999-2002, warm 2003 to 2005, cool 2006 to present, is common to all buoys and reflects the general pattern seen in the lighthouse SST data. The straight line fitted to the observations in Fig. 6 is a linear trend of -0.034 °C per year, revealing that ocean temperature near the BC coast has declined since the late 1980s, and especially after 1998. Fig. 4 also reveals a decline in temperature at shore stations over this period.

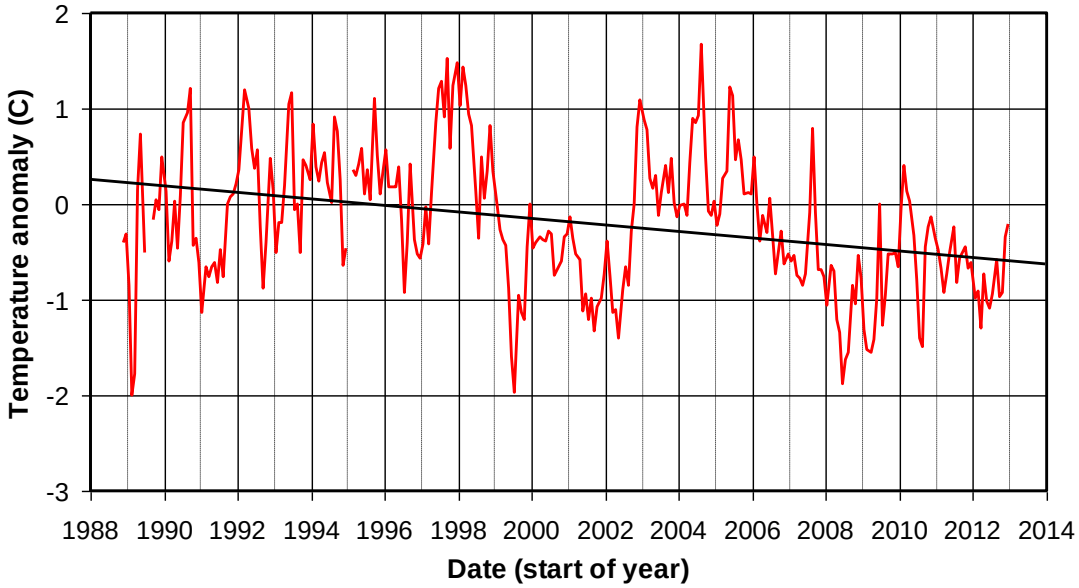

Figure 6. Time series since 1989 of the average temperature anomaly (removing first and second harmonics of a fixed annual cycle computed from data collected before 2009) for the six buoys in a north-south line off the BC west coast from Langara Island to Tofino (see Fig. 1).

2.1.4. Sea level in British Columbia, 1910 to 2012

Bill Crawford, Fisheries and Oceans Canada

The Canadian Hydrographic Service monitors sea level along the BC coast. The records below show annual sea level anomalies and the linear trend at three ports. Both Tofino and Victoria have records than began in 1910, while the record at Prince Rupert began in 1912.

Sea level anomaly in 2012 was above the century-long linear trend at each of the three ports shown in Fig. 1. At both Prince Rupert and Victoria the anomaly of 2012 was close to that of 2011, whereas the sea level anomaly at Tofino was about 8 cm higher in 2012. The years of highest sea levels (largest anomalies) at Tofino and Victoria generally coincide with El Niño events (2010, 1997, 1983) when winter winds typically blow more from the south.

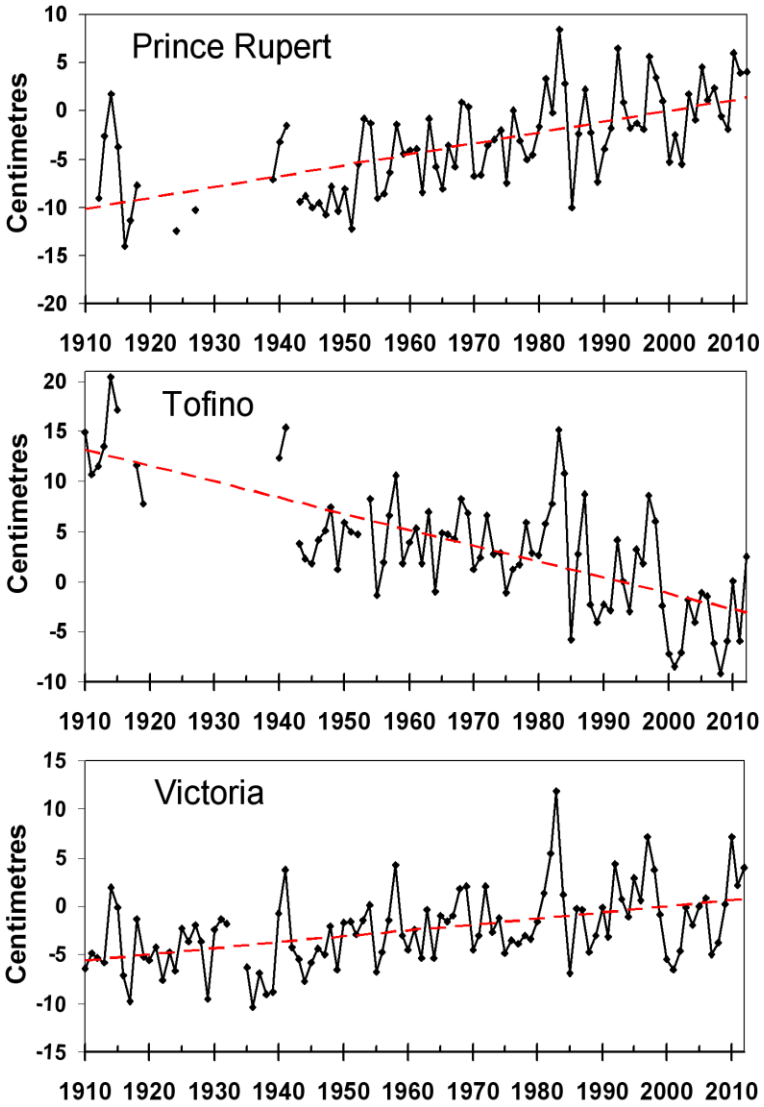

Figure 1. Sea level anomalies at three British Columbia ports. Average linear trends are plotted as dashed red lines. Reference years (i.e. mean of 0) are 1981 to 2010.

The linear trend at each port is listed below (in cm/century):

Prince Rupert +11
Victoria +6
Tofino -16

Tectonic motion is lifting the land at Tofino faster than sea level is rising, so that local sea level is dropping at an average rate of 16 cm per 100 years. The next Cascadia Subduction Zone earthquake could drop the land at Tofino by as much as a metre, and also send a major tsunami to the BC coast.

Global sea levels rose by 17± 5 cm in the 20th century. The Intergovernmental Panel on Climate Change (http://www.ipcc.ch) predicts sea level to rise by 20 to 60 cm over the 21st century, but recent observations of ice melt in Greenland and Antarctica suggest these projections might be too low. Therefore, we can expect to observe greater rates of sea level rise in British Columbia in the future than we saw in the 20th century.

2.1.5. Surface ocean variation in the PICES region

Skip McKinnell, North Pacific Marine Science Organization (PICES)

North Pacific basin scale

The temperature of the North Pacific Ocean surface varies from hour to hour because of the day/night rotation of the Earth, from day to day because of winds, tides, and currents, from month to month because of the seasonal cycle, and from year to year from the integration of forces, feedbacks in the ocean/climate system, and anthropogenic causes. The largest scale pattern of variation in the North Pacific Ocean is reflected in the Pacific Decadal Oscillation (PDO - Mantua et al. 1997). The PDO shows how the average temperatures of large parts of the surface of the North Pacific Ocean vary out of phase on decadal scales.

The PDO was originally described from 100 years of temperature records as a multi-decadal pattern of variation with warm/cold regimes lasting for 25-30 years. These stanzas are reflected in the PDO Index (Fig. 1). In the last 30 years, the period of the PDO has shortened to about 10 years (McKinnell et al. 2010); five years of cold followed by five years of warm. This pattern was used in early 2008 as the basis of a forecast that the coast of British Columbia would be cool (McKinnell 2008). Except for the brief effect of the Olympic Games El Niño of 2010, when the B.C. coast warmed for a few months, this forecast was correct. The cause of this variation is not known and cannot be attributed to any one factor, but if there is a real physical cause, the cold phase will have run its course by 2014 and a shift to warmer waters along the North American coast should be imminent. At the time of the Fisheries and Oceans Working Group (FOWG) meeting in mid-February of 2013, the PDO index reflected cooler temperatures along the North American west coast, but the decadal variation model would have it switch to warm by the 2014 meeting.

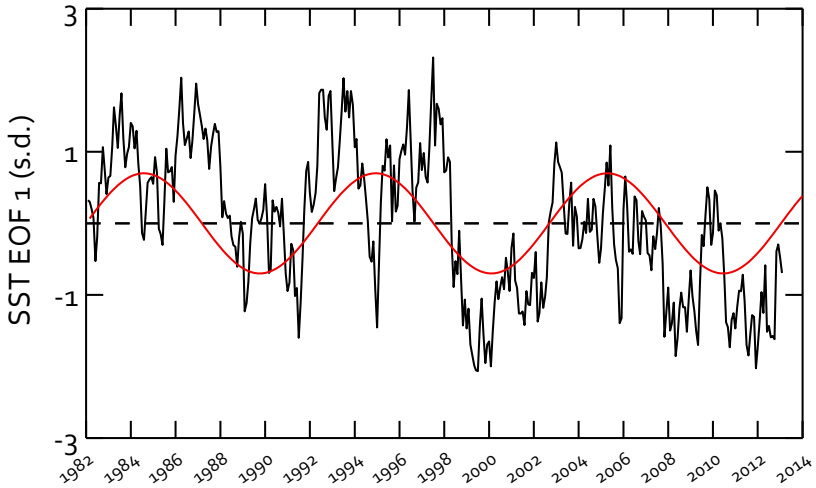

Figure 1. Temporal variability of the dominant mode of monthly sea surface temperature (SST) anomaly covariation (black) in the Pacific Decadal Oscillation region (north of 20°N) computed using only monthly SST data (Reynolds et al. 2002) on a 3° latitude by 4° longitude grid during the satellite era (approx. from 1982-present) but without adjusting the anomalies to remove a global temperature trend from the anomalies as is the practice when calculating the PDO (Mantua et al. 1997) .The red line represents the period (10.7 y) of the dominant spectral peak from a Fourier analysis of the de-trended data represented by the black line.

A second mode of surface ocean variation in the North Pacific is associated with the North Pacific Gyre Oscillation (NPGO – Di Lorenzo et al. 2008). It is calculated from sea surface

height anomalies (SSH) of the Northeast Pacific rather than from sea surface temperature (SST), although the two tend to be correlated through steric expansion and contraction. The region examined is 180°W–110°W; 25°N–62°N. Positive values of the NPGO in the past have indicated higher nitrate levels and salinity along Line P and off the coast of southern California (Di Lorenzo et al. 2009). The NPGO has been generally positive since 1998 (Fig. 2). (Crawford 1)

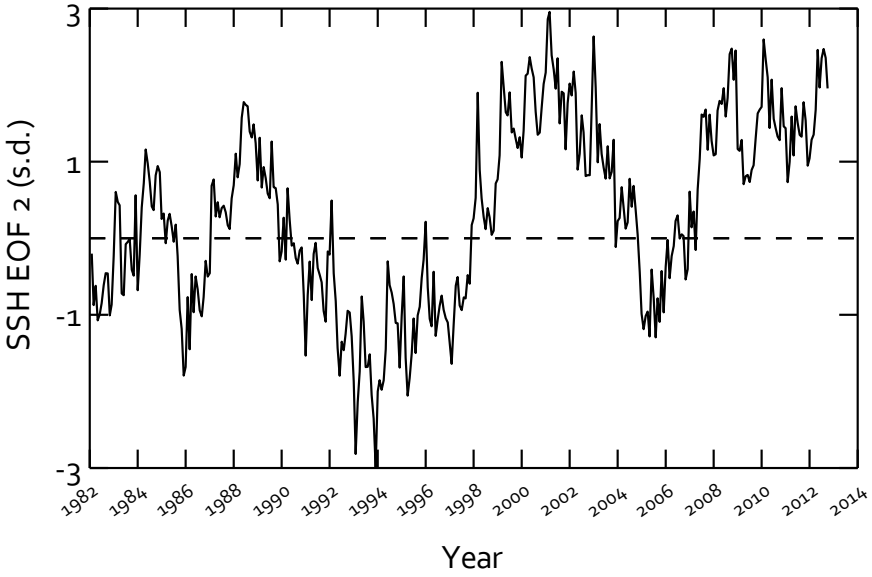

Figure 2 North Pacific Gyre Oscillation (1982-2013) of Di Lorenzo et al. (2008). The index can be downloaded from http://www.o3d.org/npgo/

Eastern North Pacific

To focus an analysis more closely on large-scale SST variation in a region of the North Pacific closer to the USA and Canadian west coast, a modal analysis of a more coastal region bordered by 30°N in the south and 145°W to the west was conducted (Fig. 3). The dominant mode of this region was correlated (r = 0.7) with the PDO mode from Fig. 1, and was also correlated (r=0.85) with Kains Island temperature in June. The subdominant mode from this analysis was correlated with the NPGO (0.56), and was negatively correlated (r=-0.69) with Kains Island temperature in January. Squaring these correlations provides an approximate indication of how much of the variability in the basin-scale oceanic patterns is reflected in the regional SST variation along the North American coast north of 30°N. Jointly, the PDO and the NPGO describe about 50% of the variation in coastal Mode 1 and about 14% of the variation in coastal Mode 2. These are relatively weak correlations, suggesting that there are significant local patterns of variation that are not captured in the basin-scale modes. This is not entirely surprising because the PDO captures only about 20% of the basin scale variation in SST (Mantua et al. 1997).

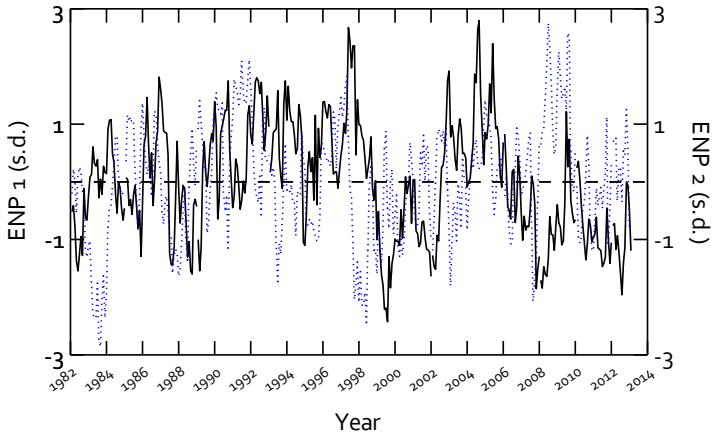

Figure 3. Dominant (black) and subdominant (blue) modes of SST in the eastern North Pacific poleward of 30°N (northern Baja California) and east of 145°W, computed from monthly SST data as in Fig. 1

Highlights

1. Basin-scale SSTs remained negative in 2012 with cooler than average temperatures along the North American coast. A recurring pattern of decadal variability since 1982 suggests that a shift to a warmer phase of SST along the USA and Canadian west coast may be not too far away if the pattern persists.
2. The NPGO has been persistently positive since 2007, which is often accompanied by higher salinity, higher nutrients and chlorophyll in some locations along the North American coast from California to British Columbia and along Line P.
3. In 2012, in the eastern North Pacific north of 30°N, SST variation associated with the PDO was relatively more energetic with relatively persistent negative values throughout the year.

References

Di Lorenzo, E., Schneider, N., Cobb, K.M., Chhak, K, Franks, P.J.S., Miller, A.J., McWilliams, J.C., Bograd, S.J., Arango H., Curchister, E., Powell, T.M. and Rivere, P. 2008. North Pacific Gyre Oscillation links ocean climate and ecosystem change. Geophysical Research Letters 35, L08607, doi:10.1029/2007GL032838.

Di Lorenzo, E., Fiechter, J., Schneider, N., Miller, A.J., Franks, P.J.S., Bograd, S.J., Moore, A.M., Thomas, A., Crawford, W., Pena, A. and Hermann, A. 2009. Nutrient and salinity decadal variations in the central and eastern North Pacific. Geophysical Research Letters doi:10.1029/2009GL038261.

Mantua, N.R., S.R. Hare, Z. Zhang, J.M. Wallace, and Francis, R.C. 1997. A Pacific decadal oscillation with impacts on salmon production. Bull. Amer. Meteor. Soc. 78, 1069-1079.

McKinnell, S. 2008. Ocean temperature to be cooler along the BC coast in 2008. pp. 46-47 In J.R. Irvine and W.E. Crawford [eds.] State of physical, biological, and selected fishery resources of Pacific Canadian marine ecosystems. DFO Can. Sci. Advis. Sec. Res. Doc. 2008/013. http://www.dfo-mpo.gc.ca/csas-sccs/publications/resdocs-docrech/2008/2008_013-eng.htm

McKinnell, S.M., Batten, S., Bograd, S.J., Boldt, J.L., Bond, N., Chiba, S., Dagg, M.J., Foreman, M.G.G., Hunt Jr., G.L., Irvine, J.R., Katugin, O.N., Lobanov, V., Mackas, D.L., Mundy, P., Radchenko, V., Ro, Y.J., Sugisaki, H., Whitney, F.A., Yatsu, A., and Yoo, S. 2010. Status and trends of the North Pacific Ocean, 2003-2008, pp. 1-55 In S.M. McKinnell and M. J.

Dagg. [Eds.] Marine Ecosystems of the North Pacific Ocean, 2003-2008. PICES Special Publication 4, 393 p.

Reynolds, R.W., N.A. Rayner, T.M. Smith, D.C. Stokes, and W. Wang. 2002. An improved in situ and satellite SST analysis for climate. J. Clim. 15, 1609-1624.

2.1.6. Wind-driven upwelling/downwelling along the northwest coast of North America, 1950 to 2012

Roy Hourston and Richard Thomson, Fisheries and Oceans Canada

Highlights of northeast Pacific Ocean coastal wind-driven upwelling in 2012 are as follows:

- Along coastal British Columbia, average- to stronger-than-average upwelling-favourable (northwesterly) and downwelling-favourable (southeasterly) winds have occurred since the late 1990s. This generally reflects stronger-than-average North Pacific Highs (summer) and Aleutian Lows (winter) and/or shifts in their geographical locations.
- In 2012 both upwelling- and downwelling-favourable winds were near average throughout most of the year and finished the year weaker than average due to a weaker-than-average and geographically shifted Aleutian Low. This change to weaker winds may also signal an end to the recent decade-long period of stronger-than average upwelling and downwelling. (Hourston and Thomson 2, and Crawford 1)

Due to their link to offshore surface Ekman transport and compensating onshore transport of nutrient-rich seawater at depth, the duration and intensity of upwelling-favourable (northwesterly) winds are good indicators of coastal productivity. To gauge low-frequency variability in coastal productivity, we have summed upwelling-favourable-only wind stresses by month along the west coast of North America from 45°-60°N latitude (Fig. 1). These wind stress are provided by a numerical analysis of the US National Centre for Environmental Prediction (NCEP).

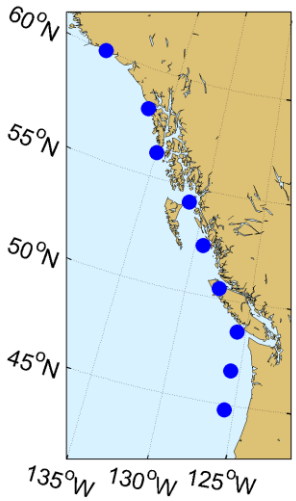

Figure 1. NCEP/National Center for Atmospheric Research (NCAR) Reanalysis-1 coastal surface wind stress grid locations.

Fig. 2 shows these monthly mean integrated upwelling anomalies smoothed using a five-year running mean over the period 1948-2012. The climate shift in the late 1970s appears as a sharp transition from stronger- than-average to weaker-than-average upwelling-favourable winds. Upwelling-favourable winds have been stronger than average throughout the 2000s. In previous State of the Ocean Reports, we speculated that a repeat of the mid 1970s regime shift to weaker-than-average upwelling appeared imminent, and Fig. 2 suggests a weakening near the end of the time series. However, an examination of the unsmoothed series reveals stronger-than-average upwelling-favourable winds continued during several of the most recent years,

2008-2011 (Fig. 3). During 2012, upwelling-favourable wind stress was average such that their anomalies were near zero.

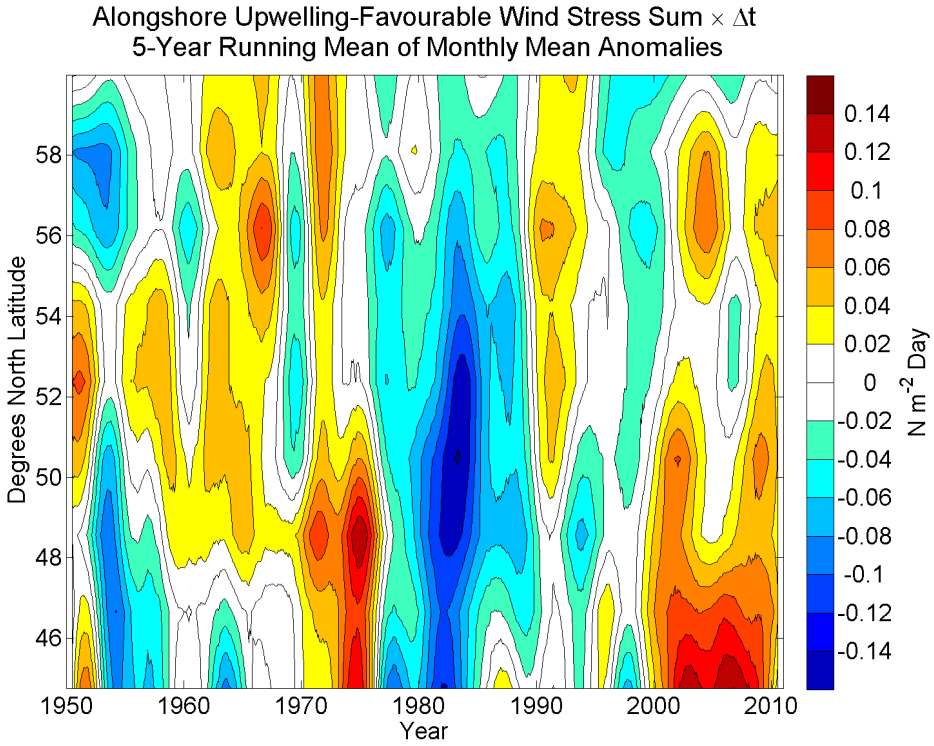

Figure 2. Five-year running means of monthly mean anomalies of monthly sums of alongshore upwelling-favourable (equatorward) wind stress at coastal grid points from 45°-60° N.

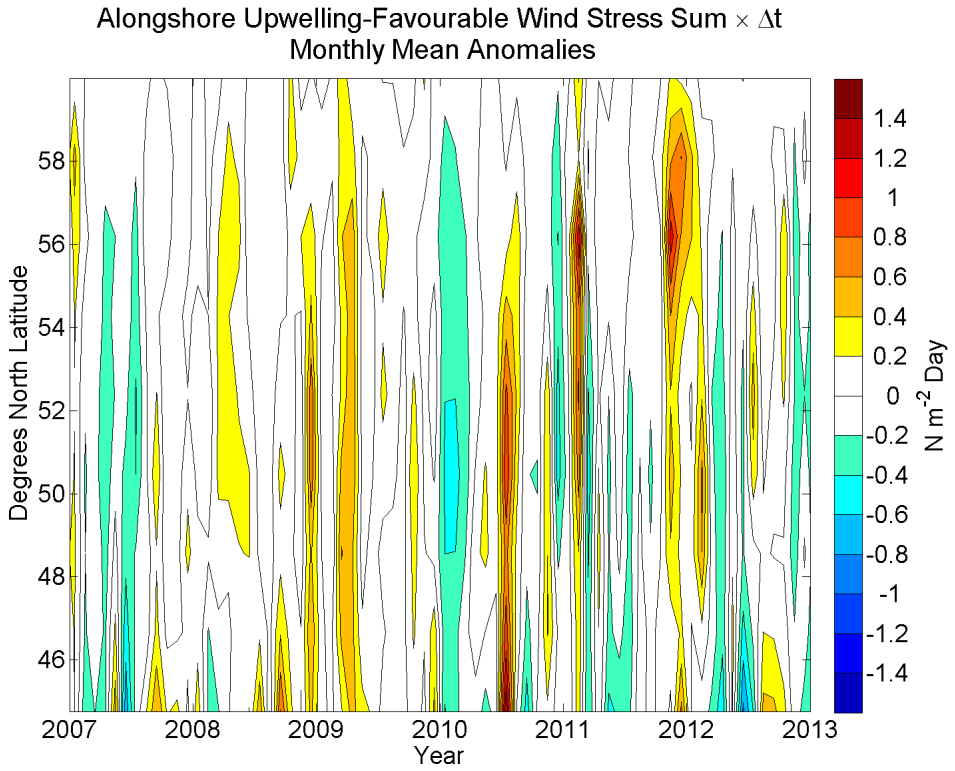

Figure 3. Recent (2007 to 2012) non-filtered monthly mean anomalies of monthly sums of alongshore upwelling-favourable (equatorward) wind stress at coastal grid points from 45°-60° N.

We have also examined the downwelling-favourable winds by considering only the poleward component of the alongshore wind stress; anomalies of the monthly poleward sums are shown in Fig. 4. Here, a shift in the late 1970s is characterized by a latitude-dependent transition. Southward of 48ºN, the transition is to weaker downwelling (shifting from average to below-average), whereas northward of this latitude the transition is to stronger downwelling (changing from below average to stronger than average). The major El Niño episodes of 1982-83 and 1997-98 are characterized by stronger than average downwelling. The largest anomalies and greatest spatial extent are positive, beginning in 1998 and extending over the range of latitude from 45-60ºN through to the present. A more detailed (non-filtered) examination of the last six years (Fig. 5) shows downwelling-favourable wind stress anomalies were either near zero (2007 to late winter 2009) or stronger than average (2010-2011). Downwelling-favourable wind stress was near average throughout most of 2012, but the year finished weaker than average.

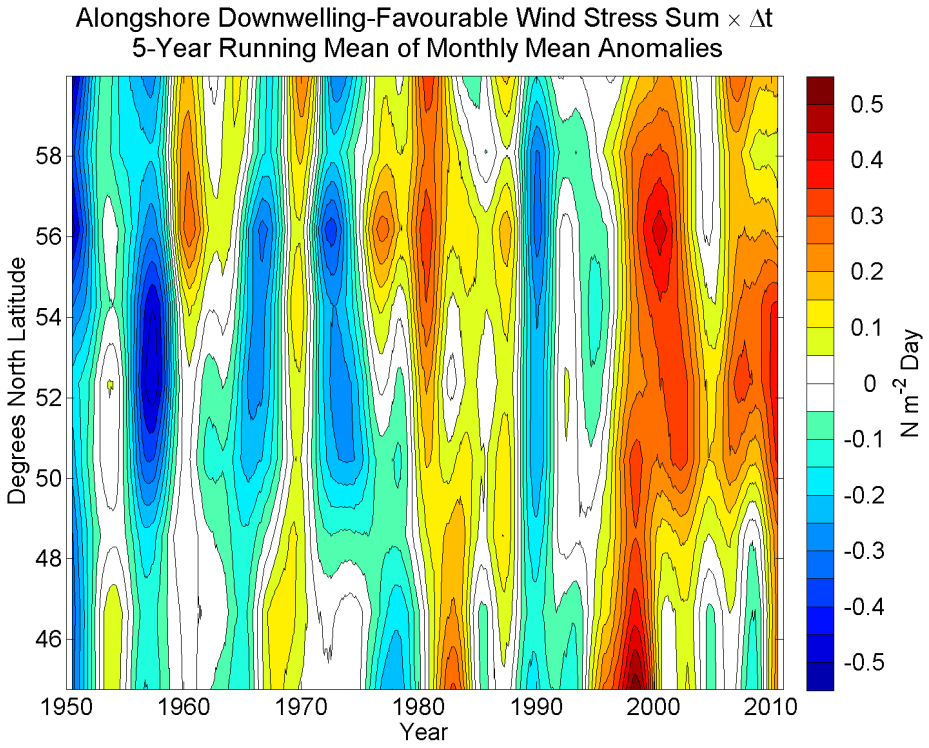

Figure 4. Five-year running means of monthly mean anomalies of monthly sums of alongshore downwelling-favourable (poleward) wind stress at coastal grid points from 45°-60° N.

As indicated in Fig. 5, the downwelling index reaches its highest magnitude during winter and fall. High winter values in early 2012 were due to intensification and/or an eastward shift of the Aleutian Low. Similarly the shift from negative to positive downwelling index values in early 2010 represented an eastward shift plus intensification of the Aleutian Low. *Thus variations in the downwelling index are due to variability in the Aleutian Low, and consist of a combination of east-west shifts of the centre of the Low and variations in its strength.* Both upwelling and downwelling indices are positive through much of the 2000s (Figs. 2 and 4), suggesting an overall increase in wind speed and wind stress, regardless of wind direction. While the effects on upwelling and alongshore advection are dependent on the wind direction, the effects on mixed-layer depth and Ekman pumping by the generally positive windstress curl in the Gulf of Alaska in winter should be mainly related to wind strength. The long-term effects in the northeast Pacific of changes in scalar wind properties is unclear, but could impact overall productivity. (Hourston and Thomson 2)

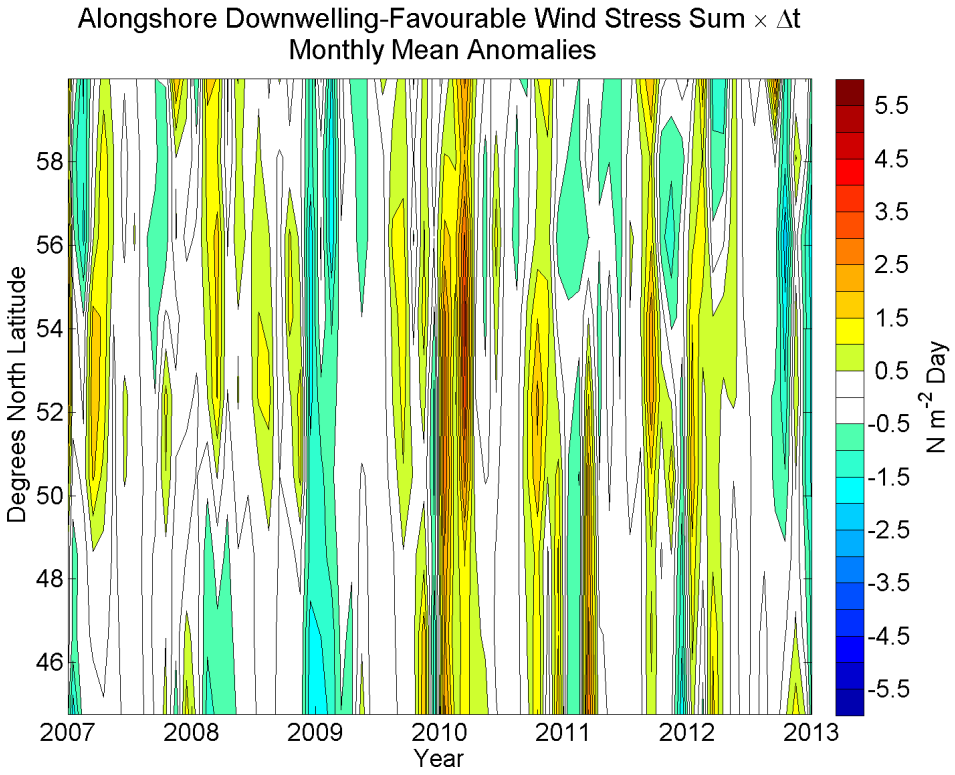

Figure 5. Recent (2007 to 2012) non-filtered monthly mean anomalies of monthly sums of alongshore downwelling-favourable (poleward) wind stress at coastal grid points from 45°-60° N.

Acknowledgements

NCEP/NCAR Reanalysis-1 wind stress provided by the National Oceanic and Atmospheric Administration /Office of Oceanic and Atmospheric Research/ Earth System Research Laboratory Physical Sciences Division, Boulder, Colorado, USA, from their Web site at http://www.esrl.noaa.gov/psd/. A literature reference for these data is given below.

Reference

Kistler, R., Kalnay, E., Collins, W., Saha, S., White, G., Woolen, J., Chelliah. M., Ebisuzaki, W., Kanamitsu, M., Kousky, V., van del Dool, H., Jenne, R., and Fiorino, M. 2001. The NCEP–NCAR 50-year reanalysis: monthly means CD-ROM and documentation. Bulletin of the American Meteorological Society 82: 247–267.l grid points from 45°-60° N.

2.1.7. Physical oceanographic conditions on the shelf/shelf-break off Vancouver Island

Roy Hourston and Richard Thomson, Fisheries and Oceans Canada

Highlights of shelf/shelf break physical oceanographic conditions off Vancouver Island in 2012 are as follows:

- 2012 west coast temperatures and surface salinities were below average.
- Winds and wind-driven near-surface currents along the coast were near average in 2012.
- The 2012 spring transition was average to late. This suggests 2012 spring productivity was average to below average.

2012 began with a La Niña (cool) event and ended with neutral El Niño/Southern Oscillation (ENSO) conditions. The Pacific Decadal Oscillation (PDO) was in a cool phase throughout 2012 (Crawford 1). These two conditions reinforced each other to produce cooler than average sea surface temperatures (SSTs) over much of the Northeast Pacific as shown in Fig. 1 for March, 2012. This figure also shows sea-level pressure anomalies, which depict a more intense than average Aleutian Low that was shifted further eastward along the coast than normal.

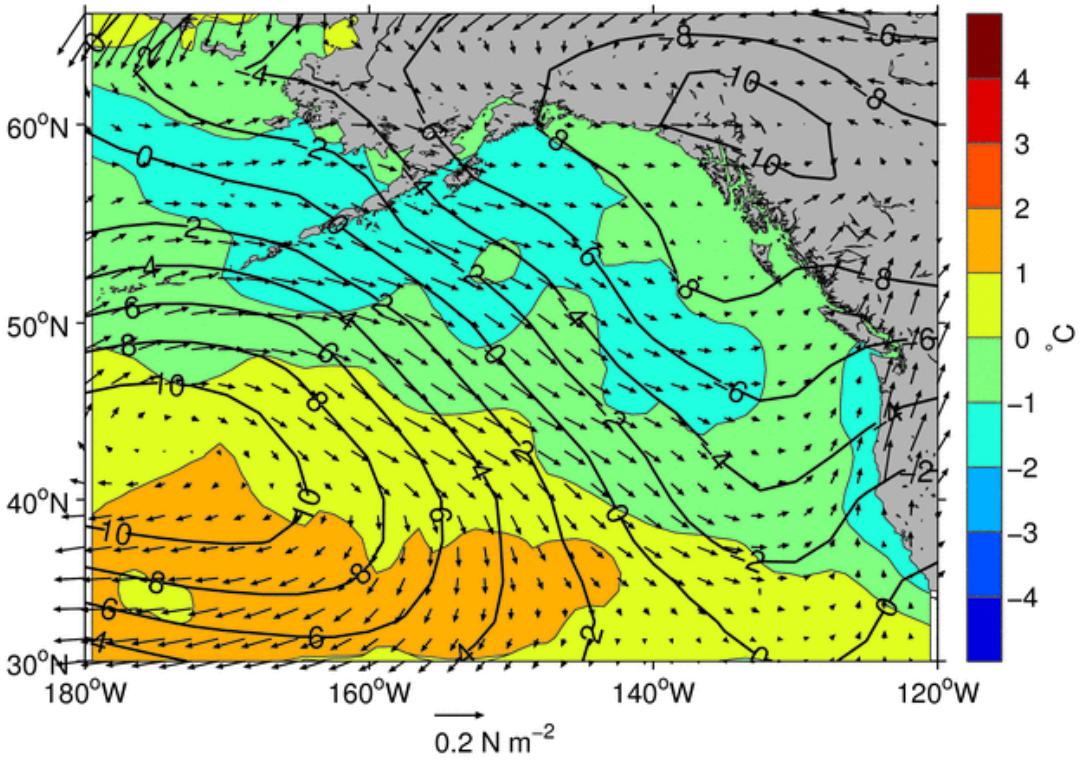

Figure 1. Anomalies (relative to 1982-2011) of sea-level pressure (contours), wind stress (vectors), and sea-surface temperature (colour contours) for the month of March, 2012

This is also clearly shown in Fig. 2. Coupled with a stronger than average North Pacific High, the resulting strong pressure gradient gave rise to the stronger than average westerly winds over the Northeast Pacific shown in Fig. 1. (Crawford 1)

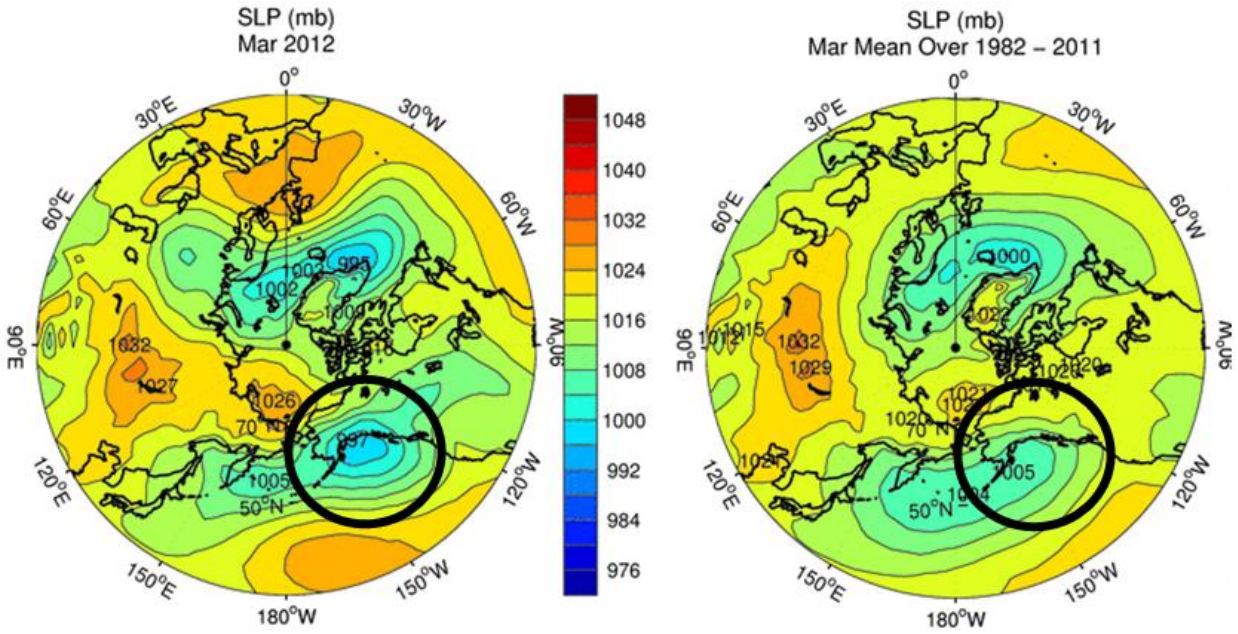

Figure 2. Sea-level pressure for the month of March 2012 (top panel), and March averaged over 1982-2011 (bottom panel). Black circles highlight the region of intensification of the Aleutian Low in 2012 compared to average.

More detailed observations along the west coast of Vancouver Island in 2012 have been examined from stations shown in Fig. 3.

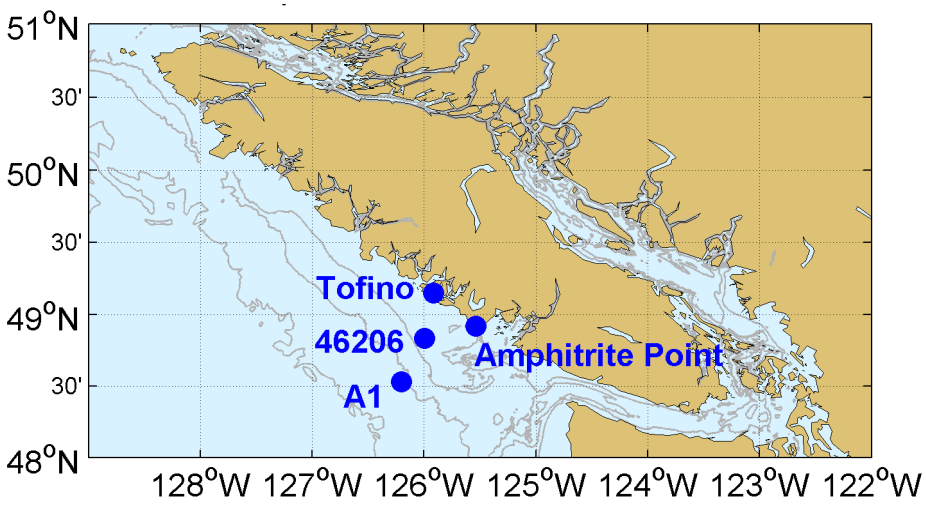

Figure 3. West coast station locations for shelf break currents (A1), sea-surface temperature and wind stress (meteorological buoy 46206), salinity (Amphitrite Point lighthouse), and water level (Tofino).

Almost 30 years of temperature variability from the surface to a nominal depth of 400 m from meteorological buoy 46206 and mooring A1 are shown in Fig. 4. Largest temperature anomalies are generally associated with strong ENSO episodes such as the 1997 El Niño and 2007 La Niña. In 2012, temperature anomalies were below average at the surface and 400 m, but not at record lows. No data was available at intermediate depths (Chandler and Gower).

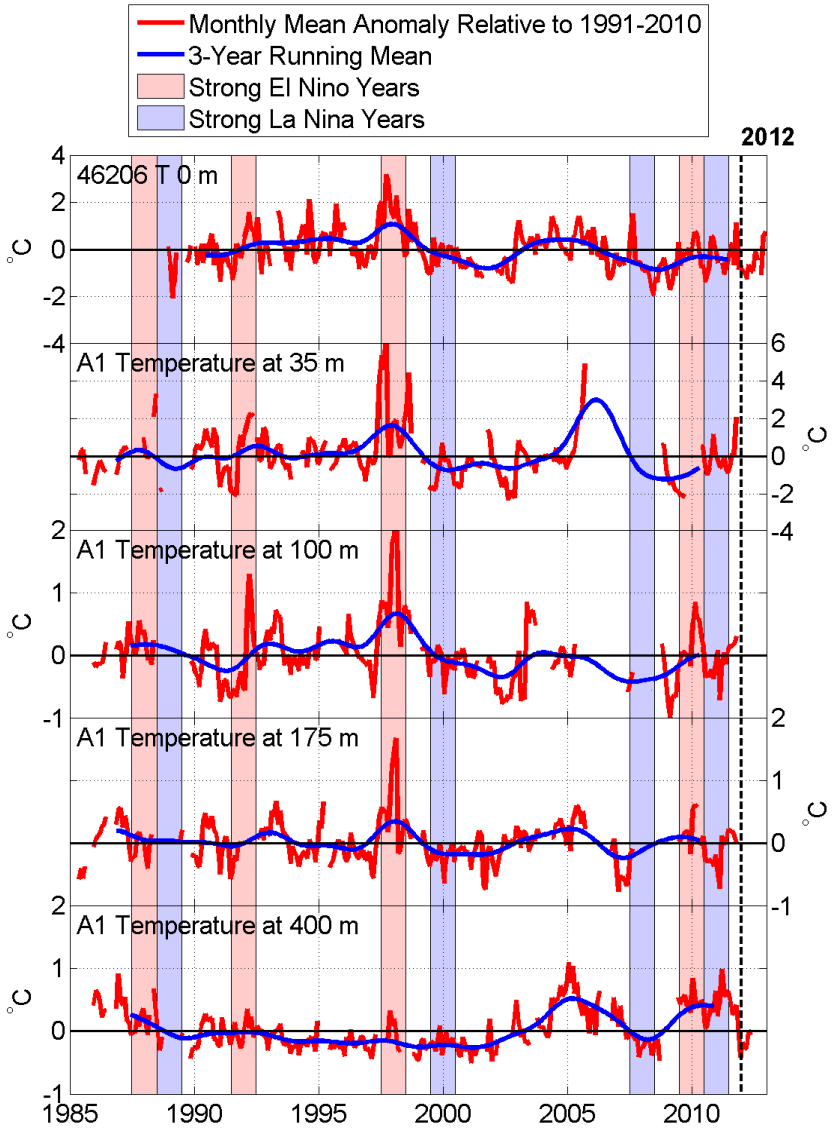

Figure 4. Monthly mean temperature anomalies off the West Coast of Vancouver Island near the shelf break at the surface (from meteorological buoy 46206) and at the nominal depths of 35, 100, 175, and 400 m (from mooring A1). 3-year running means of the anomalies are also shown in blue and were computed using the monthly data that had gaps filled by interpolation. Shaded years signify strong El Niño/La Niña events that are defined as 3 consecutive months of Nino3.4 region (5N-5S, 120-170W) temperature anomalies exceeding +/- 1.5 C.

Variability in along-shore winds and ocean currents and their effects are depicted in Fig. 5. Currents are generally more poleward (positive) during El Niño episodes (e.g., 1997) and more equatorward (negative) during La Niña episodes (e.g., 2007). Water level is higher (lower) than average during El Niño (La Niña) episodes due to onshore (offshore) Ekman transport and thermal expansion (contraction) of sea water. Wind stress and along-shore currents were about average in 2012. The year began with more equatorward flow and below average sea level that reversed to more poleward and above average sea level later in the year (Hourston and Thomson).

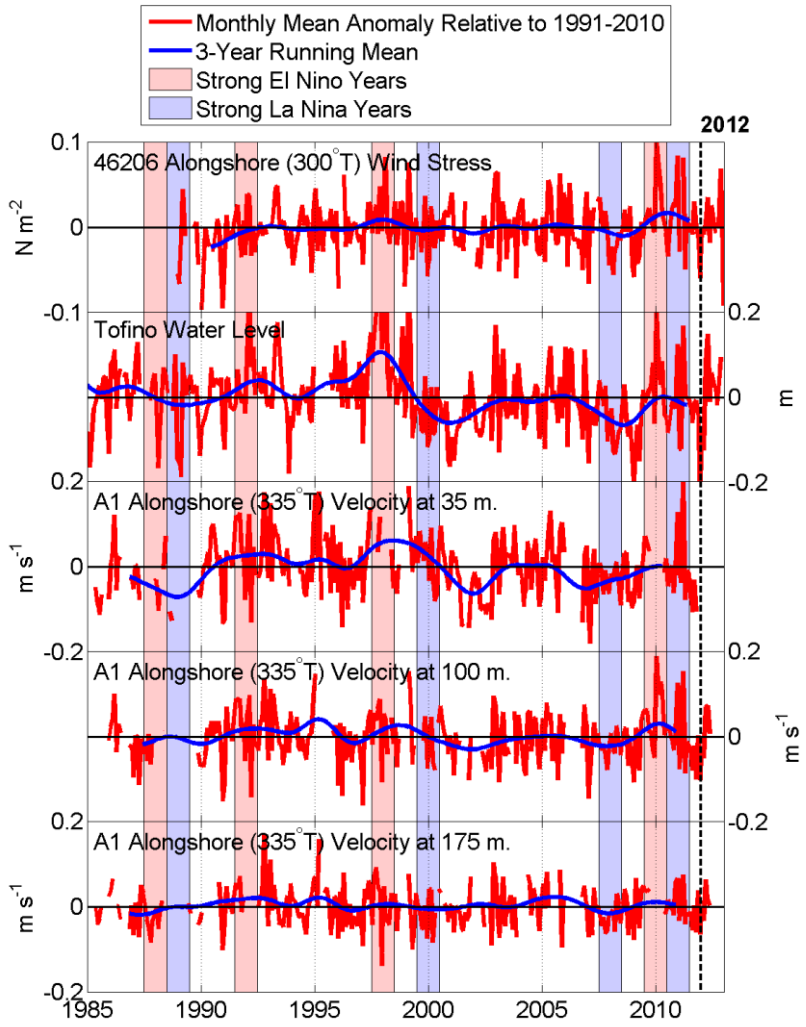

Figure 5. As for Fig. 4 but for along-shore (300 °T) wind stress at 46206, water level at Tofino, and along-shore velocity at 35, 100, and 175 metres depth at A1. Positive wind stress and current velocity indicate poleward flow, and negative values are equatorward flow. Along-shore directions were computed from an empical orthogonal function analysis of the U and V components which gives the direction of maximum variance.

Fig. 6 is a more detailed look at 2012 showing daily mean values of SST and sea surface salinity (SSS), wind stress, water level, and near-surface currents. SST was below average over the first half of the year and then finished the year above average. SSS was mostly below average. Along-shore wind stress and near-surface currents and water level were about average over 2012. This figure captures the effects of strong storms in March and April (Atkinson et al.) which resulted in large positive anomalies of poleward winds and currents and high water levels, and were associated with increases in SST and decreases in SSS due to increased downwelling. Although large and significant, these signatures of storm activity are not unusual at this time of year(Chandler and Gower).

Fig. 6 also gives an indication of spring transition timing - the onset of the coastal biologically productive season. The timing is indicated by the annual switch from generally poleward (downwelling-favourable) winds and along-shore currents to equatorward (upwelling-favourable). From the bottom panel it appears the switch from generally positive to negative along-shore currents was near average to late. This suggests 2012 coastal productivity was

average to below-average, since later spring transitions are associated with poor productivity, as was the case in 2005. A late transition in 2012 may have occurred because the Aleutian Low was stronger than average in March (Figs. 1 and 2), resulting in stronger poleward (downwelling) winds and currents along the coast in March (Figs. 1 and 6), which in turn delayed the transition to equatorward (upwelling-favourable) flow.

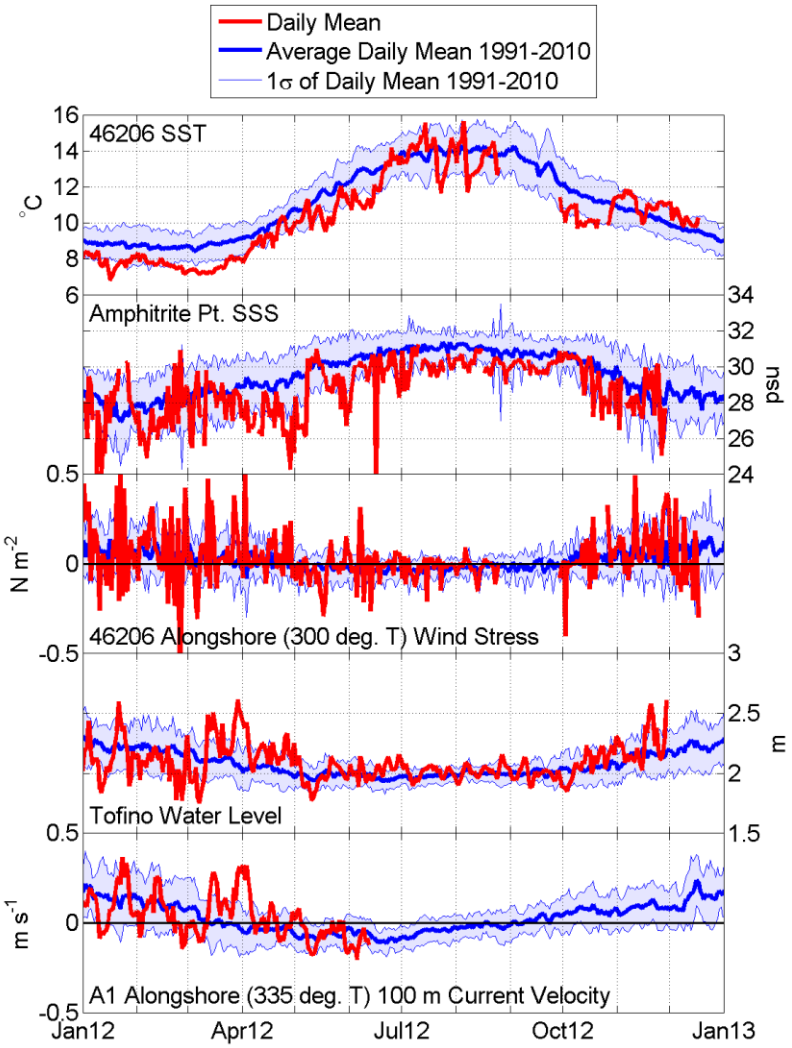

Figure 6. Daily mean (30-hour filtered) sea-surface temperature and salinity, along-shore (300 °T) wind stress, water level, and along-shore (335 °T) 100 m current velocity off the west coast of Vancouver Island in 2012 for the stations shown in Fig. 3.

Acknowledgements

Nation Centers for Environmental Prediction/ National Center for Atmospheric Research Reanalysis-1 sea-level pressure and wind stress and Reynolds Optimum Interpolation (OI) V2 SST data provided by the National Oceanic and Atmospheric Administration /Office of Oceanic and Atmoshperic Research/ Earth System Research Laboratory Physical Sciences Division, Boulder, Colorado, USA, from their Web site at http://www.esrl.noaa.gov/psd/. Literature references for these data are given below.

Sources of Information

Kistler, R., Kalnay, E., Collins, W., Saha, S., White, G., Woolen, J., Chelliah. M., Ebisuzaki, W., Kanamitsu, M., Kousky, V., van del Dool, H., Jenne, R., and Fiorino, M. 2001. The NCEP–NCAR 50-year reanalysis: monthly means CD-ROM and documentation. Bulletin of the American Meteorological Society 82: 247–267.

Reynolds, R.W., Rayner, N.A., Smith, T.M., Stokes, D.C., and Wang, W. 2002. An improved in situ and satellite SST analysis for climate. J. Climate 15: 1609-1625.

2.1.8. Observations of storms off the West Coast in 2011 and 2012 from seafloor data

David Atkinson[1], Steve Mihaly[2], Dilumie Abeysirigunawardena[2], Martin Heesemann[2]
[1]University of Victoria, [2]Ocean Networks Canada

A synoptic overview for the west Vancouver Island region for the years 2011 and 2012 is presented, along with a multi-instrument focus on a particular stormy period in January 2012. An Ocean Networks Canada bottom pressure recorder (BPR) at the Folger Passage Deep node (Fig. 1) captures wave state, which provides a useful indicator of storm activity. Common features in BPR trends observed in 2011 and 2012 reflect the broadest features of the storm climatology for the south British Columbia region; that is, relatively quiet in the summer and stormy in the fall, winter, and spring. Additional features that are apparent even with only two years of data are variations in timing of the beginning and end of the quiet season, frequency of storm events, and occurrences of multi-week trends during the stormy season.

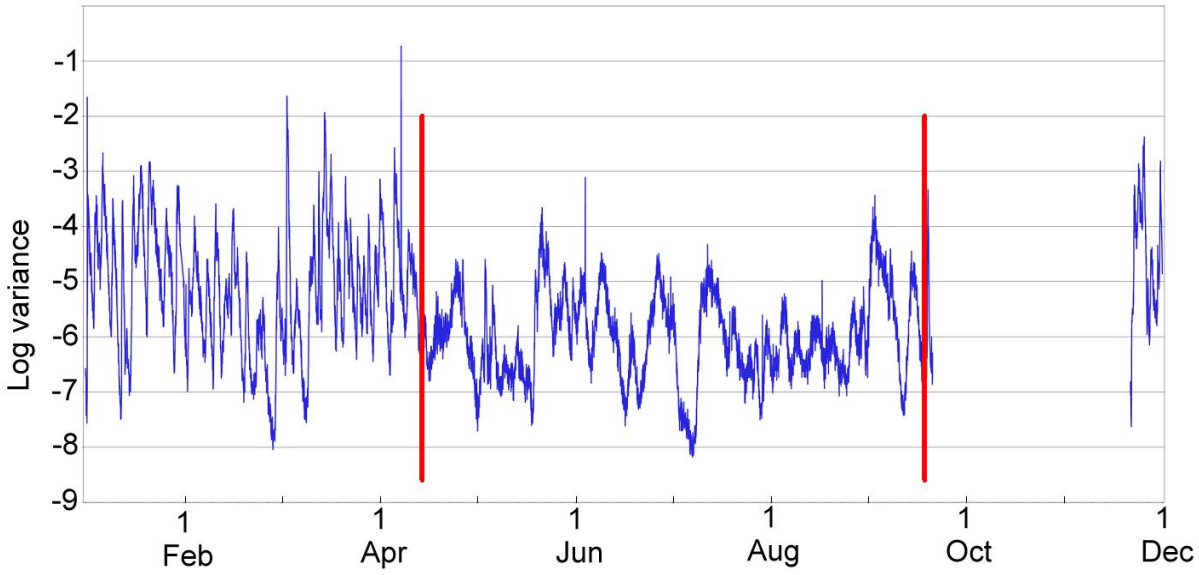

Figure 1. Bottom Pressure Recorder data recorded at the Ocean Network Canada node "Folger Passage Deep". Data are recorded every second. These data are reduced to minutely variance, and reduced again to hourly variance, to remove tidal periods, and presented as log variance to provide a clearer picture of high and low periods. This measure represents absolute wave height but also provides an indication of changes in wave height over a period of time. Greater values represent larger wave heights and more frequent changes to wave height. Thus low values in August represent small wave heights that exhibit little deviation in amplitude. Large values represent large wave amplitudes that also change rapidly, reflective of a variable wave state. Time frame is Jan 1, 2011 – Dec 1, 2011.

The annual trace of BPR log variance for 2011 (Fig. 1) indicates the change in wave state that occurs as the spring stormy season draws to a close. The frequency of the variance spikes and the background magnitude, which reflects general energy state, both drop off fairly rapidly in mid-April. Other features of note in 2011 include a general decrease to a low-activity period from mid-January through to the beginning of March, followed by an increase to a period of moderate but sustained activity. Periods of low activity included the first two weeks of May and the first week of July, which was very quiet. The vertical red bars denote the summer quiet period.

The annual trace of BPR log variance for 2012 (Fig. 2) differs from 2011 in a variety of respects. The end of the spring season is not as rapid as in 2011; instead a period of decline commences in early April that lasts until –early May. One note is the late January period, which was the

stormiest week in 2012. This was the result of a series of moderate/strong low pressure systems moving to north Vancouver Island and Haida Gwaii area. The period mid-July through August was consistently quiet, terminating with an extremely low energy period in late August. Throughout September activity picks up again. This is contrasted with locally-observed synoptic conditions, which consisted of persistently fair weather until the last week of September. This contrast suggests wave activity was not locally generated. Analysis of the BPR data in spectral form (not shown) indicates the wave activity was swell moving in from distant storms. Vertical red bars denote the summer quiet period and increasing activity in September.

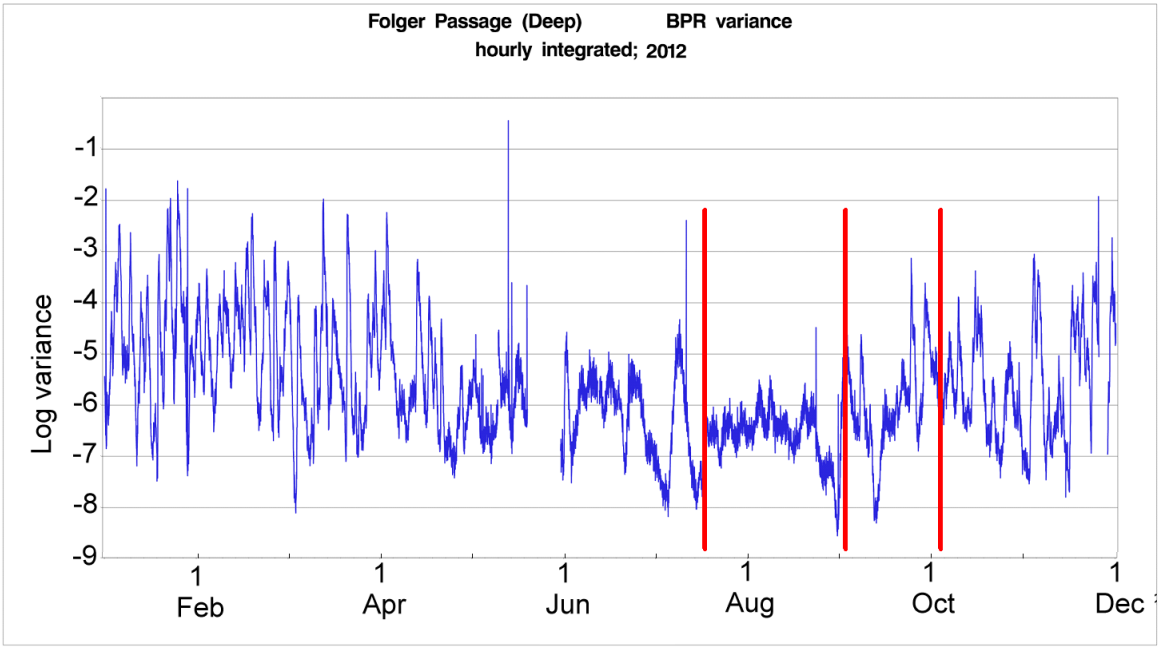

Figure 2. Bottom Pressure Recorder data recorded at the Ocean Network Canada node "Folger Passage Deep". Data are recorded every second. Those data are reduced to minutely variance, and reduced again to hourly variance, to remove tidal periods, and presented as log variance to provide a clearer picture of high and low periods. This measure represents absolute wave height but also provides an indication of changes in wave height over a period of time. Greater values represent larger wave heights and more frequent changes to wave height. Thus low values in August represent small wave heights that exhibit little deviation in amplitude. Large values represent large wave amplitudes that also change rapidly, reflective of a variable wave state. Time frame is Jan 1 2012– Dec 1, 2012.

2.1.9. 2012 water properties from Ocean Networks Canada: VENUS and NEPTUNE

Richard Dewey, Steve Mihaly, and Marlene Jefferies, Ocean Networks Canada, University of Victoria

In late 2012 the VENUS and NEPTUNE Canada observatories were formally merged, now reporting under the Ocean Networks Canada (ONC) banner. This report includes a brief summary of some key features of the data recorded on the ONC systems as they relate to the general state of the ocean around the southern portion of Vancouver Island (both in-shore, Saanich inlet and off-shore, Folger Passage near Bamfield). Challenges in 2012 include a canceled NEPTUNE maintenance cruise in September due to mechanical issues on the R/V *Thomas G. Thompson* and a failure in August of the backbone power on the VENUS cabled observatory in the Strait of Georgia. Among the 2012 successes where expansions of the observatories to included new sensors on BC Ferries and HF radar in the Strait of Georgia. These two systems provide hourly updates of the surface water properties and currents, respectively. Additional systems coming on line in 2013 include autonomous moorings in Juan de Fuca Strait measuring bottom currents and water properties, and two mobile systems, a glider and a top-down buoy profiling system, that will both provide measurements of the vertical structure in the water column.

As of February 2013 the VENUS observatory has collected seven complete years of observations in Saanich Inlet. Shown in Fig. 1 is a time series of water properties from the central mooring at 100m depth.

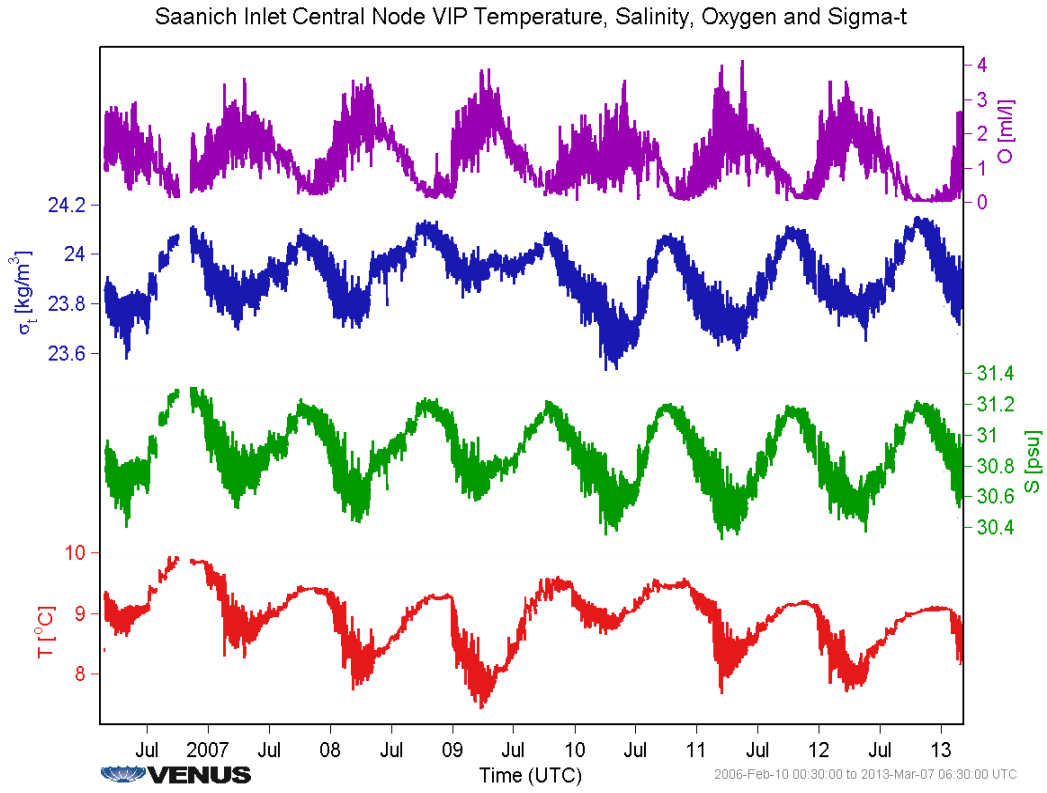

Figure 1. Seven year time series of temperature, salinity, sigma-t (a measure of seawater density) and dissolved oxygen from VENUS node at 100 m in Saanich Inlet

The time series are characterized by an annual cycle that includes summer upwelling, when temperatures warm and salinities increase, and a winter ventilation period when the temperature and salinity both drop. In Saanich Inlet, the oxygen is seen to be out of phase with both temperature and salinity, with the highest oxygen concentration at the end of winter and the lowest concentration at the end of summer.

Fig. 2 shows the same time series for just 2012. Starting in late May, the first of six distinct monthly (during the weaker of the neap tides) renewal events brings warm salty water into the bottom of Saanich Inlet, concluding with a final renewal event in mid-October. These dense water intrusions displace low oxygen water upwards in Saanich Inlet, decreasing the oxygen levels at this east side-wall site at 100 m depth. By early October the oxygen levels are extremely low, and remain low for over four months, until they begin to increase in early 2013. This was the longest duration of low oxygen water observed on the VENUS system to date.

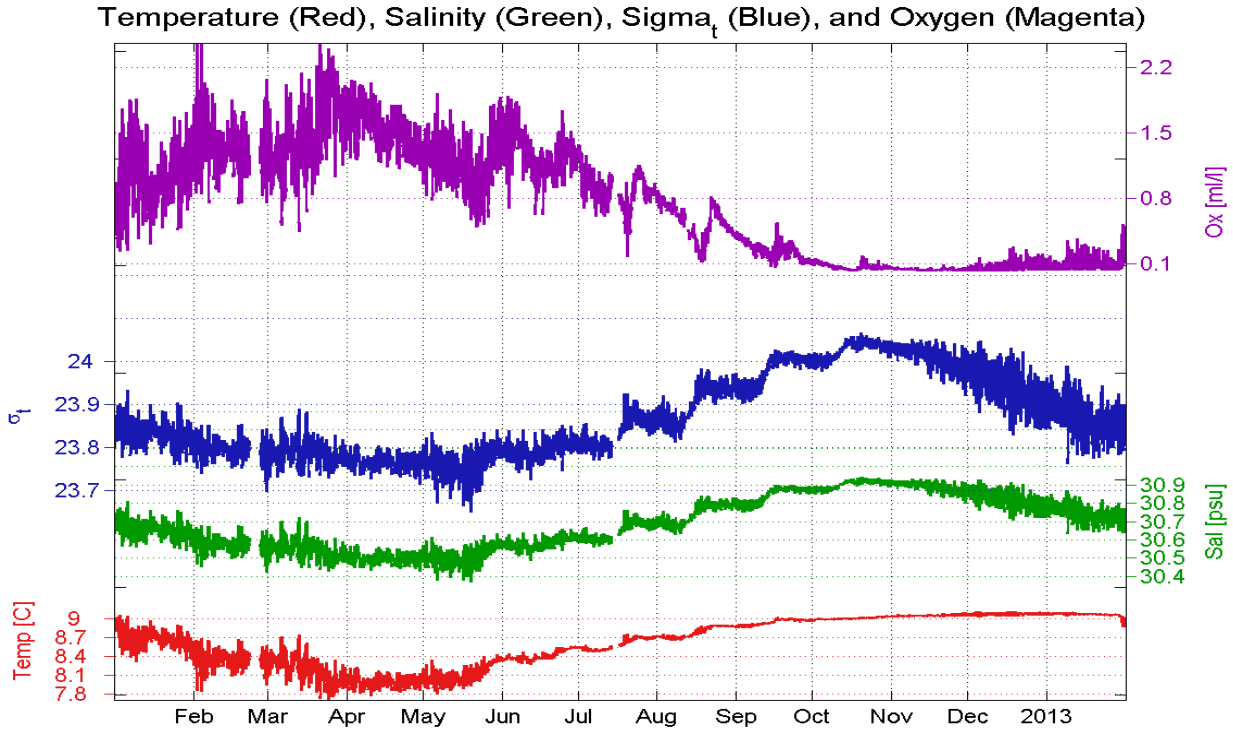

Figure 2. Time series of temperature, salinity, sigma-t (a measure of seawater density) and dissolved oxygen from VENUS node at 100 m in Saanich Inlet for 2012.

Observations from the Folger Passage (Fig. 3) site on the NEPTUNE observatory reveal a different perspective of the annual cycle (Fig. 4), more closely tied to the upwelling season. Although seawater salinity and density remain in phase in Folger Passage in Fig. 4, unlike in Saanich Inlet, the temperature signal is now out of phase with salinity, representing more oceanic condition. Cooler temperature and higher salinity are now closely tied to the on-set of upwelling conditions, while warmer temperatures and decreasing salinities correspond with downwelling periods. Oxygen concentrations mirror the salinity, with oxygen concentrations declining during upwelling (May through October) and increasing during downwelling (October through to December).

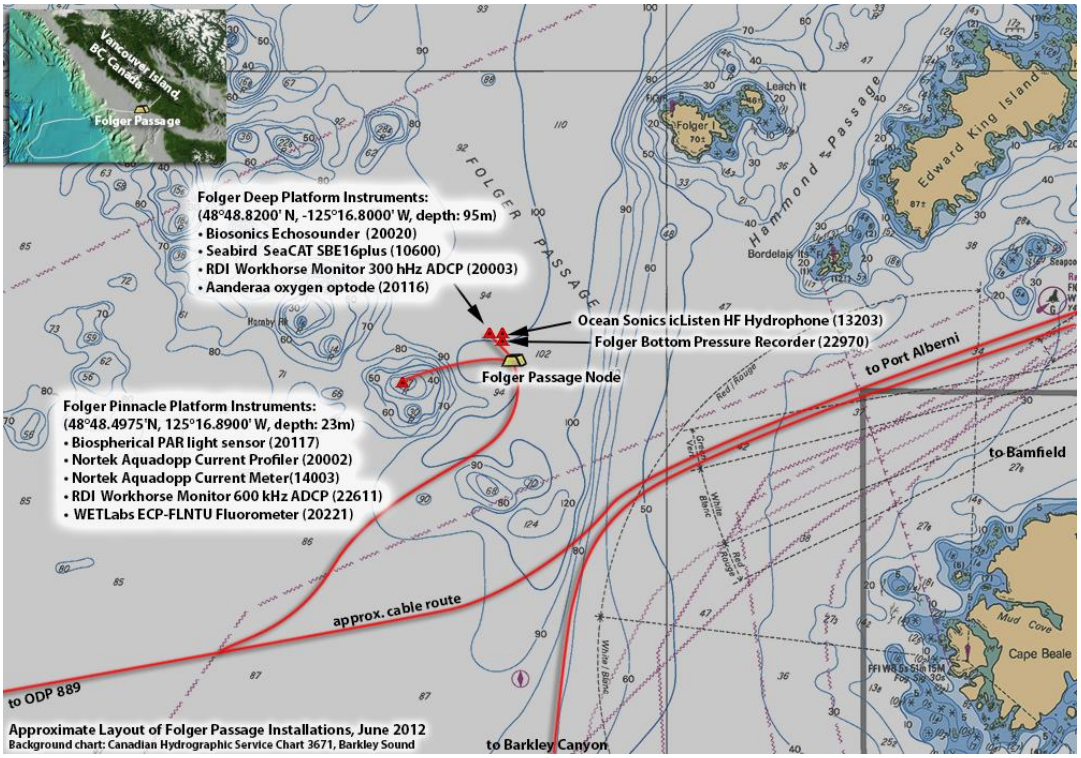

Figure 3. The Folger Passage Node of the ONC NEPTUNE Observatory, west of Bamfield.

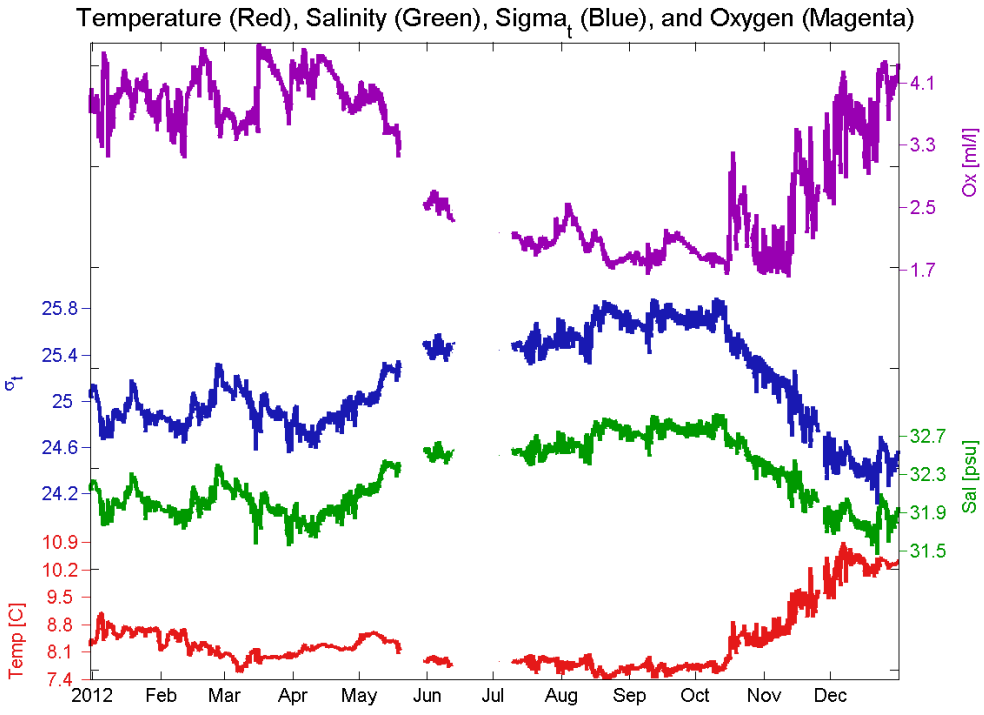

Figure 4. Time series of temperature, salinity, sigma-t (a measure of seawater density) and dissolved oxygen from the NEPTUNE node at 100 m depth at Folger Passage for 2012.

Shown in Fig. 5 is the annual-average, cumulative upwelling index at 48°N, 125°W (NOAA, Northwest Fisheries Science Center) from 1967 through 2011, and the cumulative upwelling

index for 2012. The upwelling index (Bakun 1975) is an estimate of the off-shore (positive) or on-shore (negative) transport of surface water by the along-shore winds, calculated from the along-shore wind stress divided by the local Coriolis parameter, in units of m^3s^{-1}/100m of coastline. For the point at 48°N, winds from the NNW are upwelling favorable (positive index) and winds from the SSE are downwelling (negative index) favourable. Several characteristics for 2012 are worth noting.

The 2012 upwelling season starts a little later than usual (May 7/Julian Day 128 vs April 25/Julian Day 115), and then pauses for more than a month (May 18/Julian Day 139 – June 29/Julian Day 181), before the more sustained upwelling season starts in earnest on June 30 (Julaian Day 182). Despite the delay, the net amount of upwelling in 2012 is very near the 1967-2011 average. Downwelling (southerly winds), which coincides with warmer, fresher, and higher oxygen levels, kicks in rather late, on October 11 (Julian Day 285), 2012 (Hourston and Thomson 1).

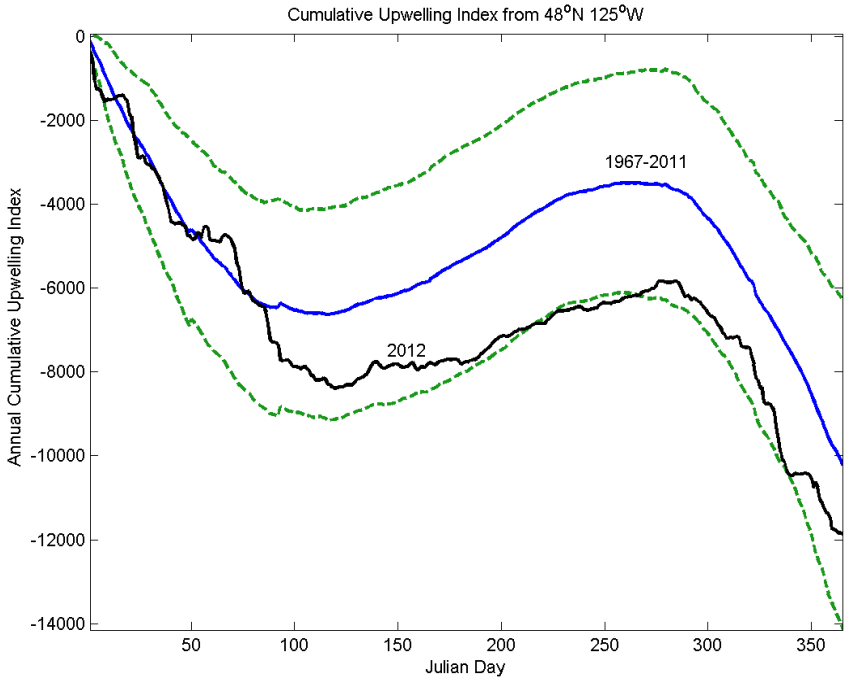

Figure 5. Cumulative Upwelling Index: Average 1967-2011 (blue) with standard deviations (green dashed), and Cumulative Upwelling Index for 2012 (black) at 48°N 125°W, NOAA, Northwest Fisheries Science Center. Julian day denotes the day of year starting at 1 on January 1. The upwelling season begins when the cumulative upwelling index is a minimum, and continues until the cumulative upwelling index reaches a maximum. For the average of 1967 to 2011, these are near Julian day 110 and 270, respectively.

Reference

Bakun, A. 1975. Daily and weekly upwelling indices, west coast of North America, 1967-73. U.S. Dept. of Commerce, NOAA Tech. Rep., NMFS SSRF-693, 114p.

2.1.10. Phytoplankton blooms on the BC coast

Jim Gower, Fisheries and Oceans Canada

The European satellite Envisat failed in orbit in April 2012, losing us the data from the spectral band at 709 nm that we have used to detect intense surface blooms, for example of *Heterosigma* along the BC coast. We can still make use of the US MODIS and VIIRS sensors to map ocean surface chlorophyll patterns and blooms of *Coccolithophores,* which often brighten BC waters in June to August. Fig. 1 shows an extensive and intense bloom on 5 July 2012. The bloom is most intense over deep water south of Estevan Point, but it extends north well past Brooks Peninsula.

Satellite observations available through NASA'a Giovanni system (http://disc.sci.gsfc.nasa.gov/giovanni) provide time series of intensity (Fig. 2), confirming 2012 as the most intense bloom year since 2006, when blooms off Vancouver Island were featured in NASA's "Picture of the Day." Presumably, this summer bloom intensity varies from year to year in response to some property of the coastal environment, such as near-surface water temperatures. However, the buoy monthly SST time series (Chandler and Gower) does not show evidence of any correlation.

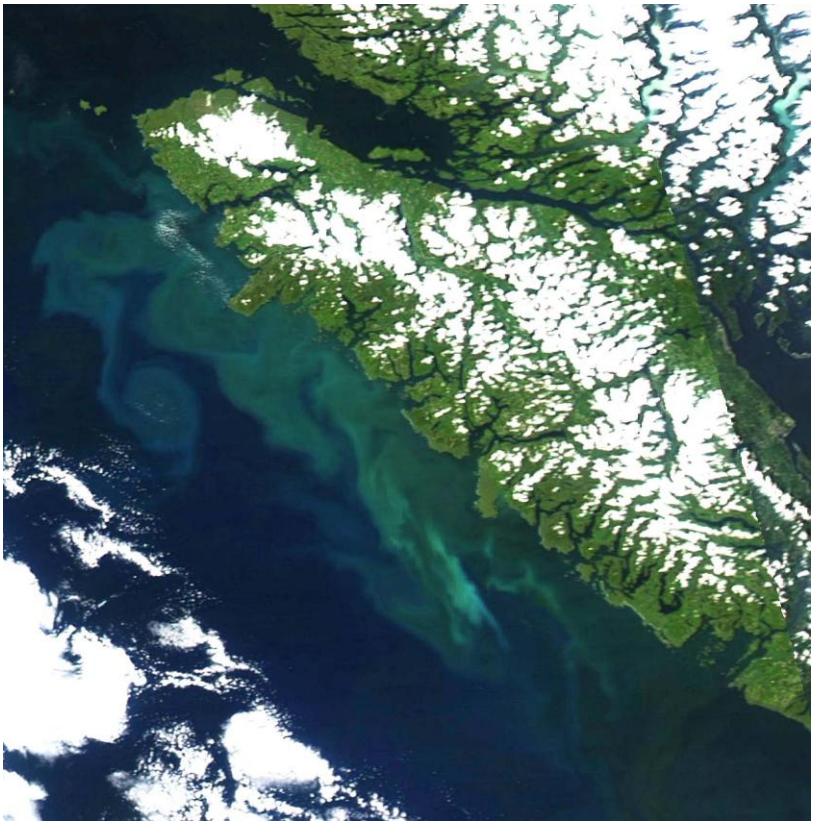

Figure 1. A MODIS Aqua true color image of a bright Coccolithophore bloom off the west coast of Vancouver Island on 5 July 2012.

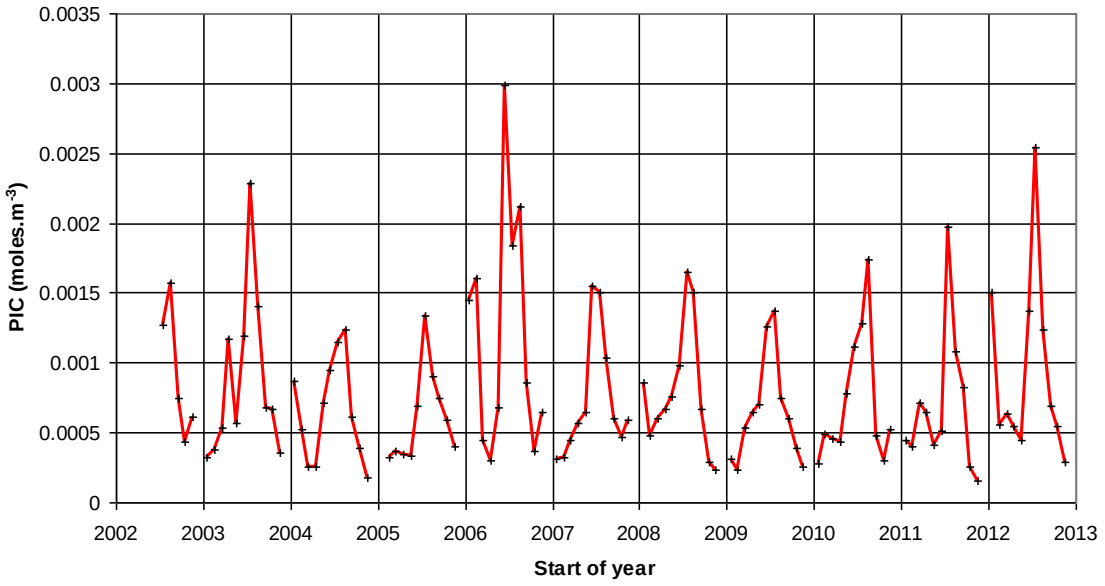

Figure 2. Monthly time series of estimates of Particulate Inorganic Carbon (PIC) derived from MODIS satellite data for the area 49° to 50°N, 126° to 128°W, showing July 2012 as the highest value after June 2006. Elevation of the sun is too low in December to allow measurement of PIC at these latitudes. Peaks in January and February in some years might be due to local sediment from rivers or storm mixing

2.1.11. Gulf of Alaska fertilization monitored by satellite ocean colour and in-situ measurements

Jim Gower, Fisheries and Oceans Canada

In August 2012, satellite water colour imagery (Fig. 1) shows areas of increased ocean surface chlorophyll concentration in the eastern Gulf of Alaska, which the Haida Salmon Restoration Corporation (HSRC) of Haida Gwaii, Canada, identify on the internet blog http://www.haidasalmon.net/blog/ as due to their iron fertilization project. When accessed on 26 March 2012, this blog contained no statement by the HSRC on fertilization location, date, amount or chemical used, except to say that the work occurred in July to September 2012. It quotes other blog sites as saying that the team motored more than 300 km west from Haida Gwaii to undertake the work, that the HSRC spread 100 tons of "iron sulfate-rich dust," or "120 tons of iron sulfate," but does not confirm these numbers or materials.

Chlorophyll, with its characteristic absorption of blue light, is readily identified by satellites that sense ocean colour. Because chlorophyll is found in phytoplankton, these satellites are able to estimate concentrations of phytoplankton at the ocean surface, but only when clouds are not present. Satellite imagery processed to estimate ocean surface chlorophyll concentration is provided by the National Oceanic and Atmospheric Administration (NOAA) Oceanwatch program at http://las.pfeg.noaa.gov/oceanWatch/oceanwatch.php and the National Aeronautics and Space Administration (NASA) site at http://disc.sci.gsfc.nasa.gov/giovanni. Colour observations are often blocked by heavy cloud cover in this area at this time of year, and indeed, the area was cloud covered throughout most of July and August 2012. Data from the NOAA site on August 8 show a small cloud-free area centred on about 52.5°N, 139°W, in which a well-defined, circular patch of relatively high chlorophyll concentration (about 10 $mg.m^{-3}$) is visible. This area is about 400 km west of Haida Gwaii.

The time sequence of satellite altimetry data (which is not sensitive to cloud cover) available from http://eddy.colorado.edu/ccar/ssh/nrt_global_grid_viewer (which provides sea surface height contours overlaid on ocean colour data) suggests that this patch of chlorophyll was in a weakened Haida eddy that formed off the west coast of Haida Gwaii about two years previously with much greater amplitude.

After August 8, satellite images were mostly blocked by clouds until the first clear day at the end of August, when areas of enhanced chlorophyll were still detected (Fig. 1). Monthly average chlorophyll imagery for late summer from September 1997 to 2011 show occasional small patches of high chlorophyll concentration in the area of boxes A to D, but nothing as extensive as in Figure 1 on 30 Aug. 2012, except in August 2008 when iron fertilization from the eruption of Mount Kasatochi caused widespread high concentrations of chlorophyll in the Gulf of Alaska. Annotation on satellite imagery on the HSRC's blog site associates areas A, B and C with the fertilization, but not areas D, E or F. If the fertilization occurred in late July 2012 at about 52.5°N, 139°W, then the HSRC's claim that they caused these high concentrations is reasonable.

Other processes can contribute to enhanced chlorophyll concentrations. In late summer, Haida eddies are often sites of higher concentrations. Altimeter data show weak eddies centred on boxes A, B and D and a stronger eddy at E. The concentration in box A is greater than associated with weak Haida eddies and is likely due to the fertilization. Closer to shore, Haida eddies can advect nutrient-rich water offshore, stimulating plankton growth and enhancing chlorophyll concentrations. The relatively strong eddy at E might be advecting chlorophyll-rich coastal water in box F further offshore to the west.

The NOAA drifting buoy archive (http://www.aoml.noaa.gov/phod/dac/index.php) shows that 12 buoys were deployed in the area in the period 14 to 22 August and a further 8 in the period 1 to 9 September 2012. The HSRC blog site referred to above notes that they launched a total of 20 drifting buoys, but gives no details of positions, dates or drift tracks. The NOAA drifting buoy data archive shows that four of the first group were launched in the eddy in box A. Three remained trapped in the eddy and one moved to between boxes B and C by August 30. Wind measured by the weather buoy WMO number 46184 near 54°N, 139°W (data from http://www.meds-sdmm.dfo-mpo.gc.ca/isdm-gdsi/index-eng.html) suggests a surface drift to the ESE from late July to August 30. Satellite altimetry suggests geostrophic surface currents which would also advect surface water at the location of the patch observed on August 8 to the ESE.

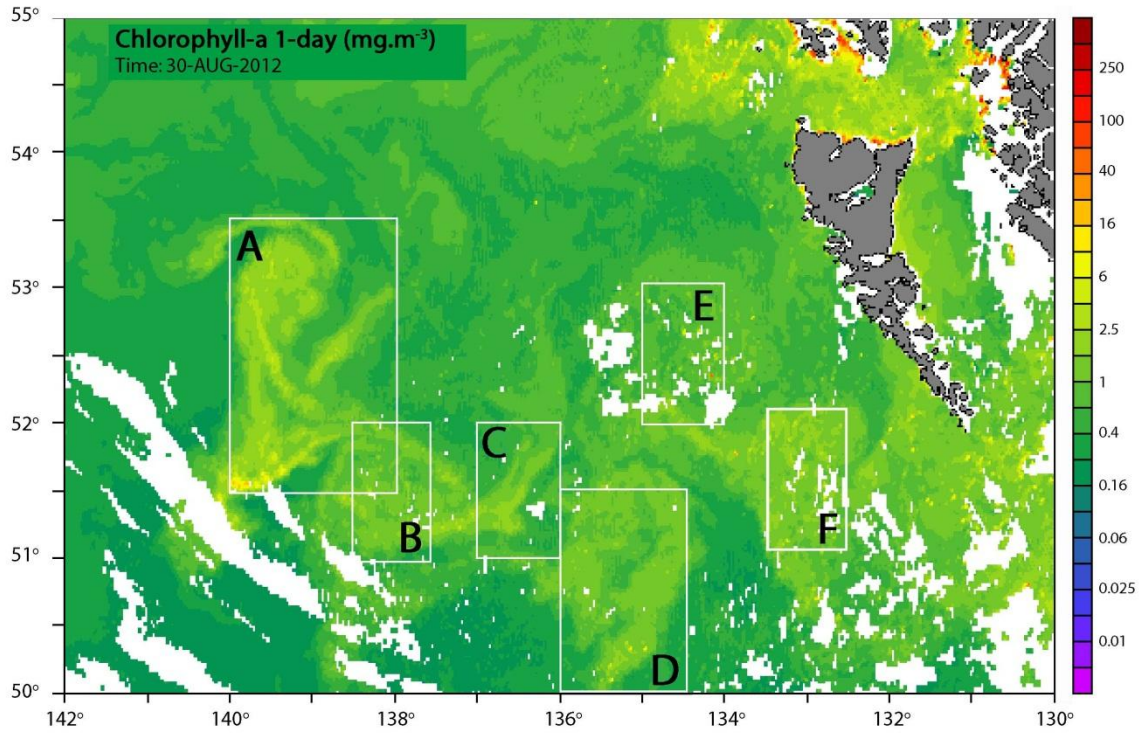

Figure 1. Image of ocean surface chlorophyll concentration in the Gulf of Alaska west of Haida Gwaii on 30 August 2012 at 2.5 km resolution, with marked areas (white boxes) A to F discussed in the text. (Data from MODIS satellite and provided by NOAA Oceanwatch: http://las.pfeg.noaa.gov/oceanWatch/oceanwatch.php)

2.1.12. Plankton in the Northeast Pacific in 2012

Sonia Batten, Sir Alister Hardy Foundation for Ocean Science, UK

Large mesozooplankton were more abundant in 2012 and seasonal timing was relatively late. Sampling with the Continuous Plankton Recorder (CPR) occurs approximately monthly 6-9 times per year between March and October in the off-shore NE Pacific (Fig. 1). Data to June 2012 have been finalised at the time of writing, while data for July to Oct 2012 are only 25% complete. In addition to mesozooplankton the CPR also retains larger hard-shelled phytoplankton (particularly chain forming diatoms and thecate dinoflagellates), so in this report a time series of diatom abundance is also included (Fig. 1). There is only weak seasonal cycle evident in the diatoms of this region with a slight dip in the summer. Observations in 2012 showed this same cycle with overall slightly lower-than-average abundance. Large diatom abundance is significantly correlated with the annual Pacific Decadal Oscillation (PDO) index so that in warm PDO positive years there are more large diatoms (R^2=0.32, p=0.02). In contrast the mesozooplankton biomass estimate of 2012 was the largest of any year in the time series (Fig. 1). It is worth noting that in only 2 years there has been a change from the lowest anomaly in 2010 to the highest in 2012. The timing of the mid-point of the seasonal cycle was also late in 2012, consistent with cool, PDO negative conditions (correlation between seasonal timing and PDO, R^2=0.4, p=0.01)

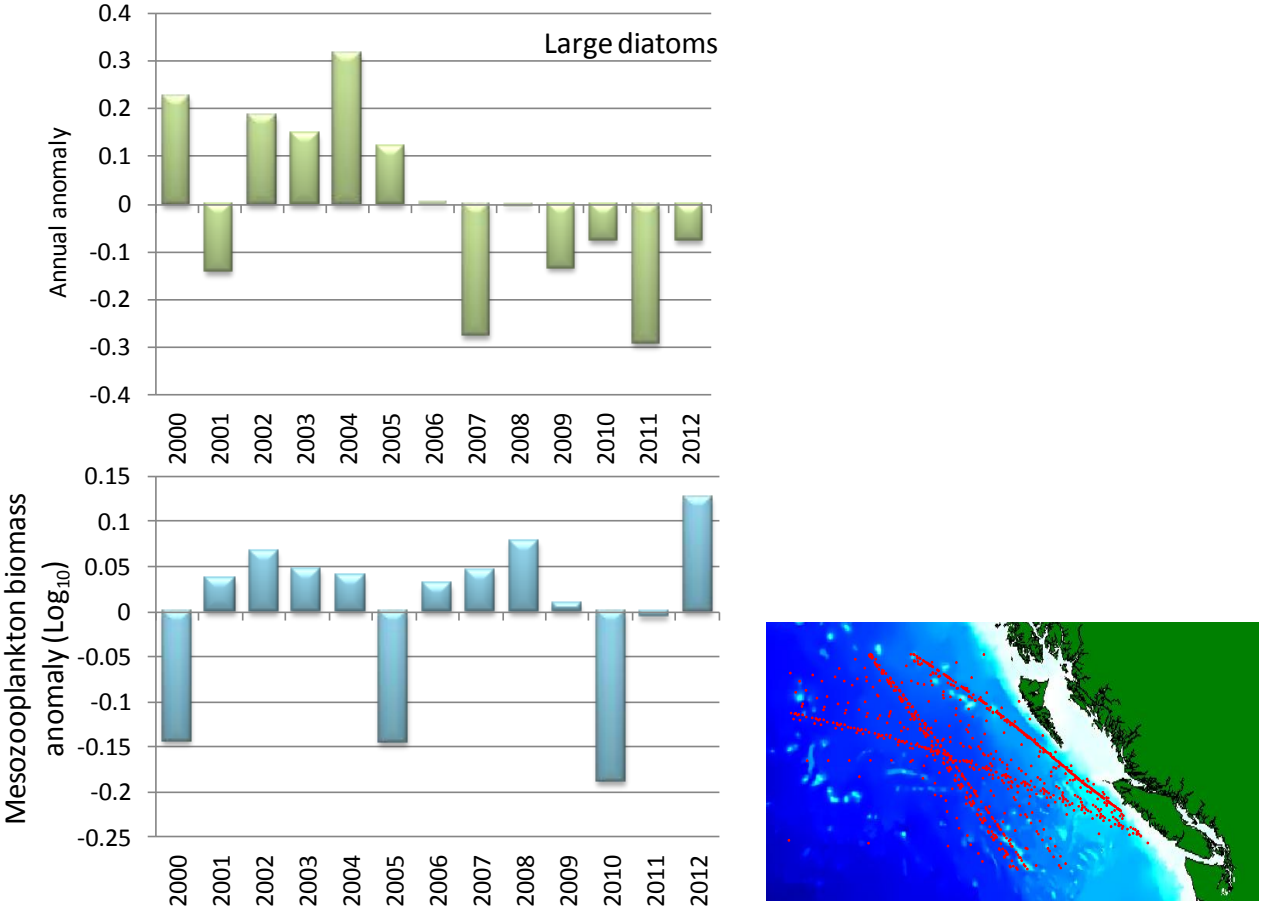

Figure 1. Annual diatom abundance (top left) and mesozooplankton biomass (bottom left) anomalies based on data from the CPR survey for the samples shown in the region above.

Seasonal timing indices for the abundant large copepod *Neocalanus plumchrus/flemingeri* are shown in Fig. 2.

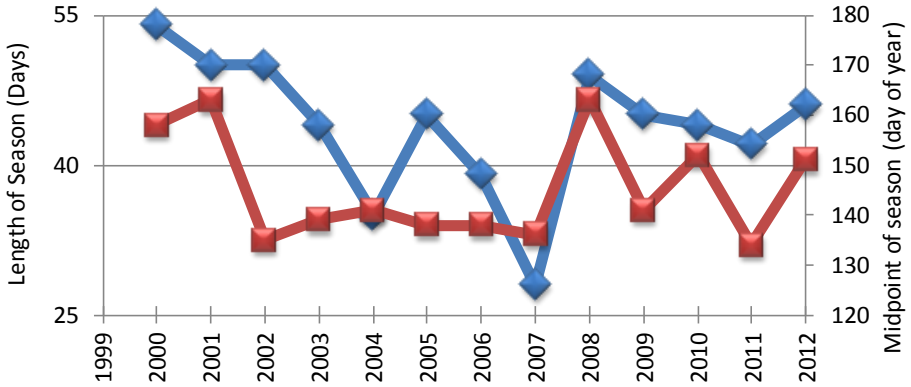

Figure 2. Day of year at which 50th percen-tile of the cumulative biomass of N. plumchrus/flemingeri was reached (red line) and length of season (blue line) as the number of days between the 25th and 75th percentile, for the offshore region

These copepods live at the ocean surface for only a month or two near time of maximum size and abundance. Changes in timing of their growth will determine when they are available as food for predators that take advantage of this organism's peak abundance. The timing of the mid-point of the season was relatively late, and its duration relatively long in 2012, but these times are in the range seen in previous years and in-line with the cool PDO-negative conditions that presently prevail. The mean annual abundance for this species in 2012 was the second highest in the time series, suggesting favourable conditions for its predators.

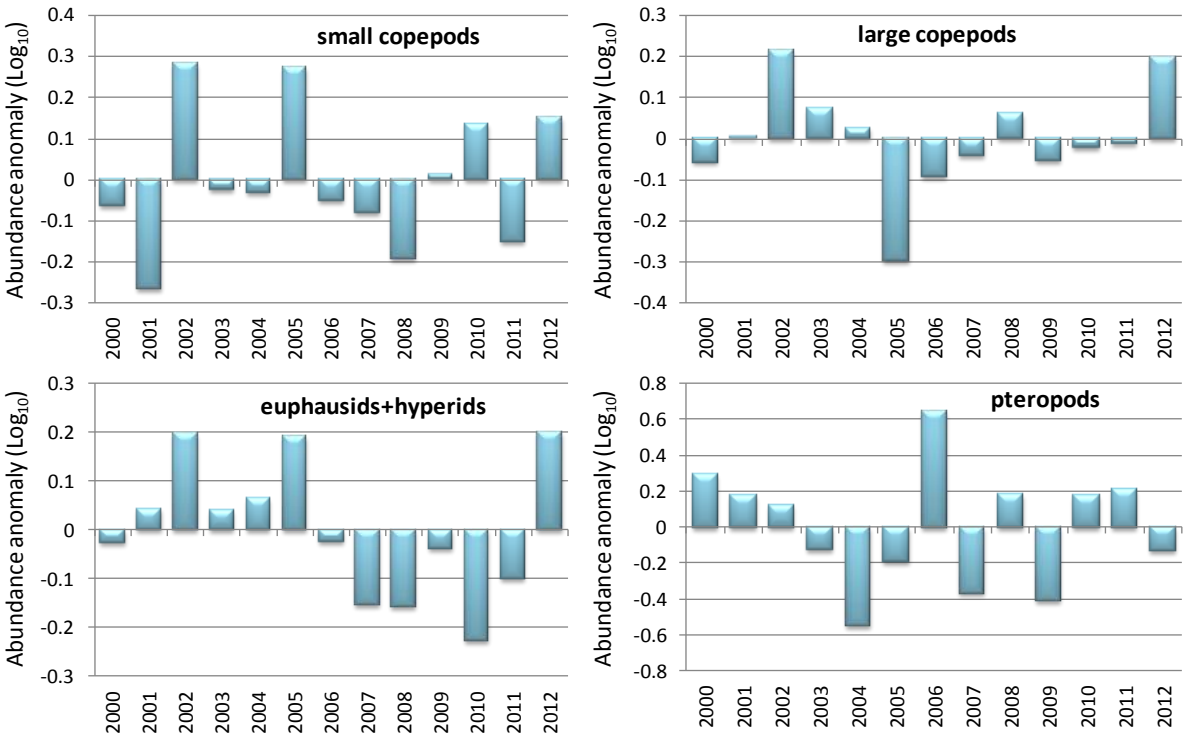

Figure 3. Annual mean abundance anomalies for broad taxonomic groups of zooplankton.

Fig. 3 shows the annual abundance anomalies for some broad taxonomic categories. Pteropods were lower than average in 2012, but copepods, both large and small, and the euphausiid/amphipod group were higher than usual (though when separated out, it was the amphipods that were particularly high in 2012). Large copepods and amphipods have a high individual biomass and it is they that have contributed most to the high biomass anomaly of mesozooplankton shown in Fig. 1.

Summer 2012 saw an iron enrichment exercise in the region sampled by the CPR, though the area with enhanced chlorophyll seen in satellite images and believed to be the planktonic response to increased iron (Gower 2), was relatively small compared to the region sampled by the CPR and whose average plankton concentrations are presented in this report. Large diatoms caught by the CPR were at or below mean monthly levels for the region as a whole through summer and fall. The zooplankton biomass as measured by the CPR was high in June, prior to the iron enrichment, and the larger copepods that we sample have an annual life cycle that is mostly completed before summer so it is unlikely that the mesozooplankton biomass was enhanced by the iron enrichment. However, small copepods were also abundant in 2012, and once the summer and fall data have been completed they will be examined more closely to determine if they were responding to the bloom. Areas sampled by the CPR outside of the region shown in Fig. 1, such as the BC shelf, northern Gulf of Alaska, and Alaskan shelf, also had strongly positive zooplankton biomass anomalies in 2012, suggesting a widespread increase across the Gulf of Alaska and adjacent coastal waters (Mackas et al. 1).

In summary, mesozooplankton conditions appear to have been favourable for their predators in 2012, with a relatively late, relatively long season and high abundance.
http://pices.int/projects/tcprsotnp/default.aspx for data and more information

2.1.13. Zooplankton along the Vancouver Island continental margin: an above-average year for "cool ocean" zooplankton.

Dave Mackas, Moira Galbraith, Doug Yelland and Kelly Young, Fisheries and Oceans Canada

Zooplankton time-series coverage of the Vancouver Island continental margin extends from 1979 to present for southern Vancouver Island (SVI), and from 1990 to present for northern Vancouver Island (NVI) (although with much lower sampling density and taxonomic resolution in 1991 to 1995). Samples are collected during DFO research surveys using vertical net hauls with black bongo nets (0.25 m^2 mouth area, 0.23 mm mesh aperture), from near-bottom to sea surface on the continental shelf and upper slope, and from 250 m to surface at deeper locations.

We estimate abundance and biomass for more than 50 zooplankton species in the SVI and NVI regions. In both regions, seasonal variability is intense and somewhat repeatable from year-to-year. However, because sampling dates vary from year to year, simple annual averages of observations confound seasonal with interannual differences. We deal with this by first estimating a multi-year average seasonal cycle (= "climatology") for each region, using the data from the start of each time series through 2005, and then using these climatologies as baselines against which we can then compare monthly conditions during any single year. To describe interannual variability, our approach has been to calculate within each year a regional, logarithmic scale biomass anomaly for each species and for each month that was sampled. We then average the monthly anomalies in each year to give an annual anomaly (see Mackas 1992 and Mackas et al. 2001 for mathematical details). It is important to note that the anomalies are log scale and therefore multiplicative on linear scale: an anomaly of +1 for a given taxon means that taxon had 10X higher biomass than in the climatology; an anomaly of -1 means the biomass was $1/10^{th}$ the climatology.

We have learned from our own and other west coast time series (Mackas et al. 2006) that zooplankton species with similar zoogeographic ranges and ecological niches usually have very similar anomaly time series. We therefore often summarize the interannual variability of multiple species by averaging within species groups. For example, the group 'boreal shelf copepods' is a composite of the copepods *Calanus marshallae*, *Pseudocalanus mimus*, and *Acartia longiremis,* all of which have distribution ranges that extend from southern Oregon to the Bering Sea. The group 'subarctic oceanic copepods' is a composite of *Neocalanus plumchrus*, *N. cristatus*, and *Eucalanus bungii*; all of which inhabit deeper areas of the subarctic Pacific and Bering Sea from North America to Asia. A third group, 'southern copepods' is a composite of five species with ranges centered about 1000 kilometers south of our study areas (either in the California Current and/or further offshore in the North Pacific Central Gyre).

The range of interannual biomass variability within a species or species group is about one log unit (i.e. factor of 10), and about 2-3 times greater than the interannual variability of total biomass. Anomalies often persist for several years and, in addition to the covariation within species groups mentioned above, there is strong covariation between some species groups. Fig.1 shows updated anomaly time series for the copepod species groups, as well as representative chaetognaths and euphausiids in the two outer coast statistical areas.

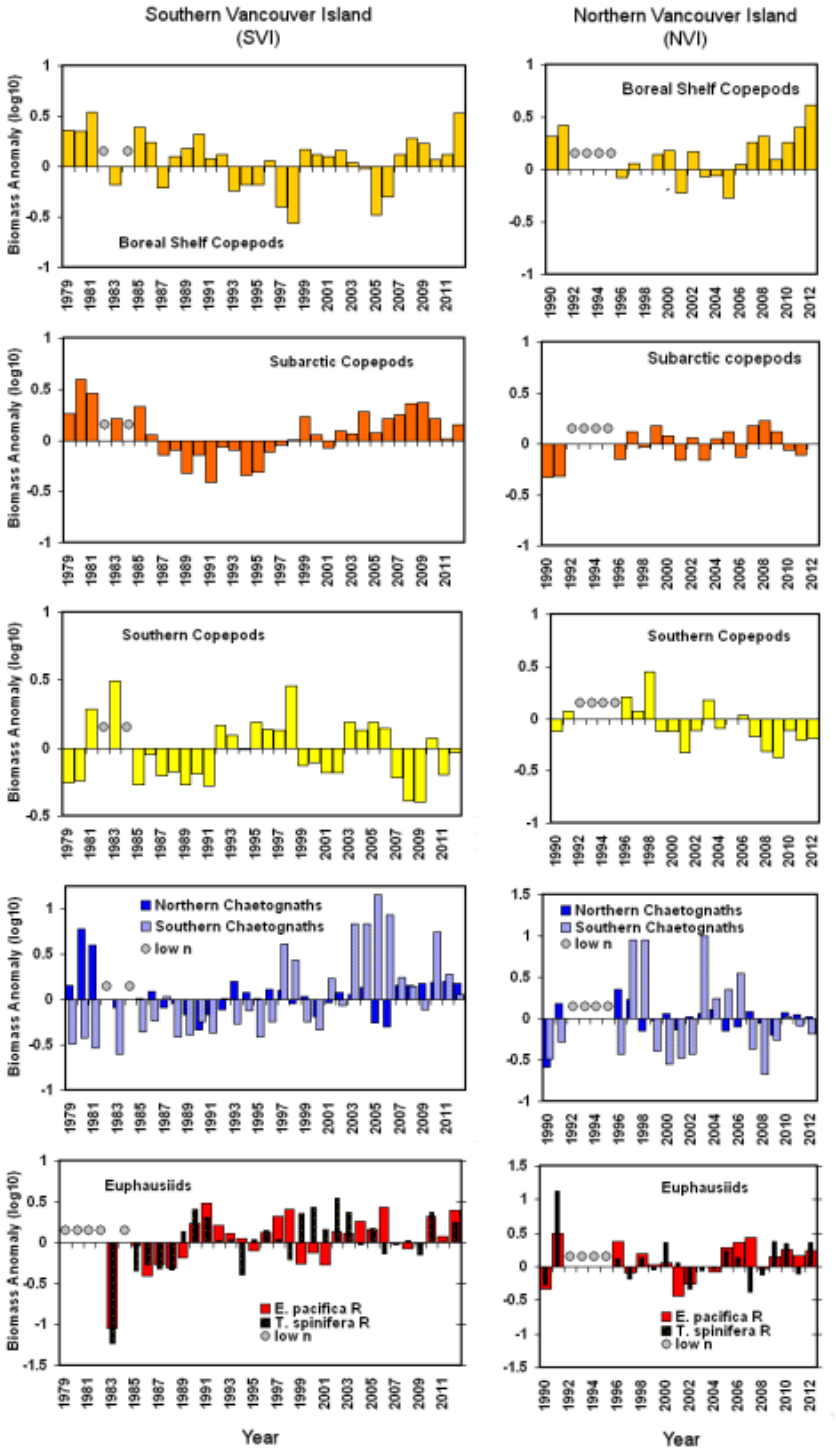

Figure 1. Zooplankton species-group anomaly time series (vs climatological baseline) for the SVI, and NVI regions. Bar graphs are annual log scale anomalies. Circles indicate years very few samples from that region. Cool years favor endemic 'northern' taxa, warm years favor colonization by 'southern' taxa.

Cool years such as the early 1980s, 1999-2002, and 2007-present tended to have positive anomalies of boreal shelf and subarctic copepods, and northern chaetognaths. Warm intervals such as 1983, 1993-1998, and 2004-2005 tend to have negative anomalies of these taxa, but

positive anomalies of southern copepods and southern chaetognaths. We now know that positive anomalies of the cool water zooplankton community off Vancouver Island are also associated with good local survival and growth of juvenile salmon, sablefish, and planktivorous seabirds (Mackas et al. 2007; M. Trudel, personal communication; Trudel et al.; Hipfner).

2012 was another cool year off the west coast. For both SVI and NVI, annual anomalies of the cool water copepod and chaetognath species groups remained positive in 2011 and 2012 (usually slightly more positive than in 2010, which was a weak El Niño year). 2012 had especially strong positive anomalies for the "boreal shelf copepod" group (highest since the early-mid 1980s). Conversely, the warm-water southern origin copepods and chaetognaths had negative anomalies, (but weaker than in 2007-2009). Euphausiid anomalies were positive and similar in magnitude to 2010.

References:

Mackas, D.L. 1992. The seasonal cycle of zooplankton off southwestern British Columbia: 1979-89. Can. J. Fish. Aquat. Sci. 49: 903-921.

Mackas, D.L., Batten, S., and Trudel, M. 2007. Effects on zooplankton of a warming ocean: recent evidence from the North Pacific. Progr. Oceanogr. 75: 223-252.

Mackas, D. L., Peterson, W. T., Ohman, M. D., and Lavaniegos, B. E. 2006. Zooplankton anomalies in the California Current system before and during the warm ocean conditions of 2005, Geophys. Res. Lett. 33, L22S07, doi:10.1029/2006GL027930.

Mackas, D.L., Thomson, R.E. and Galbraith, M. 2001. Changes in the zooplankton community of the British Columbia continental margin, and covariation with oceanographic conditions, 1985-1998. Can. J. Fish. Aquat. Sci. 58: 685-702.

2.1.14. Small-mesh bottom-trawl surveys west of Vancouver Island: update for 2012

R. Ian Perry, Dennis Rutherford, Ken Fong, Brenda Waddell, Fisheries and Oceans Canada

Bottom trawl surveys using a small-mesh net (targeting the Smooth Pink shrimp *Pandalus jordani*) have been conducted during May since 1973 in two regions, and since 1996 in three regions, off the west coast of Vancouver Island (Fig. 1). These regions, over which the total biomass of each species has been estimated, are generally bounded between the 100 m and 200 m depth contour lines for Areas 124 and 125 and the 50 m and 200 m contour lines for Area 121/123 (Fig. 2).

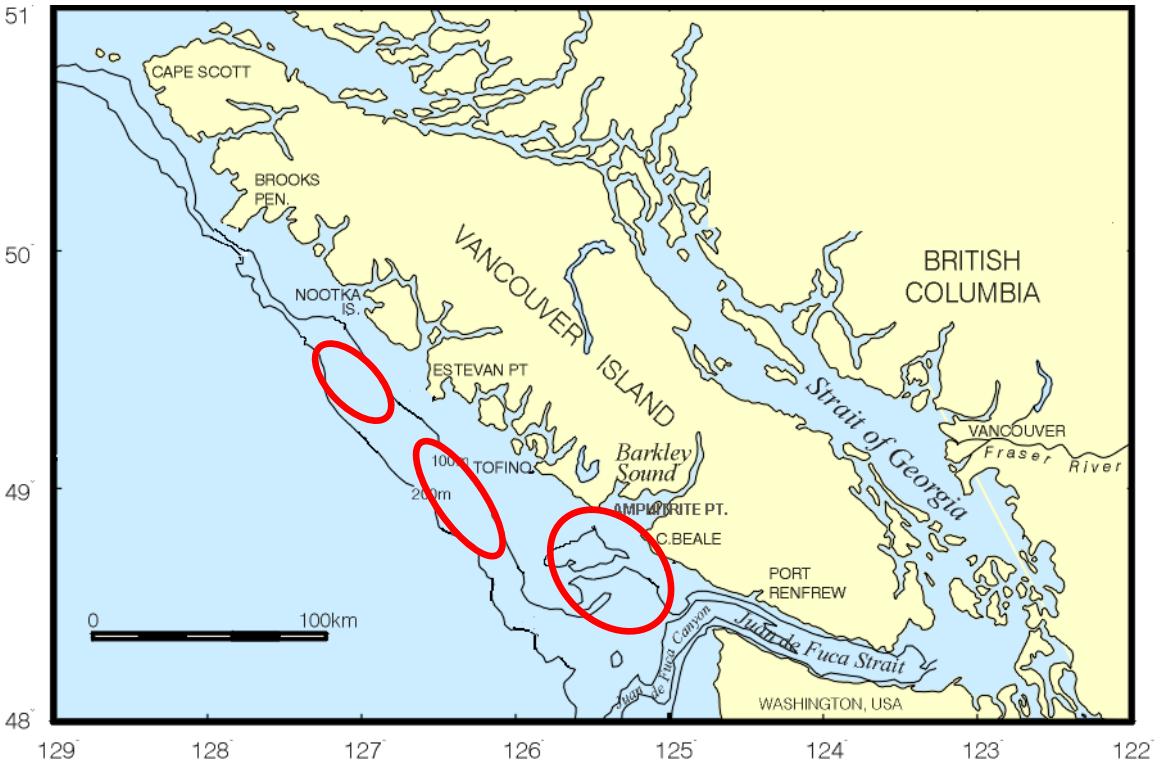

Figure 1. Map showing the three main shrimp (Pandalus jordani) fishing grounds off Vancouver Island (red ovals) considered in this report. The Nootka (Area 125) and Tofino (Area 124) Grounds are the northern and middle ovals, respectively, and have been surveyed since 1973. The southern oval represents the shrimp fishing grounds off Barkley Sound, surveyed since 1996.

This small-mesh bottom trawl survey was designed to target Smooth Pink Shrimp on the shrimp fishing grounds in a relatively small area off the west coast of Vancouver Island. Biomass estimates of other taxa caught along with Smooth Pink Shrimp may, or may not, be reliable depending on whether these other taxa are highly mobile in and out of the survey area or are highly patchy in their distribution. An autocorrelation analysis suggests that of the 36 taxa regularly sampled by this survey, 16 of them appear to be well-sampled (i.e. have positive autocorrelations of at least lag 1 year). Of those species shown in Fig. 3, all are well-sampled by this survey gear except for Spiny Dogfish and Pacific Hake (English Sole is marginally sampled by this survey).

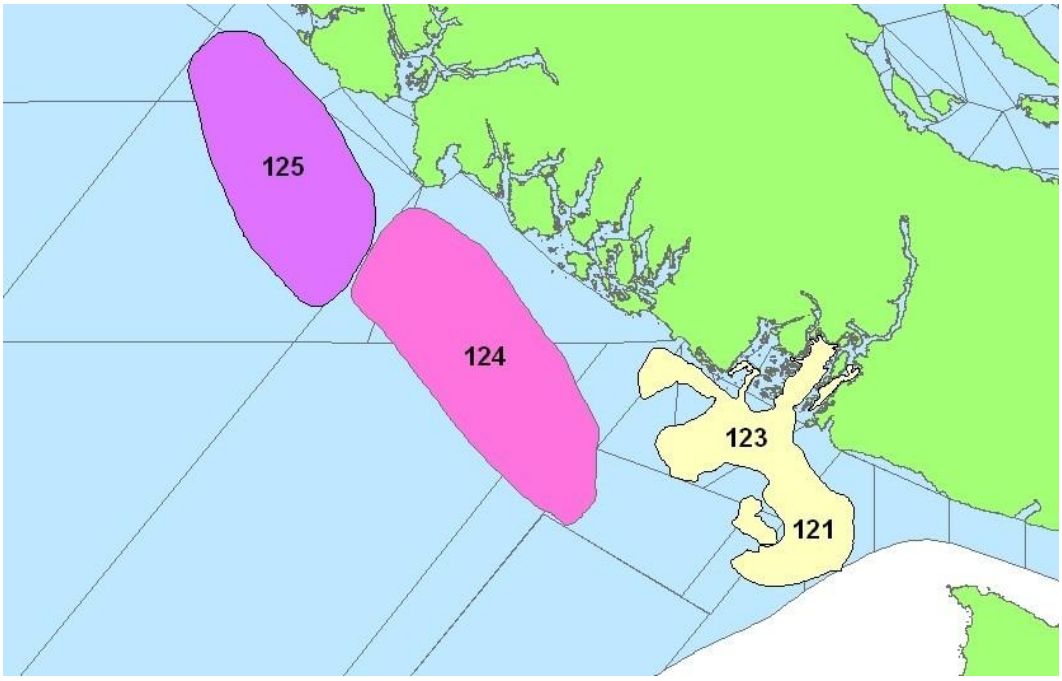

Figure 2. Areas used to calculate total abundances of each taxon. The numbers within each mask represent the Pacific Fisheries Management Statistical Area (shown by the blue lines in the figure). Area 125 is the Nootka ground, 124 is the Tofino ground, and 121 and 123 are the Barkley Sound grounds.

Surveys in May 2012 found the biomass of *Pandalus jordani* Shrimp off central Vancouver Island had increased from the low value in 2011 (Fig. 3). Pink Shrimp biomass in Areas 121-123 off Barkley Sound show roughly similar trends over time to those in Areas 124-125, although the biomass in 2012 was higher in Areas 121 and 123 than in previous recent years. The biomass of "core" flatfish species remained lower in all surveyed areas in 2012 compared with the early 2000's, but higher than during the 1970's and 1980's. The biomass of Walleye Pollock (*Theragra chalcogramma*, a cold water species) was particularly high in 2012 in Areas 124-125, and slightly higher in Areas 121-123, compared with previous years.

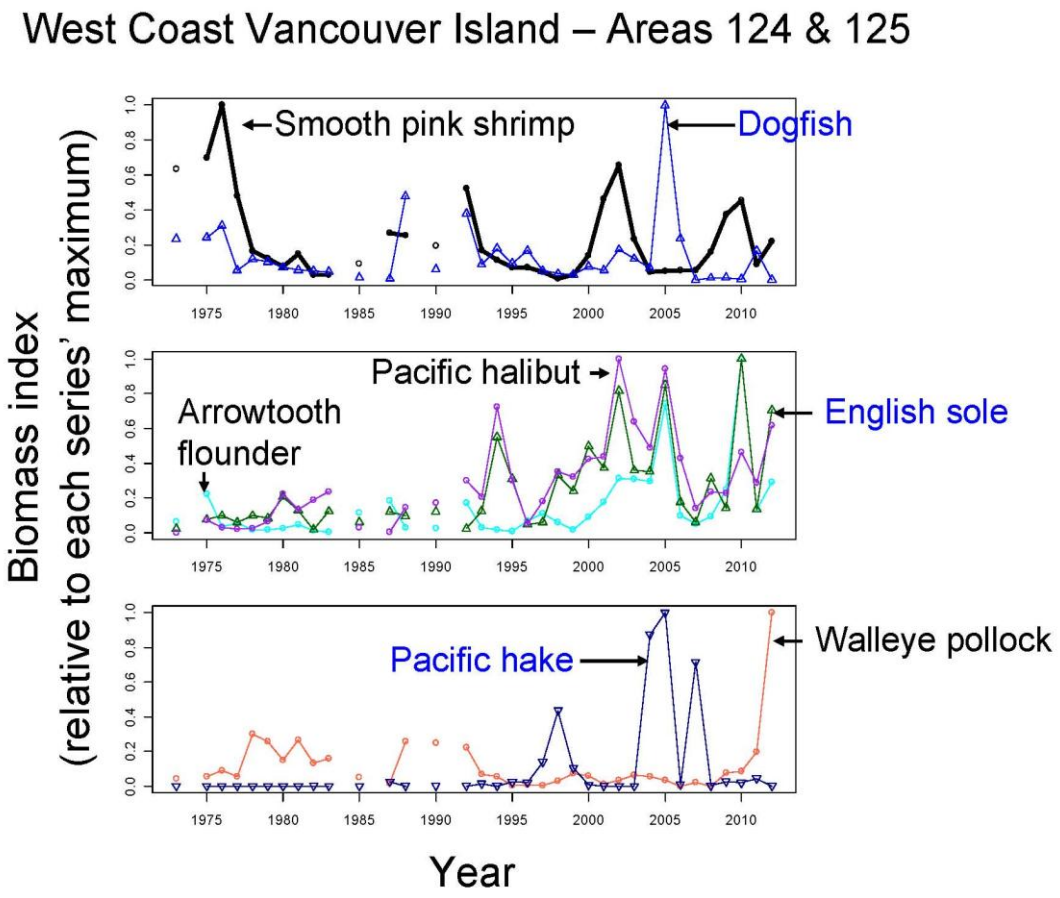

Figure 3. Time series of normalised (to maximum biomass) survey catches in Areas 124 and 125 of Smooth Pink Shrimp, dogfish, Pacific Halibut, Arrowtooth Flounder, English Sole, Pacific Hake and Walleye Pollock. Sampling was conducted in May of each year. Blue text identifies those taxa believed to be not well-sampled by the survey, based on an autocorrelation analysis.

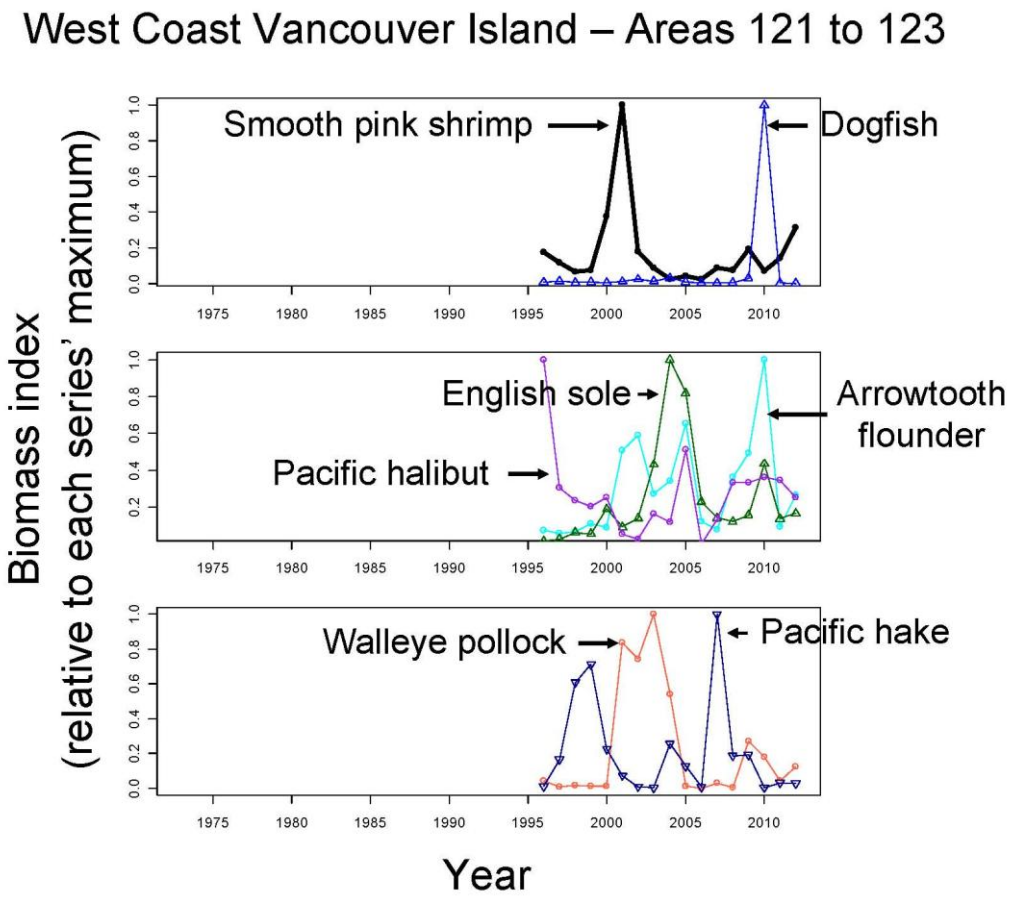

Figure 4. Time series of normalised (to maximum biomass) survey catches in Areas 121 and 123 (off Barkley Sound) of Smooth Pink Shrimp, dogfish, Pacific Halibut, Arrowtooth Flounder, English Sole, Pacific Hake and Walleye Pollock. Sampling was conducted in May of each year.

2.1.15. Eulachon

Jake Schweigert, Bruce McCarter, Chris Wood*, Doug Hay*, Jennifer Boldt, Tom Therriault, Heather Brekke, Fisheries and Oceans Canada, *DFO Emeritus

Description of indices

Three indices of Eulachon (*Thaleichthys pacificus)* population trends are: 1.) Eulachon catches occurring in annual offshore shrimp trawl surveys off the West Coast of Vancouver Island (WCVI, 1973-2012) and in Queen Charlotte Sound (QCS, 1998-2012), 2.) commercial Eulachon catches in the Fraser (1900-2004) and Columbia (1888-2010) River systems, and 3.) a spawning stock biomass estimate based on annual Fraser River Eulachon egg and larval surveys, 1995 to 2012 (http://www.pac.dfo-mpo.gc.ca/science/species-especes/pelagic-pelagique/herring-hareng/herspawn/pages/river1-eng.htm)

In the past, information from these indices was used to assess population trends and provide science advice regarding Eulachon catch recommendations. Offshore indices of juvenile Eulachon abundance, however, do not necessarily reflect the abundance of adult Eulachon that return to rivers (Schweigert et al. 2012).

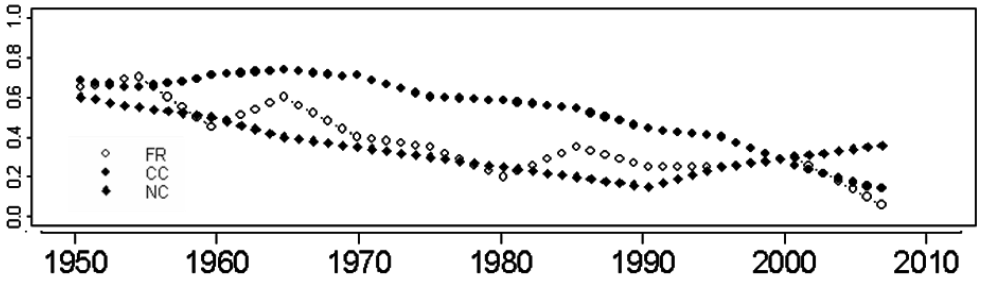

Figure 1. Estimated relative abundance trends for the three BC Eulachon designated units (DU); adapted from Schweigert et al. (2012). FR = Fraser DU, CC = central coast DU, NC = Nass/Skeena DU (symbols with post-1990 increasing trend). Y-axis is expressed in unit-less, relative values.

Status and trends

Eulachon have experienced long-term declines in many rivers throughout their distribution from California to Alaska. Indices of Eulachon abundance in central and southern British Columbia rivers remain at low levels (Fig. 1). The estimated Eulachon spawning stock biomass in the Fraser River decreased during 1994-2010 with slight increases in 2011 and 2012 (Fig. 2; note the y-axis is on a log-scale). The spawning stock biomass has been below the action level (a management-derived level, below which steps are implemented to ensure conservation, 150 tonnes) since 2004. The biomass in the Fraser River will be estimated by an egg and larval survey in April-May, 2013. Catches in the Columbia River system decreased dramatically in the early-1990s. Columbia River Eulachon were federally-listed in the U.S.A. as threatened under the Endangered Species Act (ESA) effective May 17, 2010 and all Eulachon-directed fisheries were closed in 2011 (http://www.nmfs.noaa.gov/pr/pdfs/fr/fr75-13012.pdf).

The Committee on the Status of Endangered Wildlife in Canada (COSEWIC) assessed Eulachon in BC as three populations (or designated units): the Central Pacific coast population and Fraser River populations were assessed as endangered, and the Nass/Skeena Rivers population is currently being reassessed (COSEWIC 2011, Schweigert et al. 2012). A recovery potential assessment is completed and available online (Schweigert et al. 2012; http://www.dfo-mpo.gc.ca/csas-sccs/Publications/ResDocs-DocRech/2012/2012_098-eng.html).

Factors causing those trends

It is unknown what caused declining trends in Eulachon abundance. Schweigert et al. (2012) state that "No single threat could be identified as most probable for the observed decline in abundances among DUs or in limiting recovery. However, mortality associated with coastwide changes in climate, fishing (direct and bycatch) and marine predation were considered to be greater threats at the DU level, than changes in habitat or predation within spawning rivers."

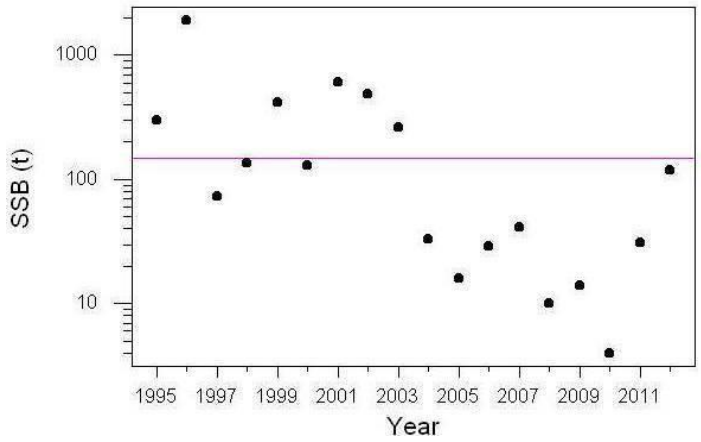

Figure 2. Estimated spawning stock biomass (SSB in tonnes) of Eulachon in the Fraser River, 1995-2012. Y-axis is on a log-scale. Horizontal line shows 150-tonne action level.

Implications of those trends

Reduced biomass of eulachon has negative implications for First Nations and commercial fishers. Eulachon are socially and culturally significant to local First Nations and are fished by First Nations, recreational and commercial fishers.

Reduced Eulachon abundance also likely has negative impacts on their predators. Important predators of Eulachon include: marine mammals particularly sea lions in the estuarie, and porpoises, Chinook and Coho Salmon, Spiny Dogfish, Pacific Hake, sturgeon, Pacific Halibut, Walleye Pollock, sablefish, rockfish, Arrowtooth Flounder (Levesque and Therriault 2011). Diet data time series of all animals in the ecosystem would improve our ability to examine temporal trends in predator-prey interactions and the implications of those trends.

Sources of Information

COSEWIC. 2011. COSEWIC assessment and status report on the Eulachon, Nass/Skeena Rivers population, Central Pacific Coast population and the Fraser River population *Thaleichthys pacificus* in Canada. Committee on the Status of Endangered Wildlife in Canada. Ottawa. xv + 88 pp. http://www.sararegistry.gc.ca/virtual_sara/files/cosewic/sr_eulachon_0911_eng.pdf.

Hay, D.E., Wes, K.C., and Anderson, A.D. 2003. Indicators and 'response' points for management of Fraser River eulachon: a comparison and discussion with recommendations. DFO Can. Sci. Advis. Sec. Res. Doc. 2003/051 ii + 44p. http://www.dfo-mpo.gc.ca/CSAS/Csas/DocREC/2003/RES2003_051_e.pdf

Levesque, C.A. and Therriault, T.W. 2011. Information in Support of a Recovery Potential Assessment of Eulachon (*Thaleichthys pacificus*) in Canada. DFO Can. Sci. Advis. Sec. Res. Doc. 2011/101 viii + 71p. http://www.dfo-mpo.gc.ca/Csas-sccs/publications/resdocs-docrech/2011/2011_101-eng.pdf

Schweigert, J., Wood, C., Hay, D., McAllister, M., Boldt, J., McCarter, B., Therriault, T.W., and Brekke, H. 2012. Recovery Potential Assessment of Eulachon (*Thaleichthys pacificus*) in

Canada. DFO Can. Sci. Advis. Sec. Res. Doc. 2012/098. Vii + 121p. http://www.dfo-mpo.gc.ca/csas-sccs/Publications/ResDocs-DocRech/2012/2012_098-eng.html

2.1.16. Herring

Jennifer Boldt, Jaclyn Cleary, Jake Schweigert , Kristen Daniel, Charles Fort, Ron Tanasichuk, Matt Thompson, Fisheries and Ocean Canada

Description of indices

Model estimates of Pacific Herring biomass, based on commercial and test fishery biological samples (age, length, weight, sex, etc.), Herring spawn dive survey data, and commercial harvest data, provide an index of Herring population trends for five major fishing stocks: Strait of Georgia (SOG), west coast of Vancouver Island (WCVI), Prince Rupert District (PRD), Haida Gwaii (HG; previously referred to as the Queen Charlotte Islands stock), and the central coast (CC), and two minor stocks (Area 2W and Area 27) (DFO 2012; Fig. 1).

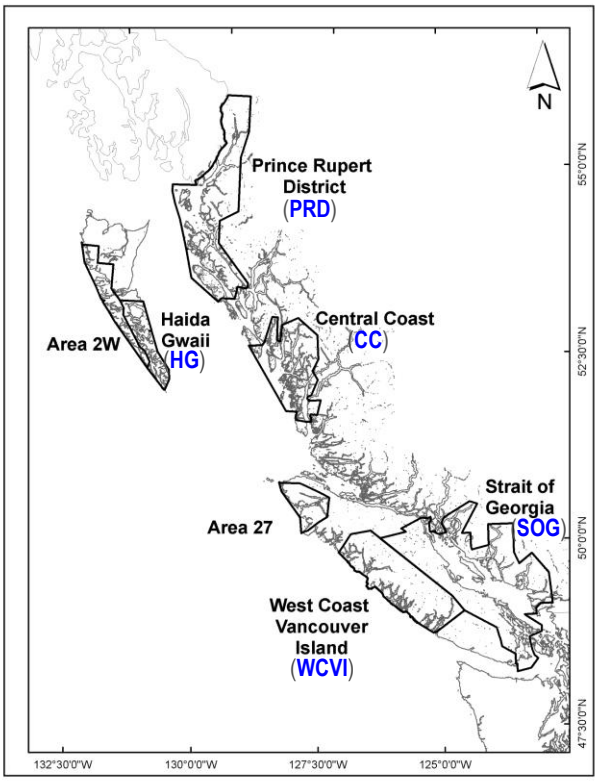

Figure 1. Location of the five major (Strait of Georgia, west coast of Vancouver Island, Prince Rupert, Haida Gwaii, and the Central Coast) and two minor (Area 2W and Area 27) Pacific Herring fishing stocks in British Columbia.

In 2012, an integrated statistical catch-age model provided biomass estimates for Pacific Herring (DFO 2011). A second index is an annual, offshore survey that provides an index of recruitment to the WCVI and the SOG herring stocks, based on the catch-per-unit-effort (CPUE)-weighted proportion of age-3 pre-recruit herring in their common summer feeding area off the WCVI (both these stocks occupy the WCVI region in summer). A third index of herring recruitment trends is obtained with the juvenile herring survey conducted annually in the SOG and CC (*not updated here*). These three indices provide information on population trends and inform Fisheries and Oceans Canada science advice regarding catch recommendations.

Status and trends

West Coast Vancouver Island (WCVI): Herring biomass off the WCVI has experienced continual declines since the late 1980s. Current low levels of biomass are consistent with levels observed in the late 1960s following the reduction fishery (1951-1968), despite the absence of commercial fishing for the majority of the past decade (DFO 2012; Fig. 2).

Biomass estimates in 2012 were similar to low levels observed since 2006 and, in 2012 (Fig. 2), are below the fishery threshold (14,067 tonnes). Since about 1977, the recruitment of Herring off the WCVI has been generally poor, interspersed with a few good year-classes (Fig. 3). Recruitment in 2012 was poor and results from the summer 2012 off-shore trawl survey indicate poor recruitment for 2013. There has been little evidence of stock recovery in this area, despite the absence of commercial fishing since 2006. WCVI Herring weight-at-age has declined since the mid-1970s or mid-1980s (Fig. 4).

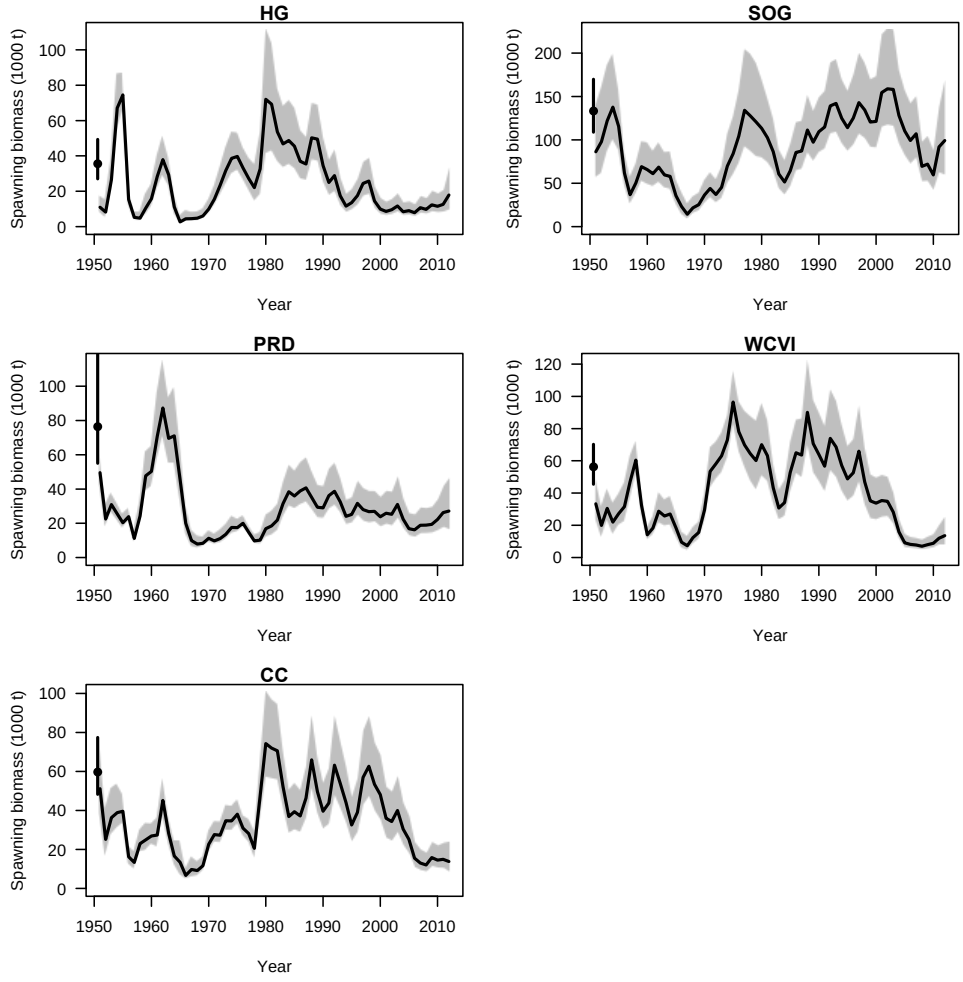

Figure 2. Median posterior density estimates of spawning stock biomass (Bt) for the five major stock areas, 1950-2012. Biomass is in thousands of metric tonnes (Bt) and scales differ between panels. The shaded envelope represents 90% of the distribution in estimates of Bt. Dark circle and extending vertical lines (at year 1950) represent the median estimates of unfished biomass, for the entire time series, and their distribution, for the major stocks only.

Strait Of Georgia (SOG): The biomass of Herring in the SOG reached near historic high levels from 2002-2004 at over 100,000 tonnes (Cleary and Schweigert 2010; Fig. 2). Current spawning

biomass is still relatively high and is well above the fishery threshold (33,318 tonnes). Since 1995, recruitment to this stock has been average or good except in 2008 and 2010 (Fig. 3). In 2012, recruitment was good and the summer off-shore trawl survey indicates average recruitment for 2013. SOG herring weight-at-age has declined since the mid-1970s (Fig. 4).

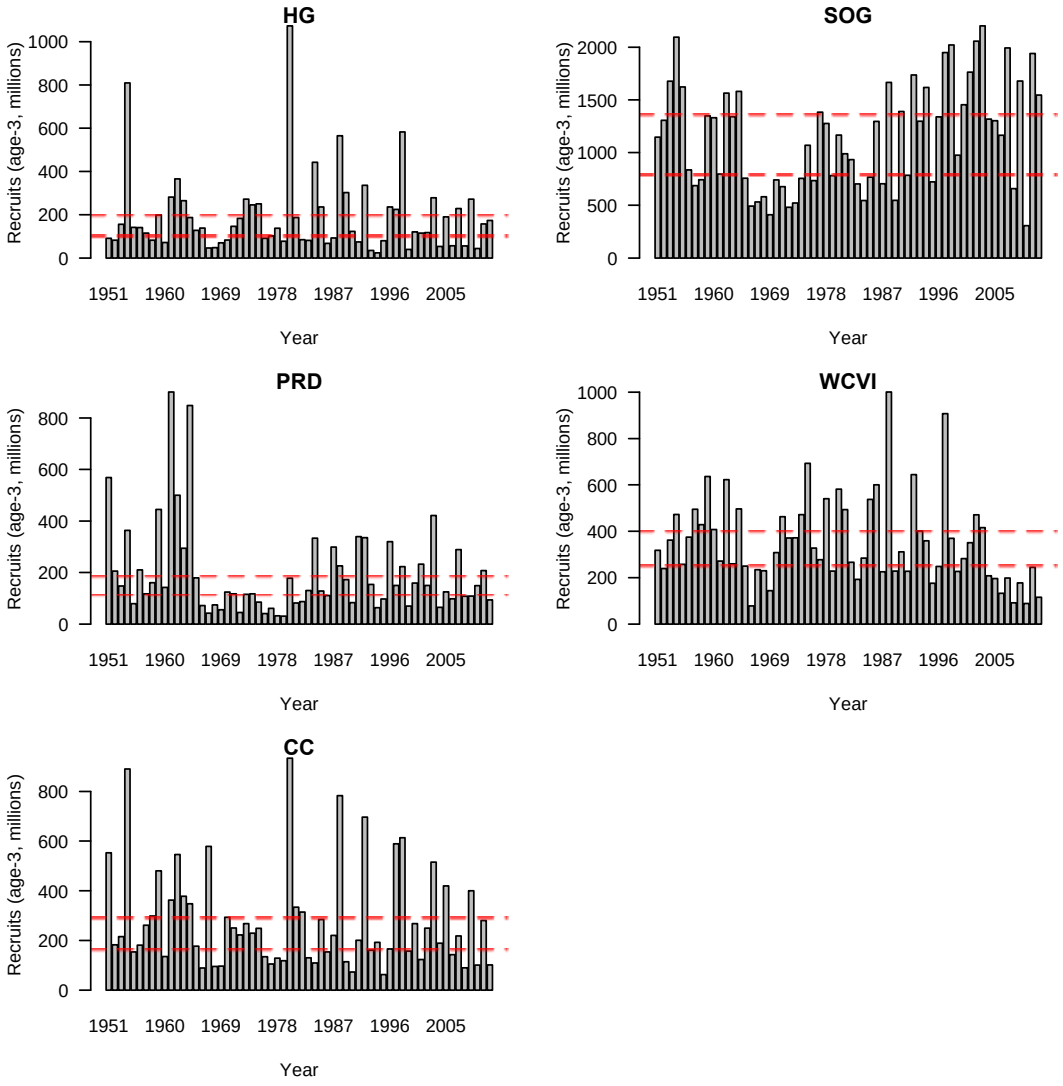

Figure 3. Estimated numbers of age-3 recruits presented for each of the five major stock areas, 1951-2012. Lower horizontal dashed red line represents lower 33rd percentile of recruits; upper horizontal dashed line represents upper 67th percentile of recruits. Dashed lines demark recruitment categories of poor, average and good. Note: scales differ between panels.

Prince Rupert (PRD), Haida Gwaii (HG), and Central Coast (CC): Exploitable herring biomass in the Pacific North Coast Integrated Management Area (PNCIMA) region represents a combination of migratory stocks from the HG, PRD and CC areas (DFO 2012). Herring biomass in HG (Fig. 2) was at low, stable levels during the past decade; small increases in 2011 and 2012 resulted in biomass estimates similar to the fishery threshold (8,892 tonnes). The biomass in the CC decreased during the past 13 years and is currently below the fishery threshold (14,930 tonnes). The biomass in PRD has remained relatively stable (Fig. 2), and is above the fishery threshold (19,107 tonnes). PRD, HG, and CC herring weight-at-age has declined since the mid-1970s (Fig. 4).

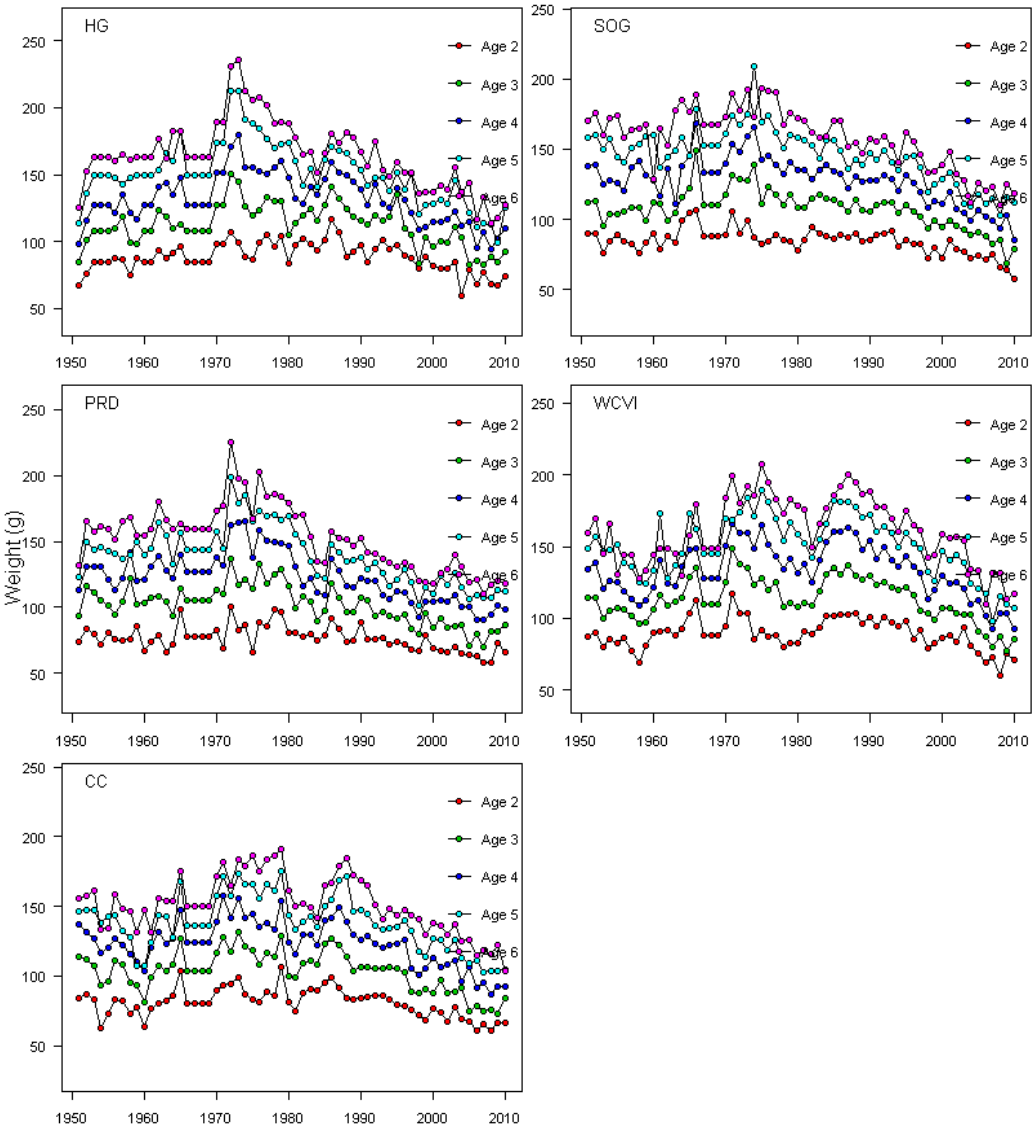

Figure 4. Weight-at-age (ages 2-6) of Pacific Herring in the five major fishing stocks in British Columbia (1951-2010).

Factors causing those trends

The biomass of three major fishing stocks (HG, CC, WCVI) have been below fishery thresholds in recent years (Schweigert et al. 2009; DFO 2012) despite being closed to fishing; whereas, two areas that are open to fishing have stable or high biomass estimates (PRD, SOG). Consideration of these biomass trends in combination with the declining trend in herring weight-at-age observed for all fishing stock areas, suggests that factors other than fishing may be influencing Herring population trends. Changes in food supply and quality, predator abundance, and competition are factors that could affect trends in herring biomass and weight-at-age (Schweigert et al. 2010; Hay et al. 2012).

Pacific Herring are zooplanktivorous, consuming primarily euphausiids (krill) and some copepods (Wailes 1936). Changes in ocean conditions, such as temperature or currents, could affect the amount and types of prey available. For example, a northerly current direction could

result in the presence of California current waters off the WCVI, bringing California Current zooplankton species that have a lower energetic value, creating poorer feeding conditions for herring (Schweigert et al. 2010, Mackas et al. 2004). In addition, Tanasichuk (2012) relates WCVI herring recruitment to the biomass of euphausiids.

There are a wide variety of herring predators, including Pacific Hake, lingcod, Spiny Dogfish, Pacific Cod, sablefish, Arrowtooth Flounder, Pacific Halibut, Steller Sea Lions, Northern Fur Seals, Harbour Seals, California Sea Lions, and Humpback Whales (Schweigert et al. 2010). Off the WCVI, fish predator abundance has decreased in recent years, while the abundance of most marine mammal predators has increased (Olesiuk 2008, Olesiuk et al. 1990). This has resulted in a relatively stable or slightly decreasing trend in the amount of WCVI herring consumed by predators since 1973 (Schweigert et al. 2010). Although a significant proportion of the herring population could be cropped annually by predation, trends in natural mortality of WCVI Herring were not found to be directly attributable to trends in estimates of predation (Schweigert et al. 2010). Herring recruitment, however, has been correlated with piscivorous hake biomass (piscivorous hake are those hake that are large enough to consume herring), suggesting predation may be an important factor influencing WCVI Herring recruitment (Tanasichuk, 2012).

Competition may also be a factor affecting Herring population trends. Since the late 1990s, a substantial component of the Pacific Sardine population off the west coast of North America has migrated into Canadian waters annually (Schweigert et al. 2009). Reduced survival of adult Herring is most pronounced in areas exposed to offshore influences (WCVI, HG, and to a lesser extend CC; Schweigert et al. 2010), where sardine migrate. The large increases in Pacific Sardine in the early 1990s to 2000s in Canadian waters may have increased competition for food with herring, and/or attracted predators (Schweigert et al. 2010). A Strategic Program for Ecosystem-Based Research and Advice (SPERA) project was funded (2012/13) to assess the impact of increasing Sardine abundance on the current depressed Herring populations.

Implications of those trends

Pacific Herring comprise an important component of commercial fisheries in British Columbia. Estimated biomass of herring relative to the commercial fishery threshold has implications for herring fisheries. The biomass forecasts for SOG and PRD herring were above fishery thresholds; therefore these areas are open to commercial harvest for the 2012/13 season (DFO 2012). Following the herring harvest control rule, the maximum available harvest is based on a 20% harvest rate of the mature herring biomass (Cleary and Schweigert 2010). Biomass estimates for HG, CC and WCVI stocks all remain at relatively low stock abundance levels. Biomass forecasts for HG and CC stocks are below the fishery threshold and commercial harvest is not recommended for 2012/13 in these areas. The long-term recommendation for management of HG, CC and WCVI stocks is the development of stock rebuilding strategies.

Trends in herring biomass have implications for herring predators, such as fish, marine mammals and seabirds. The relative importance of herring in each predator's diet varies; however, herring may represent up to 88% of lingcod diet (Pearsall and Fargo 2007), 40 % of Pacific Cod and Pacific Halibut diets (Ware and McFarlane 1986), and 35% - 45% of pinniped diets (Olesiuk et al. 1990, Womble and Sigler 2006, Trites et al. 2007, Olesiuk 2008). Depending on the level of diet specialization and ability to switch to alternate prey, herring abundance and condition may affect predators' growth and abundance. Time series of diets of animals in this ecosystem would improve our ability to examine temporal trends in predator-prey interactions and implications of those trends.

Sources of Information

Cleary, J.S. and Schweigert, J.F. 2012. Stock Assessment and Management Advice for the British Columbia Herring Stocks: 2010 Assessment and 2011 Forecasts. DFO Can. Sci. Advis. Sec. Res. Doc. 2011/115. viii + 90p.

DFO. 2011. Stock assessment report of Pacific herring in British Columbia in 2011. DFO Can. Sci. Advis. Sec. Sci. Advis. Rep. 2011/061.

DFO. 2012. Stock Assessment Report on Pacific Herring in British Columbia in 2012. DFO Can. Sci. Advis. Sec. Sci. Advis. Rep. 2012/062.

Hay, D., J. Schweigert, J., Boldt, J., Cleary, J., Greiner, T.A., and Hebert, K. 2012. Decrease in herring size-at-age: a climate change connection? In Irvine, J.R. and Crawford, W.R. 2012. State of the physical, biological, and selected fishery resources of Pacific Canadian marine ecosystems in 2011. DFO Can. Sci. Advis. Sec. Res. Doc. 2012/072. xi +142 p. pages 66-69

Mackas, D.L., W.T. Peterson, and J.E. Zamon. 2004. Comparisons of interannual biomass anomalies of zooplankton communities along the continental margins of British Columbia and Oregon. Deep-Sea Research II 51: 875-896.

McFarlane, G. A., Schweigert, J., MacDougall, L., and Hrabok, C. 2005. Distribution and biology of Pacific sardine (*Sardinops sagax*) off British Columbia, Canada. California Cooperative Oceanic Fisheries Investigations Reports, 46: 144–160.

Olesiuk, P. F. 2008. Abundance of Steller sea lions (*Eumatopias jubatas*) in British Columbia. DFO Can. Sci. Advis. Sec.Res. Doc. 2008/063. iv + 29p.

Olesiuk, P. F., Bigg, M. A., Ellis, G. M., Crockford, S. J., and Wigen, R. J. 1990. An assessment of the feeding habits of harbour seals (*Phoca vitulina*) in the Strait of Georgia, British Columbia, based on scat analysis. Canadian Technical Report of Fisheries and Aquatic Sciences 1730. 135 pp.

Pearsall, I. A., and Fargo, J. J. 2007. Diet composition and habitat fidelity for groundfish assemblages in Hecate Strait, British Columbia. Canadian Technical Report of Fisheries and Aquatic Sciences, 2692.

Schweigert, J.F., Boldt, J.L., Flostrand, L., and Cleary, J.S.. 2010. A review of factors limiting recovery of Pacific herring stocks in Canada. ICES J. Mar. Sci. 67:1903-1913.

Schweigert, J., Christensen, L. B., and Haist, V. 2009. Stock assessments for British Columbia herring in 2008 and forecasts of the potential catch in 2009. DFO Can. Sci. Advis. Sec. Res. Doc. 2009/019. iv + 61 p.

Tanasichuk, R. 2012. Euphausiids and west coast Vancouver Island fish production. In Irvine, J.R. and Crawford, W.R. 2012. State of the physical, biological, and selected fishery resources of Pacific Canadian marine ecosystems in 2011. DFO Can. Sci. Advis. Sec. Res. Doc. 2012/072. xi +142 p. pages 47-49.

Trites, A. W., Calkins, D. G., and Winship, A. J. 2007. Diets of Steller sea lions (*Eumatopias jubatus*) in southeast Alaska, 1993–1999. Fishery Bulletin, 105: 234–248.

Wailes, G. H. 1936. Food of *Clupea pallasi* in southern British Columbia waters. Journal Biological Board of Canada, 1: 477–486.

Ware, D. M., and McFarlane, G. A. 1986. Relative impact of Pacific hake, sablefish and Pacific cod on west coast of Vancouver Island herring stocks. International North Pacific Fisheries Commission Bulletin, 47: 67–78.

Womble, J. N., and Sigler, M. F. 2006. Seasonal availability of abundant, energy-rich prey influences the abundance and diet of a marine predator, the Steller sea lion *Eumatopias jubatus*. Marine Ecology Progress Series, 325: 281–293.

2.1.17. Sardine

Linnea Flostrand, Jennifer Boldt, Jake Schweigert, Vanessa Hodes, Fisheries and Oceans Canada

Description of indices

Indices of Pacific Sardine (*Sardinops sajax*) population trends are based on an annual surface trawl survey by DFO off the west coast of Vancouver Island (WCVI), a population stock assessment led by scientists in the United States (U.S.) and commercial sardine landings from British Columbia (B.C.) waters. Annual WCVI catch per unit effort (CPUE) and commercial catch estimates are applied to estimate the regional biomass of Sardines in Canadian waters. The WCVI survey began in 1997, and switched to night-time sampling in 2006, after a 2005 survey found the mean results of day and night sampling to be comparable but day sampling had greater variance. Results from the WCVI survey and the U.S. assessment of the population are used to estimate sardine migration rates into B.C. waters (Figs. 1-3). This information has been used to forecast subsequent seasonal abundance and to advise on recommended catch levels (e.g. DFO 2012).

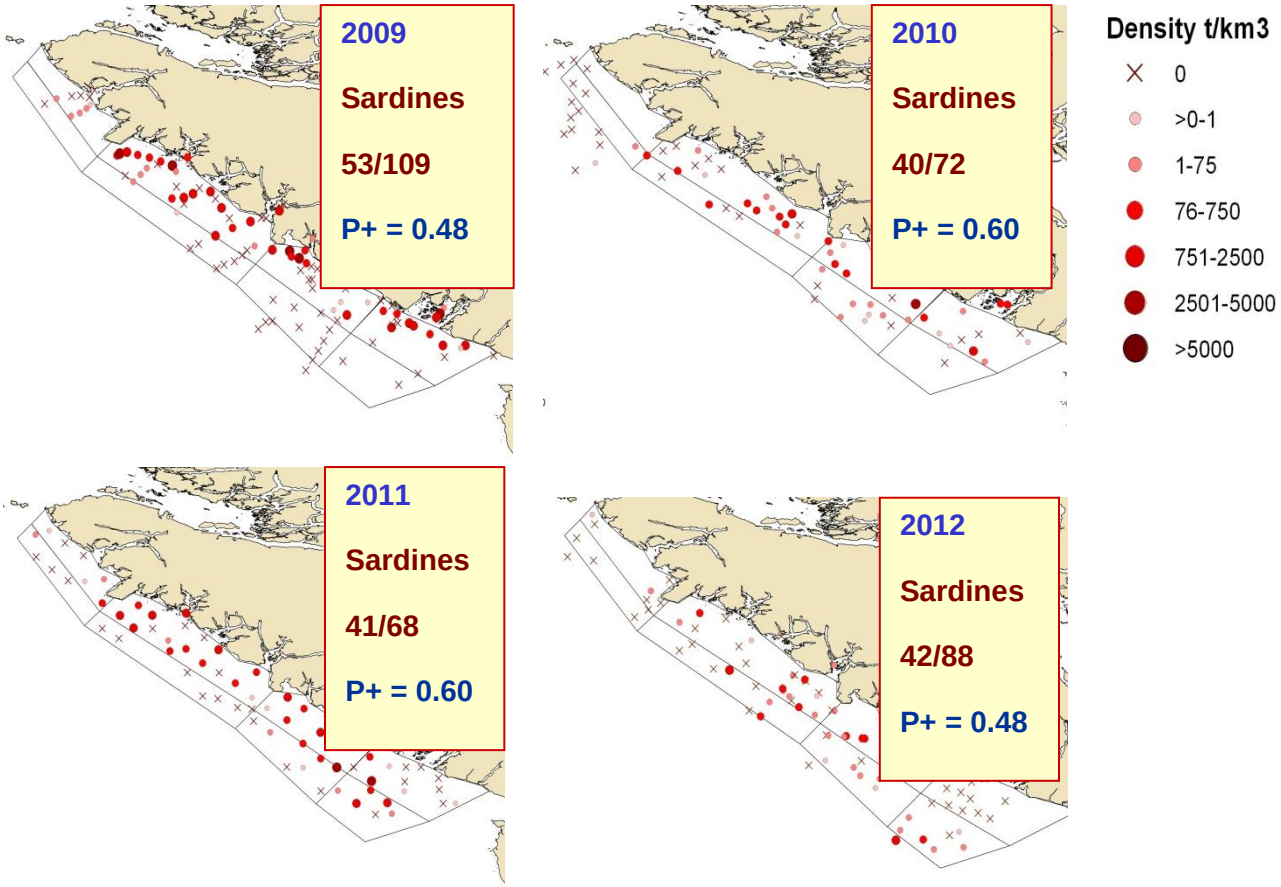

Figure 1. West coast of Vancouver Island (WCVI) summer trawl survey sampling locations and relative sardine catch densities for 2009-2012 (tonnes per km^3 trawled). P+ = the fraction of tows where sardine were caught.

Status and trends

Pacific Sardine is a migratory species, annually migrating between southern California where they spawn during winter and spring months to the rich feeding areas off WCVI where they mainly forage during summer and fall months; the older and larger fish tend to move even further north (Clark and Janssen 1945, Flostrand et al. 2011). The B.C. sardine fishery collapsed in 1947 and the California fishery collapsed by the early 1950s. Sardine returned to southern Vancouver Island waters in 1992 after a 45-year absence, and expanded their seasonal distribution northward throughout the west coast of Vancouver Island, Hecate Strait and Dixon Entrance by 1998 (McFarlane et al. 2001). In 2012, WCVI survey catch densities of Sardine decreased considerably from 2011 and density estimates were lower than other observations since 2006 (Fig. 1). The extremely low densities (with a mean that approximately half of the mean for 2010) may be due to a combination of survey timing and unfavourable oceanographic conditions as well as decreased population abundance (Fig. 2).

The most recent U.S. Sardine assessment suggests that the biomass in the California Current (Northeast Pacific) Sardine population off the U.S., Canada and northwest Baja Peninsula increased rapidly through the 1980s and 1990s, peaking at approximately 1,300,000 tonnes in 1999, and in 2006 and 2007 (Hill et al. 2012, Fig. 3). The population assessment shows declines from 2006 to 2012, which may be related to declines in mean WCVI Sardine densities and migration rate estimates (Fig. 2). The most current population biomass estimate for age 1 year and older sardine is approximately 660,000 tonnes (as of July 2012).

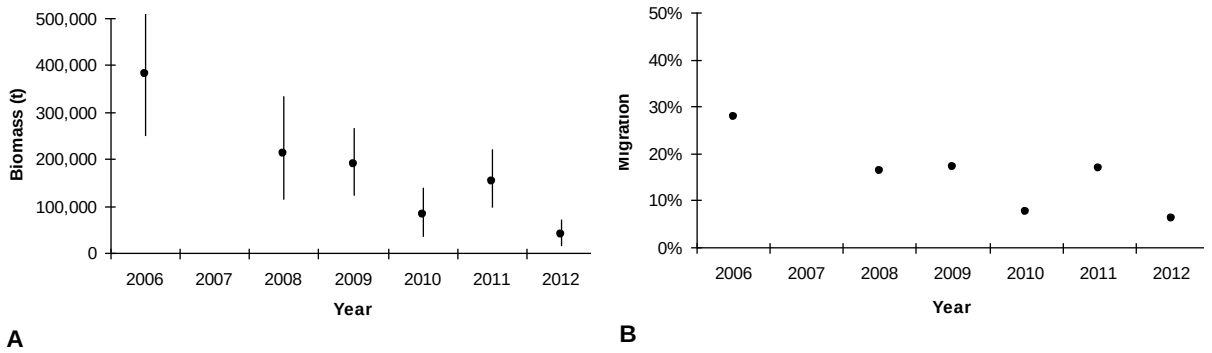

Figure 2. West coast of Vancouver Island (WCVI) summer trawl survey 2006, 2008-2012 (A) biomass estimates and 90% confidence intervals, and (B) migration rate estimates (calculated by year as WCVI biomass (panel A means) divided by age 1+ population biomass (Fig. 3 below from Hill et al., 2012). Migration rates are estimates of the proportions of the adult population that seasonally migrate into waters off the WCVI by mid summer when the DFO survey is conducted (late July/early August).

In B.C., commercial purse seine fishing for Sardine has been conducted in sheltered waters (especially inlets) along the southern central coast, within Queen Charlotte Strait and Queen Charlotte Sound, and the WCVI, represented by several Pacific Fishery Management Areas (PFMAs, Table 1, Fig. 4). Relatively small proportions of the annual total allowable catches were realized during initial years following the re-opening of the commercial fishery in 2002, due, in part, to modest Sardine markets at the time and competing fisheries for vessel and plant resources. Most B.C. waters have been open to commercial Sardine fishing except where there are permanent fishing closures or bycatch concerns. In 2012, the total sardine catch from B.C. waters was 20,621 tonnes, approximately 95% of the total allowable catch of 21,917 tonnes. All commercial harvest occurred off the WCVI, with the majority of catch coming from Pacific Fishery Management Areas 23, 25 and 123.

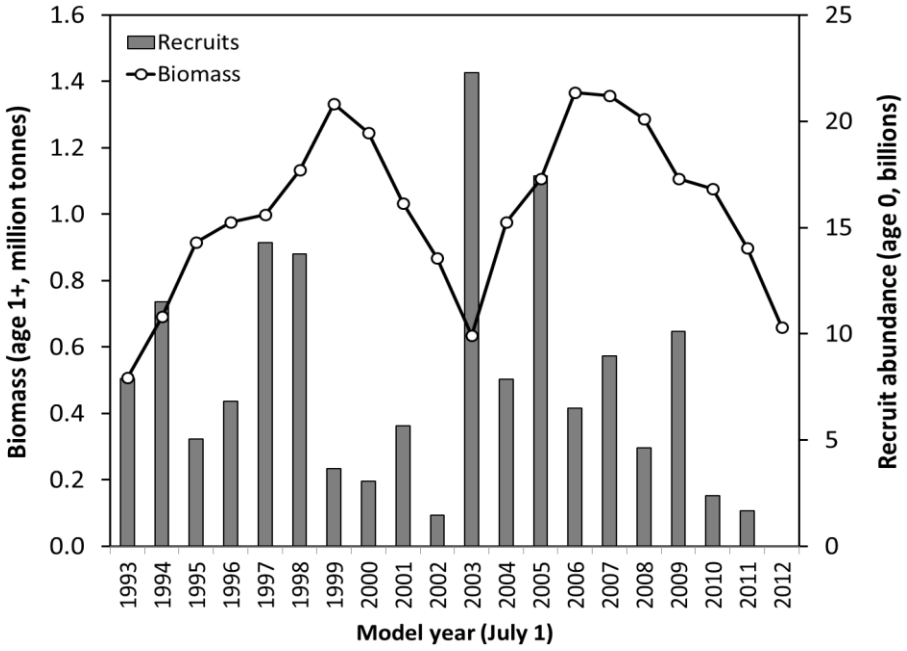

Figure 3. Abundance trends for spawning stock (age 1 year and older) biomass (line plot, left axis millions of tonnes) and year-class strength (bar plot, right axis billions of age-0 fish). Information from Hill et al. 2012, model "X6e").

Factors causing trends in abundance and distribution

Historical Sardine abundance has been extremely variable along the US and Canadian west coast, cycling over approximately 60-year periods (Cushing 1971, Hill et al. 2011). The abundance of Sardines and the timing of their annual northward migration are influenced, in part, by environmental factors and stock size, age and size composition and recruitment relationships that are not well understood (Lo et al. 2010, Hill et al. 2012). The decline in Sardine biomass in the late 1940s was attributed to environmental conditions and overfishing (Clark and Marr 1955, Jacobson and MacCall 1995). During cold years, such as in the 1950s to 1970s, Sardine productivity was low and their distribution was contracted in the southern part of their range (Hill et al. 2011, Jacobson and MacCall 1995). Recent warm years, associated with increased Sardine productivity (Jacobson and MacCall 1995) and larger stock size have resulted in a more northerly seasonal distribution of the stock (McFarlane et al. 2001, Hill et al. 2011, Zwolinski et al. 2011, Zwolinski et al. 2012).

Implications of those trends

The resurgence of a B.C. sardine fishery began in 1995 as experimental until a commercial designation in 2002, with only a small proportion of the total allowable catch (TAC) being harvested in the early years. More recently (2008-2012) commercial B.C. Sardine landings have increased (10,435-22,538 tonnes) and, with increases in population and seasonal abundance estimates in 2011 (Fig. 2), the TAC for the 2012 fishing season was 27,279 tonnes, which was the highest level since the fishery re-opened after the population collapsed in the 1950s (Table 4). Approximately 70% of the 2012 TAC was landed.

In British Columbia waters, Pacific Sardine are consumed by a variety of fish, such as Coho and Chinook Salmon (Chapman 1936), Spiny Dogfish and other sharks, Albacore Tuna and other tuna, Pacific Hake, jack mackerel as well as by marine mammals, such as Humpback Whales, California Sea Lions and other pinnipeds. Historically, Sardine populations have undergone

extreme variations in abundance and it is likely that predators have adapted to utilize this resource when it is abundant. Time series of diets of animals in this ecosystem would improve our ability to examine temporal trends in predator-prey interactions and the implications of those trends.

Table 1. Annual Sardine total allowable catch (TAC) and purse seine landings in British Columbia (B.C.) by Pacific Fishery Management Area (PFMA) for 2006-2012 (in tonnes).

Region	**Year:**	**2006**	**2007**	**2008**	**2009**	**2010**	**2011**	**2012**
B.C.	TAC:	13,500	19,800	12,491	18,196	23,166	21,917	27,279
	PFMA	**B.C. sardine fishery landings by year and PFMA**						
Mainland	7	0	26	0	0	0	0	0
	8	0	0	358	564	18	0	0
	9	0	25	522	3,370	1,925	0	0
	10	0	0	1,421	3,196	1,049	0	0
	12	1,558	1,181	2,462	131	320	0	0
	Subtotal	*1,558*	*1,232*	*4,764*	*7,262*	*3,312*	*0*	*0*
WCVI	20	0	168	0	0	0	0	
	23	0	105	820	3,655	5,178	5,145	8,700
	24	0	0	301	57	1,149	677	201
	25	0	1	2,025	3,188	6,008	5,787	8,423
	26	0	0	1,179	249	133	1,593	964
	27	0	0	0	0	3,486	1,694	56
	121	0	0	0	0	0	77	0
	123	0	0	1,346	916	3,185	4,683	423
	124	0	0	0	0	46	703	151
	125	0	0	0		42	199	120
	126	0	0	0	0	0	62	89
	Subtotal	*0*	*274*	*5,671*	*8,065*	*19,227*	*20,621*	*19,127*
B.C.	**All**	**1,558**	**1,507**	**10,435**	**15,327**	**22,538**	**20,621**	**19,127**

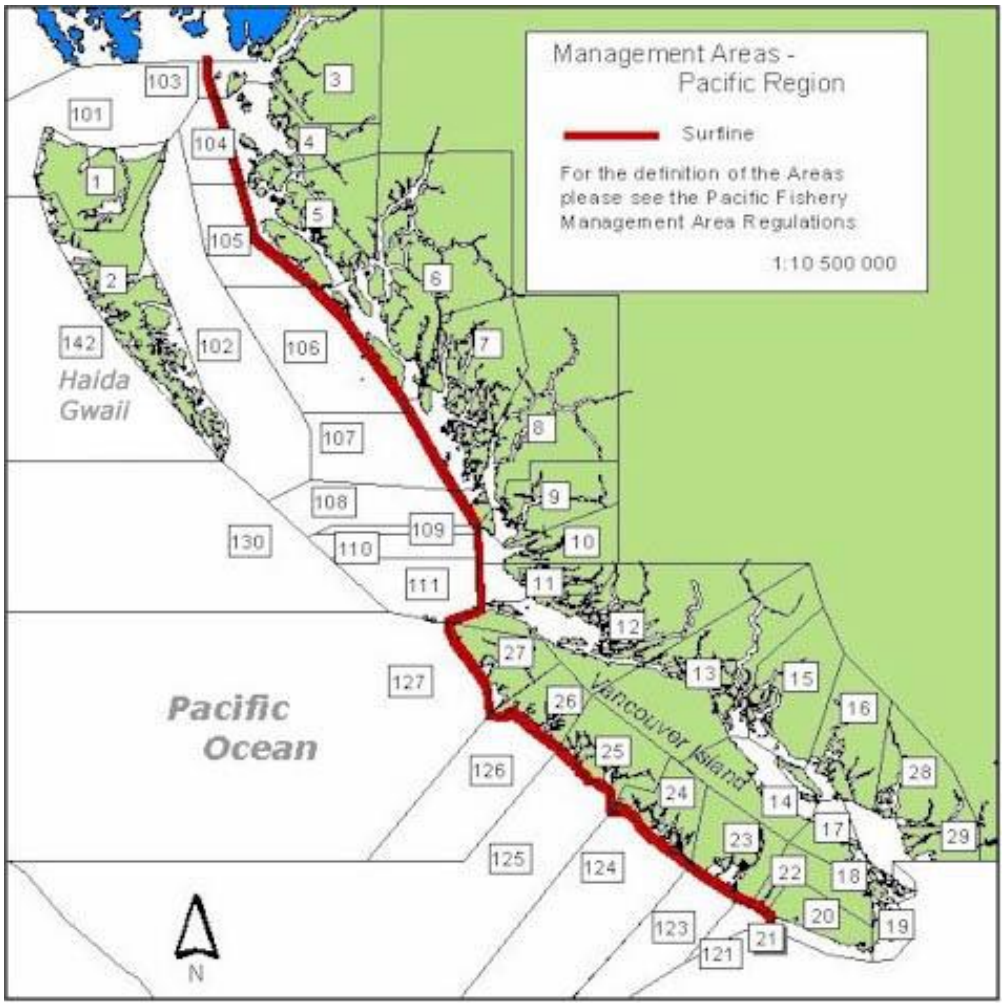

Figure 4. Pacific Fishery Management Areas of Fisheries and Oceans Canada.

Multispecies observations from the WCVI trawl survey

In addition to Sardine observations, catch compositions from the 88 trawl tows made during the DFO 2012 WCVI trawl survey included information on the prevalence and distribution of other species. Notable observations of other species, due to having a relatively high prevalence (proportion of tows), high catch densities, or both, included Pacific Herring (55 tows), Jack Mackerel (34 tows), Chub Mackerel (33 tows), Chinook Salmon (83 tows), Coho Salmon (72 tows) and whitebait smelt (25 tows). The range in fork lengths of both species of Mackerel was 23-30cm, which overlapped with the range in fork lengths for sardine (21-26 cm). The size distributions and degrees of prevalence of mackerel observed in the WCVI summer trawl survey are fairly atypical.

References

Chapman W.M. 1936. The pilchard fishery of the state of Washington in 1936 with notes on the food of the silver and Chinook salmon off the Washington coast. Dept. of Fisheries, State of Washington, Biological Rept. 36. 30p.

Clark, F. N., and Janssen, J. F. Jr. 1945. Movements and abundance of the sardine as measured by tag returns. Calif. Div. Fish Game Fish. Bull. 61: 7-42.

Clark, F. N., and Marr, J. C. 1955. Population dynamics of the Pacific sardine. CalCOFI Prog. Rep. 1 July 1953-31 March 1955: 11-48.

Cushing, D. H. 1971. The dependence of recruitment of parent stock on different groups of fishes. J. Cons. Int. Explor. Mer. 33: 340-362.

DFO. 2012. Pacific Region Integrated Fisheries Management Plan for Pacific Sardine (June 1, 2012 to February 9, 2013).

Flostrand, L., Schweigert, J., Detering, J., Boldt, J., and S. MacConnachie. 2011. Evaluation of Pacific sardine (*Sardinops sagax*) stock assessment and harvest guidelines in British Columbia. DFO Can. Sci. Advis. Sec. Res. Doc. 2011/096.

Hill, K., Crone, P., Lo, N., Macewicz, B., Dorval, E., McDanniel, J., and Gu, Y. 2011. Assessment of the Pacific sardine resource in 2011 for U.S. management in 2012. Pacific Fishery Management Council, Nov 2011 Briefing Book, Agenda Item I.2.b. Attachment 8.

Hill, K.T., Crone, P., Lo, N.C.H., Demer, D.A., Zwolinski, J.P., and Macewicz, B.J. 2012. Assessment of the Pacific sardine resource in 2012 for U.S. management in 2013. Pacific Fishery Management Council, Nov 2012 Briefing Book, Agenda Item I.2.b. 193 p.

Jacobson, L. J. and MacCall, A. D. 1995. Stock-recruitment models for Pacific sardine (*Sardinops sagax*). Can. J. Fish. Aquat. Sci. 52:566-577.

Lo, N.C.H., Macewicz, B.J., and Griffiths, D. 2010. Biomass and reproduction of Pacific sardine (*Sardinops sagax*) off the Pacific northwestern United States 2003-2005. Fishery Bulletin 108: 174-192.

McFarlane, G.A., and MacDougall, L.A., Schweigert, J. and Hrabok, C. 2001. Distribution and biology of Pacific sardine (*Sardinops sagax*) off British Columbia, Canada. CalCOFI Report 46: 144-160.

Zwolinksi, J.P., Emmett, R.L., and Demer, D.A. 2011. Predicting habitat to optimize sampling of Pacific sardine (*Sardinops sajax*). ICES Journal of marine Science, 68: 867-879.

Zwolinksi, J.P., Demer, D.A., Byers, K.A., Cutter, G.S., Renfree, J.S., Sessions, T.S., and Macewicz, B.J. 2012. Distributions and abundances of Pacific sardine and other pelagic fishes in the California Current *Ecosystem during spring 2006, 2008, and 2010,* estimated from acoustic-trawl surveys. Fishery Bulletin. 110:110–122.

2.1.18. Annual variability in nearshore fish assemblages in Pacific Rim National Park Reserve

Jennifer Yakimishyn and Yuri Zharikov, Pacific Rim National Park Reserve

We review the annual variation in fish species composition in four kelp forest beds in Barkley Sound (BS) surveyed from 2008 to 2012, and 24 eelgrass meadows sampled from 2004 to 2012 in Barkley and Clayoquot Sound (CS) (Fig. 1). We also present abundance trends of individual fish species and fish species groups common to both the kelp forest and eelgrass meadow surveys. Kelp forest fish surveys were conducted using scuba transects that involved four 25-metre transects placed at similar depths (approximately 10 m) with all fish identified, counted and total length measurements recorded to the nearest centimetre. Eelgrass meadows were sampled using triplicate beach seine sets made at low tide, where all fish captured within a 90m^2 area were counted, identified, subsampled for length and weight, and returned to the ocean (see Robinson et al. 2011 for details).

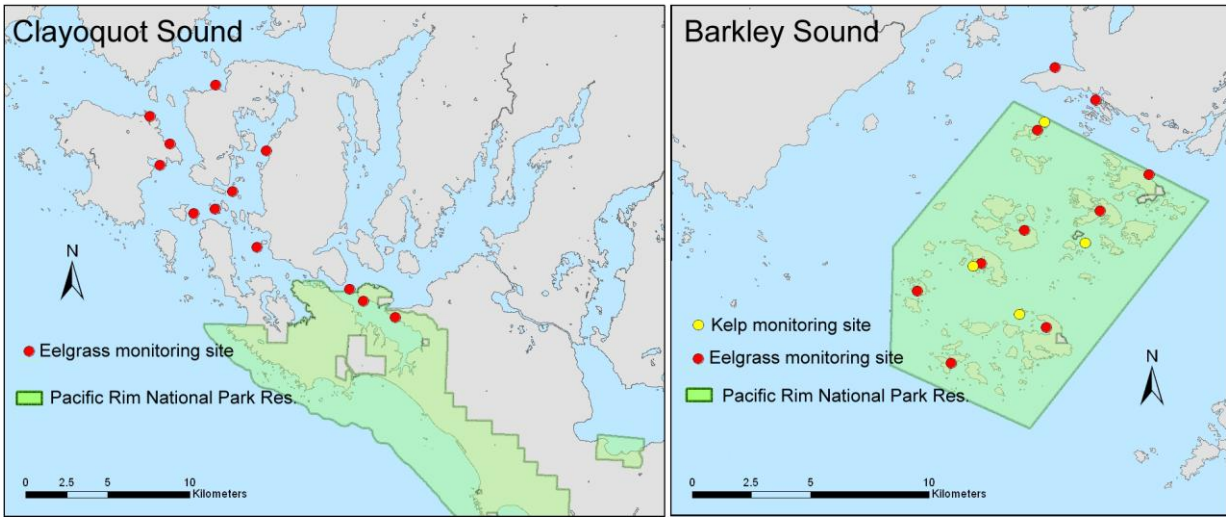

Figure 1. Kelp and eelgrass monitoring sites in Pacific Rim National Park Reserve. The green areas indicate the national park boundaries, yellow circles are kelp monitoring site locations and red circles are eelgrass monitoring site locations.

Abundance trends of individual fish species and fish species groups

Temporal trends for five individual species and two species groups that were common and abundant in both kelp and eelgrass fish surveys were evaluated: Black-Yellowtail Rockfish complex (*Sebastes melanops/flavidus*), Copper-Quillback Rockfish complex (*Sebastes caurinus/maliger*), rockfish species group, Kelp Greenling (*H. decagrammus*), Kelp Perch (*B. frenatus*), and seaperch species group (Table 1). Shiner Perch (*C. aggregata*) were evaluated for eelgrass meadows because they are abundant representatives of eelgrass meadow fish assemblages. In comparison, Shiner Perch were not observed every year in kelp forest surveys, but Kelp Perch were the abundant seaperch representative of kelp forest fish assemblages.

The fish species assessed can be assigned to three distinctive reproductive strategies. Rockfish are viviparous (gives birth to live young) and release larvae into the water column in late winter-early spring. Kelp Greenlings are oviparous (egg-laying) benthic spawners and guard their eggs until the larvae hatch into the water column in late winter to early spring. Seaperch are viviparous and give birth to well-developed young in late spring.

Table 1. Summary of overall individual fish species and fish species group trends and recent trends as determined by the most recent break point in the slope. All slopes are coded in red for decreasing abundance and green for increasing abundance.

Species	Region & habitat	Overall trend (years), Slope (se)	Recent trend (years)	2012 Abundance
Black rockfish	BS kelp	Steep decline (2008-12), **-35.0 (±3.5)%**	See overall trend	Among lowest on record
	BS eelgrass	Uncertain (2004-12)	Mostly declining 2008-12	Lowest on record
	CS eelgrass	Strong increase (2004-12), **16.8 (±4.6)%**	Declining 2010-12	Among lowest on record
Copper rockfish	BS kelp	Uncertain (2008-12)		About average
	BS eelgrass	Moderate increase (2004-12), **21.9 (±9.2)%**	Mostly increasing 2009-12	Among highest on record
	CS eelgrass	Steep decline (2004-12), **-16.5 (±5.8)%**	Declining 2010-12	About average
Rockfish species	BS kelp	Steep decline (2008-12), **-30.5 (±4.5)%**	See overall trend	Among lowest on record
	BS eelgrass	Uncertain (2004-12)	Uncertain, high year-to-year variability	Lowest since 2004
	CS eelgrass	Uncertain (2004-12)	Declining 2010-12	Among lowest on record
Kelp greenling	BS kelp	Steep decline (2008-12), **-35.4 (±6.0)%**	See overall trend	Lowest on record
	BS eelgrass	Moderate increase (2004-12), **7.6 (±2.4)%**	Declining 2008-12	Lowest on record
	CS eelgrass	Moderate decline (2004-12), **-7.2 (±3.4)%**	Uncertain, high year-to-year variability	About average
Kelp perch	BS kelp	Uncertain (2008-12)		About average
	BS eelgrass	Strong increase (2004-12), **57.6 (±6.7)%**	Increasing 2008-12	Highest since 2004
	CS eelgrass	Uncertain (2004-12)	Declining 2010-12	Among lowest on record
Shiner perch	BS eelgrass	Strong increase (2004-12), **16.4 (±4.9)%**	Increasing 2010-12	Highest since 2004
	CS eelgrass	Moderate decline (2004-12), **-9.3 (±3.0)%**	Declining 2010-12	Among lowest on record
Seaperch	BS kelp	Moderate decline (2008-12), **-20.4 (±9.1)%**	See overall trend	About average
	BS eelgrass	Strong increase (2004-12), **15.9 (±4.5)%**	Increasing 2010-12	Highest since 2004
	CS eelgrass	Moderate decline (2004-12), **-9.2 (±3.0)%**	Declining 2010-12	Among lowest on record

Overall, Black-Yellowtail Rockfish show a recent decline in abundance in both kelp and eelgrass habitats (Table 2, Fig. 2). Specifically, young-of-the-year settlement into eelgrass meadows was poor for 2012, suggesting poor winter spawning conditions in 2012 for this species. This trend was also observed for the abundance of Kelp Greenlings in 2012 (Table 1, Fig. 2), also suggesting poor winter spawning conditions in 2012. Copper-Quillback Rockfish showed

different trends both in habitats and region. In 2012, BS eelgrass meadows had higher than average Copper-Quillback abundances, whereas both CS eelgrass and BS kelp had about average abundance (Table 1, Fig. 2). These numbers may reflect recruitment from previous years, where most Black-Yellowtail Rockfish in eelgrass meadows are young-of-the-year individuals.

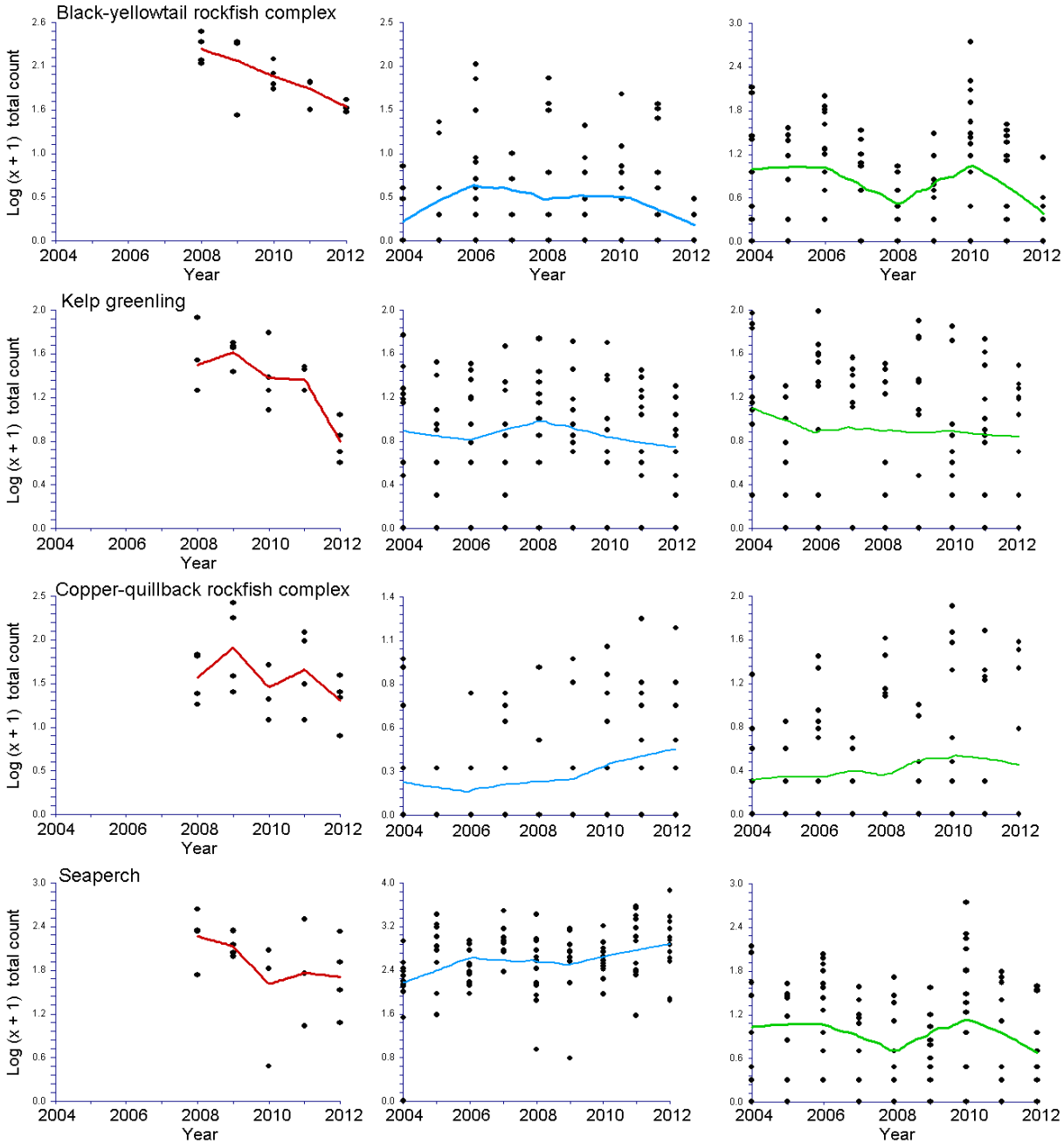

Figure 2. Temporal trends in Log (x+1) transformed fish species abundance (total count per survey – all transects/sets combined) in kelp forest sites (left panel, LOESS trend in red), Barkley Sound eelgrass sites (center panel, LOESS trend in blue) and Clayoquot Sound eelgrass sites (right panel, LOESS trend in green). Data plotted are estimates for individual surveys.

In comparison, seaperch species abundance varied among habitats and regions (Table 1, Fig. 2). Overall, seaperch abundances were relatively stable in kelp forest habitats. In

comparison, the seaperch had the lowest abundance on average in Clayoquot Sound eelgrass meadows in 2012, but had one of the highest abundances in the Barkley Sound eelgrass meadows in 2012.

Examination of within-meadow temperatures indicates that Clayoquot Sound had lower-than-average temperatures in June of 2012, compared to higher-than-average within-meadow temperatures in Barkley Sound in 2012 (Fig. 3). Higher seaperch abundances may depend more on within-meadow temperatures than on regional oceanographic temperatures.

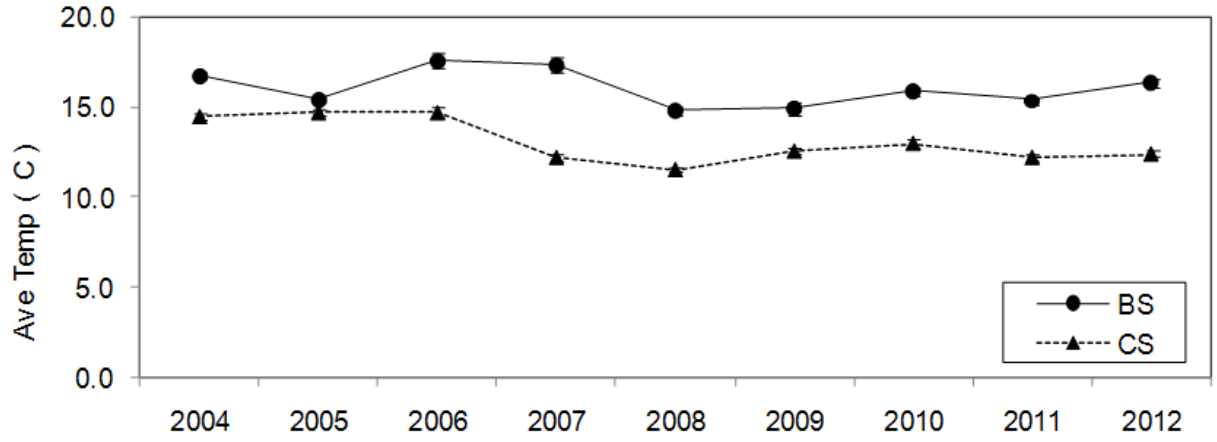

Figure 3. Average within-eelgrass-meadow temperature taken during fish sampling event.

Annual variation in fish species composition

All fish species composition analysis was conducted using PRIMER software. A semi-parametric permutational multiple analysis of variance (PERMANOVA; Anderson 2001) indicated if the clouds of species assemblages differ by location in multivariate space. The PERMANOVA analysis was conducted within each habitat (kelp or eelgrass) and/or region (BS or CS) using a 2-factor model with the random factors site and year. If years differed significantly in the PERMANOVA analysis, *a posteriori* pair-wise comparison was made among levels of the factor (Anderson et al. 2008). Lastly, a similarity percentage analysis (SIMPER) was used to identify the fish species mainly responsible for distinguishing inter-annual differences in fish assemblages. Annual trends in individual fish species and species groups abundances were analysed for overall slope (trend) as well as break points across the entire time series using generalized estimating equations implemented in TRIM (http://www.ebcc.info/trim.html).

The PERMANOVA analysis revealed significant differences in fish species composition among sites (kelp forest or eelgrass meadow) and over the years sampled (Table 2). The greatest component of the variation occurred at the smallest spatial scale, within a site, for kelp forest fish assemblage (17.5%), whereas the greatest component of variation occurred among sites for eelgrass fish assemblages (BS eelgrass 28.3%, CS eelgrass 26.1%). Annual variation contributed the least to eelgrass fish compositional dissimilarity (BS eelgrass 12.5%, CS eelgrass 11.4%), but was higher for kelp forest fish compositional dissimilarity (12.6%). Post-hoc pair-wise year comparisons were made within each habitat types and/or regions. Annual variability, expressed as significant differences between consecutive years, was higher for eelgrass meadows (BS eelgrass 83%, CS eelgrass 89%), than for kelp forest sites (30%).

A SIMPER analysis was performed on each habitat and/or region separately to determine which discriminating species contributed the most to significant differences between 2012 and all other years. A good discriminating species had a discrimination index value > 1.0 (Ley 2005) and

accounted for at least 50% of the pair-wise dissimilarity between years. Overall, BS kelp had between 3 to 4 discriminating species, and both BS and CS eelgrass meadows had 9 to 10 discriminating species. Discriminating species varied between habitat and/or region. Kelp forest fish assemblages had no consistent discriminating fish species that contributed to dissimilarities observed between 2012 and the four other years (2008, 2009, 2010, 2011). Eelgrass meadows in both regions had four good discriminating species that consistently contributed to the dissimilarities between 2012 and all other years sampled (2004 through 2011). However, the discriminating species differed between regions. In BS eelgrass, Kelp Perch (*Brachyistius frenatus*), Shiner Perch (*Cymatogaster aggregata*), Crescent Gunnel (*Pholis laeta*), and Plainfin Midshipman (*Porichthys notatus*) were the four consistent discriminating species for differences between 2012 and all other years, whereas in CS eelgrass, the Threespine Stickleback (*Gasterosteus aculeatu*), Kelp Greenling (*Hexagrammos decagrammu*), English Sole (*Parophrys vetulu*), and Kelp Clingfish (*Rimicola muscarum*) comprised the four consistent discriminating species. In summary, fish assemblages in both kelp forest and eelgrass meadows assessed in these surveys did not appear to vary in 2012 any more than was observed in previous years, and variation in fish assemblages was better explained by spatial variation then temporal.

Table 2. Results from permutational multivariate analysis of variance PERMANOVA of site and year differences in species composition obtained using 999 permutations, based on Bray-Curtis similarity measure with kelp forest, eelgrass meadows and regions analysed separately.

Fish assemblage	Source of variation	df	SS	MS	Pseudo-F	P	Estimated variance component (sqrt)
BS kelp	Site	3	3761	940	3.0705	<0.001	9.8
	Year	4	2357	785	2.566	<0.01	12.6
	Residual	12	3674	306			17.5
BS eelgrass	Site	11	77059	7005	11.818	<0.001	28.3
	Year	8	18061	2258	3.8085	<0.001	12.5
	Residual	77	45644	593			24.3
CS eelgrass	Site	11	66145	1843	14.185	<0.001	26.1
	Year	8	14743	6013	4.3476	<0.001	11.4
	Residual	79	33488	424			20.6

References

Anderson, M.J. 2001. A new method for non-parametric multivariate analysis of variance. Austral Ecology 26: 32-46.

Anderson, M.J., Gorley, R.N., and Clarke, K.R. 2008. PERMANOVA+ for Primer: Guide to Software and Statistical Methods. PRIMER-E: Plymouth, UK. 214 pp.

Ley, J.A. 2005. Linking fish assemblages and attributes of mangrove estuaries in tropical Australia: criteria for regional marine reserves. Marine Ecology Progress Series 305: 41-57.

Robinson, C.L.K., Yakimishyn, J., and Dearden, P. 2011. Habitat heterogeneity and eelgrass fish assemblage diversity and turnover. Aquatic Conservation: Marine Science and Freshwater Ecosystem 21: 625-635.

2.1.19. Spawner escapement trends for Pink Salmon and possible links to oceanography

Jim Irvine[1], Michael O'Brien[1], Catherine Michielsens[2], and Michael Folkes[1]
[1]Fisheries and Oceans Canada, [2]Pacific Salmon Commission

All Pink Salmon spawn at 2 years of age such that fish that return to spawn in odd and even numbered years are genetically isolated from each other. Regional differences in even and odd year abundances have been known for more than a century. We reviewed trends in yearly Pink Salmon spawner escapement abundance in BC and asked State of the Ocean workshop participants if they were aware of biological oceanographic differences that might explain the differences in trends we found between odd and even year cycles.

We assembled and analysed BC Pink Salmon spawner escapement time series, extending from the early 1950s to 2011, the latter being the most recent year data were available. We used 5 statistical approaches to evaluate trends in the population time series of 23 Conservation Units (CUs), which are largely genetically distinct biological units (10 of these CUs return on even years and 13 on odd years). Each of the 5 statistical approaches had two bench marks that categorised population trends as increasing (green), neutral (amber), or decreasing (red).

Almost without exception, odd year CUs are doing better than even year CUs. Generally, even year CUs tended to have mostly neutral (amber) abundance trends while abundances of odd year CUs were increasing (green). In those areas with CUs of both even and odd year returning salmon, trends in odd years are always more positive than trends in even years (Fig. 1).

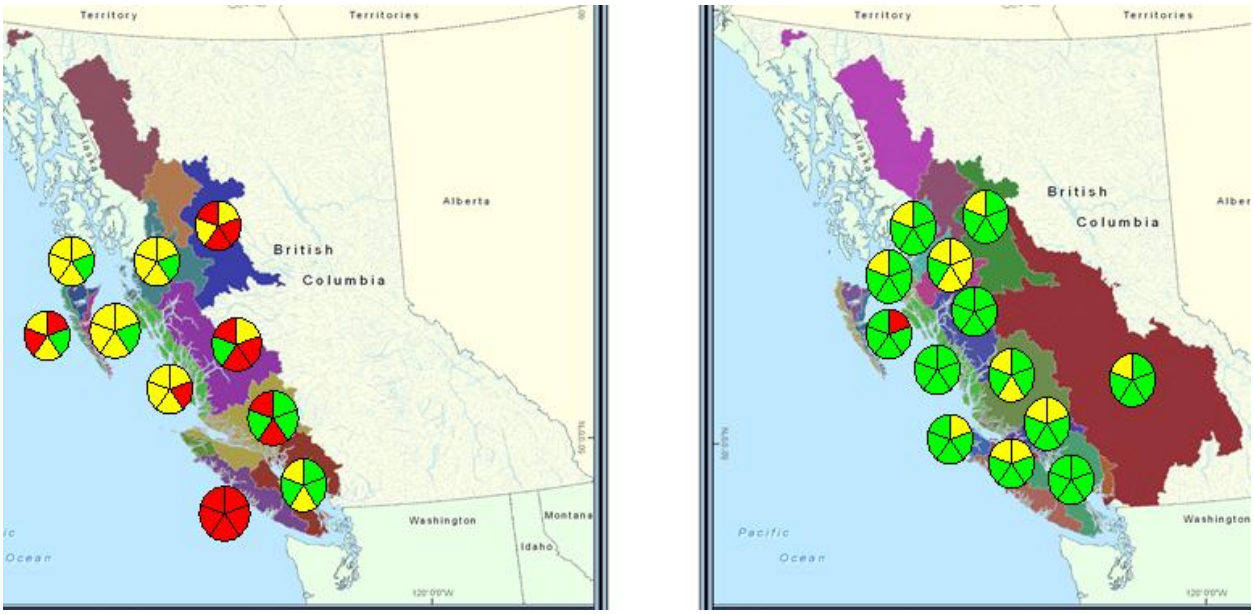

Figure 1. Provisional categorisation of population trends for even (left panel) and odd (right panel) year returning Pink Salmon CUs. Each pie represents 1 CU with each pie segment providing the result of 1 of 5 types of time series analyses, Colours denote population trends as increasing (green), neutral (amber), or decreasing (red).

It has been more than 50 years since Ricker (1962) proposed 8 possible hypotheses to explain differences in abundance between even and odd year Pink Salmon. Yet there remains no consensus on why these differences occur. Our finding of opposite trends implies that density dependent interactions between the cycle lines may play a role, as hypothesised by Ricker (1962) and supported by Krkosek et al. (2011). It is possible that large numbers of adults from

one line deplete food resources for fry of the other, or vice versa. For example Adrievskaya (1970) found that adult Pink Salmon in the Sea of Okhotsk feed on the adult form of a hyperiid amphipod of which the larvae are an important food resource for juvenile Pink Salmon, thereby depleting this food resource for juveniles (Adrievskaya 1970). In the subarctic North Pacific Ocean large numbers of odd year returning Pink Salmon have been shown to lower the amount of zooplankton in odd years (Shiomoto et al. 1997), although whether or not this impacts even year returning Pink Salmon has not been demonstrated.

References

Andrievskaya, L.D. 1970. Feeding of Pacific salmon juveniles in the Sea of Okhotsk. News of the Pacific Research Institute of Fisheries and Oceanography 78: 105-115. Translation series 2441.

Krkosek, M., Hilborn, R., Peterman, R.M., and Quinn, T.P. 2011. Cycles, stochasticity and density dependence in Pink salmon population dynamics. Proc. R. Soc. B. 278 (1714): 2060. doi:10.1098/rspb.2010.2335

Ricker, W.E. 1962. Regulation of the abundance of Pink salmon populations. MacMillan lectures in fisheries, symposium on Pink Salmon: 155-201. University of British Columbia Institute of Fisheries.

Shiomoto, A., Tadokoro, K., Nagasawa, K., and Ishida, Y. 1997. Trophic relations in the subarctic North Pacific ecosystem: possible feeding effect from pink salmon. Marine Ecology Progress Series 150(1): 75-85. doi:10.3354/meps150075

2.1.20. Sockeye Salmon indicator stocks – regional overview of trends, 2012 returns, and 2013-2015 outlook

Kim Hyatt, Margot Stockwell, Howard Stiff and Rick Ferguson, Fisheries and Oceans Canada

Studies by Mueter et al. (2002a, 2002b) and Pyper et al. (2005) suggest associations between Pacific salmon survival and coastal environmental variables (*upwelling index, sea surface temperature (SST), and sea surface salinity (SSS)*) are strongest at local spatial scales (<500-800 km intervals) for adjacent stocks and exhibit little to no co-variation at scales larger than 1000 km. Correlation scales for SST in summer most closely matched the correlation scales for salmon survival. Regional averages of SST appeared to be better predictors of survival than large-scale measures of SST variability (*e.g.* the Pacific Decadal Oscillation, Mueter et al. 2002b). Regional-scale variations in coastal SST's may reflect processes causing co-variation in survival rates of neighbouring stocks. Thus, neighbouring stocks may exhibit stronger similarities in survival and production variations than widely separated stocks. In addition, geographical overlap of salmon species during freshwater and early marine life stages appear more important in determining shared environmental effects on survival rates than life history differences between species (Pyper et al. 2005).

Comparisons of forecasts and observed returns of Sockeye Salmon for major rivers and fisheries in BC have been completed annually by DFO personnel for decades (Fig. 1). Given the observations above, production trends for major sockeye populations or stock aggregates (*i.e.* "indicator-stocks") may reflect environmental changes and production trends for other salmon species originating from coastal-areas constituting separate production domains. Trend comparisons (1970-2012) among sockeye indicator-stocks permit the following generalizations:

- Return variations are large, with maximum annual returns at 10-90 times minimum returns.
- Maximum returns for all Sockeye indicator stocks from the North Coast to the Fraser occurred in the early 1990s in association with the powerful 1989 La Niña event 2-3 years earlier. Similarly, a major La Niña event in 2008 was followed in 2010-11 by record to near-record returns of Vancouver Is. (Barkley), Fraser R. (Chilko), and Columbia R. (Okanagan) indicator stocks, dramatically reversing their recent, sub-average, return trends (Fig. 1).
- As anticipated earlier (Hyatt et al. 2011), southern Sockeye stocks, with sea-entry into the northern California Current upwelling domain (Okanagan, Barkley sockeye) exhibited rapid rebuilding to near record returns in 2009-2011 i.e. the decadal-scale, geographically-widespread, production-decline of Sockeye from southeast Alaska to southern BC, reported by Peterman and Dorner (2012), is over.
- By contrast, Transboundary (Tahltan, Tatsamenie) and North Coast (Nass, Skeena) stocks continued a decadal-scale, sub-average return trend through 2012 with apparently little response associated with the 2008 La Niña (i.e. no major elevation of returns in 2010-12).
- Although there are several examples in each sockeye indicator series for which observed returns diverged greatly from pre-season forecasts (Fig. 1), the latter commonly anticipate decadal-scale trends within each of their six coastal production domains of origin. SST and ENSO indices in the Pacific remained negative to neutral in 2011 and 2012 so Columbia River (principally Okanagan) and west coast Vancouver

Island sockeye (principally Barkley Sound) salmon marine survivals are likely to remain near their all-year average for the 2011-2012 ocean entry years (i.e. 2013-2015 adult return years).

- Persistent, sub-average marine survivals exhibited by Sockeye indicator stocks originating from production domains on the Central Coast (Rivers and Smith Inlets), North Coast, and Transboundary (Tatsamenie, Tahltan) areas (Hyatt et al., unpublished observations) suggest total returns there will remain sub-average in 2013 through 2015.

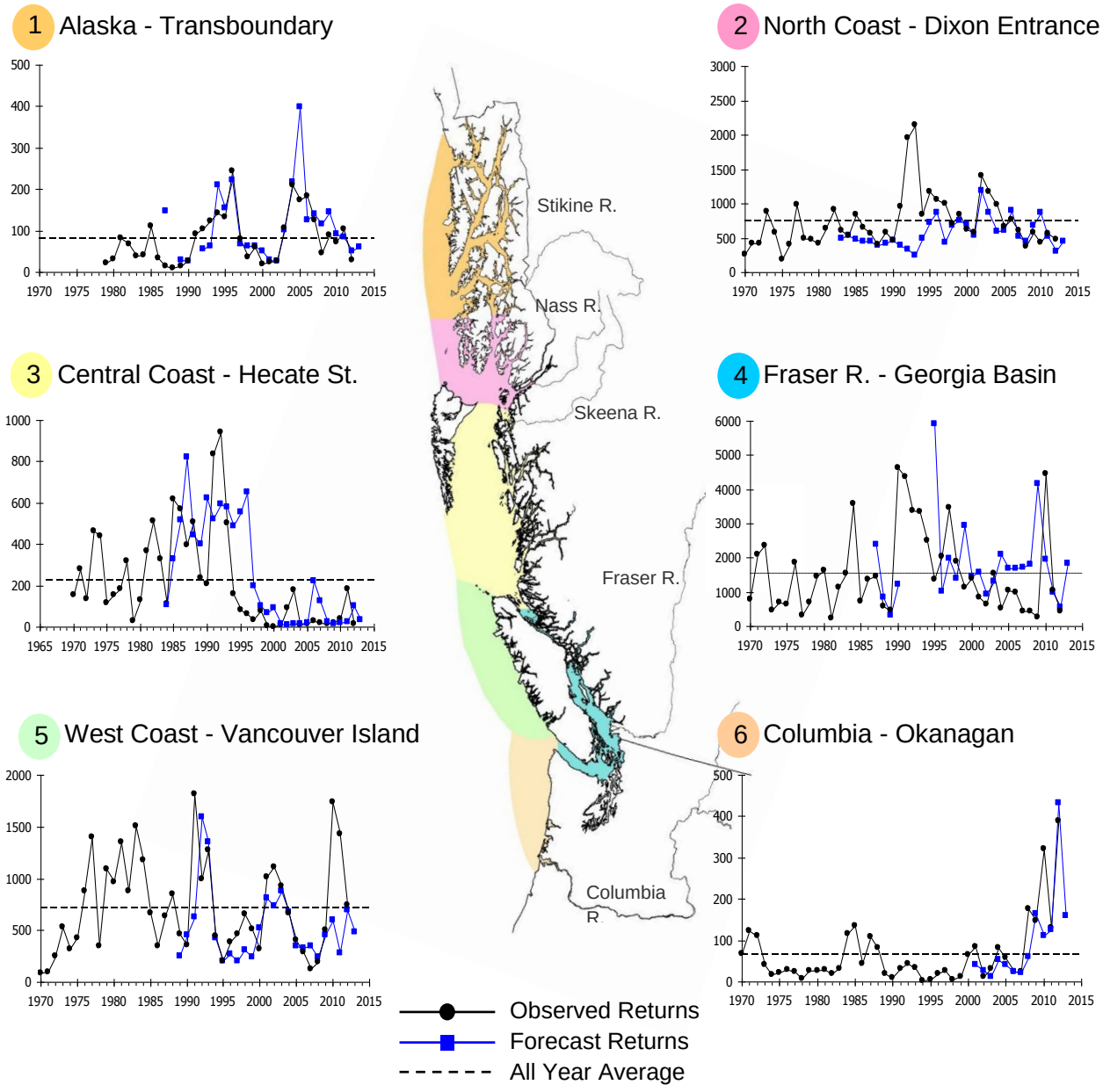

Figure 1. Trends in the total returns and forecasts for British Columbia sockeye index stocks including: 1. Tahltan R., representing Alaska-Trans B.; 2. Nass, North Coast; 3. Smith's Inlet rivers, Central Coast-Hecate St.; 4. Chilko Lake, Fraser-Georgia Basin; 5. Barkley Sound Rivers, West Coast VI; and 6.Okanagan Sockeye Salmon, Columbia-Okanagan. Y-axis represents returns in thousands of fish.

Sources of Information

Hyatt, K. D. and W. Luedke. 1999. West Coast Vancouver Island Sockeye. DFO Science Stock Status Report D6-05. 5p. http://www.dfo-mpo.gc.ca/csas/Csas/status/1999/D6-05e.pdf

Hyatt, K. D., M. M. Stockwell and D. P. Rankin. 2011. Sockeye salmon index stocks- Regional overview of trends and 2010 returns pp. 157-163 *in* Crawford, W.R. and J.R. Irvine. 2011. State of physical, biological, and selected fishery resources of Pacific Canadian marine ecosystems in 2010. DFO Can. Sci. Advis. Sec. Res. Doc. 2011/054. http://www.dfo-mpo.gc.ca/csas-sccs/Publications/ResDocs-DocRech/2011/2011_054-eng.pdf

Mueter, F. J., Ware, D. M., and Peterman, R. M. 2002a. Spatial correlation patterns on coastal environmental variables and survival rates of salmon in the north-east Pacific Ocean. Fish. Oceanogr. 11: 205-218.

Mueter, F. J., Peterman, R. M., and Pyper, B. J. 2002b. Opposite effects of ocean temperature on survival rates of 120 stocks of Pacific salmon (*Oncorhynchus* spp.) in northern and southern areas. Can. J. Fish. Aquat. Sci. 59: 456-463.

Peterman, R. M. and Dorner, B . 2012. A widespread decrease in productivity of sockeye salmon (*Oncorhynchus nerka*) populations in North America. Can. J. Fish. Aquat. Sci. 69: 1255-1260.

Pyper, B. J., Mueter, F. J., and Peterman, R. M. 2005. Across-species comparisons of spatial scales of environmental effects on survival rates of northeast Pacific salmon. Trans. Am. Fish. Soc. 134: 86-104.

2.1.21. Increased catches and improved growth of Juvenile Salmon off WCVI in 2012 relative to 2011

Marc Trudel, Mary Thiess, John Morris, Strahan Tucker, Tyler Zubkowski, Yeongha Jung, and Steve Baillie, Fisheries and Oceans Canada

Ocean surveys for juvenile salmon have been used to assess the distribution, growth, condition, and survival of Pacific salmon in different parts of the British Columbia coastal ecosystem since 1998. These surveys are usually conducted in late spring-early summer (June-July) and in the fall (October-November). In addition, juvenile salmon have been collected during winter (February-March) since 2001. This work assumes that marine survival will be higher in years when salmon are rapidly growing and are in good condition than in years of poor growth and condition. Hence, marine survival is expected to be positively correlated to indicators of juvenile salmon growth rate (Trudel et al. 2008).

Mean June-July catch-per-unit-effort (CPUE) of juvenile Chum, Sockeye, Coho and Chinook Salmon increased off the west coast of Vancouver Island (WCVI) in 2012 relative to 2011 and was at or above the 1998-2012 long-term average for all species (Fig. 1). A similar pattern was observed for the central coast of British Columbia (Fig. 2). The utility of using these CPUEs as early indicators of future adult returns is not clear, as CPUEs may be correlated with smolt production from south of our region, smolt survivals, or both.

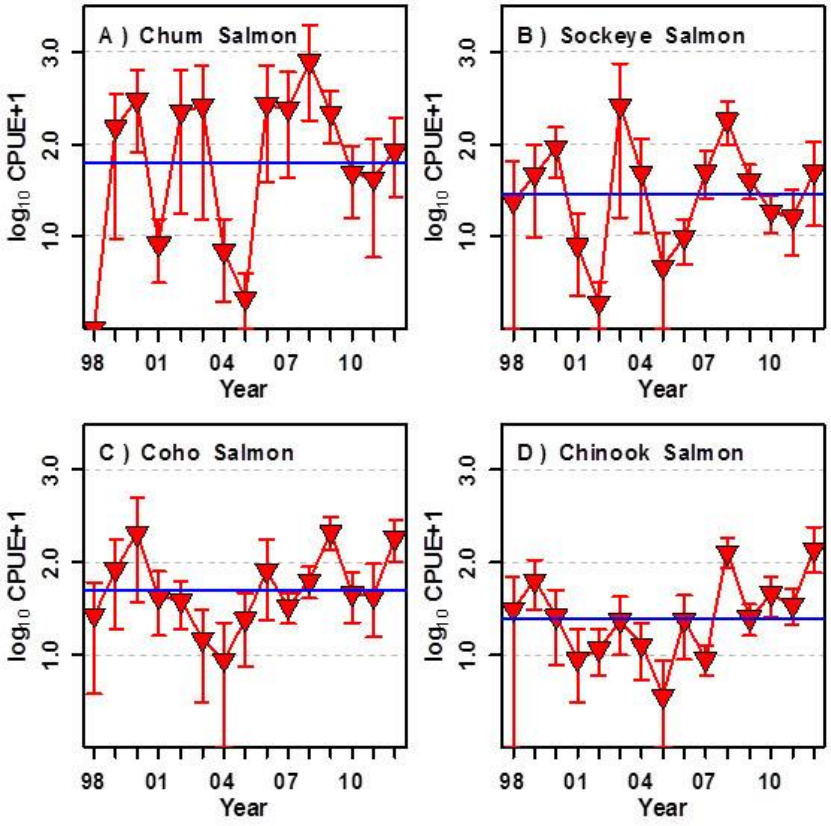

Figure 1. Catch-per-unit-effort (CPUE) of juvenile Chum Salmon, Sockeye Salmon, Coho Salmon, and Chinook Salmon on the continental shelf off the west coast of Vancouver Island in June-July 1998-2012. The blue line represents the average value for the time series. Average CPUE and 95% confidence intervals (vertical red lines) were obtained by bootstrapping.

Juvenile Sockeye Salmon CPUE was expected to increase in 2012 and reach high levels, as these were the offspring of record high returns in 2010 to the Fraser River, Barkley Sound, and Columbia River. Although catches were large in 2012, they were not as high as some earlier years (Fig. 1-2). This may be due to various factors such as decreased freshwater or marine survival, or delayed coastal migration.

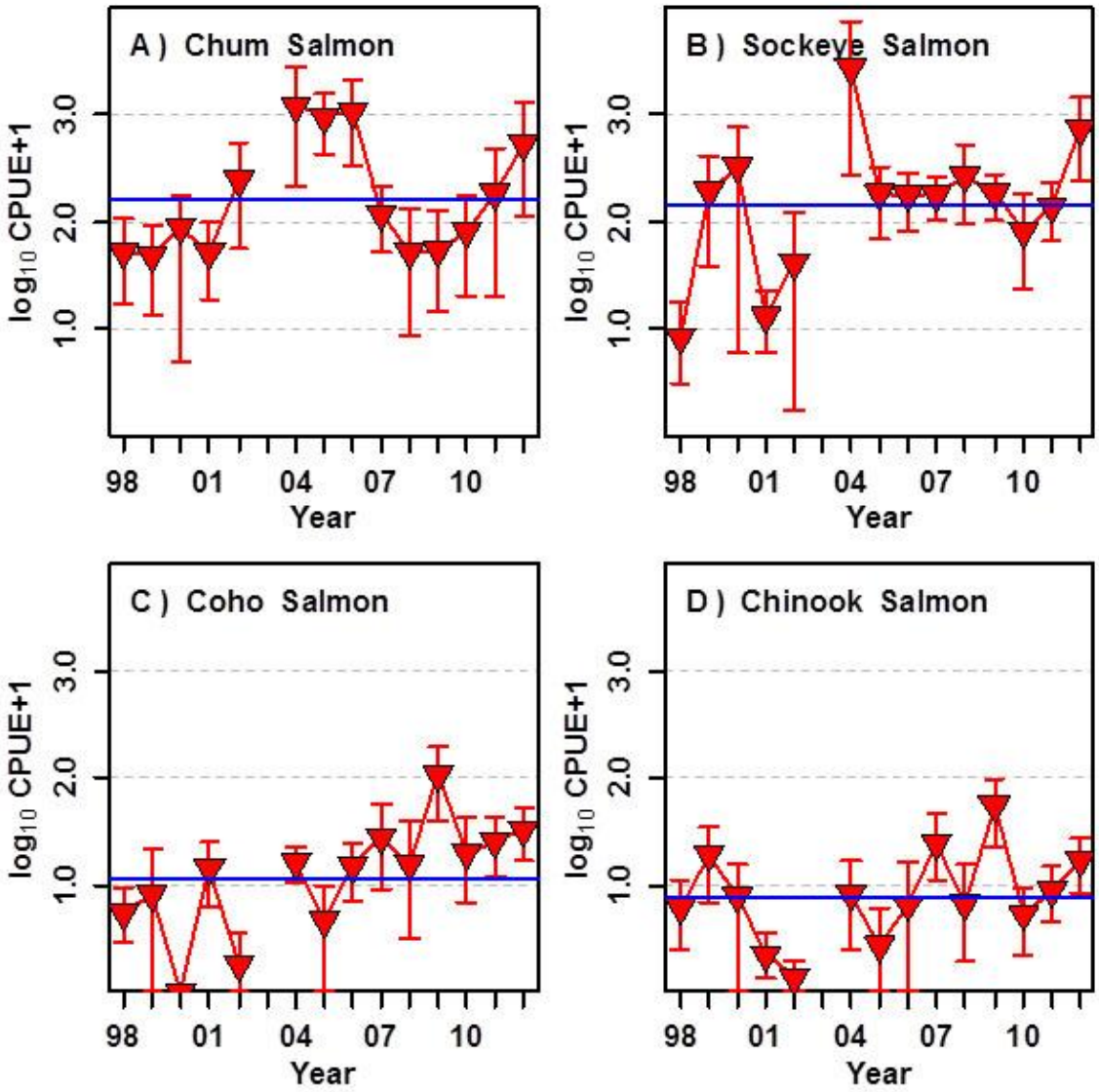

Figure 2. Catch-per-unit-effort (CPUE) of juvenile Chum Salmon, Sockeye Salmon, Coho Salmon, and Chinook Salmon on the continental shelf in the central coast of British Columbia (Queen Charlotte Sound, Hecate Strait, and the west coast of the Haida Gwaii) in June-July 1998-2012. The blue line represents the average value for the time series. Average CPUE and 95% confidence intervals (vertical red lines) were obtained by bootstrapping.

Growth rates of juvenile Coho Salmon off WCVI increased above the 1998-2011 average in 2012 (Fig. 3). As our analyses indicate that the marine survival of WCVI Coho Salmon stocks is strongly correlated to their growth (Trudel et al. 2008), recent increases in growth suggest that marine survival will be average to above average for WCVI Coho Salmon returning in 2013 relative to 1999-2012 (Fig. 4).

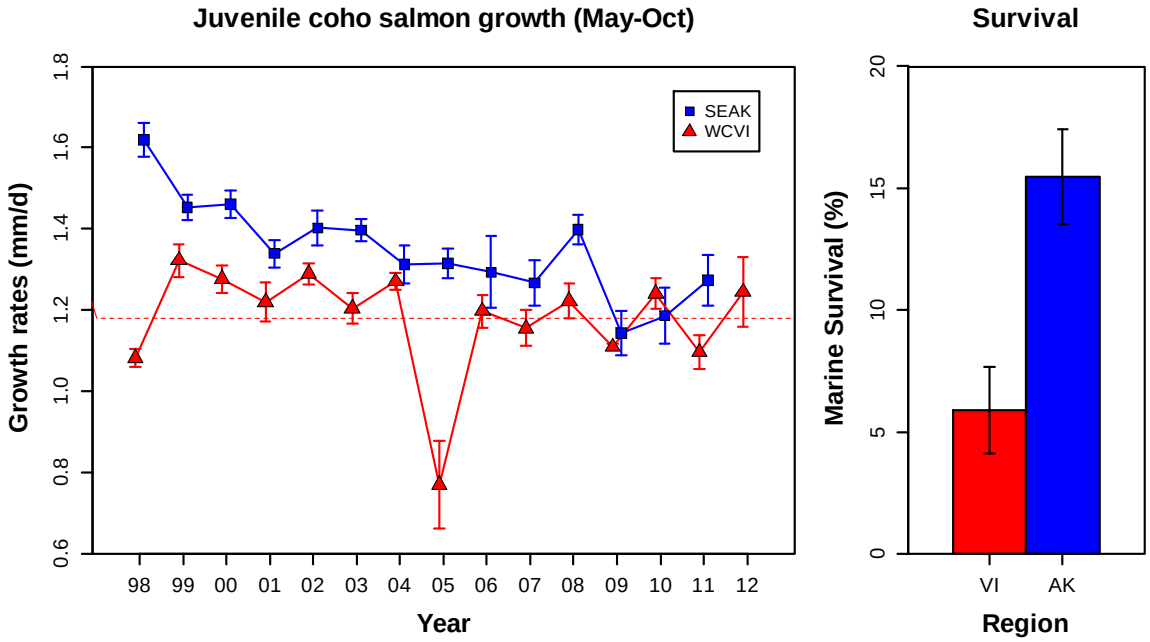

Figure 3. Growth rates (May-October) of juvenile Coho Salmon off the west coast of Vancouver Island (red triangles) and Southeast Alaska (blue squares). The blue and red dotted lines represent the 1998-2012 average values for Southeast Alaska and the west coast of Vancouver Island, respectively. The error bars are 2 times the standard error. Details on the procedure used to estimate growth rate are provided in Trudel et al. (2007).

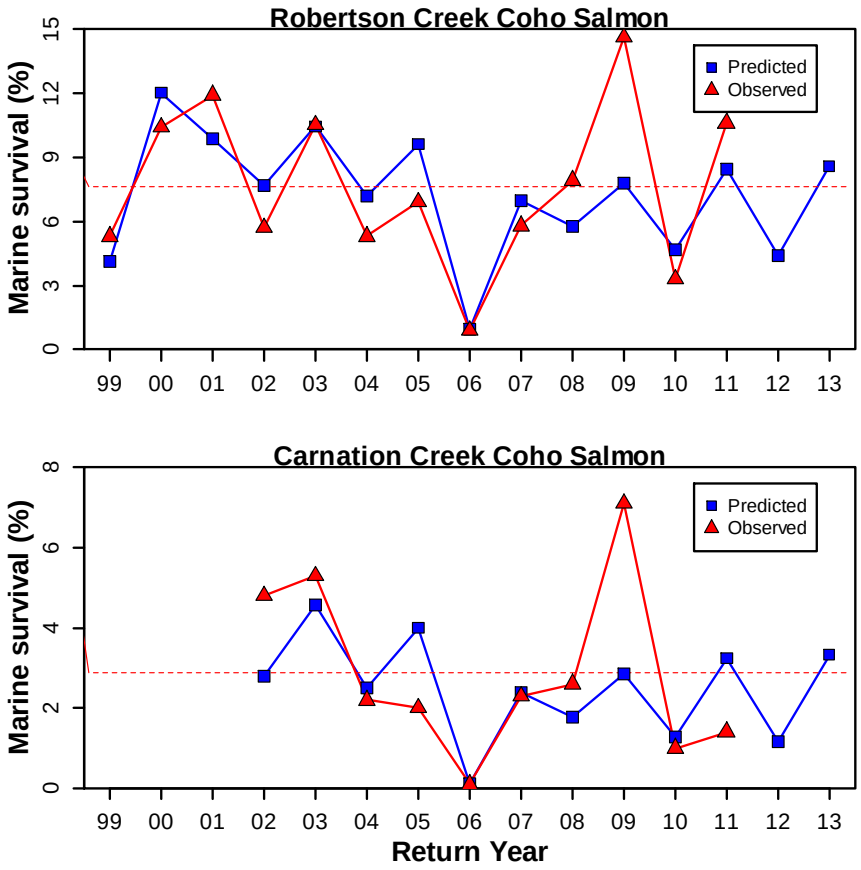

Figure 4. Marine survival and forecast of Robertson Creek and Carnation Creek Coho Salmon. Predicted values were obtained by regressing the logit of marine survival with juvenile Coho Salmon growth off the west coast of Vancouver Island. The dashed red line represents the average marine survival for 1999-2011 return years (here estimated as ocean entry year plus one).

Interestingly, juvenile Coho Salmon growth has generally been higher in even years than odd years since 2001 (Fig. 3). It is unclear what is the underlying mechanism generating this pattern. In marine waters of southern British Columbia, juvenile Pink Salmon are typically most abundant in even years (Irvine et al.). However, they rarely show up off WCVI during summer, and are only present in moderate numbers during fall in even years. Moreover, they are thought to compete with juvenile Coho Salmon in the Strait of Georgia (Beamish et al. 2008).

References

Beamish, R.J., Sweeting, R.M., Lange, K.L., and Neville, C.M. 2008. Changes in the population ecology of hatchery and wild coho salmon in the Strait of Georgia. Trans. Am. Fish. Soc. 137: 503-520.

Trudel, M., Thiess, M.E., Bucher, C., Farley, E.V., Jr., MacFarlane, B., Casillas, E., Morris, J.F.T., Murphy, J.M., and Welch, D.W. 2007. D.W. Regional variation in the marine growth and energy accumulation of juvenile Chinook salmon and coho salmon along the west coast of North America. Am. Fish. Soc. Symp. Ser. 57: 205-232.

Trudel, M., Baillie, S., Parken, C., and O'Brien, D. 2008. Average growth for coho salmon in southern British Columbia. pp. 82-83 In Irvine, J. and B. Crawford (Eds). 2008. State of physical, biological, and selected fishery resources of Pacific Canadian marine ecosystems. DFO Can. Sci. Advis. Sec. Res. Doc. 2008/013.

2.1.22. Albacore Tuna in BC waters: below average catches in 2012

John Holmes, Fisheries and Oceans Canada

Albacore Tuna (*Thunnus alalunga*) is a highly migratory pelagic species widely distributed in tropical and temperate waters of all oceans. There are two distinct stocks of albacore in the Pacific Ocean, one in the South Pacific and one in the North Pacific. Juvenile albacore from two to four years of age in the North Pacific stock are the primary target of the Canadian troll fleet along the west coast of North America and the adjacent high seas waters.

Annual variations in the distribution and abundance of albacore in coastal waters are affected by water temperature and food distribution (Alverson 1961; Laurs et al. 1984). Juvenile albacore are attracted to areas of sharp temperature and salinity gradients (fronts) in the transition zone between the subarctic and subtropical gyres in the North Pacific (Laurs and Lynn 1977). Based on fishery data, water temperatures between 14 and 19°C within the transition area are important for albacore, and albacore in coastal areas are found primarily seaward of the continental shelf edge. On average, transition zone waters between 14 and 19°C are observed within the Canadian exclusive economic zone (200 mile limit) beginning in mid to late July and persisting through October. Juvenile albacore forage on small pelagic fishes (anchovy, sardine, saury, mackerel, hake) and squids (Glaser 2010) at the edge of the continental shelf.

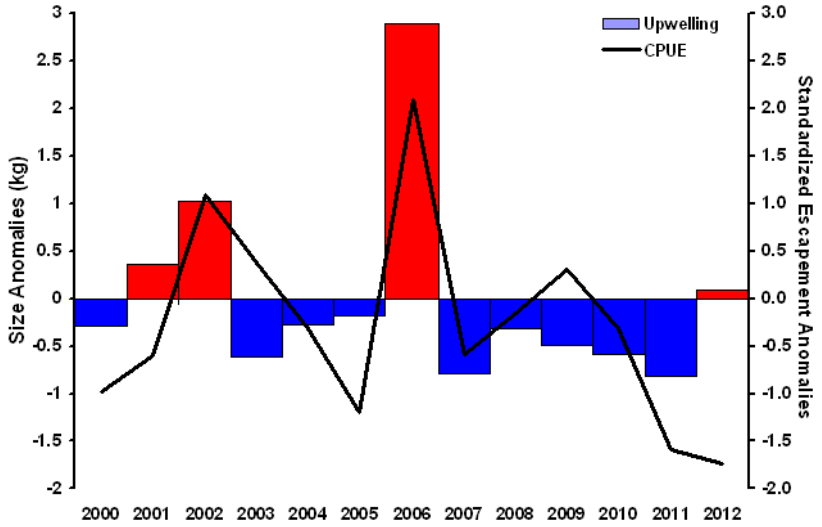

Figure 1. Standardized anomalies of catch rate (fish/day) in Canadian waters (black line) and July-October upwelling index values at 48°N, 125°W (bars). Zero (0) on both scales is the average for 2000-2009. Standardized anomalies (A) are calculated as:

$$A_{2011} = \frac{(X_{2011} - \overline{X}_{2000\text{-}2009})}{s_{2000\text{-}2009}}$$

Where X is the observed value, $\overline{X}$ is the average for 2000-2009, and s is the standard deviation.

Scientists often use catch-per-unit-effort (CPUE) or catch-rate (total catch divided by the effort to achieve that catch) to index fish abundance. Annual CPUEs for albacore in BC coastal waters averaged 66 fish/day during the 2000-2009 period, and catch rate in 2012 was well below average at 31 fish/day (Fig. 1). Catch rates in five of the last six years since 2006 have been below average, consistent with cooler sea surface temperature in the eastern Gulf of Alaska

during these years. The 2000-2009 period is used as the base period for averaging because the data are from logbooks and logbook reporting has exceeded 80% for this period. Albacore catch rates are positively correlated (r = 0.70) with July-Oct upwelling index anomalies at 48°N, 125°W (www.pfeg.noaa.gov/products/PFEL/modeled/indices/upwelling/NA/upwell_menu_NA.html), where positive anomalies indicate higher than average upwelling during the summer and fall and negative anomalies are lower than average upwelling for the same period. A potential explanation for this correlation is that above average upwelling supports higher productivity in lower trophic levels on the continental shelf, which in turn enhances albacore foraging opportunities on small pelagic fish and squids at the edge of the continental shelf. Stronger upwelling winds blow from the northwest along the Vancouver Island shelf, and not only upwell more nutrient-rich water near shore, but also push this water and its richer marine life toward the outer edge of the continental shelf, where tuna prefer to feed. This stronger offshore flow of surface waters might also intensify the frontal features offshore of the shelf break, concentrating prey for tuna.

Although food production was probably sufficient in 2012 based on average upwelling conditions (Figure 1), transition zone waters arrived later than normal in August, only extended as far north as Cape St. James, Haida Gwaii, and left early in October. The highest CPUEs occurred in sporadic locations along the continental shelf and more consistently in offshore waters (Fig. 2). Historically, about 80% of the Canadian albacore catch has occurred in coastal waters off of Washington and Oregon (through access provisions in the Canada-US Albacore Tuna Treaty), approximately 14% in Canadian waters, and the remainder in adjacent high seas waters. Canadian vessels were not licensed to fish in coastal waters of the United States in 2012 because treaty access provisions expired at the end of 2011 and were not replaced. As a result, harvesting activity by the Canadian fleet was focused in Canadian and adjacent high seas waters. Total catch of albacore in Canadian waters was 2,058 t (81% of the fishery), which is a 207% increase relative to the catch in 2011 (670 t) and reflects a 184% increase in effort in Canadian waters relative to 2011.

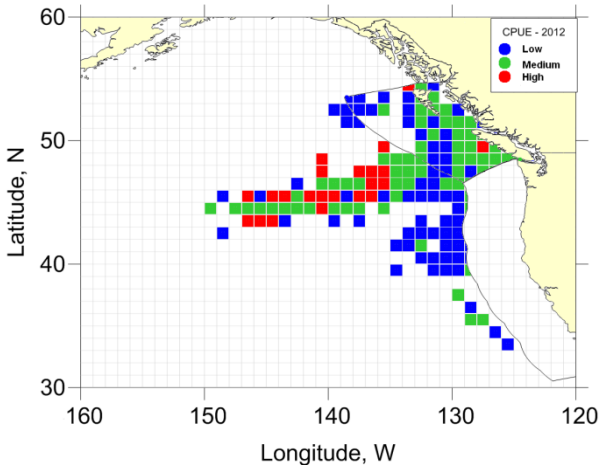

Figure 2. Distribution of catch rates (fish/vessel-day) by the Canadian albacore fishery in 2012. Data are plotted for 1° x 1° spatial blocks. Catch rates are estimated as the total number of fish caught within a block from June through October divided by the total number of vessel-days (effort) in that block during the same period.

2012 was a poor year for the Albacore Tuna fishery and was characterized by the late arrival of the transition zone waters and early departure from the Canadian EEZ, leading to a reduced overlap in time and space between these waters and the continental shelf edge where upwelling dominates productivity and creates foraging opportunities for tuna.

Assessments of interannual temporal and spatial variation in albacore distribution and abundance may benefit from considering indices of environmental processes at various spatial scales.

References

Alverson, D.L. 1961. Ocean temperatures and their relation to albacore tuna (*Thunnus germo*) distribution in waters off the coast of Oregon, Washington, and British Columbia. J. Fish. Res. Board Can. 18: 1145-1152.

Glaser, S.M. 2010. Interdecadal variability in predator-prey interactions of juvenile North Pacific albacore in the California Current system. Mar. Ecol. Prog. Ser. 414: 209-221.

Laurs, R.M., and Lynn. R.J. 1977. Seasonal migration of North Pacific albacore, *Thunnus alalunga*, into North American coastal waters - distribution, relative abundance, and association with transition zone waters. Fish. Bull. 75:795-822.

Laurs, R.M., Fielder, P.C., and Montgomery, D.R. 1984. Albacore tuna catch distributions relative to environmental features observed from satellites. Deep-Sea Res. 31: 1085-1099.

2.1.23. Seabird breeding on Triangle Island in 2012: a relatively good year for Cassin's Auklets

Mark Hipfner, Environment Canada

Triangle Island Background and Species Natural History

Marine birds can be effective indicators of the state of marine ecosystems because they gather in large and highly visible aggregations to breed and because, as a group, they feed at a variety of trophic levels (zooplankton to fish). Seabird breeding success is closely tied to the availability of key prey species, and as a result, can vary widely among years, depending on ocean conditions. Triangle Island (50°52' N, 129°05' W) in the Scott Island chain off northern Vancouver Island, supports the largest and most diverse seabird colony along the coast of British Columbia. Since 1994, researchers from the Centre for Wildlife Ecology (a collaboration between Environment Canada and Simon Fraser University), have visited Triangle Island to collect annual time-series information on seabird demography and ecology. This report presents key indicators of seabird breeding at Triangle Island in 2012, and places 2012 results within the context of the 1994-2011 time series.

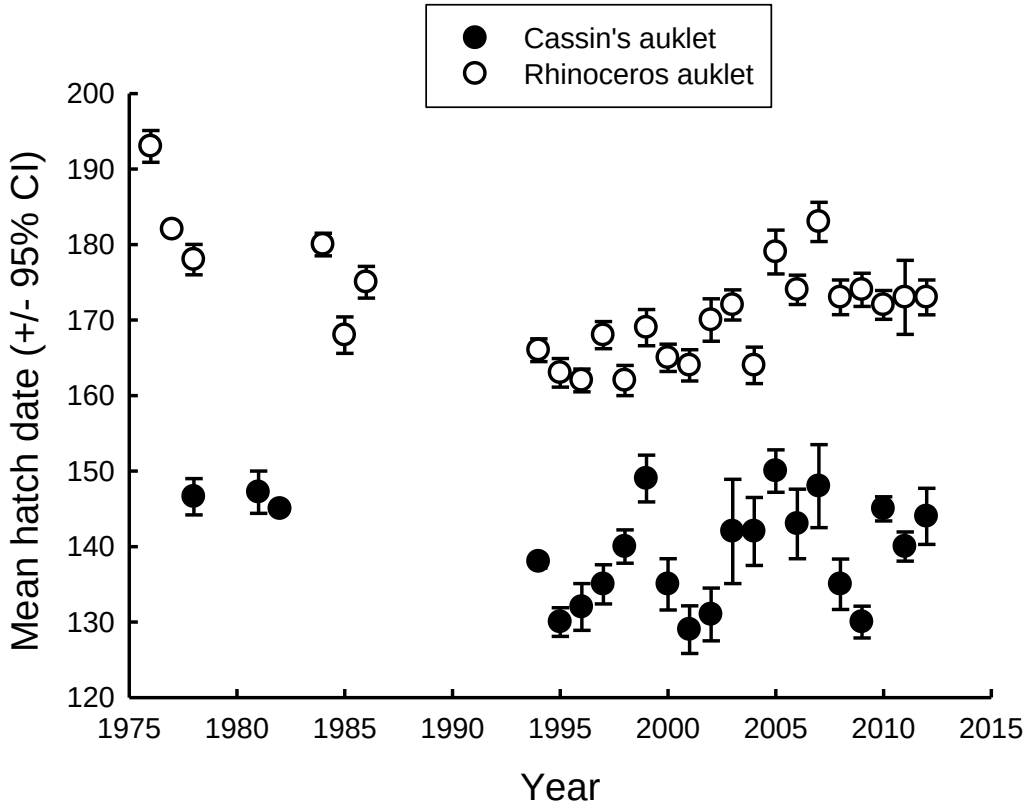

Figure 1. Timing of breeding for two focal seabirds – zooplanktivorous (plankton-eating) Cassin's Auklet and more piscivorous (fish-eating) Rhinoceros Auklet - on Triangle Island, British Columbia, 1976-2012. Timing of breeding was close to long-term averages in both Cassin's Auklets and Rhinoceros Auklets.

Timing of breeding

Variation in the timing of avian breeding is determined primarily by female condition prior to and during the period of egg formation, which is itself related to food availability early in the season. Over the last 18 years Cassin's Auklets in general have tended to lay earlier in cold-water years

and to breed more successfully as a result. In 2012, timing of breeding in Cassin Auklets was close to the long-term average, and somewhat later than during the La Niña years of 2008 and 2009 (Fig. 1). For Rhinoceros Auklets, timing of breeding in general has remained consistent in recent years, including 2012, and close to long-term averages (Fig. 1).

Breeding success

The mean mass at 25 days of age of Cassin's Auklet nestlings in 2012 was above the 1996-2011 average (Fig. 2). In general, the auklets' offspring grow more quickly and fledge at heavier masses in cold-water years, because timing of their hatching is strongly temporally matched with the phenology of an important prey species, the copepod *Neocalanus cristatus*. Thus, the above-average 25-day mass was expected based on the relatively cold spring sea-surface temperatures in 2012.

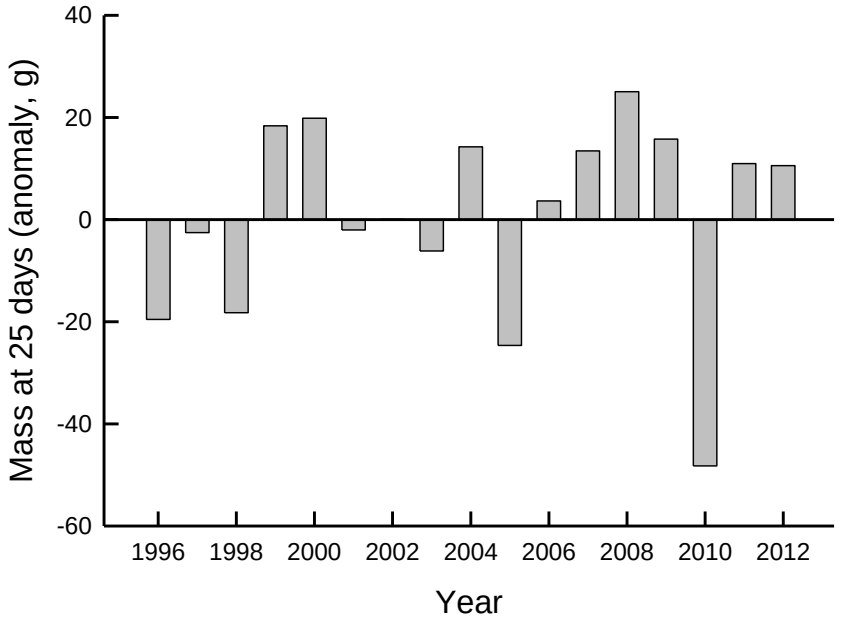

Figure 2. Mass of nestling Cassin's Auklets at 25 days of age, averaged for each year

Consumption of salmon by Rhinoceros Auklets

Provisioning Rhinoceros Auklets deliver meals consisting of 1 to 30 whole fish to their nestlings. Diets tend to be dominated by Pacific Sandlance, especially in years with an early spring bloom, but salmon smolts (Sockeye, Pink and Chum) are a common secondary prey type in some years. In 2012, the percentage of meals that contained salmon was much higher than in any other from 2006-2011 at both Triangle and Pine islands.

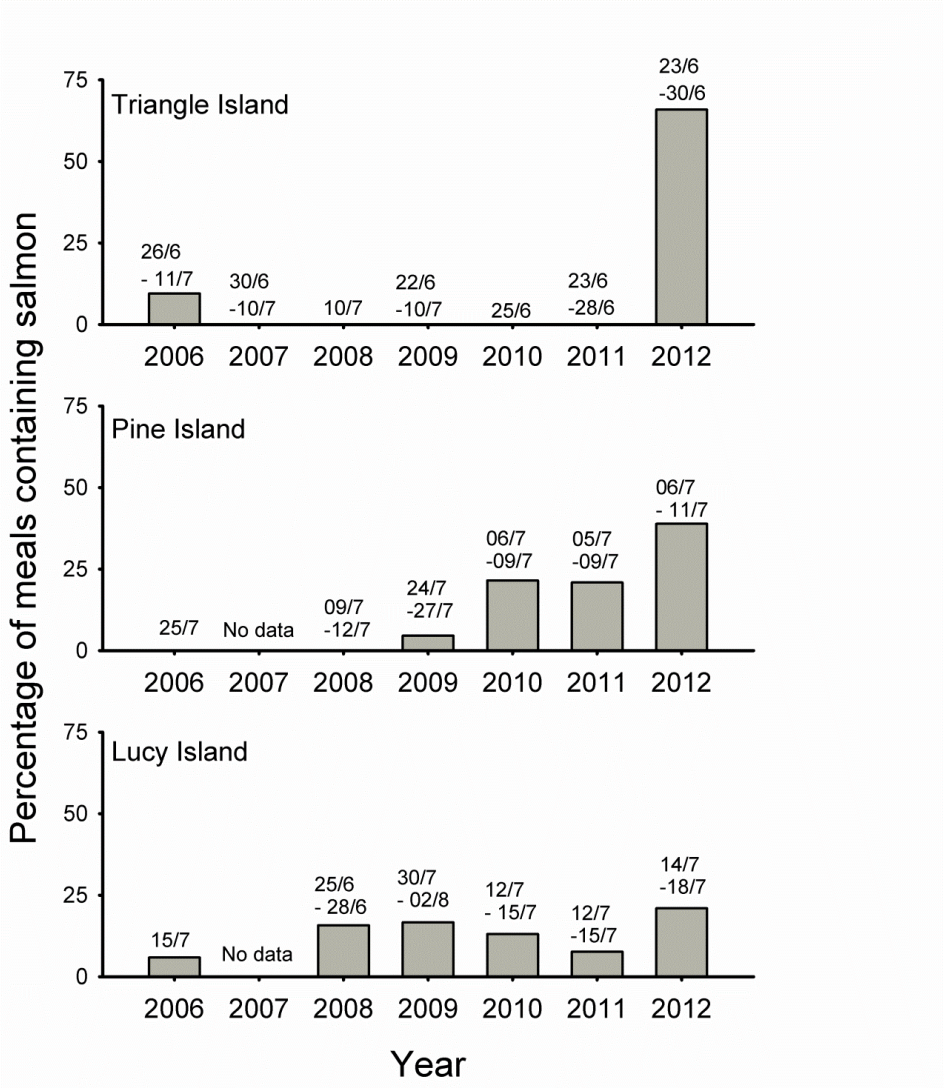

Figure 3. Percentage of meals delivered to nestlings by Rhinoceros Auklet parents that contained one or more salmon smolts at three colonies in 2006-2012: Triangle Island in the Scott Island Group, Pine Island in Queen Charlotte Strait, and Lucy Island in Chatham Sound in northern BC. Sampling dates (day/month) above bars. Note that salmon was much more common in meals in 2012 than in other years at Triangle and Pine islands.

Links

Environment Canada Contact: Mark Hipfner (mark.hipfner@ec.gc.ca)

2.2. SALISH SEA

2.2.1. Salish Sea: cold conditions persist in 2012

Diane Masson, Fisheries and Oceans Canada

Waters of the Salish Sea are illustrated in Figure 1a below. The red dot in Fig. 1a marks the location of the Nanoose sampling station where ocean temperature and salinity have been measured regularly by the Canadian Navy since the 1960s. Scientists of the Institute of Ocean Sciences have sampled at locations in Fig. 1b since 1999.

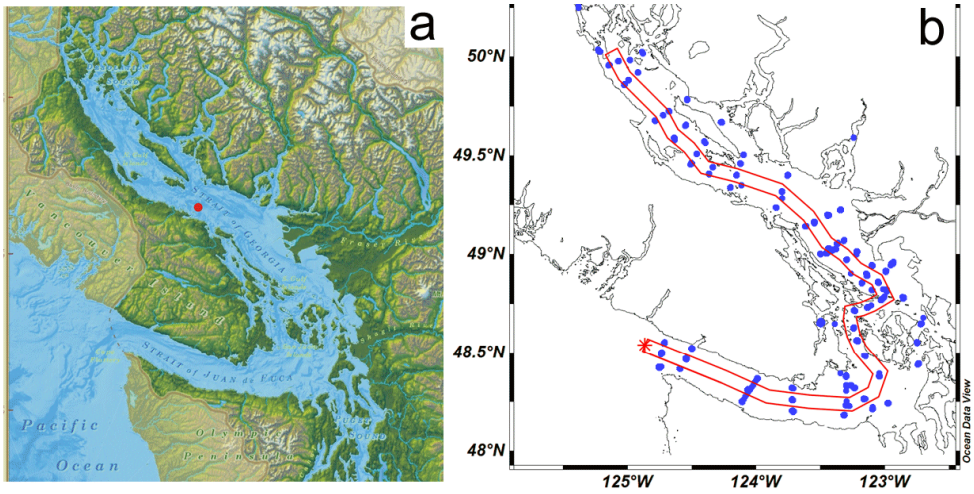

Figure 1. (a) Salish Sea with Nanoose Station (49° 18.7' N, 124° 2.7' W) marked by red dot. (b) Ocean stations sampled by Fisheries and Oceans Canada several times per year (blue dots). Data from stations enclosed by red lines in (b) are plotted in Fig. 3.

In 2012, water temperatures at the Nanoose Station remained slightly below normal. Fig. 2 gives temperature anomalies there since 2005. The anomalies are relative to the 30-year average computed over the period 1971-2000. Since the middle of 2011, temperature anomalies have been moderately negative (< -0.5 ^{o}C) through most of the water column.

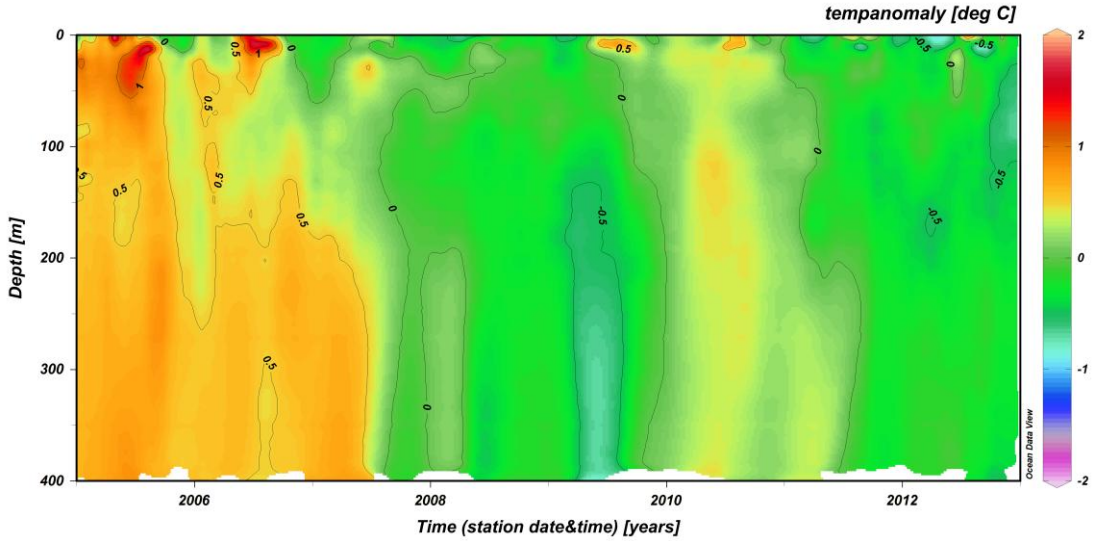

Figure 2. Temperature anomalies measured at the Nanoose Station. Anomalies are computed relative to the climatological mean for 30-year period 1971-2000.

In addition, a late spring transition was associated, in April 2012, with a weak upwelling signal in western Juan de Fuca Strait. On Fig. 3, water temperatures, measured during the spring seasonal survey, are contoured along a vertical section located on the thalweg of the coastal basin, from the mouth of Juan de Fuca Strait to the northern end of the Strait of Georgia (see Figure 1b and inset to Fig. 3 for section location). The temperatures measured in April 2012 show unusually weak evidence of the cold upwelled deep water entering western Juan de Fuca Strait at this time of year, as well as relatively cold temperatures for the most of the coastal basin.

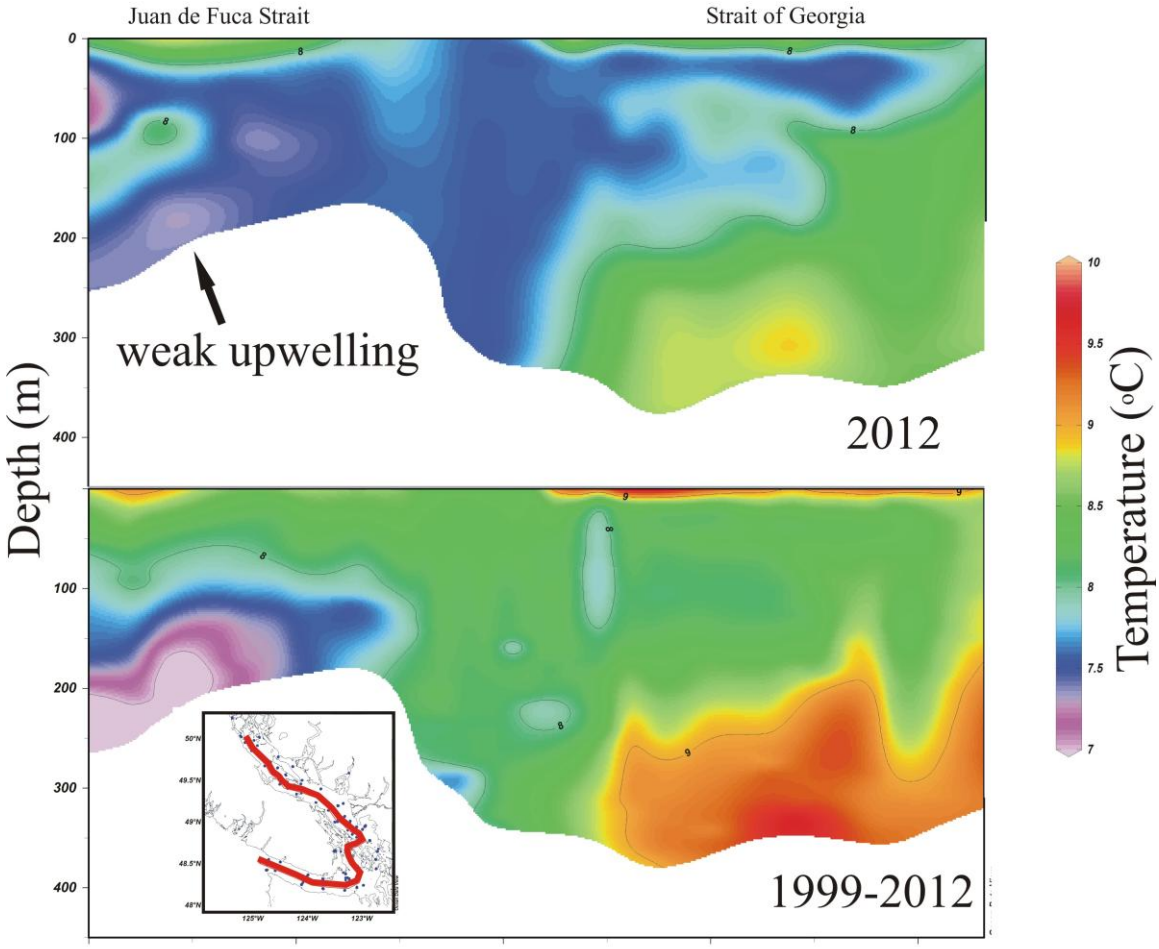

Figure 3. Temperature contours along a vertical section following the thalweg (see inset, bottom panel, for section location), measured in 2012 (top panel) and averaged over 1999-2012 (bottom panel).

2.2.2. Oxygen in the deep Strait of Georgia, 1951-2010

Sophia Johannessen, Diane Masson and Robie Macdonald, Fisheries and Oceans Canada

Tidal mixing, deep-water renewal, diffusion and respiration together determine the concentration of oxygen in the deep Strait of Georgia (Johannessen et al., in press). Hypoxic (low oxygen concentration), upwelled ocean water flows eastward along the bottom of Juan de Fuca Strait and into Haro Strait, where it is partially reoxygenated by contact with the surface water during the vigorous tidal mixing. During the late spring and late summer repeated deep-water renewal events replace the pre-season bottom water in the Strait of Georgia with mixed water from Haro Strait (Fig. 1). Diffusive mixing rapidly reduces the concentration of oxygen in the new bottom water, while remineralization of organic matter continues to consume oxygen throughout the year, some of which is replaced by mixing from above.

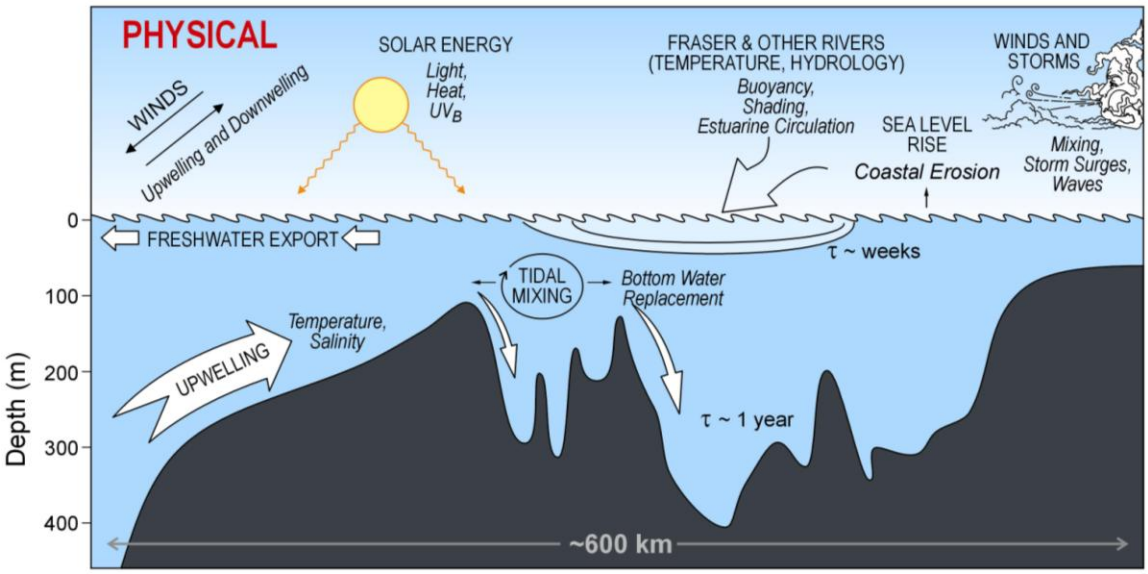

Figure 1. Physical circulation of the Strait of Georgia and approaches. The figure represents a transect from the mouth of Juan de Fuca Strait (at left, labelled upwelling) through Haro Strait (in left-centre, labelled tidal mixing), where the strong mixing occurs, and then into the southern and northern basins of the Strait of Georgia (Figure from Johannessen and Macdonald, 2009. Climate Research 40: 1-21.)

Dissolved oxygen is declining in subsurface seawater around the world (Gilbert et al., 2010). In some coastal waters, eutrophication caused by the anthropogenic discharge of nutrients has led to hypoxia. The Strait of Georgia is not very sensitive to the addition of anthropogenic nutrients, because the phytoplankton are mainly light-limited (Mackas and Harrison, 1997). However, the concentration of oxygen in the deep water has declined at a rate of about 0.02 ml L^{-1} yr^{-1} since 1971 (Johannessen et al., in press) and now seasonally crosses the precautionary threshold of 3 ml L^{-1} which applies to many species of marine animals. With a winter minimum of 2.0 to 2.5 ml L^{-1}, the oxygen concentration is approaching biological thresholds for tolerance of hypoxia.

The decline in oxygen has resulted principally from the increasing hypoxia of Pacific Ocean water along the continental margin of southern British Columbia (e.g. Crawford and Peña, 2013, who report a decrease of 0.025 ml L^{-1} yr^{-1} at 200 m depth over the past 30 years). We attribute the decline in the Strait of Georgia to this advection of more hypoxic water into the strait by rejecting other possible processes. Neither local anthropogenic loadings of organic

carbon nor increased primary production at the surface can explain the observed reduction in bottom water oxygen in the Strait of Georgia. Increased microbial respiration due to increasing seawater temperature could theoretically increase biochemical oxygen consumption, but there is no evidence that this has yet made a measurable difference to the concentration of oxygen in the Strait of Georgia (Johannessen et al., in press).

Linear extrapolation of the long-term trend indicates that parts of the Strait could become episodically hypoxic (< 1.4 ml L^{-1}; < 62.5 µmol L^{-1}) as early as 2040. However, water mass modelling shows that the mixing with surface water in Haro Strait limits the potential of the shelf water to reduce the oxygen concentration in the deep Strait: even should the shelf water become completely anoxic, the concentration of oxygen in bottom waters of the Strait of Georgia would level off just above 2 ml L^{-1} after three years. Increasing surface water temperature will reduce the solubility of oxygen, but this effect is projected to cause a further decline of only 0.05 ml L^{-1} over the next 25 years. In addition, since the concentration of oxygen was lower in the 1950s and 1960s than in the 1970s, the current decline may, in part, be associated with a multi-decadal cycle.

The range of pH in the Strait of Georgia is about 7.8-8.1 at the surface and 7.3-7.6 at depth (Johannessen et al., unpublished data). We lack time series to assess pH change in the Strait of Georgia. However, pH tends to change in concert with oxygen, because remineralization both consumes oxygen and releases CO_2, which reduces pH. Since acidification has been documented in the hypoxic, subsurface water off the west coast of North America (Feely et al., 2008), which is the source water for deep-water renewal, pH in the deep Strait of Georgia is likely declining.

References

Crawford, W. R. and Peña, M. A. 2013. Declining oxygen on the British Columbia continental shelf. Atmosphere-Ocean, DOI:10.1080/07055900.2012.753028.

Feely, R. A., Sabine, C. L., Hernandez-Ayon, J. M., Ianson, D., and Hales, B. 2008. Evidence for upwelling of corrosive" acidified" water onto the continental shelf. Science 320: 1490-1492.

Gilbert, D., Rabalais, N. N., Diaz, R. J., and Zhang, J. 2010. Evidence for greater oxygen decline rates in the coastal ocean than in the open ocean. Biogeosciences 7: 2283-2296.

Johannessen, S. C. and Macdonald, R. W. 2009. Effects of local and global change on an inland sea: the Strait of Georgia, British Columbia, Canada. Climate Research 40: 1-21.

Johannessen, S., Masson, D. and Macdonald, R.in press. Oxygen in the deep Strait of Georgia, 1951-2009: the roles of mixing, deep-water renewal and remineralization of organic matter. Limnology and Oceanography.

Mackas, D. L., and Harrison, P. J. 1997. Nitrogenous nutrient sources and sinks in the Juan de Fuca Strait / Strait of Georgia / Puget Sound estuarine system: assessing the potential for eutrophication. Estuarine, Coastal and Shelf Science 44: 1-21.

2.2.3. Eutrophication in Puget Sound

Christopher Krembs, Washington State Department of Ecology, ckre461@ecy.wa.gov

This report addresses aspects of eutrophication in Puget Sound: How do trends from 1999 to 2012 relate to estuarine processes as well as atmospheric and oceanographic boundary conditions? Is eutrophication fuelling the microbial food web?

Puget Sound (Fig. 1) is a deep fjord and is located at the southern reaches of the Salish Sea, receiving ocean water through Juan de Fuca Strait and Admiralty Reach. The Long-term Marine Monitoring Program at the Washington State Department of Ecology samples 27 core stations monthly in the Puget Sound region. The program's focus centers on detecting long-term patterns of variability and trends relative to statistically established baseline conditions from 1999 to 2008.

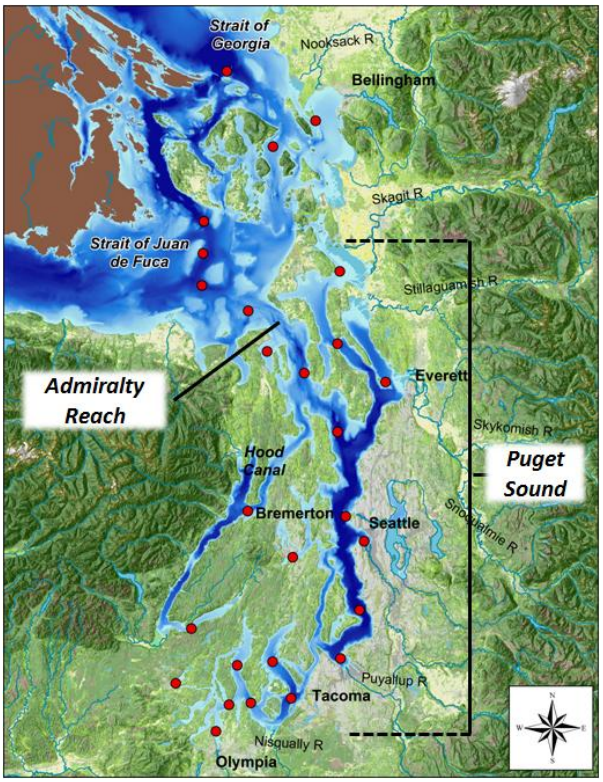

Figure. 1. Puget Sound constitutes the southern portion of the Salish Sea and is located in Washington State. Included are Ecology's long-term marine monitoring stations that are visited monthly [by boat in the Strait of Juan de Fuca and by sea plane at all other stations] (red dots).

To increase the signal-to-noise ratio, all variables at the 27 stations are *a priori* depth integrated. Measurements by CTD (temperature, salinity, oxygen, transmissivity, chlorophyll *a*) are integrated over 0- to 50-m depth. Nutrient samples and sensor calibration samples are sampled at discrete depth by Niskin bottles (0, 10 and 30 m) and medians of the 3 samples are taken to reduce noise. All data are converted into anomalies relative to baseline conditions that are specific for each station and month. This effectively overcomes the strong seasonal and geographic patterns in the dataset.

Oceanic boundary conditions significantly affect Puget Sound's water quality variables over larger temporal and spatial scales (Fig. 2A, C, E and G). Despite depth integration and

conversion of the dataset into anomaly space, an appreciable noise remains among individually sampled stations (Fig. 2B, D, F and H). The remaining noise is overcome by taking a temporally (yearly) and spatially (entire Puget Sound) averaged approach.

The Pacific Decadal Oscillation (PDO) showed a warm phase from 2003 to 2005 that significantly (Spearman Rank Correl. $p<0.05$, $n=14$) affected the thermal energy content in Puget Sound in the upper 0-50 m (Fig. 2A). The anomaly strongly permeated the entire station network (Fig. 2B). Anomalies in salt content (0-50 m) (Fig. 2C,D) significantly (Spearman Rank Correl. $p<0.05$, $n=14$) follow the Upwelling Index at 48°N, 125°W (Fig. 2C) on an annual Puget Sound-wide scale. The correlation corroborates the strong influence of upwelled ocean water on the solute balance in Puget Sound upper water layers.

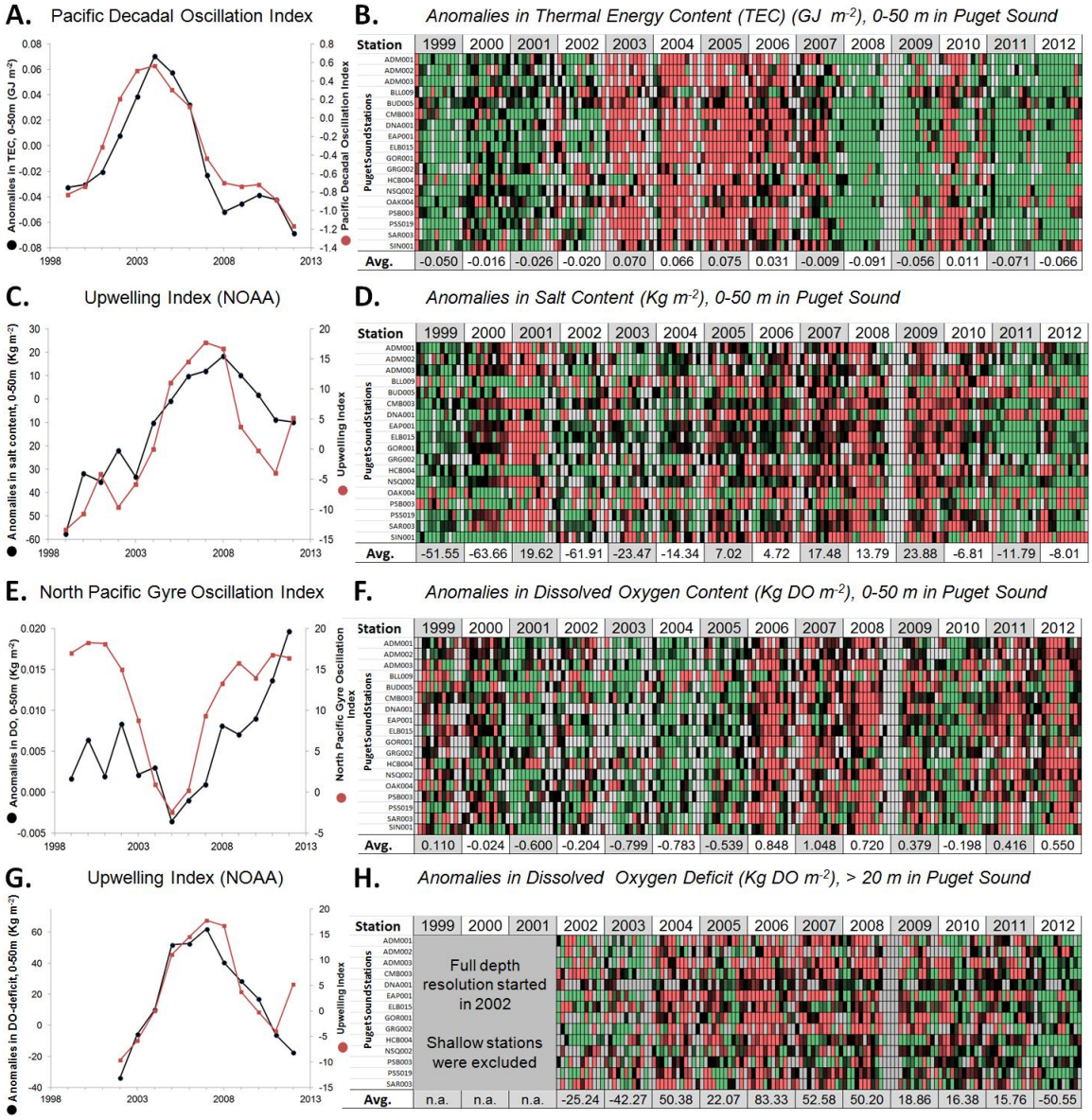

Figure 2. The influence of ocean boundary conditions on depth integrated water quality variables presented as anomalies relative to site- and seasonal-specific baseline conditions established from 1999 to 2008. A: The yearly averaged anomalies in thermal energy content of 0-50 m in Puget Sound correlate significantly with the Pacific Decadal Oscillation Index (both series are shown as a 3-year running average). B: Monthly anomalies (in color) in the thermal energy content (0-50 m) are shown for individual

stations that went into generating graph A. Red and green highlight anomalies outside the 25th and 75th percentiles, respectively; black values fall near the median; gray color illustrates missed sampling events. C and D: The significant correlation between the Upwelling Index at 48°N, 125°W and the salt content (0-50 m) for Puget Sound (C) and anomalies in salt content by individual stations (D) following the format of panels A and B. E and F: The significant correlation between the North Pacific Gyre Oscillation Index and dissolved oxygen anomalies in Puget Sound (E) and anomalies in dissolved oxygen by individual stations (F) following the format of panels A and B. G and H: The significant correlation between the Upwelling Index at 48°N, 125°W and the anomalies in the oxygen deficit at (>20 m to bottom) in Puget Sound (G) and anomalies in the oxygen deficit by individual stations (H) following the format of panels A and B. Significant correlations (Spearman Rank Correl, p <0.05) are based on yearly averages of ocean indices and Puget Sound-wide anomaly values.

Larger variability exists in the anomalies of depth-integrated dissolved oxygen (0-50 m) (Fig. 2F). High anomalies in dissolved oxygen imply higher oxygen concentrations relative to expected conditions. On an annual Puget Sound-wide scale, dissolved oxygen anomalies significantly (Spearman Rank Correl. p<0.05, n=14) follow the North Pacific Gyre Oscillation (NPGO) (Fig. 2E). This suggests that the NPGO, which predicts productivity patterns along the western coast of North America (Di Lorenzo et al. 2009), extends also into Puget Sound waters.

Upwelling along the Washington west coast brings nutrient-rich and oxygen-depleted deeper ocean water onto the shelf. The water traverses Juan de Fuca Strait and enters Puget Sound at depth via Admiralty Reach. Upwelled water can strongly influence Puget Sound's deeper water bodies. To describe the severity of low oxygen in Puget Sound, we calculate the anomalies in the depth-integrated oxygen deficit from 20 m below the ocean surface down to the ocean bottom (denoted as >20-m depth). The oxygen deficit is the amount of oxygen needed to re-saturate the under-saturated portions of the water column with oxygen. High numbers imply that the water below 20 m is worse in respect to expected under-saturated oxygen levels. A significant positive correlation exists (Spearman Rank Correl. p<0.05, n=14) between upwelling intensity and the dissolved oxygen deficit at >20-m depth, (Fig. 2G)

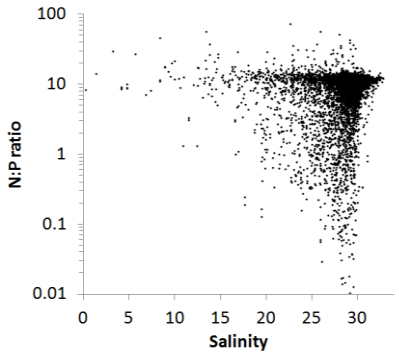

Figure 3. Puget Sound-wide data of the ratio of nitrogen to phosphate (N:P) in relation to salinities plotted from 1999 to 2012. Data clouds show a well defined N:P range between 10-11 in the higher salinity range (salinities >30). For salinities <30, salinity to N:P ratios significantly scatter and fall predominantly below ratios of more oceanic origin (higher salinity)

Upwelled, deep ocean water is low in oxygen concentrations and has reduced N:P ratios relative to ocean surface water. This is due to microbial denitrifaction and selective reduction of nitrogen in low oxygen zones. Ratios in N:P in Puget Sound are often even lower than upwelled deep ocean water (Fig. 3), a result of high primary productivity and selective removal of nitrogen from the water and the large microbial denitrification potential of the benthos (Braker et al. 2001, USGS study, http://pubs.usgs.gov/sir/2006/5106/section7.html). A significant positive correlation (Spearman Rank Correl. p<0.05, n=14) between upwelling intensity and the ratio of

nitrogen to phosphorus (N:P) at depth of 0-30 m can therefore be seen in Fig. 4A. Over the last 14 years, higher N:P ratios occurred during stronger upwelling years and restored lower N:P ratios in Puget Sound to near ocean conditions.

While all three indices showed extrema near the middle of the last decade (PDO-2004, NPGO-2005, and Upwelling-2007) and have significantly affected water quality variables, macro nutrients (nitrogen and phosphorus) continued to steadily increase in Puget Sound (Fig. 5A). Puget Sound-wide nitrate increased at a rate of 3 µM per decade (phosphorus increased 0.3 µM per decade, data not shown) (Fig. 5A). This affected noticeably the silicate to dissolved inorganic nitrogen (Si:DIN) ratio, which showed a decline of 10 units per decade (Fig. 5B).

Changes in the Si:DIN ratios are considered a sign of human nutrient inputs (Harashima, 2007). The significant decline (Spearman Rank Correl. $p<0.05$, $n=13$) in the Si:DIN ratio paired with increases in macro nutrients (nitrate, Figs. 5A and B) favors the growth of non-silicified phytoplankton species such as dinoflagellates *Noctiluca* (Fig. 6D and E) among others.

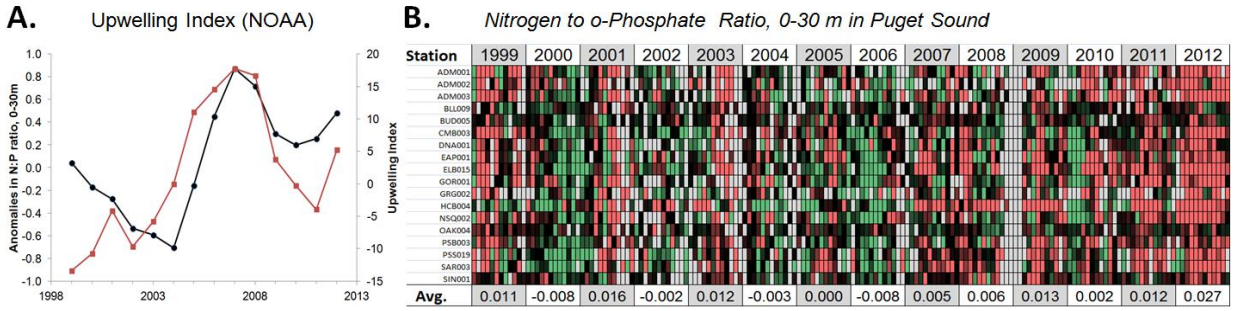

Figure 4. The influence of ocean boundary conditions on N:P ratios at 0- to 30-m depth relative to site- and seasonal-specific baseline conditions established from 1999 to 2008. A: Puget Sound-wide yearly averaged anomalies in N:P ratios correlate with the Upwelling Index at 48°N, 125°W (both series are shown as a 3-year running average). B: Monthly anomalies (in color) in the N:P ratios shown for individual stations that went into the generation of graph A, show many high values in 2012. Red and green highlight anomalies outside the 25th and 75th percentiles, respectively; black values fall near the median; gray color illustrates missed sampling events. Significant correlations (Spearman Rank Correl, $p<0.05$) are based on yearly averages of ocean indices and Puget Sound-wide anomaly values.

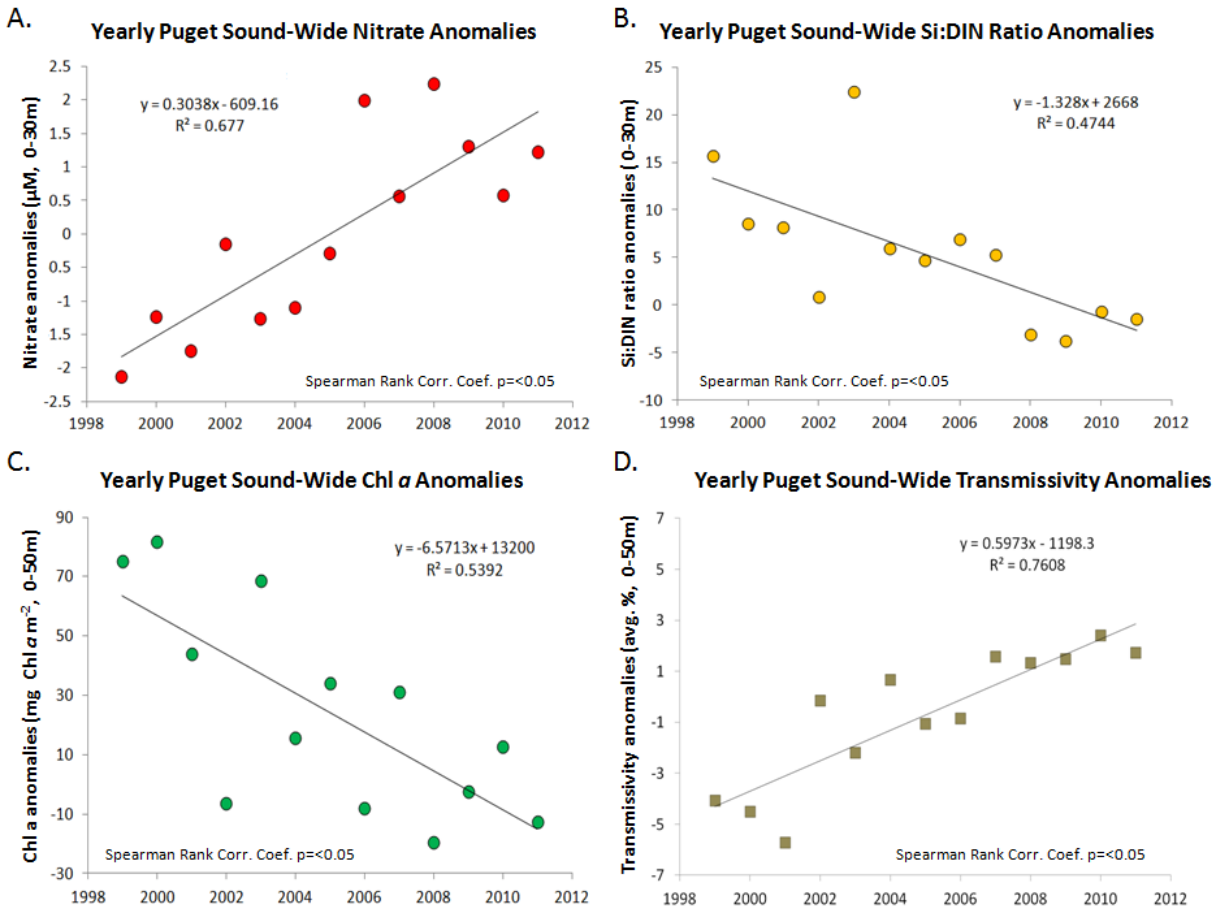

Figure 5. Long-term trends in yearly Puget Sound-wide anomalies for nitrate (A), the silicate to dissolved inorganic nitrogen ratio (Si:DIN) (B), chl a (C) and water transmissivity (D). While nitrate significantly increased at a rate of 3 µM per decade resulting in a significant decrease in the Si:DIN ratio of about 10 units per decade, overall sub-surface chl a concentrations have declined by 65 mg m^{-2}. A transmissivity sensor independently confirmed the decline with a significant increase in water clarity.

Generally, 2012 was marked by lower than expected salinities and temperatures, and higher than expected dissolved oxygen concentrations relative to a 1999-2008 baseline (Fig. 2B,D,F) shown) at most depths. Chl *a* concentrations (0-50 m) were slightly higher than in 2011 but still below expected values. Very high abundances of jellyfish started in August 2012 in south Puget Sound and Sinclair Inlet and persisted over the winter well into January 2013 (http://www.ecy.wa.gov/programs/eap/mar_wat/eops/EOPS_2012_11_08.pdf).

Over the last two years, Ecology's Eyes Over Puget Sound reports (EOPS) (http://www.ecy.wa.gov/programs/eap/mar_wat/surface.html) have documented extensive near-surface blooms of *Noctiluca* and other dinoflagellates in many locations in Puget Sound starting as early as February and lasting well into November. Despite large, frequent and extensive near-surface blooms of dinoflagellates, depth integrated chl *a* concentrations (0-50 m) in Puget Sound have significantly declined at a rate of 80 mg per decade (Spearman Rank Correl. $p<0.05$, $n=13$) (Fig. 5C). Coincidently, water clarity has significantly (Spearman Rank Correl. $p<0.05$, $n=13$) increased (Fig. 5D) which independently corroborates the decline in chl *a*.

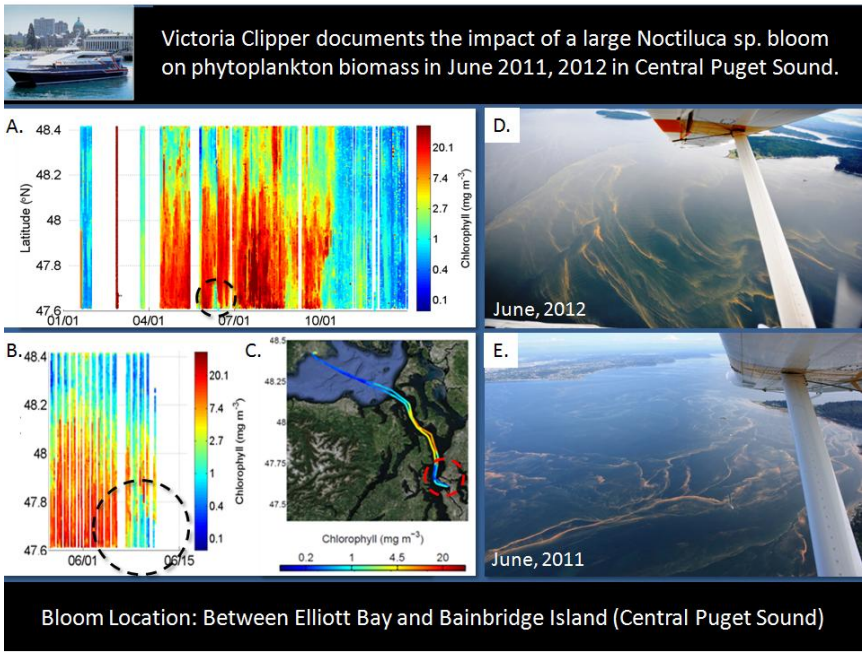

Figure 6. The dinoflagellate Noctiluca sp. formed intense blooms in June 2011 and 2012 that could be seen in a rapid decline of in situ chl a concentrations measured with the Victoria Clipper en route ferry monitoring system (A and B) (dotted circles). The more localized and intense bloom in 2012 clearly diminished chl a concentrations between 47.6 ^{0} and 47.8 ^{0} north (B) along the ferry transect (C).

Noctiluca sp. can be autotrophic (green form photosynthesizes with the help of endosymbionts) and heterotrophic (red and orange forms need to feed) (Hansen 1991, Padmakumar et al. 2010) and is frequently associated with eutrified coastal environments (Vasas et al., 2007). Over the course of the last two years, 2011 and 2012, we documented two extensive orange-red *Noctiluca* blooms in Central Puget Sound (Fig. 6B, E). A very large bloom in 2011 and a more localized but intense bloom in 2012 both quickly reduced chl *a* concentrations in the water column. The impact of dinoflagellate *Noctiluca* grazing on phytoplankton biomass appeared in Ecology's ferry sensor system (Victoria Clipper) (Fig. 6A). The grazing of phytoplankton was independently corroborated by other moorings (data not shown). Chl *a* dropped within days of the *Noctiluca* bloom that had visibly accumulated at the surface during calm wind conditions. Images of the blooms can be found in the EOPS reports for June 20, 2011 and June 12, 2012:

- http://www.ecy.wa.gov/programs/eap/mar_wat/eops/EOPS_2011_06_20.pdf,
- http://www.ecy.wa.gov/programs/eap/mar_wat/eops/EOPS_2012_06_12.pdf.

References

Braker G., Ayala-del-Río1 H.L., Devol A.H., Fesefeldt A. and Tiedje, J.M. 2001. Community Structure of Denitrifiers, Bacteria, and Archaea along Redox Gradients in Pacific Northwest Marine Sediments by Terminal Restriction Fragment Length Polymorphism Analysis of Amplified Nitrite Reductase (nirS) and 16S rRNA Genes. Appl. Environ. Microbiol. Vol. 67 no. 4, p. 1893-1901. doi: 10.1128/AEM.67.4.1893-1901.2001

Di Lorenzo, E., Fiechter, J., Schneider, N., Bracco,A., Miller, A.J., Franks, P.J.S., Bograd, S. J., Moore ,A. M., Thomas, A. C., Crawford, W., Pena, A. and Hermann, A. J. 2009: Nutrient and salinity decadal variations in the central and eastern North Pacific. Geophysical Research Letters, 36, doi:10.1029/2009GL038261.

Hansen J, 1991. Quantitative importance and trophic role of heterotrophic dinoflagellates in a coastal pelagial food web. Mar. Ecol. Prog. Ser. 73, p. 253-261.

Harashima A., 2007. Evaluating the effects of change in input ratio of N:P:Si to coastal marine ecosystem. J. Environ. Sci. Sustainable Soc., 1, p. 33-38.

Padmakumar K.B., SreeRenjima G., Fanimol C.L., Menon N.R., and V.N. Sanjeevan, 2010. Preponderance of heterotrophic Noctiluca scintillans during a multi-species diatom bloom along thesouthwest coast of India. International Journal of Oceans and Oceanography. 4, no. 1, p. 55-63.

Vasas A., Lancelot C., Rousseau V. and Jordan, F. 2007. Eutrophication and overfishing in temperate nearshore pelagic food webs: a network perspective. Mar. Ecol. Prog. Ser., 336, p. 1-4.

2.2.4. Spring phytoplankton bloom in the Strait of Georgia

Susan E. Allen[1], Douglas J. Latornell[1], Jim Gower[2] and Benjamin Moore-Maley[1]
[1]University of British Columbia, [2]Fisheries and Oceans Canada

The spring phytoplankton bloom in the Strait of Georgia develops in the late winter or early spring as light becomes more available to phytoplankton. Light becomes stronger because: 1) the season is changing, bringing longer days and the sun higher in the sky; 2) the mixing layer is becoming shallower because wind speeds tend to drop; 3) the cloud fraction in the sky decreases allowing more sunlight to reach the ocean. The bloom decreases when the near surface nutrients are consumed by the phytoplankton. The first species to bloom in the Strait of Georgia are *Thalassiosira* spp. (Harrison et al., 1983; Collins et al., 2009). The interannual variation in the spring bloom is seven weeks (Collins et al., 2009; Allen and Wolfe, in press.), ranging in date from 24 February to 14 April. We have developed a computer model for the physics and lower trophic levels in the Strait of Georgia which can successfully hindcast the spring bloom (Collins et al., 2009).

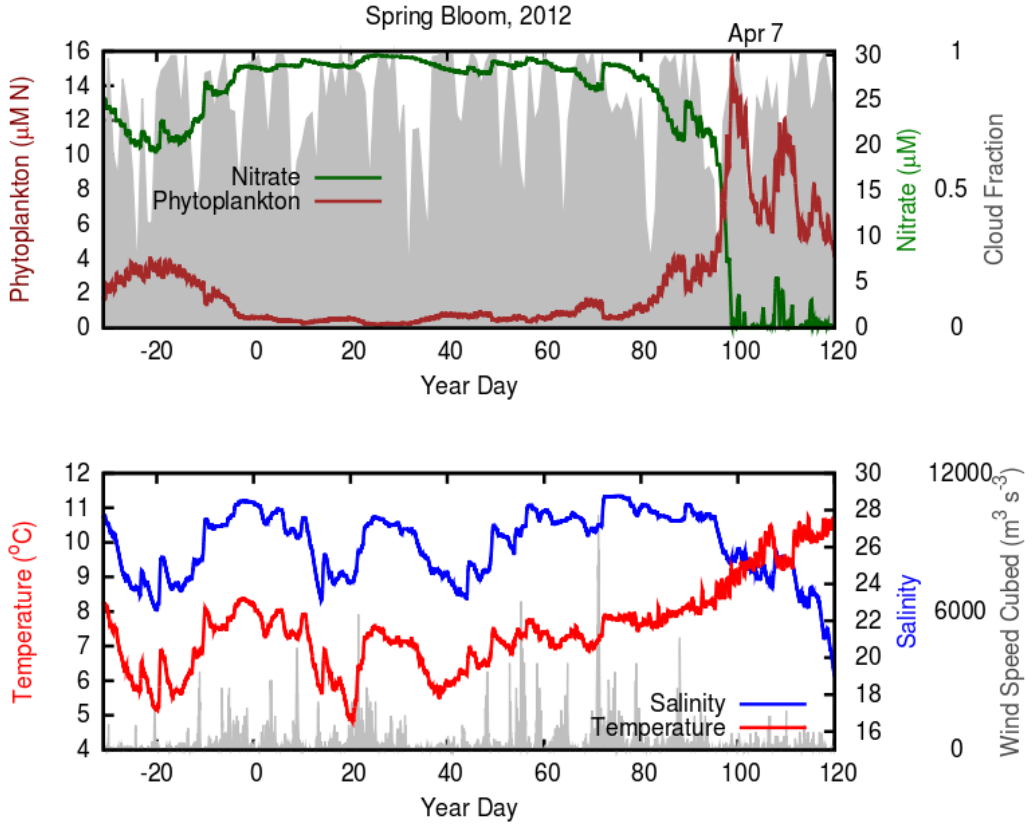

Figure 1. Hindcast of the 2012 spring bloom and related conditions in the Strait of Georgia, illustrating model outputs of temperature, salinity, nitrate and phytoplankton, and measured winds and clouds. The lower panel shows temperature (in red) and salinity (in blue) averaged over the upper 3 m of the water column; in grey is the wind-speed cubed which is directly related to the strength of the mixing.

One can clearly see the mixing associated with the storm about day 70; salinities sharply increase as deeper, high-salinity water is mixed into the surface waters and temperatures also sharply increase as deeper, warmer water is mixed upward. The top panel shows phytoplankton biomass (in dark red) and nitrate (in green); in grey is the cloud fraction averaged

over the day. One can see the evidence of mixing due to storms such as the day 70 storm; nitrate rapidly increases and phytoplankton biomass decreases. One can also see the influence of low-wind, low cloud-fraction periods such as that around day 30 and again around day 80. Here phytoplankton biomass steadily increases and nitrate decreases. The 2012 spring bloom was late (Apr 7) because of the large number of storms and associated high-cloud fraction.

The 2012 Spring Bloom

The winter and early spring of 2012 were windy and cloudy. Both high winds and high cloud-fraction delay the spring bloom and the bloom was indeed late (Fig. 1). Peak biomass date is hindcast by the model as Apr 7. The onset of the spring bloom (as opposed to the peak biomass date) is determined as that date when the fluorescence signal from surface chlorophyll equivalent measured by satellite is observed to be more than about 5 $mg.m^{-3}$ over 30% or more of the surface of the Strait. In 2012, the onset of the spring bloom was observed to be late, on about March 31. These two dates (onset March 31, peak Apr 7) compare well with the peak of the bloom also estimated by satellite (Costa et al.).

According to the model, spring blooms from 2006-2011 were all later than March 29 (Allen and Wolfe, in press), meaning we have been in a period of stable, late spring blooms (Fig. 2). According to the satellite estimates the onsets of the blooms in 2007, 2008 and 2009 were much earlier. In these years, the satellite imagery shows phytoplankton biomass increases in the fjords bordering the Strait early in the year and shows this phytoplankton biomass being advected into the Strait and thus seeding the Strait spring bloom (Gower et al., in press). Now that more data is available in the Strait we are hoping for a seeding event in future years to investigate this discrepancy.

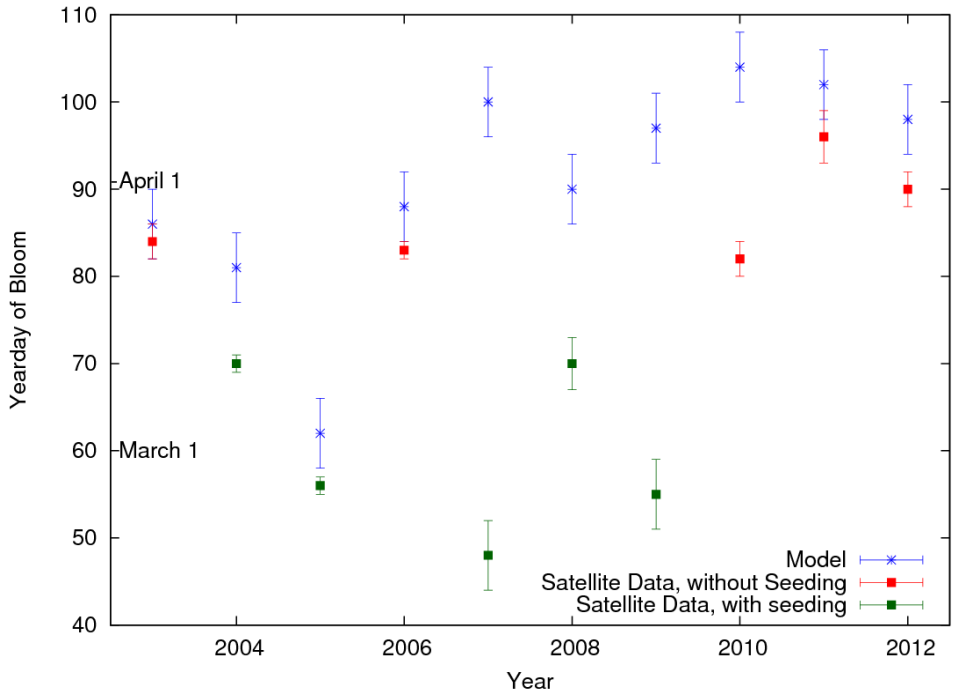

Figure 2. Model-derived peak bloom dates in blue. Satellite-derived onset dates for the spring bloom in years with seeding from bordering fjords (in green) and in years without seeding from bordering fjords (in red). The year 2012 shows a late spring bloom.

The 2013 Spring Bloom

The model can also be run using current weather data in a nowcast mode. After the current day, we can hypothesize the future weather and estimate the day of this year's peak bloom. We use three different future weathers: 1) the average weather (1968-2010) with a small correction so that if it is used from the previous autumn, it does give the average spring bloom date; 2) the weather from 1999 which led to the latest spring bloom (14 April) in the 1968-2010 period; and 3) the weather from 1993 which led to the earliest spring bloom (24 February) in the same period. The current forecast can be seen at http://eos.ubc.ca/~sallen/SoG-bloomcast/results.html. For comparison, observational data from the BC ferries measured by VENUS can be found at http://venus.uvic.ca/data/data-plots/strait-of-georgia-plots/strait-of-georgia-bc-ferries-vancouver-nanaimo-today/

As of Mar 1, 2013, weather data was available until the end of Feb 26, 2013. At this point, the prediction for the 2013 spring bloom is Apr 1, 2013 with the range running from Mar 28 (if the weather is light winds and sunny) to Apr 13 (if the weather is strong winds and cloudy). So the prediction is for a late to very late spring bloom, similar to the previous 7 years.

Details of the coupled-biophysical Model

The model is a vertical-mixing layer model forced by observed winds at Sand Heads, observed air temperature, humidity and cloud fraction at Vancouver International Airport (YVR), Fraser River flow at Hope and Englishman River flow at Parksville (Environment Canada, 2012 a and b). The latter is multiplied by 55 to represent all river flows into the Strait other than the Fraser River. The physical model is based on the Large et al. (1994) KPP-model with an estuarine circulation model added (Collins et al., 2009). To model a spring bloom, only a simple nitrate-diatom biological model is used. The diatom growth parameters are taken from the literature based on the first phytoplankton to bloom in the Strait (*Thalassiosira* spp.). The model zooplankton concentration was taken from observations (Sastri and Dower, 2009) and the model was tuned by adjusting the phytoplankton growth rate (Allen and Wolfe, in press) within the range measured in the laboratory. The model was tuned, within 4 days, for the spring blooms of 2002-2005 for which detailed observations were made as part of the STRATOGEM project (Allen and Wolfe, in press).

DFO's spring bloom monitoring for 2012

To study the onset of the spring bloom in 2012, we were able to use satellite imagery from MERIS and MODIS, recording fluorometers on buoy 46146 on Halibut Bank and on a dock at Egmont between Jervis and Sechelt Inlets, and a fluorometer on the *Spirit of Vancouver Island* ferry, sailing intermittently between Tsawwassen on the mainland and Swartz Bay on Vancouver Island. A bloom was observed by satellite and fluorometer in Sechelt Inlet in early March, but this did not trigger a bloom in Jervis Inlet and did not provide a “seeding” bloom into the Strait.

References

Allen, S. E. and Wolfe, M.A. In press. Hindcast of the timing of the spring phytoplankton bloom in the Strait of Georgia, 1968-2010. Prog. Oceanogr.

Collins, A. K., Allen, S. E., and Pawlowicz, R. 2009. The role of wind in determining the timing of the spring bloom in the Strait of Georgia. Can. J. Fish. Aquat. Sci. 66: 1597-1616.

Environment Canada, 2012a. Climate database [online]. http://www.climate.weatheroffice.gc.ca/climateData/canada_e.html

Environment Canada, 2012b. Hydrometric data [online]. http://www.ec.gc.ca/rhc-wsc/

Gower, J., King, S., Statham, S., Fox, R.and Young, E.In press. The Malaspina Dragon: a newly-discovered pattern of the early spring bloom in the Strait of Georgia, British Columbia, Canada. Prog. Oceanogr.

Harrison, P.J., Fulton, J.D., Taylor, F.J.R and Parsons, T.R. 1983. Review of the biological oceanography of the Strait of Georgia: Pelagic environoment. Can. J. Fish. Aquat. Sci. 40: 1064-1094.

Large, W.G., McWilliams, J.C., and Doney, S.C. 1994. Oceanic vertical mixing: A review and a model with a nonlocal boundary layer parameterization. *Rev. Geophys*. 32(4): 363–403.

Sastri, A.R., and Dower, J.F. 2009. Interannual variability in chitobiase-based production rates of the crustacean zooplankton community in the Strait of Georgia, British Columbia, Canada. Mar. Ecol. Prog. Ser. 388: 147–157.

2.2.5. Spatial-temporal phytoplankton bloom metrics in the Strait of Georgia derived from MODIS imagery: 2012 and previous years

Maycira, Costa[1], Tyson Carswell[1], Erika Young[1], Rusty Sweeting[2], Jim Gower[2], Rich Pawlowicz[3], Gary Borstad[4]
[1]University of Victoria, [2]Fisheries and Oceans Canada, [3]University of British Columbia, [4]ASL Environmental Sciences Inc.

Satellite remote sensing offers a synoptic, cost effective and repeatable method in deriving *ocean surface chlorophyll (Chl)* concentrations as a proxy for phytoplankton biomass, over traditional ship-based methods. The objective of this report is to illustrate the methods and associated results to determine phytoplankton bloom metrics (initiation, amplitude, and duration) in the Strait of Georgia (SoG) for 2007, 2008, and 2012 based on imagery from the MODIS satellite. Future work will include the analysis of the 10-year time series data of MODIS-derived bloom metrics and juvenile sockeye indices for the SoG.

The 2007, 2008, and 2012 Bloom Metrics

Image data (level 1a) were accessed from NASA's OceanColor web portal, and processed in SeaDAS (Seawifs Data Analysis System) environment. All available MODIS-Aqua images (n=3469, entire data base 2002-2012; n=465, 2007, 2008, and 2012) were processed. The images were firstly atmospheric calibrated and validated (R^2=0.7, slope 1.16; n=101) according to a Management Unit of the North Sea Mathematical Models (MUMM) and shortwave infrared wavelengths (SWIR) (Komick and Costa, submitted). Secondly, the empirical Ocean Color version 3-MODIS (OC3M) *Chl* algorithm was chosen and validated (R^2=0.7; slope 1.09; n=12 points) for the SoG. This was selected over other models as it is commonly used in global *Chl* monitoring, and achieves reasonably accurate estimates of *Chl* concentrations for the SoG when compared to other global models (Komick et al. 2009).

Thirdly, all *Chl* images were spatially binned and finally temporally binned to derive mean 8-day *Chl* concentrations. Mean 8-day *Chl* concentrations were collected for one region located in the south SoG, coinciding with the route of the ferry *Spirit of Vancouver Island*, which is equipped with a fluorometer as part of the 'Victoria Experimental Network Under the Sea' (VENUS). The number of available binned (8-day) images are 20 (2007); 19 (2008); 21 (2012).

In order to derive bloom dynamics that help describe underlying physical and biological forcing, a set of objective metrics must be applied to the imagery dataset. To quantify the characteristics of the spring blooms for the region, a shifted Gaussian function of time was fitted to the time-series of binned 8-day *Chl* concentrations (Zhai. et al., 2011). Timing of initiation is defined as the date where *Chl* concentrations are 20 percent of maximum amplitude. Duration of the bloom is defined as the cumulative time where chlorophyll concentrations are above the 20% threshold.

The results of the Gaussian fit representing the spring bloom are seen in Fig. 1. In the following discussion, a week is 8 days duration to match the binning period. The earliest timing of initiation (week 6.6 – mid February) was defined in 2008. This is much earlier than 2007 and 2012 years, week 12.0 (~end March) and week 12.8 (~beginning of April), respectively (Table 1). Further, 2007 and 2012 are also similar in regard to week of maximum observed *Chl* (~week 15) and maximum observed concentrations (~16.0 mg m^{-3}). Much lower maxima *Chl* were determined in 2008 (3.4 mg m^{-3}) but for a long duration (~ 80 days). The lower *Chl* in 2008 was also detected by the *Spirit of Vancouver Island* fluorometer (3.8 mg m^{-3}) for the same region; however the MODIS biomass metrics determined higher *Chl* for the central (13.7 mg m^{-3}) and northern (5.2 mg m^{-3}) regions of SoG (Carswell et al., 2012). The determined week of initiation

of bloom conditions in 2012 was on the second week of April, 10 days later than the defined bloom initiation by Allen et al. Our methods further defined that the 2012 maximum *Chl* was approximately 16.0 mg m^{-3}, happened on the third week of April, and the bloom lasted for about 42 days (Fig. 2). The day of bloom maximum happened approximately two weeks after the prediction of the coupled-biophysical model by Allen et al.

Determining inter-annual relationships between the timing/magnitude/duration of the spring bloom and the residence/condition of juvenile salmon entering from nursery lakes may be paramount for ecological based fisheries management. Our approach applied to a 10-year time series of data will help to understand these relationships.

(a) (b)

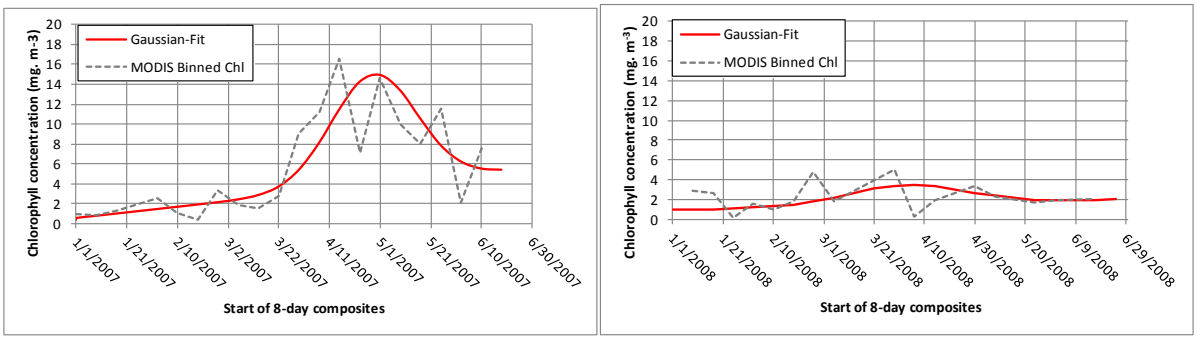

(c)

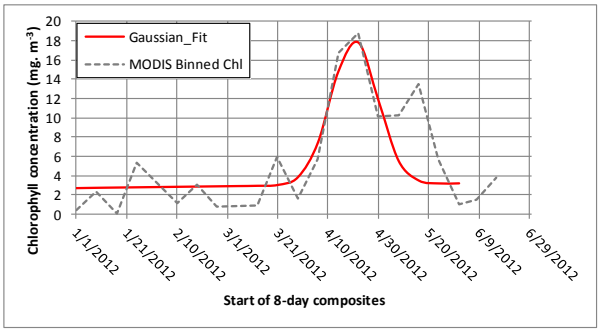

Figure 1. Gaussian fit curves of ocean surface chlorophyll, in red for (a) 2007, (b) 2008, and (c) 2012. Black lines are the 8-days binned MODIS-based chlorophyll concentrations.

Table 1. Biomass metrics of phytoplankton blooms based on Gaussian statistical fitting to MODIS chlorophyll concentrations at ocean surface in the southern Strait of Georgia.

Year	Week of Initiation	Week of Maxima	Duration (days)	Maximum Amplitude (Chl mg m^{-3})
2007	12.0 (6-April)	15.7 (5-May)	60	16.3
2008	6.6 (21-February)	11.7 (2-April)	82	3.4
2012	12.8 (11-April)	14.8 (27-April)	32	16.2

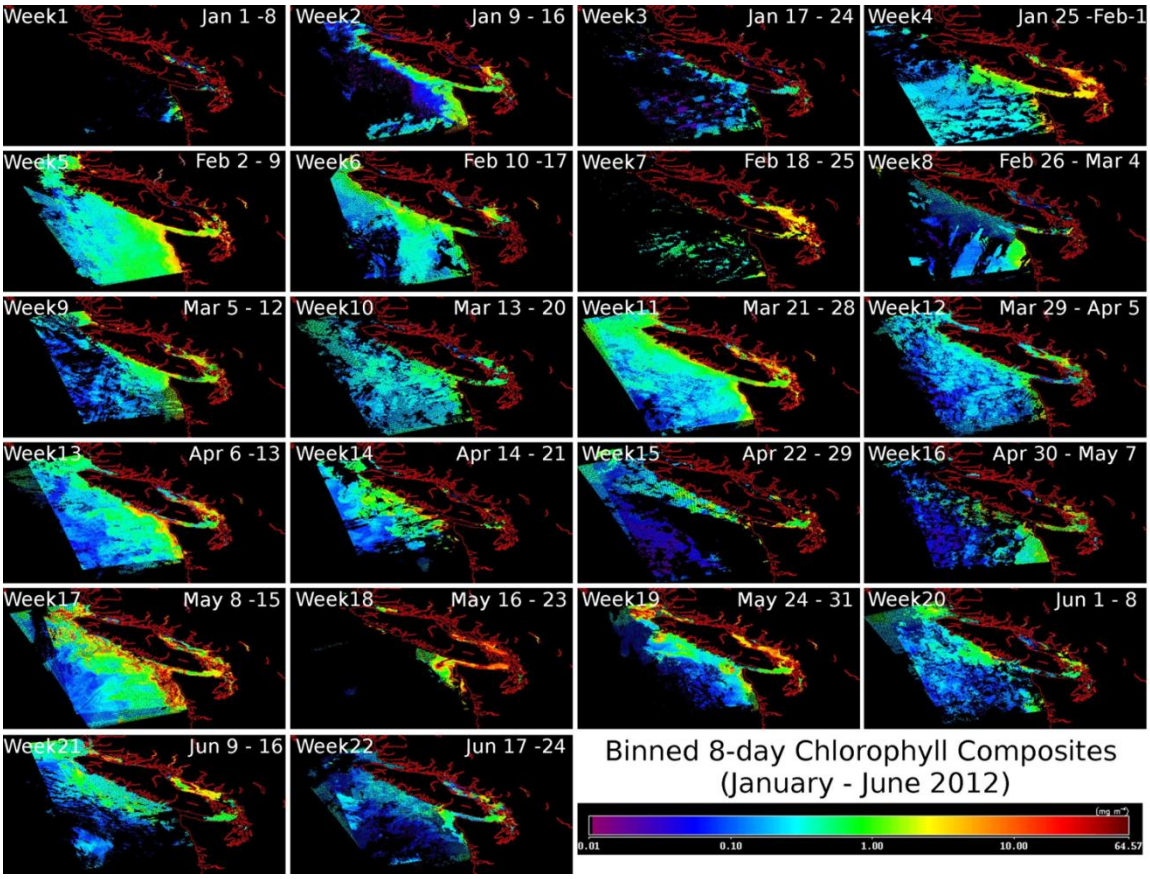

Figure 2. Spatial-temporal MODIS derived Chl products – January to June 2012.

Sources of Information

Carswell, T.K., Costa, M., Zhai, L., Komick, N., Gower, J., and Sweeting, R. 2012. Utilizing ship of opportunity fluorometry data coupled with satellite imagery to determine spring phytoplankton bloom dynamics in the Strait of Georgia, Canada. Ocean Optics Conference, October 8-12, Glasgow, Scotland.

Collins, A., Allen, S. E., and Pawlowicz, R. 2009. The role of wind in determining the timing of the spring bloom in the Strait of Georgia. Canadian Journal of Fisheries and Aquatic Sciences, 66(9), 1597-1616.

Costa, M; Carswell, T.; Young, E.; Komick, N; Zhai, L. MODIS atmospheric correction and chlorophyll products in the Strait of Georgia, British Columbia, Canada. In: International Ocean Colour Science Meeting, Darmstadt, Germany, May 6-8, 2013.

Kleppel,G. 1993. On the diets of calanoid copepods. Marine Ecology Progress Series, 99, 183-195.

Komick, N., Costa, M., and Gower, J. 2009. Bio-optical algorithm evaluation for MODIS for western Canada coastal waters: an exploratory approach using *in-situ* reflectance. Remote Sensing of Environment, 113(4), 794-804.

Mackas, D., Greve, W., Edwards, M., Chiba, S., Tadokoro, K, et al. 2011. Changing zooplankton seasonality in a changing ocean: Comparing time series of zooplankton phenology. Progress in Oceanography, 97-100, 31-62.

Marmorek, D., D. Pickard, A. Hall, K. Bryan, L. Martell, C. Alexander, K. Wieckowski, L. Greig and C. Schwarz. 2011. Fraser River sockeye salmon: data synthesis and cumulative impacts. ESSA Technologies Ltd. Cohen CommissionTech. Rep. 6. 273p. Vancouver, B.C. www.cohencommission.ca.

Rensel, J., Haigh, N., Tynan, T. 2010. Fraser river sockeye salmon marine survival decline and harmful blooms of Heterosigma akashiwo. Harmful Algae, 10(1), 98-115.

Stuart, V., Platt, T., and Sathyendranath, S. 2011. The future of fisheries science in management: a remote-sensing perspective. International Journal of Marine Science, 68(4), 644-650.

Thomson, R.E., Beamish R. R., Beacham, T.D., Trudel, M., Whitfield, P.H., and Hourston, R.A.S. 2012. Anomalous ocean conditions may explain the recent extreme variability in Fraser River sockeye salmon production. Marine and Costal Fisheries: Dynamics, Management, and Ecosystem Sciences, 4:415-437.

Zhai, L., Platt, T., Tang, C., Sathyendranath, S., and Hernandez Walls, R. 2011. Phytoplankton phenology on the Scotian Shelf. ICES Journal of Marine Science, 68(4),781-791.

2.2.6. Zooplankton in the Strait of Georgia: continued recovery of large-bodied "cool ocean" zooplankton from low levels 2005-2007

Dave Mackas, Moira Galbraith, and Kelly Young, Fisheries and Oceans Canada

Unlike the Vancouver Island outer coast (see Mackas et al. 1 and Mackas et al. 2001, 2007), zooplankton sampling in the Strait of Georgia (SOG) has been intermittent, and done by a number of separate and shorter-term sampling programs. However, as part of the 2008-2010 Strait of Georgia "Ecosystem Research Initiative", we were able to compile and analyze historic zooplankton data dating back to 1990 (earlier data were also compiled, but in most cases the earlier samples were processed for only one or a few target species, rather than the entire zooplankton community). Because of time varying taxonomic resolution (especially for pre-adult zooplankton life stages), our analysis of the SoG zooplankton community has merged the source data into broader categories (size classes within major taxa) than the species level resolution used in our outer coast time series. In addition, many of the dominant zooplankton taxa in the SOG make extensive vertical migrations at daily and/or seasonal time scales. For this reason, we have focused our analysis on a subset of samples that were collected at deep locations using net tows that sampled all or most of the water column. From 1990-1995 and 1998-2010, sampling by DFO and the Universities of Victoria and British Columbia provided a methodologically-consistent and year-round set of time series samples that meet these criteria. This report is a brief summary of an analysis of the 1990-2010 time series recently completed by Mackas et al. (in press). An additional analysis by Li et al. (in press) focused on a different subset of samples (1992-2007) collected by 0-50 m net tows around the margins of the Strait.

Both Li et al. (in press) and Mackas et al. (in press) report large decadal changes in the SOG zooplankton community. The SoG zooplankton interannual variability differs in time scale and phasing from the outer coast time series described above. Within the SoG, there is little or no oscillation between 'northern' and 'southern' communities, and somewhat more evidence of sustained trends and/or very low frequency fluctuations. Both in earlier years (Harrison et al. 1983) and since 1990 (Mackas et al., in press), total zooplankton dryweight biomass has been dominated by copepods (~40%) and euphausiids (~29%). Post 1990 time series for these two categories are shown in Fig. 1. Along with many other zooplankton taxa, copepods and euphausiids had low biomass in 1994-95 and very low biomass in 2005-07.

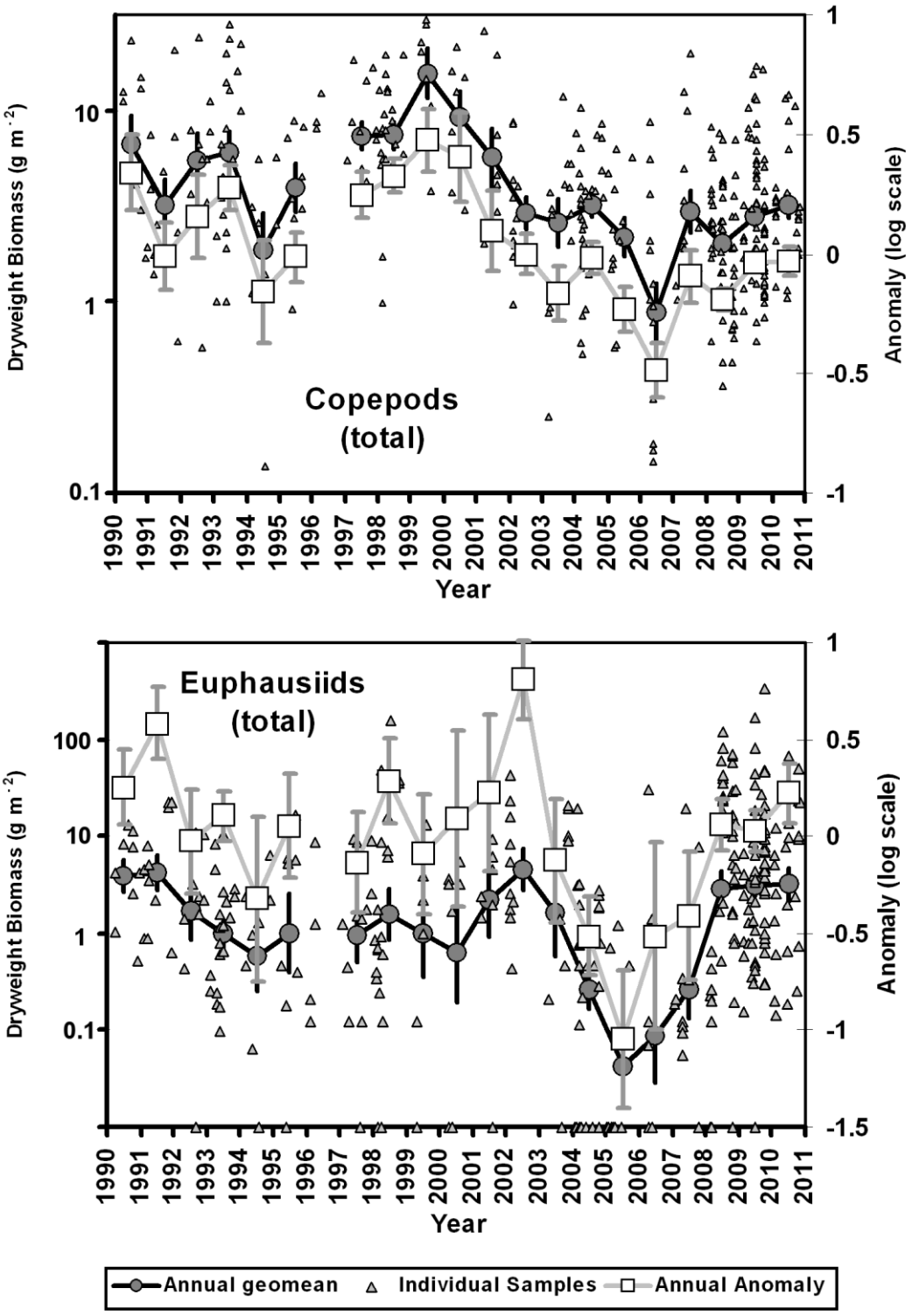

Figure 1. Examples of 1990-2010 zooplankton time series from the Strait of Georgia (from Mackas et al. in press). Top panel shows total copepods, bottom panel shows total euphausiids. Squares indicate log-scale anomalies relative to average seasonal cycle. Grey circles indicate annual geomean dryweight biomass; small triangles are biomass in individual samples. 1996 had too few samples to report annual geomean and anomaly.

Interannual variability of the entire zooplankton community is often summarized using a statistical technique called Principal Components Analysis (PCA). For the Strait of Georgia, nearly 36% of the total community variability projects onto the first principal component (time series shown in Fig. 2a). This component had positive coefficients for nearly all of the zooplankton taxa (i.e. a positive PC1 score indicates above-average biomass for most taxa). It also correlated strongly with below average temperature in the Strait, and with a North Pacific climate index called the North Pacific Gyre Oscillation (NPGO) (Fig. 2b).

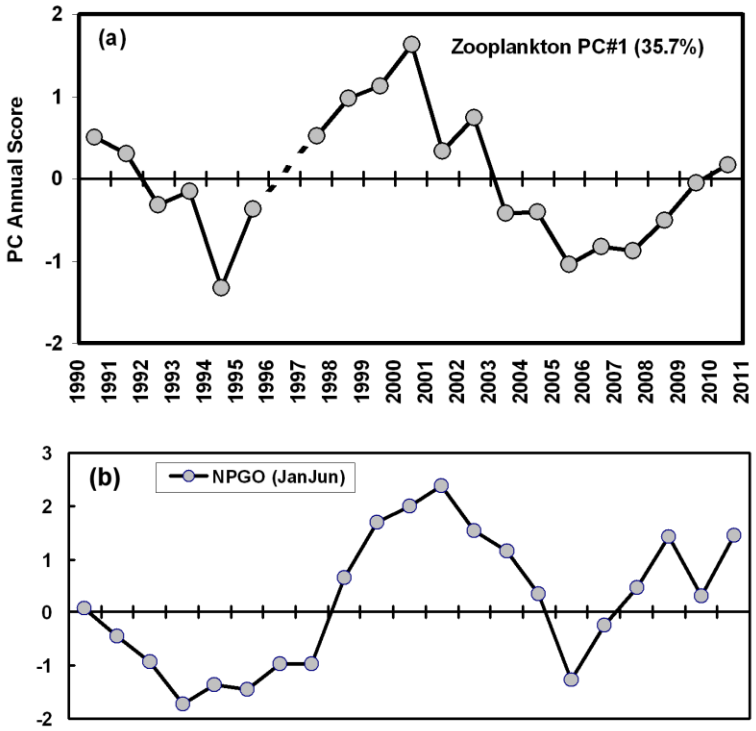

Figure 2. Time series of annual scores for the lead zooplankton PC, and for the North Pacific Gyre Oscillation Index (NPGO). Summarized from Mackas et al. in press.

ERI funding for the Strait of Georgia zooplankton analysis ended in 2010. However, in December 2012, we received supplementary DFO funding to process and analyze additional zooplankton samples that were collected opportunistically in 2011 and 2012. This analysis is not yet complete, but results to date indicate that the recovery from the 2005-2007 minimum of zooplankton biomass continued into 2012. Current levels appear to be similar to those in 1999-2002.

Sources of Information

Bornhold, E.A. 2000. Interannual and interdecadal patterns in timing and abundance of phytoplankton and zooplankton in the central Strait of Georgia, with special reference to *Neocalanus plumchrus*. MSc thesis, University of British Columbia, Vancouver

Campbell, R.W., Boutillier,P, and Dower, J.F. 2004.Ecophysiology of overwintering in the copepod *Neocalanus plumchrus*: changes in lipid and protein contents over a seasonal cycle. Mar. Ecol. Progr. Ser. 208, 211-226

El-Sabaawi, R., Dower, J.,Kainz, M., Mazumder, A. 2009. Characterizing dietary variability and trophic positions of coastal calanoid copepods: insight from stable isotopes and fatty acids. Marine Biology, 156, 225-237.

Fulton, J. 1973. Some aspects of the life history of *Calanus plumchrus* in the Strait of Georgia. J. Fisheries Research Board Canada 30, 811-815.

Harrison, P.J., Fulton, J.D., Taylor, F.J.R., Parsons, T.R. 1983. Review of the biological oceanography of the Strait of Georgia: Pelagic environment. Canadian Journal of Fisheries and Aquatic Sciences, 40, 1064-1094.

Li, L., Mackas,D. Hunt,B, Schweigert,J., Pakhomov, E., Perry,R.I., Galbraith,M., Pitcher,T.J. 2013 in press. Large changes in zooplankton communities in the Strait of Georgia, British Columbia, covary with environmental variability. Progress in Oceanography.

Mackas, D.L., S. Batten, and M. Trudel. 2007. Effects on zooplankton of a warming ocean: recent evidence from the North Pacific. Progr. Oceanogr. 75: 223-*252*.

Mackas, D.L., R.E. Thomson and M. Galbraith. 2001. Changes in the zooplankton community of the British Columbia continental margin, and covariation with oceanographic conditions, 1985-1998. Can. J. Fish. Aquat. Sci. 58: 685-702.

Mackas, D.L., Galbraith, M.D., Faust, D., Masson, D., Romaine, S., Shaw, W., Trudel, M., Dower, J., Campbell, R., Sastri, A., El Sabaawi, R. 2013 in press. Zooplankton time series from the Strait of Georgia: Results from year-round sampling at deep water locations, 1990-2010. Progress in Oceanography.

2.2.7. Juvenile salmon surveys in the Strait of Georgia 2012

Chrys Neville and Ruston Sweeting, Fisheries and Oceans Canada

Juvenile salmon generally enter the Strait of Georgia from April to June, many remaining there until the fall. In 2012 juvenile salmon were sampled during trawl surveys June 22 - July 2 and September 15 - 26. These surveys fished standard track lines sampled since 1998 following the protocol in Beamish et al. (2010). In this report we use a combination of the catch rates along with oceanographic conditions in the Strait of Georgia to estimate the relative strength of returning adults (return year dependent on species) for juvenile salmon that entered the ocean in 2012. Beamish et al. (2010) reported on the relationship between the catch rates of juvenile Coho Salmon and subsequent adult returns. In this report we apply the same methodology to all juvenile salmon catch rates with the assumption that early marine survival is a major component of determining total marine survival. The estimates provided are not for absolute returns but for the relative strength of returns compared to the survey time period.

The surface water temperature (SST) in 2012 continued the cooling trend of the past few years with an average SST from May to July of 14.5°C. This was similar to temperatures that had been observed in 2000 (Fig. 1), a strong production year. Surface salinity during this early summer period averaged 24.6 psu and was also lower than the previous few years (Chandler and Gower). Fraser River discharge in April increased over the previous four years but was within the variability observed over the past 12 years (Fig. 2). The cooler SST and lack of extreme flow conditions suggest that productivity conditions in the Strait of Georgia for juvenile salmon in 2012 were generally good.

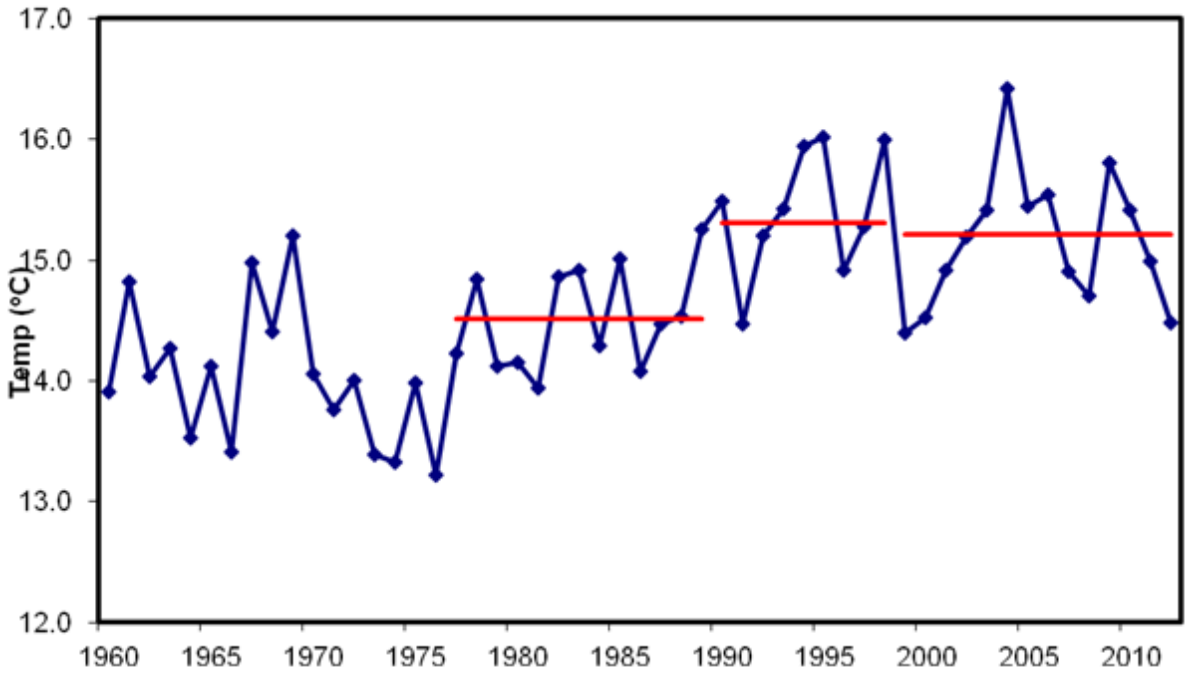

Figure 1. Average surface water temperature (SST) in May-July 1960-2012 in the Strait of Georgia. Measurements are averaged from five locations throughout the strait, including Cape Mudge, Chrome Island, Departure Bay, Entrance Islands, and Sisters Island. Data available from http://www.pac.dfo-mpo.gc.ca/science/oceans/data-donnees/lighthouses-phares/index-eng.htm*. The red bars are regime averages.*

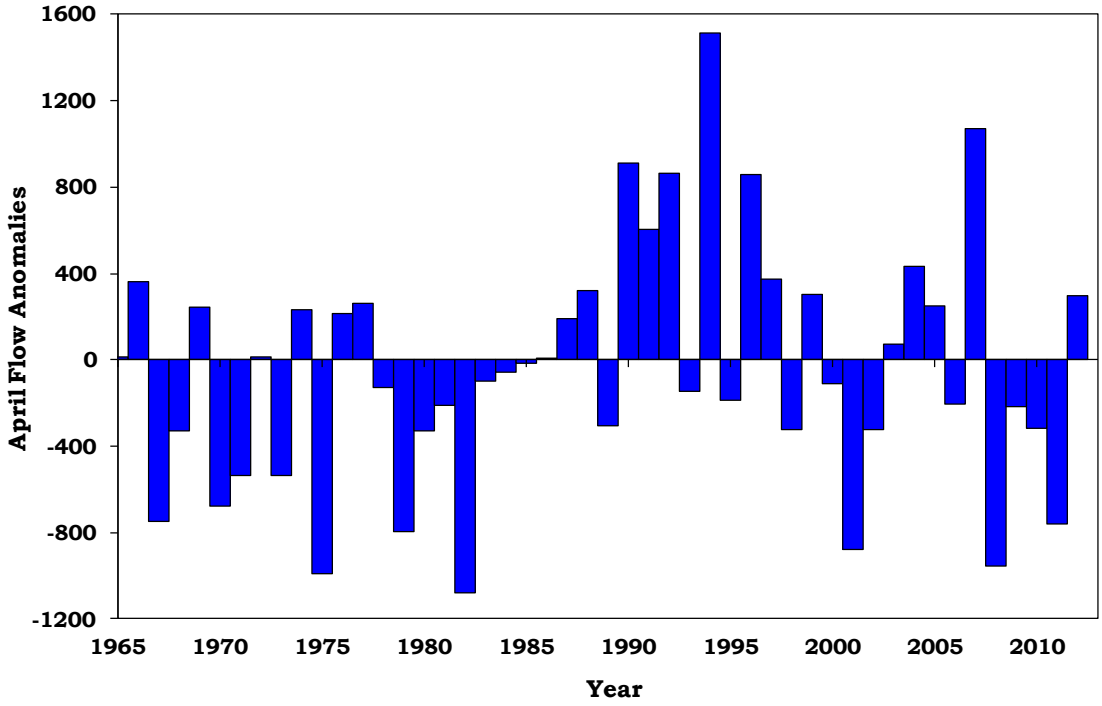

Figure 2. Anomaly of Fraser River flow (cubic meters per second) at Hope for April 1965-2012. Data are from station # 08MF005 provided by Water Resources Branch, Environment Canada

Many of the juvenile Sockeye Salmon that entered the Strait of Georgia in 2012 were progeny of the record return of Sockeye Salmon to the Fraser River in 2010. It was, therefore, not surprising that the CPUE of juvenile Sockeye Salmon in the early summer survey was the highest in the time series and almost double the long term average (Fig. 3A). While the length of these fish was the smallest observed in the time series (Fig. 3B), the size of sockeye juveniles in 2008, which resulted in the large 2010 return, was also small. Therefore, if there is no additional impact of the small size and if marine conditions are favourable along their subsequent migration route, we expect a **good** return of sockeye in 2014.

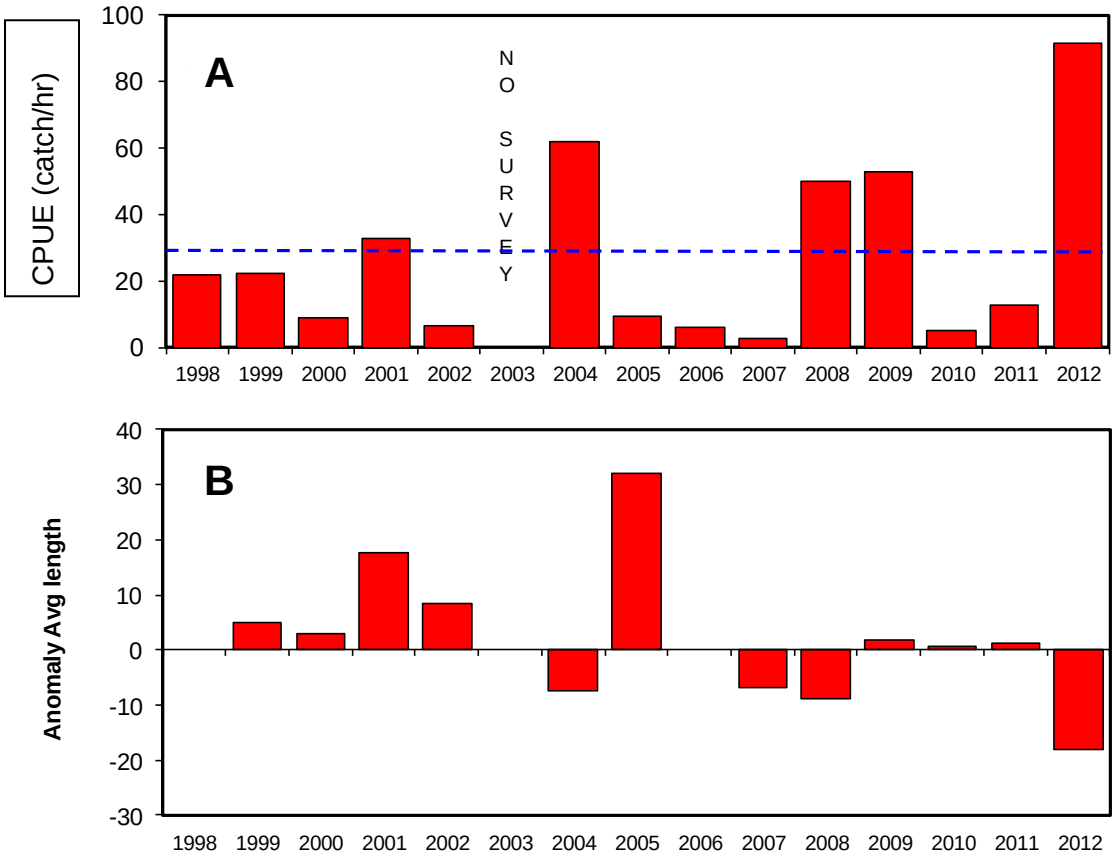

Figure 3. (A) CPUE and (B) anomaly of average length for juvenile Sockeye Salmon caught in the June/July trawl surveys in the Strait of Georgia 1998-2012. The juveniles in 2012 are from the record adult return to the Fraser River in 2010. Dashed line in (A) is average CPUE for 1998-2012.

Coho salmon generally spend one winter in the ocean, therefore, most juveniles that entered the ocean in 2012 will return in 2013. Juvenile Coho Salmon generally remain in the Strait of Georgia until fall (Chittenden et al. 2009) and this region is important in determining brood year strength (Beamish et al. 2010). The CPUE of Coho Salmon in July 2012 was similar to 2011 and below the time series average (Fig. 4A). However, the CPUE of Coho Salmon in the September 2012 survey was the highest in the time series (Fig. 4B). The estimated abundance of Coho Salmon in the Strait of Georgia in September 2012 was 4.0 million juveniles. Based on an update of the analysis described in Beamish et al. (2010) of the abundance of Coho Salmon in the September surveys compared to the total marine survival and the cooler SST in 2012 (Sweeting et al. 2010), a **good** return of Coho Salmon is expected in 2013.

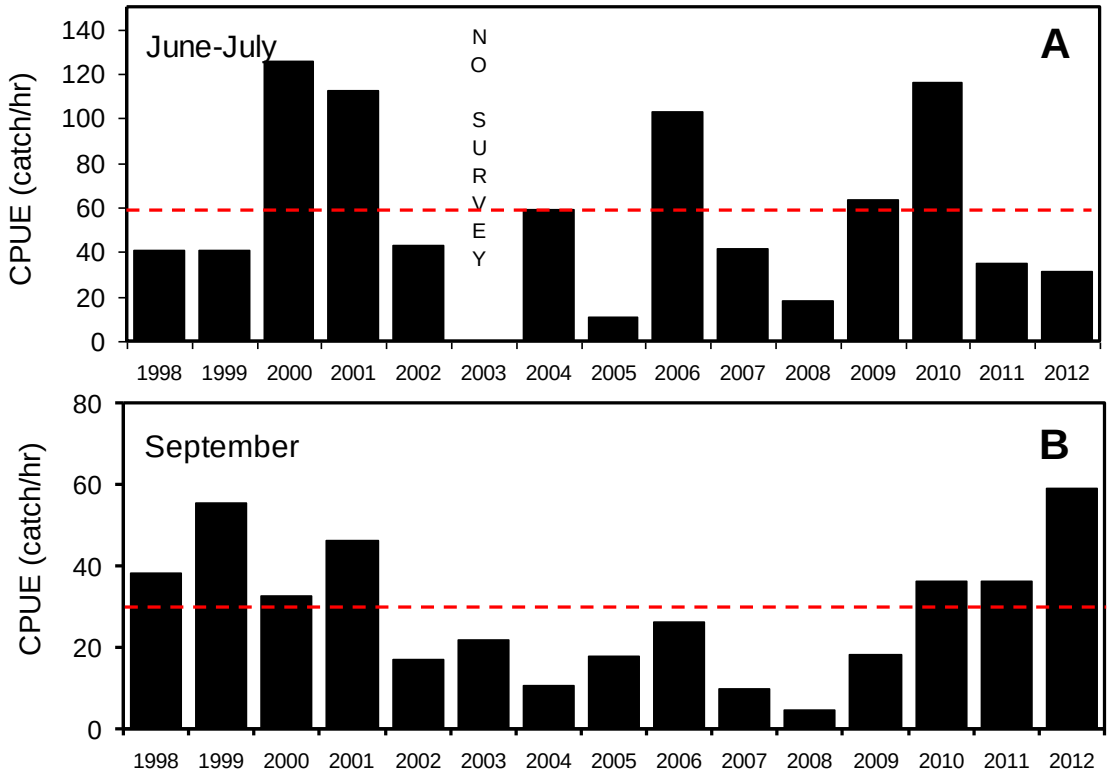

Figure 4. CPUE of Coho Salmon in (A) June-July and (B) September 1998-2012 in the Strait of Georgia. Dashed lines are average CPUE for 1998-2012.

Chum salmon enter the ocean in the year they emerge from the gravel and typically spend three winters in the ocean. The CPUE of Chum Salmon that entered the ocean in 2012 and were caught in the early summer survey was very low and similar to 2011 (Fig. 5). These two years were two of the four lowest observed in our time series. In addition, the juveniles in both these years were small. Based on the lower than average CPUE and size we expect **poor** returns of Chum Salmon in both 2014 and 2015.

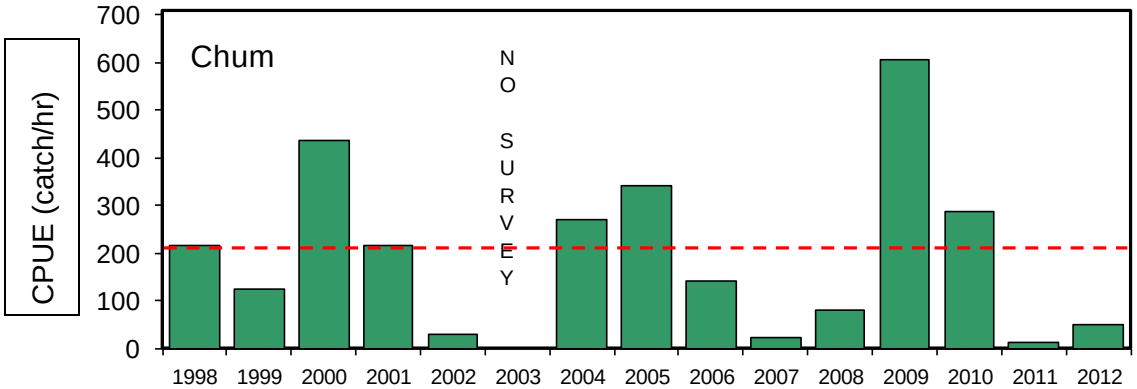

Figure 5. CPUE of Chum Salmon in the June-July trawl surveys in the Strait of Georgia 1998-2012. Dashed line is average CPUE for 1998-2012.

Chinook Salmon early life history is complex with variation in life history type (ocean and stream-type), age at ocean entry and timing of ocean entry. Results of DNA analysis of Chinook Salmon described in Beamish et al. (2011) indicated that catches in the June/July surveys are a mixture of ocean and stream type Chinook Salmon. The CPUE of Chinook Salmon that entered the ocean in the spring/early summer of 2012 and were caught in the early summer survey continued a declining trend from 2006 and was below the long term average (Fig. 6A). The average size of these fish was the largest we had observed in the time series (Fig. 6B) but we cannot determine if this is related to shifts in the proportion of ocean and stream type fish without further analysis. In general, we expect continued **poor** marine survival for Chinook Salmon and poor returns in 2014 and 2015.

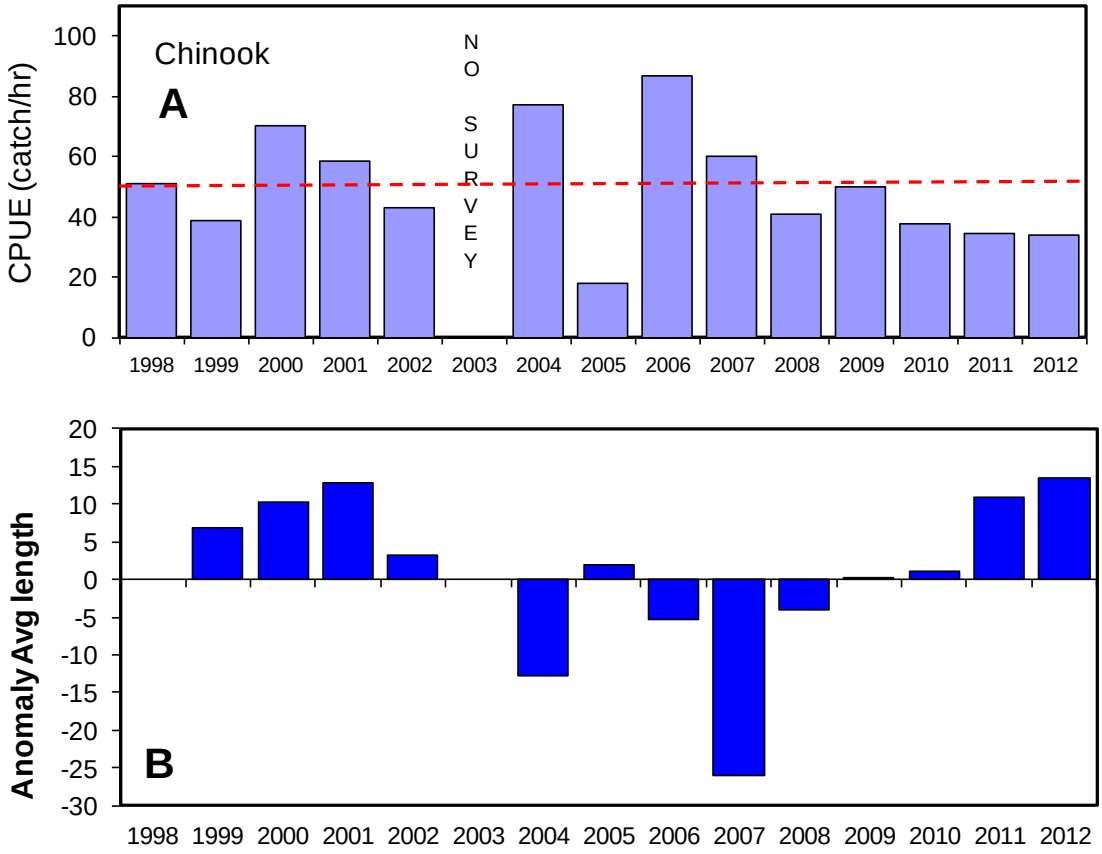

Figure 6. (A) CPUE and (B) anomaly of average length of juvenile Chinook Salmon caught in the June/July trawl surveys in the Strait of Georgia 1998-2012. Dashed line in (A) is average CPUE for 1998-2012.

The CPUE of Pink salmon in the early summer survey in 2012 was similar to observations in 2000 to 2008 (Fig. 7). It was not near the record high catches observed in 2010 although moderately strong related to the other even numbered years. We expect to see **good** returns of Pink Salmon to the Fraser River in 2013.

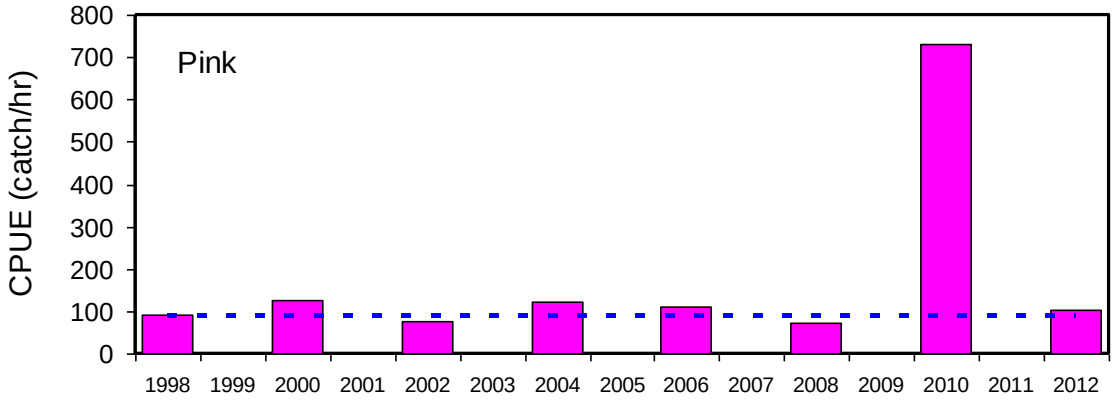

Figure 7. CPUE of Pink Salmon caught in the June/July trawl surveys in the Strait of Georgia 1998-2012. Dashed line is average CPUE for 1998-2012 excluding 2010.

References

Beamish, R.J., Sweeting, R.M., Lange, K.L., Noakes, D.J., Preikshot, D., and Neville, C.M. 2010. Early marine survival of coho salmon in the Strait of Georgia declines to very low levels. Marine and Coastal Fisheries: Dynamics, Management, and Ecosystem Science 2:424-439

Beamish, R.J., Lange, K.L., Neville, C.E., Sweeting, R.M., and Beacham, T.D. 2011. Structural patterns in the distribution of ocean- and stream-type juvenile chinook salmon populations in the Strait of Georgia in 2010 during the critical early marine period. NPAFC Doc. 1354, 27 p

Chittenden, C.M., Beamish, R.J., Neville, C.M., Sweeting, R.M., and McKinley, R.S. 2009. The use of acoustic tags to determine the timing and location of the juvenile coho salmon migration out of the Strait of Georgia, Canada. Transactions of American Fisheries Society 138:1220-1225

Sweeting, R., Lange, K., Neville, C., and Beamish, R. 2010. Juvenile salmon surveys in the Strait of Georgia. Pages 133-134 *in* W.R. Crawford and J.R. Irvine (eds.) State of physical, biological, and selected fishery resources of Pacific Canadian marine ecosystems. DFO Canadian Science Advisory Secretariat Research Document 2010/053.

2.2.8. Telemetry-based estimates of early marine survival and residence time of juvenile Sockeye Salmon in the Strait of Georgia and discovery passage, 2012

Erin L. Rechisky†, David W. Welch†, Aswea D. Porter†, Marika K. Gale^, Timothy D. Clark‡, Nathan B. Furey* and Scott G. Hinch*
†Kintama Research Services Ltd.; ‡Australian Institute of Marine Science; ^Freshwater Fisheries Society of British Columbia; *University of British Columbia

We used a large-scale acoustic telemetry array to track two year old Chilko Lake Sockeye Salmon smolts during the initial 1000 km of their freshwater and marine migration. Salmon smolts were surgically implanted with a uniquely coded acoustic transmitter ("tag") and then tracked with a network of acoustic sensors positioned within the Fraser River basin and at multiple sites in the Salish Sea (Fig. 1). By reconstructing the movements of each individual salmon from the data recorded by the array it was possible to estimate survival from Chilko Lake into the Fraser River and through the Strait of Georgia, Discovery Passage and Queen Charlotte Strait using the Cormack-Jolly-Seber model (Cormack 1964; Jolly 1965; Seber 1965) and to determine residence time (transit time) in these key areas. This report focuses on components of the west coast array that are variously managed by Kintama Research Services, the University of British Columbia and the Ocean Tracking Network (OTN).

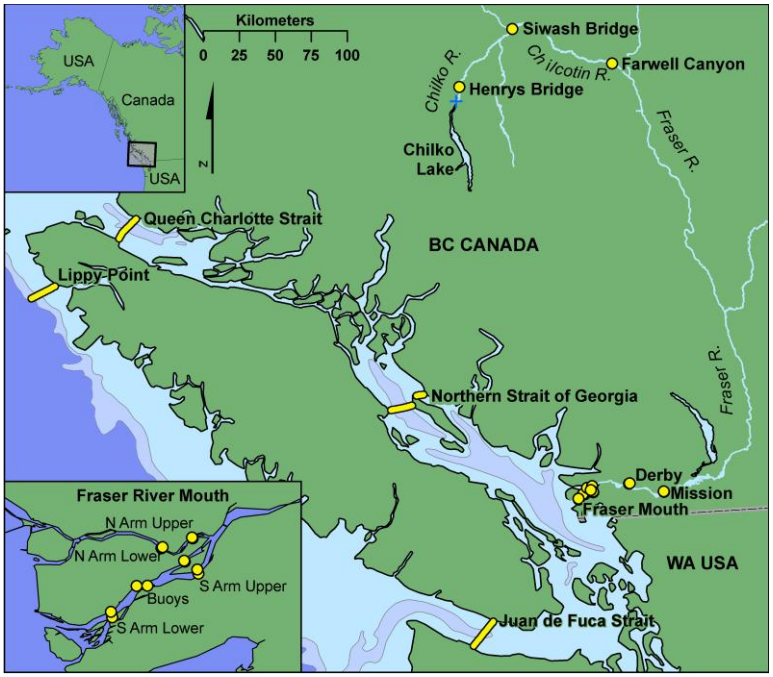

Figure 1. Map of the acoustic receiver array (yellow lines and dots) used to track juvenile Chilko Lake (Fraser River) Sockeye Salmon. The blue cross represents Chilko Lake release site in 2010, 2011 and 2012. Isobaths (200 and 500 meter) are coloured in pale blue. The Salish Sea includes Puget Sound to the south, Johnstone Strait to the north and Juan de Fuca Strait to the west

Chilko Lake Sockeye Early Survival Estimates

In 2012, freshwater survival from the DFO counting fence at the outlet of Chilko Lake to the Fraser River mouth was 29% (SE=3%) for smolts tagged with a 7 mm diameter tag (n=386) and 34% (SE=3%) for smolts tagged with a 5 mm tag (n=199). This is consistent with survival in 2011 (31% (SE=4%) and 32% (SE=5%) for smolts tagged with 7 mm (n=254) and 6 mm tags (n=200) and released at the fence, and higher than the 2010 estimate of 21% (SE=4%) for

smolts tagged with 7 mm tags and released at the fence (n=199; Fig. 2). Much of this mortality, however, appears to have occurred within the first 178 km (in the Chilko and Chilcotin rivers), and very little mortality occurred during the nearly 400 km migration through the Fraser River. This was further demonstrated by an additional treatment group release in 2011: smolts tagged with 7 mm transmitters were transported downstream of the high mortality area in the Chilko River and released near Siwash Bridge (Fig. 1). Mortality in the Chilcotin River was similar to the other treatment groups, and very little mortality occurred once smolts reached the Fraser River (Fig. 2).

Subsequent survival from the Fraser River mouth through the Strait of Georgia was 77% (SE=18%) for smolts tagged with 7 mm tags in 2012, considerably higher than the 2011 estimate (38%, SE=10%, excluding transported smolts) but similar to survival in 2010 (76% (SE=23%); 5 mm and 6 mm tags could only be detected in freshwater). Survival from the northern Strait of Georgia through Discovery Passage and much of Queen Charlotte Strait was highly variable: 31% (SE=10%) in 2012, 61% (SE=18%) in 2011 and 17% (SE=9%) in 2010. Thus, early marine survival from the Fraser River mouth to northeastern Vancouver Island was 24% (SE=6%) in 2012, 23% (SE=7%) in 2011, and 13% (SE=8%) in 2010.

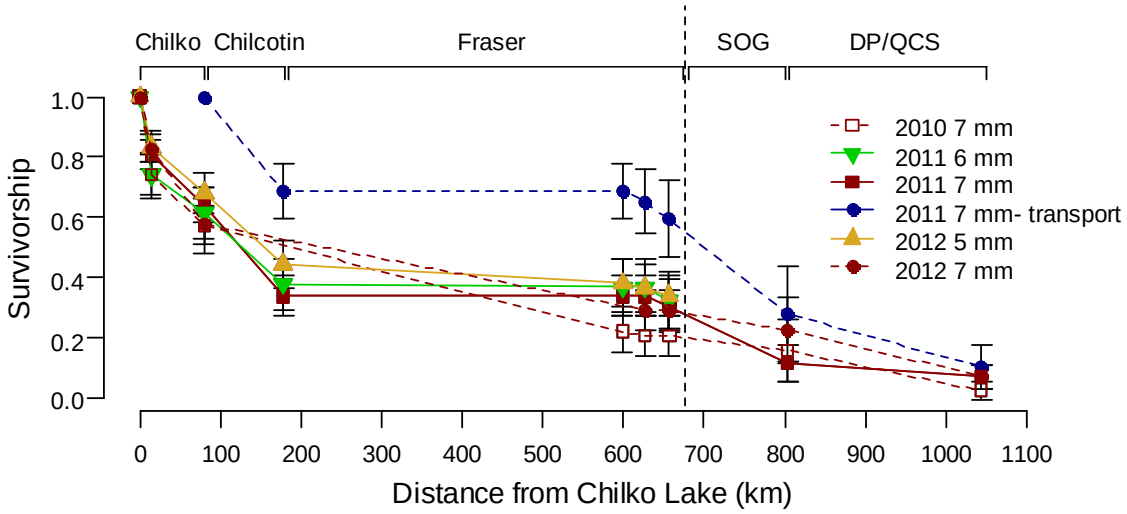

Figure 2. Cumulative survival of wild, two-year-old Chilko Lake sockeye smolts from release at the DFO counting fence near the outlet of Chilko Lake to Queen Charlotte Strait (QCS; NE Vancouver Island). SOG=Strait of Georgia, DP/QCS=Johnstone Strait/Queen Charlotte Strait. Smolts were implanted with 5 mm, 6 mm, or 7 mm diameter VEMCO transmitters (5 mm and 6 mm tags could only be detected in freshwater). In 2011, an experimental group of smolts was transported to an area near the confluence of the Chilko and Chilcotin rivers. The dashed vertical line represents the Fraser River mouth. Error bars are 95% confidence intervals. In 2010 and 2012 we could not separate Chilcotin and Fraser River survival for smolts tagged with 7 mm tags because either receivers were not deployed (2010) or did not detect smolts at that location (2012).

Cumulative survival from Chilko Lake to northern Vancouver Island, a distance of 1044 km, was 7% (SE=2%) for smolts in 2012, similar to survival in 2011 (7%, SE=2%) and higher than 2010 (only 3% (SE=2%); Fig. 2). No smolts were detected migrating via the southern route through Juan de Fuca Strait in 2010 and 2012. In 2011, three smolts were detected on the Juan de Fuca Strait sub-array; two of these three fish were later detected on the Lippy Point sub-array on the northwest end of Vancouver Island.

2012 was the third year for which we estimated survival of wild Chilko Lake sockeye smolts; however, in 2004-07, we made similar measurements for young hatchery-reared Cultus Lake Sockeye Salmon migrating down the Fraser River and through the Salish Sea, including the

crucial 2007 smolt outmigration year which led to extremely low returns in 2009 (see Welch et al. 2009). Thus, we now have seven years of direct, telemetry-based survival measurements for sockeye smolts along the inner coast of Vancouver Island. As with Chilko smolts, early marine survival of Cultus Lake smolts was variable: survival in the Strait of Georgia (SOG) ranged between 38-92%, and 37-60% through Discovery Passage and much of Queen Charlotte Strait.

Sockeye Daily Survival Rates

Daily survival rates of Chilko Lake Sockeye in freshwater were lower than Cultus Lake Sockeye (Fig. 3), presumably due to the high mortality experienced over a short period of time in the Chilko and Chilcotin rivers (Fig. 2). Chilko Sockeye smolts had relatively high and stable daily survival rates in the SOG in all years, and these survival rates were consistent with survival rates measured for Cultus Lake sockeye in prior years. Subsequent rates of survival during migration through the Johnstone Strait, Discovery Passage, and Queen Charlotte Strait region were generally lower and more variable than in the SOG for both Chilko and Cultus Lake smolts.

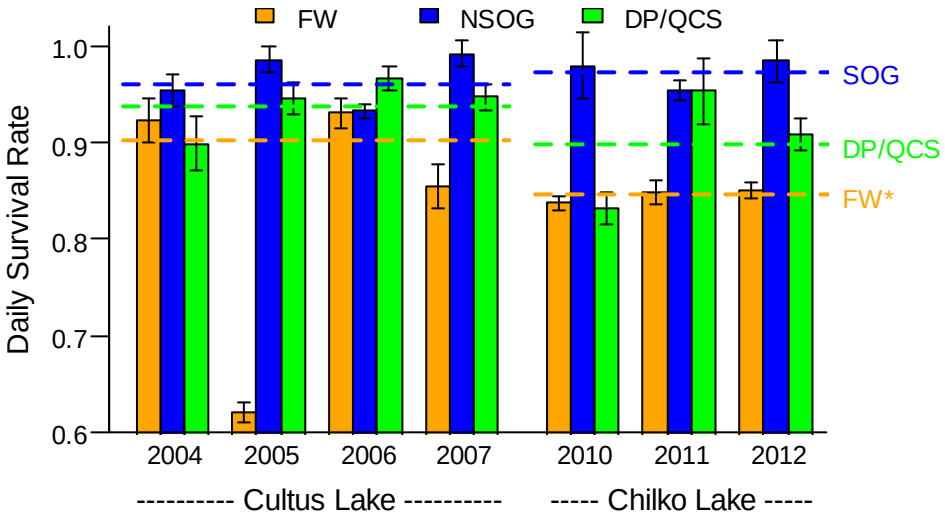

*Figure 3. Daily survival rate for two-year-old hatchery-reared Cultus and wild Chilko Lake sockeye smolts in the Fraser River basin (FW), Strait of Georgia (SOG) and Discovery Passage/Queen Charlotte Strait (DP/QCS). The six dashed horizontal lines indicate the multi-year average survival rate for each population in each of three habitats. *The FW average excludes 2005 Cultus Lake sockeye survival (see Welch, et al. 2009). Error bars show 95% confidence intervals.*

Chilko Smolt Residence Time in the Strait of Georgia and Queen Charlotte Strait

Travel time from Chilko Lake to the Fraser River mouth was approximately one week in all years (median travel time ranged from 5-9 days). Median travel time through the Strait of Georgia (Fraser River mouth to the Northern Strait of Georgia (NSOG) sub-array, 147 km) was 16.4 days in 2012, 18.6 days in 2011 and only 9.1 days in 2010 (Fig. 4) indicating that two year old smolts migrate quickly through the SOG (i.e. brief residence time). Smolts were last detected at NSOG in early June 2012, and in mid-June in 2010 and 2011. Travel time through Discovery Passage and QCS (from the NSOG sub-array to the QCS sub-array, 240 km) was even more rapid: 14 days in 2012, 10.8 days in 2011 and 9.4 days in 2010. Smolts were last detected in mid-June in 2012 and late June in 2010 and 2011.

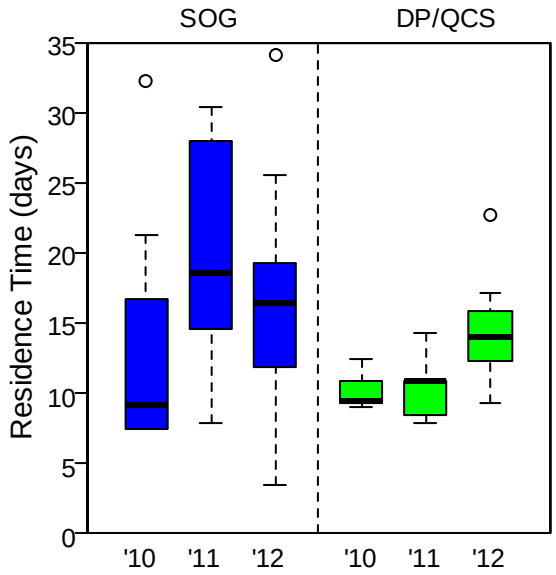

Figure 4. Residence time of acoustic tagged two-year-old Chilko Lake sockeye smolts in the Strait of Georgia (SOG) and Johnstone Strait/Queen Charlotte Strait (DP/QCS), 2010-2012 . The central band within the box is the median, the top and bottom side of each box are the 25th and 75th percentiles, and the whiskers extend to the minimum and maximum values exclusive of outliers. Outliers are beyond 1.5 times the interquartile range and are shown as open circles.

Summary

Our multi-year results indicate that survival patterns of Chilko Lake Sockeye smolts are remarkably consistent among years, that freshwater mortality appears to be largely confined to clear water tributaries upstream of the Fraser confluence, presumably due to predation, and survival down the Fraser River mainstem is very high. Once in the ocean, survival declines, and survival rates in the Strait of Georgia are more stable relative to survival rates in the Discovery Passage/Queen Charlotte Strait region. Transit times indicate smolts are rapidly migrating out of the SOG and QCS.

References

Cormack, R. M. 1964. Estimates of survival from the sighting of marked animals. Biometrika 51:429-438.

Jolly, G. M. 1965. Explicit estimates from capture-recapture data with both death and immigration- Stochastic model. Biometrika 52:225-247.

Seber, G. A. F. 1965. A note on the multiple recapture census. Biometrika 52:249-259.

Welch, D. W., M. C. Melnychuk, E. R. Rechisky, A. D. Porter, M. C. Jacobs, A. Ladouceur, R. S. McKinley, and G. D. Jackson. 2009. Freshwater and marine migration and survival of endangered Cultus Lake sockeye salmon (*Oncorhynchus nerka*) smolts using POST, a large-scale acoustic telemetry array. Canadian Journal of Fisheries and Aquatic Sciences 66(5):736-750.

2.2.9. Fraser Sockeye Salmon productivity: forecasts, indicators, and uncertainty

Sue Grant, Fisheries and Oceans Canada

Salmon forecasts remain highly uncertain, in large part due to wide variability in annual salmon productivity (recruits-per-spawner). For Fraser Sockeye, quantitative and qualitative indicators of productivity explored to date have not reduced forecast uncertainty and remain an active area of research. The limited understanding of mechanisms affecting Fraser Sockeye productivity is due to the broad range of environments these stocks occupy throughout their life-history. Fraser Sockeye generally spend their first two winters in freshwater, followed by their last two winters in the marine environment. In the freshwater environment, they spend their first winter as eggs incubating in their spawning gravel and their second winter rearing as fry in their rearing lakes, and then migrate downstream to the Strait of Georgia as smolts. In the marine environment, they migrate rapidly northward in the Strait of Georgia (Preikshot et al. 2012), and move into the North Pacific via the Johnstone Strait. Fraser Sockeye continue their northward migration along the continental shelf, and move into the Northeast Pacific in their first winter at sea (Tucker et al. 2009), and spend one more winter in the marine environment before they return to their natal spawning grounds to spawn.

Considerable mortality and inter-annual variability in mortality occurs in the freshwater and marine ecosystems, as indicated by freshwater and marine survival of Chilko River Sockeye (Fraser Sockeye indicator stock) (Fig. 1). Chilko is the only Fraser Sockeye stock with a long and complete time series of smolt data (counted through an enumeration weir located at the outlet of Chilko Lake), which can be used with escapement and return data to partition total survival into freshwater and ‘marine’ (‘marine’ survival includes their migration downstream from the counting weir to the Strait of Georgia). Therefore, it is likely that a number of factors in both the freshwater and marine environments influence Fraser Sockeye productivity, and these factors may vary between stocks and inter-annually.

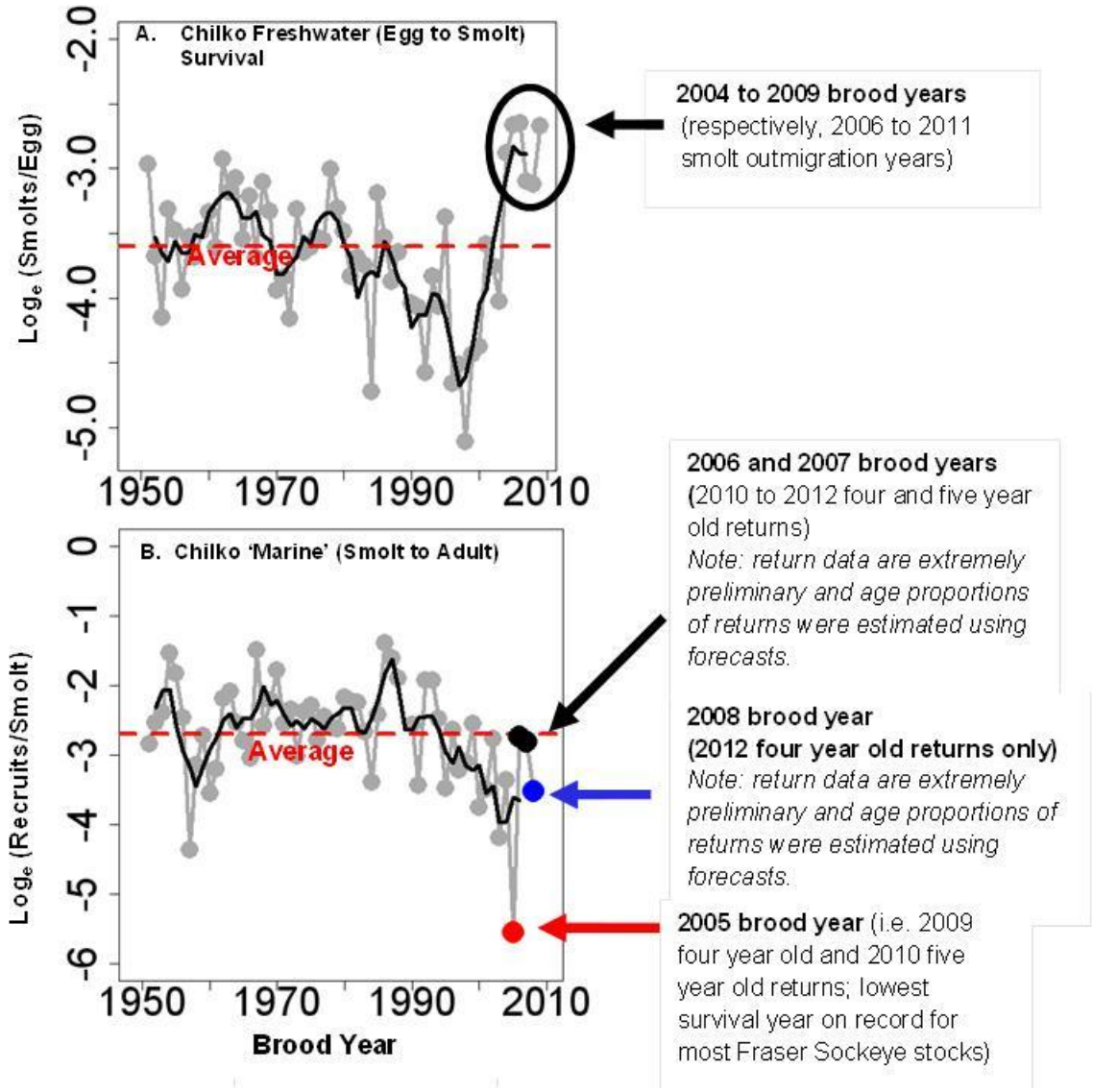

Figure 1. Chilko River Sockeye A. freshwater (log_e smolts-per-egg) and B. 'marine' (log_e recruits-per-smolt) annual survival (filled grey circles and lines) and smoothed four-year running average survival (black lines). Note: Chilko 'marine' survival includes a freshwater period during their downstream migration as smolts from the outlet of Chilko Lake to the Strait of Georgia. Red dashed lines in both plots indicate average survival. Reprinted from Grant and MacDonald 2013).

In the absence of leading indicators of productivity, Fraser Sockeye forecasts have been particularly uncertain in recent years, due to the systematic declines in productivity exhibited by the Fraser Sockeye aggregate (all stocks combined), which culminated in the lowest productivity on record in the 2005 brood year (2009 four year old and 2010 five year old returns) (Grant et al. 2010; Grant et al. 2011; Peterman and Dorner 2012) (Fig. 2). In subsequent years (2006 to 2008 brood years), productivity has improved (Fig. 2). The Fraser Sockeye total aggregate productivity largely represent trends exhibited by the most abundant Summer Run timed stocks (e.g. Chilko and Quesnel), however individual stock productivity trends vary (Fig. 3).

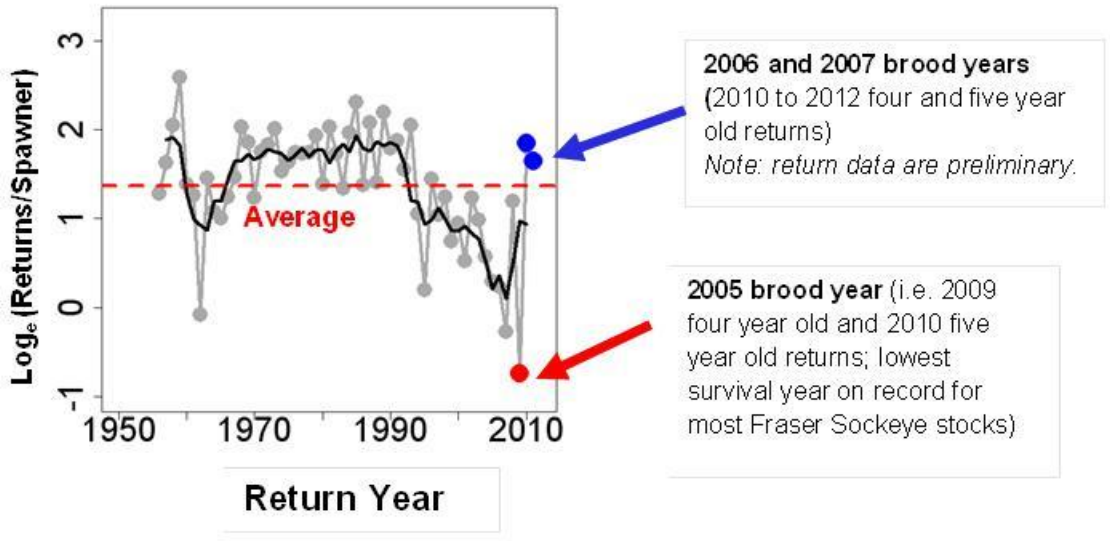

Figure 2. Total Fraser Sockeye productivity (log_e (returns/total spawner)) up to the 2012 return year. The light grey filled circles and line presents annual productivity and the black line presents the smoothed four year running average. Returns for 2009 (red filled circle) to 2012 are preliminary. The red dashed line indicates average survival.

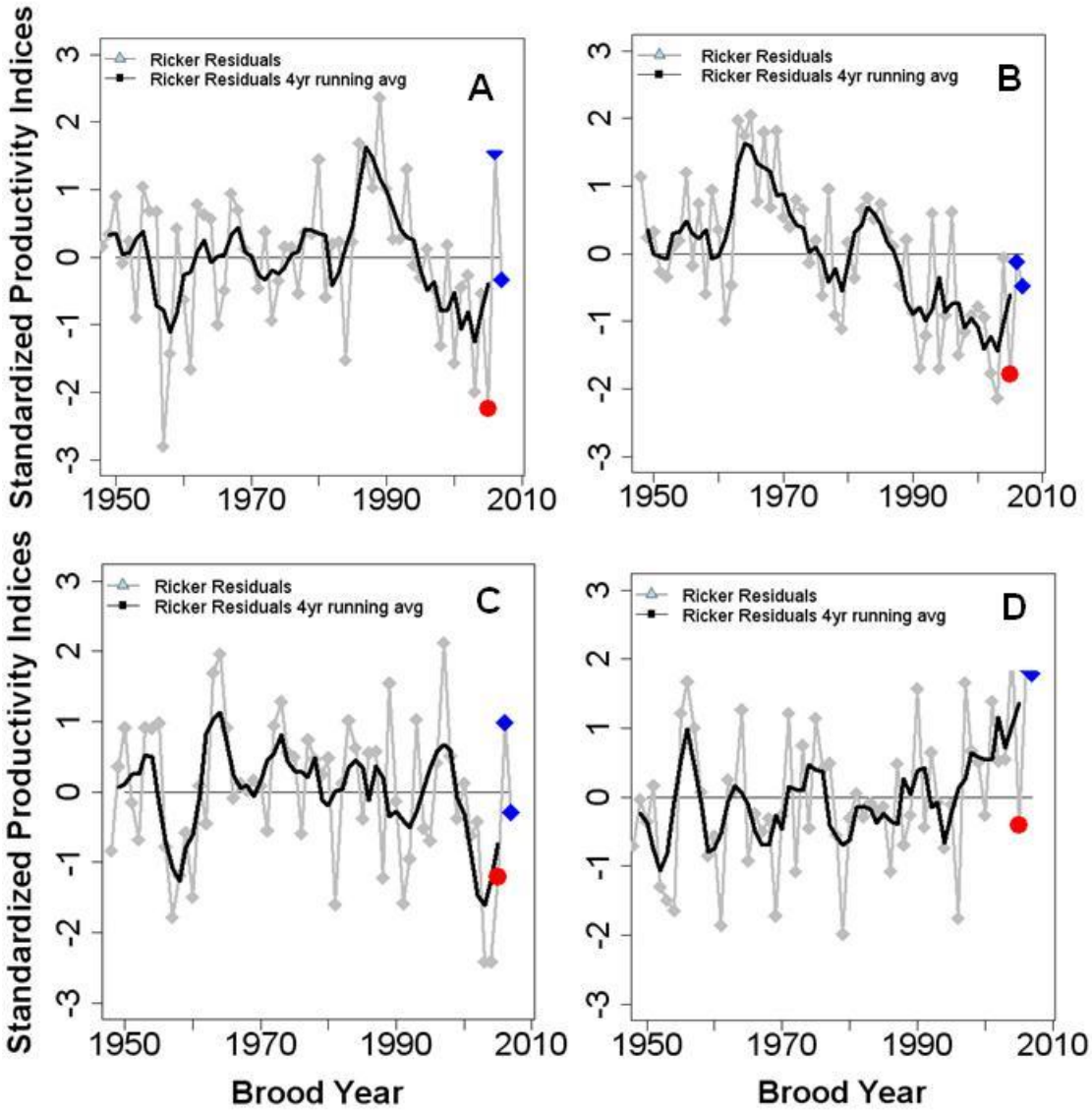

*Figure 3. Fraser Sockeye productivity (standardized z-scores of Ricker model residuals) up to the 2012 return year for **A.** Chilko Sockeye; **B.** Early Stuart Sockeye; **C.** Late Shuswap Sockeye; and **C.** Harrison Sockeye. The grey filled circles and line presents annual productivity and the solid black line presents the smoothed four-year running average. The 2005 (red circle) and 2006-2007 brood years (blue diamonds) are indicated; these recent data are preliminary.*

To capture inter-annual random (stochastic) uncertainty in Fraser Sockeye forecasts (largely attributed to variations in productivity), forecasts are presented as standardized cumulative probabilities (10%, 25%, 50%, 75%, and 90%), using Bayesian statistics, rather than as single deterministic point estimates (Grant et al. 2010; Grant and MacDonald 2013). At the 25% probability level, for example, there is a one in four chance the actual return will fall at or below the specified return prediction, given the historical data. Fisheries and Oceans Canada (DFO) fisheries managers use these forecast probability distributions to frame out the range of fishing opportunities that stakeholders may expect in the upcoming year. These return forecasts are also applied, in concert with run timing forecasts, as additional information for test-fishery and hydro-acoustic models, used to manage the fisheries in-season. As the fishing season proceeds

and more in-season data become available, the pre-season forecasts have a diminishing influence on in-season return estimates.

The 2013 forecast indicates a one in ten chance (10% probability) the total Fraser Sockeye return will be at or below 1,554,000 (lowest observed on this cycle) and a nine in ten chance (90% probability) it will be at or below 15,608,000, assuming productivity is similar to past observations (Grant and Macdonald 2013) (Fig. 3). The mid-point of this distribution (50% probability) is 4,765,000 (there exists a one in two chance the return will be at or below this value). The four year old percentage of the total forecast is 90%, and ranges from 13% to 100%, depending on the stock. The 2013 forecast is larger than the 2012 forecast, attributed to higher escapements in the 2009 versus 2008 brood year. Summer Run stocks, particularly Chilko and Quesnel, contribute 78% to the total return forecast, whereas Late Run (12%), Early Summer (5%) and Early Stuart Run stocks (4%) each contribute considerably less. The Harrison 2013 forecast is particularly uncertain, and returns have a higher likelihood of falling outside the forecast distribution. The total forecasted 2013 Fraser Sockeye return largely falls (up to a three in four chance, based on past observations) below the cycle average (8,579,000), due to the below average 2009 and 2008 brood year escapements for most stocks. Conversely, there is a one in four chance the return will be above the cycle average, if Fraser Sockeye productivity falls at the high end of past observations.

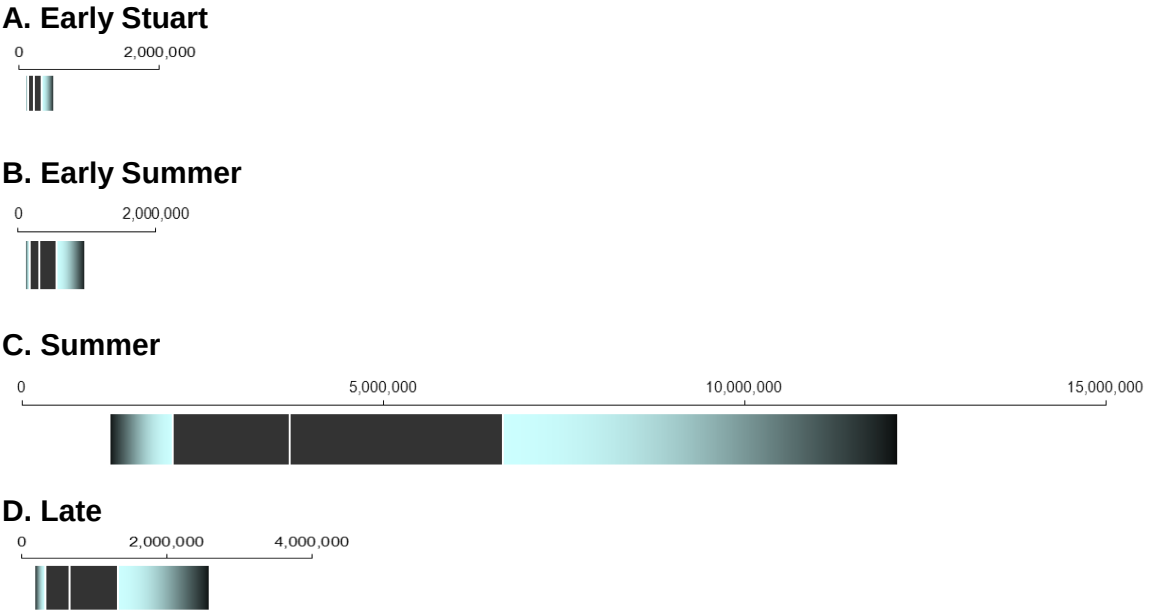

*Figure 4. Fraser Sockeye 2013 forecast probability distributions for **A**. Early Stuart; **B**. Early Summer; **C**. Summer and **D**. Late Run timing groups. These figures describe the stochastic (random) uncertainty in Fraser Sockeye forecasts as probability distributions. The width of the blue (or grey) bars represents the 10% and 90% probability levels, the width of the black bars represents the 25% to 75% probability levels, and the white line in the centre of the black bars represents the 50% probability level.*

As work proceeds on potential indicators of salmon productivity, exploration of environmental-recruitment correlations will benefit from the inclusion of uncertainties into these relationships. For the forecast process, Bayesian prediction intervals can be used quantitatively to describe the uncertainty in the model fit to the data, or qualitatively to frame out the ability of a particular correlation to distinguish between different survival conditions, which depend on the overlap between prediction intervals over the time series. For example, using Peterson's (National Ocean and Atmospheric Administration: NOAA) stop light approach, Bayesian prediction intervals may demonstrate that many environmental variables can only be used to resolve two

categories of survival conditions, such as Red/Amber (low to average) and Amber/Green (average to high), rather than the three categories typically presented (Red, Amber, and Green). For Fraser Sockeye, further work is on-going to see if a multi-criteria stop light approach, which includes the use of Bayesian methods, can reduce uncertainty in the official quantitative forecasts.

References

Grant, S.C.H. and MacDonald, B.L. 2013. Pre-season run size forecasts for Fraser Sockeye (*Oncorhynchus nerka*) and Pink (*O. gorbuscha*) in 2013. DFO Can. Sci. Advis. Sec. Res.Doc. 2012/045. vi + 42 p.

Grant, S.C.H., MacDonald, B.L., Cone, T.E., Holt, C.A., Cass, A., Porszt, E.J., Hume, J.M.B., and L.B. Pon. 2011. Evaluation of uncertainty in Fraser Sockeye (*Oncorhynchus nerka*) Wild Salmon Policy Status using abundance and trends in abundance metrics. DFO. Can. Sci. Advis. Sec. Res. Doc. 2011/087. viii + 183 p.

Grant, S.C.H., Michielsens, C. G. J., Porszt, E. J., and A.J. Cass. 2010. Pre-season run size forecasts for Fraser Sockeye (*Oncorhynchus nerka*) in 2010. CSAS Res.Doc. 2010/042, - vi + 127.

Peterman, R.M. and Dorner, B. 2012. A widespread decrease in productivity of Sockeye salmon (*Oncorhynchus nerka*) populations in western North America. *Can. J. Fish. Aquat. Sci*. 69:1255-1260.

Preikshot, D., Beamish, R.J., Sweeting, R.M., Neville, C.M., Beacham, T.D. 2012. The residence time of juvenile Fraser River Sockeye salmon in the Strait of Georgia. *Marine and Coastal Fisheries: Dynamics, Management, and Ecosystem Science* 4: 438-449.

Tucker, S., Trudel, M., Welch, D.W., Candy, J.R., Morris, J.F.T., Thiess, M.E., and Wallace, C. 2009. Seasonal stock-specific migrations of juvenile sockeye salmon along the West Coast of North America: implications for growth. *Trans. Am. Fish. Soc.* 138: 1458-1480.